

**“DEVELOPMENT OF siRNA NANO-CONSTRUCTS TO
POTENTIATE EFFECTS OF CHEMOTHERAPEUTICS FOR
EFFECTIVE TREATMENT OF LUNG CANCER”**

A thesis submitted to The Maharaja Sayajirao University
of Baroda for the Degree of

**DOCTOR OF PHILOSOPHY
IN
PHARMACY**

By

Mr. Nirav I. Khatri

M.Pharm

Supervised by

Dr. Ambikanandan Misra

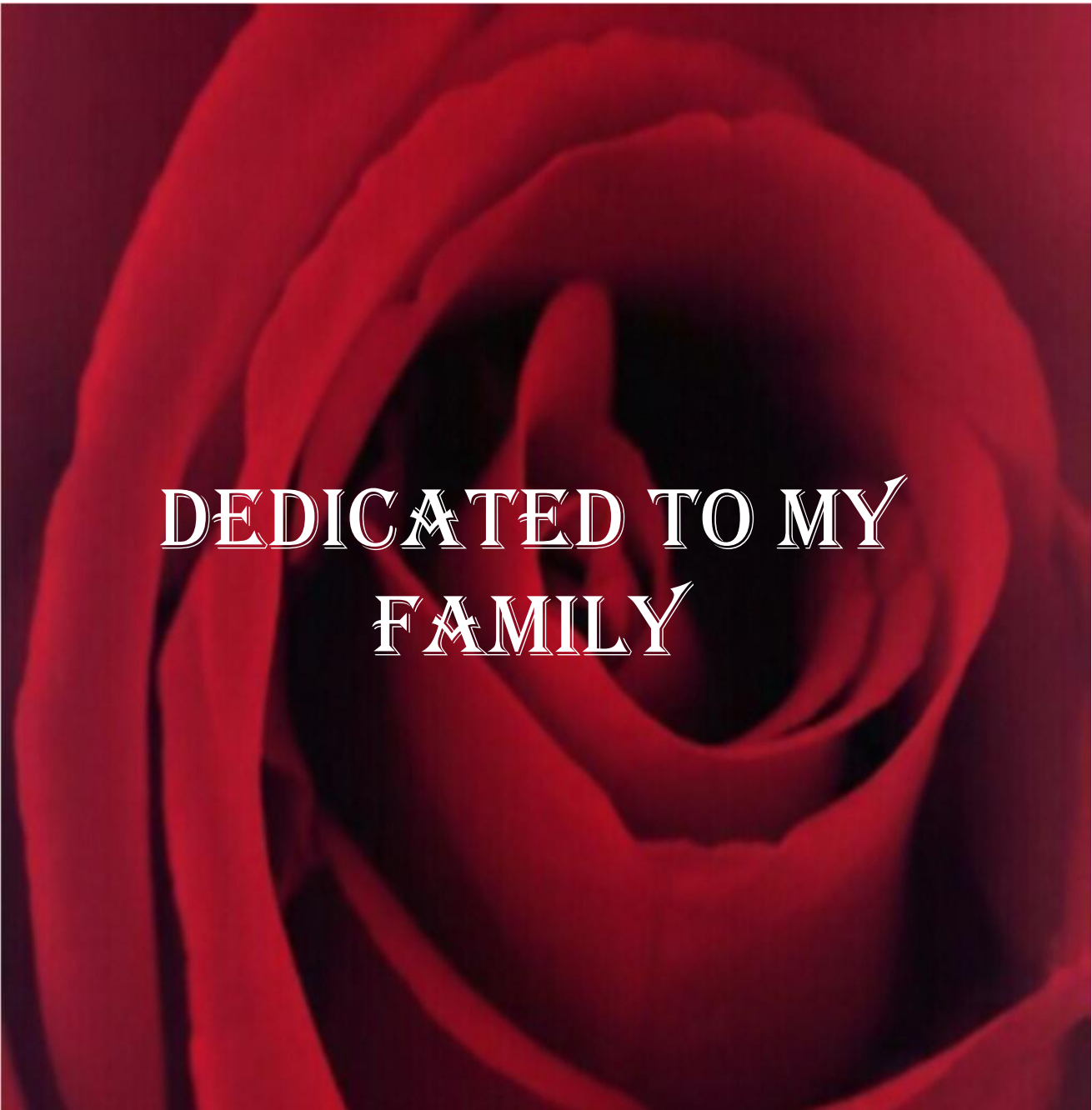
Professor of Pharmacy



Pharmacy Department

Faculty of Technology and Engineering
The Maharaja Sayajirao University of Baroda
Vadodara -390001, Gujarat, India

MAY, 2013



DEDICATED TO MY
FAMILY

May 21, 2013

CERTIFICATE

This is to certify that the thesis entitled “Development of siRNA Nano-Constructs to Potentiate Effects of Chemotherapeutics for Effective Treatment of Lung Cancer”, submitted for Ph.D. degree in Pharmacy by Nirav I. Khatri comprises the original research work carried out by him under my guidance and supervision.

Guide

Prof. Ambikanandan Misra

Pharmacy Department

Head

Pharmacy Department

Dean

Faculty of Technology and Engineering

DECLARATION

I hereby declare that the thesis on the topic entitled “Development of siRNA Nano-Constructs to potentiate effects of chemotherapeutics for effective treatment of lung cancer” which is submitted herewith to ‘The Maharaja Sayajirao University of Baroda, Vadodara’ for the award of Ph.D. in Pharmacy is the result of work done by me in the Pharmacy Department, Faculty of Technology & Engineering, The Maharaja Sayajirao University of Baroda, under the able guidance of Prof. Ambikanandan Misra, Pharmacy Department, Faculty of Technology & Engineering, The Maharaja Sayajirao University of Baroda, Vadodara.

I further declare that the result of this work has not been previously submitted for any degree.

(Nirav I. Khatri)

Place: Vadodara

Date: May 21, 2013

Certified by and forwarded through the research guide,

Ambikanandan Misra

Professor in Pharmacy & Dean,

Faculty of Technology & Engineering,

The Maharaja Sayajirao University of Baroda,

Vadodara-390001.

Acknowledgement

With vital devotion, I express my foremost heartfelt gratitude in the name of Almighty for directing and navigating me to and through this project to the successful accomplishment of my long cherished dream of this thesis with strength, assets, confidence and faith.

*Words are too trivial and scarce to convey my profound sense of indebtedness, gratefulness and honour for being driven by revered guidance of **Professor Ambikanandan Misra**, Pharmacy department, Dean, Faculty of Technology and Engineering, The Maharaja Sayajirao University of Baroda. His encouraging, patient and insightful guidance towards innovative and quality work has pervaded in me the essence of dedication, hard work, morality and sincerity towards research and investigation. His constructive ideas, intelligent, determined and qualitative approach has served my way not only to complete this project but also to face further challenges of life. I would always ruminate to his genuine concern and support during hard times and right direction during difficult decisions. I take this golden opportunity to express the feel of pride and good fortune to have such a kind and preeminent individuality as my supervisor.*

Special thanks to Prof. M. R. Yadav, Head of Pharmacy department for kind support and for providing me necessary facilities for research work. I shall thank Dr. (Mrs) K. K.Sawant, co-ordinator, G.H. Patel, Pharmacy Department, Prof. S. H. Misra, Mrs. S. Rajput and Prof. R. Balaraman for their helpful suggestions and encouragement.

I also express my special thanks to Prof. Sarita Gupta, co-ordinator, DBT-ILSPARE for providing all the required materials, equipments and facilities to carry out cell culture

studies. I take a special note of thanks to Akhilesh, Tushar and Komal for their untoward help to carry out different research activities of cell line studies.

I am thankful to Department of Biotechnology (DBT-SBIRI) for providing funds for my research project.

I offer sincere thanks to Mr. Dipesh Bardia, Mr. Iman Vohra and Ms. Jagruti Desai for constant help and co-operation during the tenure of research work as well as their unconditional support.

I would like to thank my all colleagues, Mohan Rathi, Chetan Yewale, Atul Kolte, Hardik Gandhi, Dr. Manisha Lalan, Bhavik Shah, Dr. Gaurang Patel, Dr. Sachin Naik, Dr. Jigar Lalani, Dr. Deepa Patel, Dr. Gitanjali Kher, Sonia Trehan, Sandeep, Girish Kore, Kailash, Piyush and all research Scholars who had help me directly or indirectly, for their fruitful advice and constant co-operation during tenure of research work.

Thanks are also due for Office staff of Faculty of Technology and Engineering and The Maharaja Sayajirao University of Baroda for their support and cooperation.

Nirav I. Khatri

Index

Chapter 1. Introduction

1.1. Introduction	1
1.2. Objective of the Proposed Work	8
1.3. Rationale	8
1.4. Hypothesis	9
1.5. Research Design and Method	9
1.6. Expected Results	9
1.7. Work Plan	9
1.8. References	10

Chapter 2. Literature Review

2.1. Lung Cancer	13
2.1.1. Causes of the Lung Cancer	13
2.1.2. Symptoms that Suggest Lung Cancer Include	13
2.1.3. Pathogenesis	14
2.1.4. Prevention and Treatment	14
2.2. Drug Profile	18
2.2.1. Mechanism of Action	18
2.2.2. Absorption, Fate, and Elimination	19
2.2.3. Therapeutic Uses	20
2.2.4. Clinical Toxicities	20
2.2.5. Problem Associated with Gemcitabine Hydrochloride	21
2.2.6. Chemoresistance with Gemcitabine Hydrochloride	21
2.2.7. Chemosensitization	22
2.3. Liposomes	24
2.3.1. Composition of Liposomes	24
2.3.1.1. Phospholipids	24

2.3.1.2. Sterols	25
2.3.1.3. Other Non-Structural Components	25
2.3.2. Types of Liposomes	26
2.3.3. Methods of Preparation of Liposomes	26
2.3.4. Characterization of Liposomes	26
2.3.4.1. Size and Size Distribution	26
2.3.4.2. Lamellarity	27
2.3.4.3. Determination of Percentage Capture	27
2.3.5. Stability of Liposomes	27
2.3.6. Liposomes as Drug Delivery Systems	29
2.4. Formulation Optimization	31
2.4.1. Experimental Designs	34
2.4.1.1. Factorial Designs	37
2.4.1.2. Design Augmentation	37
2.4.2. Response Surfaces	37
2.4.3. Mathematical Models	41
2.5. RNA Interference	42
2.5.1. Development of RNAi Technology	43
2.5.2. Targets of RNAi	44
2.5.3. Challenges to RNAi Delivery	45
2.5.3.1. Physiological Barriers	45
2.5.3.2. Cellular Barriers	47
2.5.4. Cellular Mechanisms of RNAi	48
2.5.5. Small Interfering RNA (siRNA)	50
2.5.6. RNAi as Therapeutics	51
2.5.7. <i>In vivo</i> Delivery Vectors	56
2.5.8. <i>In vivo</i> Delivery of RNAi	59
2.5.8.1. Systemic Delivery of RNAi Therapeutics	59

2.5.8.2. Clinical Trials and RNAi	62
2.5.9. Delivery of Therapeutic siRNA in cancer	65
2.5.10. siRNA Application in Lung Cancer	68
2.6. RGD Peptide for Targeting	70
2.7. References	72

Chapter 3. Analytical Method Development

3.1. Preparation of Calibration Plot of siRNA	96
3.1.1 Reagents	96
3.1.2 Method of Analysis	96
3.1.3 Accuracy and Precision of Method	97
3.2. Analysis of Calcium Content of Liposomes	99
3.2.1. Introduction	99
3.2.2. Reagents	104
3.2.3. Method of Analysis	104
3.2.4. Accuracy and Precision of Method:	105
3.3. siRNA Gel Electrophoresis: Gel Retardation Assay	107
3.3.1. Introduction	107
3.3.2. Method of Analysis	108
3.3.3. Determination of Quantifiable Range of siRNA for Gel Retardation Assay	108
3.3.4. Relative Quantification	109
3.3.5. Accuracy and Precision of the Method	111
3.4. References	113

Chapter 4. Formulation Development

4.1. Selection of siRNA	114
4.1.1. Sense-strand Analysis	114
4.1.1.1. MALDI-Mass Spectrometry of siRNA	114

4.1.1.2. Capillary Gel Electrophoresis (CGE) Analysis of siRNA	115
4.1.2. Antisense-strand Analysis	115
4.1.2.1. MALDI mass Spectrometry of siRNA	115
4.1.2.2. Capillary Gel Electrophoresis (CGE) analysis of siRNA	116
4.1.3. Gel Electrophoresis of siRNA	116
4.2. Development of Cationic siRNA loaded liposomes	119
4.2.1. Introduction	119
4.2.1.1. DOTAP	119
4.2.1.2. DOPE	120
4.2.1.3. Negatively Charged Lipid- DMPG	121
4.2.1.4. mPEG ₂₀₀₀ -DSPE	123
4.2.1.5. Cholesterol	124
4.2.2. Development of Cationic Liposomes	127
4.2.2.1. Preparation of pre-formed liposomes	127
4.2.2.2. Development of siRNA Liposomes	128
4.2.2.3. Optimization of Parameters	128
4.2.2.4. RGD Grafting on the Surface of Liposomes	128
4.2.2.5. Lyophilization of siRNA Liposomes	129
4.2.2.6. Assay	130
4.2.2.7. Entrapment Efficiency	131
4.2.2.8. Particle Size and Zeta Potential	131
4.2.2.9. Residual Water content	131
4.2.2.10. Cryo-Transmission Electron Microscopy (Cryo-TEM)	132
4.2.2.11. Statistical Analysis	132
4.2.3. Result and Discussion	132
4.2.3.1. Preparation of Pre-formed Liposomes	132
4.2.3.2. Preparation of Cationic siRNA Liposomes:	134
4.2.3.3. Optimized Formulations	143

4.2.3.4. Lyophilization	144
4.2.3.5. Assay	146
4.2.3.6. Entrapment Efficiency	147
4.2.3.7. Particle size and Zeta potential	148
4.2.3.8. Residual Water Content	150
4.2.3.9. Transmission Electron Microscopy	151
4.3 Development of Calcium Phosphate mediated siRNA Loaded in Liposomes	152
4.3.1. Methodology	150
4.3.2. Preparation of Calcium Phosphate Encapsulated siRNA Liposomes	153
4.3.2.1. Preparation of calcium phosphate liposomes	153
4.3.2.2. RGD Grafting on the Surface of Liposomes	154
4.3.2.3. Loading of siRNA in Calcium Phosphate Entrapped Liposomes	154
4.3.3. Formulation Optimization	154
4.3.4. Calcium Entrapment	156
4.3.5. Particle Size and Zeta Potential	157
4.3.6. Assay	157
4.3.7. siRNA Entrapment Efficiency	157
4.3.8. Cryo-Transmission Electron Microscopy (Cryo-TEM)	157
4.3.9. Statistical Analysis	158
4.3.10. Results and Discussion	158
4.3.10.1. Optimization of Calcium Phosphate Entrapped Liposomes	158
4.3.10.2. Optimization for Loading of siRNA in Calcium Phosphate Entrapped Liposomes	175
4.3.10.3. Incorporation of RGD	195
4.3.10.4. Calcium Entrapment	196
4.3.10.5. Assay	196
4.3.10.6. siRNA Entrapment Efficiency	197
4.3.10.7. Particle size and Zeta Potential	197

4.3.10.8. Transmission Electron Microscopy	200
4.4. References	201

Chapter 5. *In Vitro* Characterization

5.1. Cell-line Studies	207
5.1.1. <i>In vitro</i> Cytotoxicity Assay (MTT Assay)	207
5.1.2. <i>In vitro</i> Cell Uptake Studies	208
5.1.2.1. Flow Cytometry	208
5.1.2.2. Confocal Microscopy	210
5.1.3. Sub-inhibitory Concentration (Cell Cycle Analysis)	211
5.1.4. Transfection Studies/Gene expression by real time PCR	213
5.1.5. Statistical Analysis	218
5.1.6. Results and Discussion	218
5.1.6.1. <i>In Vitro</i> Cytotoxicity Assay (MTT Assay)	218
5.1.6.2. <i>In Vitro</i> Cell Uptake	223
i. Flow Cytometry	223
ii. Confocal Microscopy	229
5.1.6.3. Sub-inhibitory Concentration (Cell Cycle Analysis)	239
5.1.6.4. Transfection Studies	240
5.2. Chemosensitization Studies	246
5.2.1. Method	246
5.2.2. Result and Discussion	247
5.3. Serum Stability Study (In vitro Release)	256
5.3.1. Methods	256
5.3.2. Result and discussion	257
5.4. Haemolysis Study	261
5.4.1. Method	261
5.4.2. Results and Discussion	263

5.5. Electrolyte Induced Flocculation Test	267
5.5.1. Method	267
5.5.2. Results and Discussion	268
5.6. References	271

Chapter 6. *In Vivo* Toxicity Study

6.1. Acute Toxicity Study	274
6.2. Description of the Methods	275
6.2.1. Selection of Animals Species	275
6.2.2. Housing and Feeding Conditions	275
6.2.3. Preparation of Animals	276
6.2.4. Preparation of Doses	276
6.2.5. Procedures	276
6.2.5.1. Administration of Doses	276
6.2.5.2. Main Test	277
6.2.5.3. Sighting Study	277
6.2.5.4. MTD Determination	277
6.2.5.5. Numbers of Animals and Dose Levels	278
6.2.5.6. Observations	278
6.3. Results and Discussion	279
6.4. References	282

Chapter 7. Stability Studies

7.1. Stability Studies of Liposomes	283
7.2. Method	283
7.3. Results and Discussion	284
7.3.1 Stability Testing of RGD-DDHC Liposomes(2%)	284
7.3.2 Stability Testing of RGD-CPE Liposomes(2%)	285

7.4. References	287
-----------------	-----

Chapter 8. Summary and Conclusion

8.1. Summary	289
--------------	-----

8.2. Conclusions	300
------------------	-----

List of Tables

Table 1.1 Some Putative siRNA targets against cancer

Table 2.1 Drug Profile

Table 2.2 Major Modes of Liposomal Action and Related Applications

Table 2.3 Modes of Rnai Delivery and Potential Targets in Various Diseases

Table 2.4 Therapeutic intervention using siRNA

Table 2.5 siRNA – Clinical Trials

Table 2.6 Examples of siRNA delivery systems for treatment of cancers

Table 3.1 UV Spectrophotometric Absorbance of siRNA

Table 3.2 Accuracy of the Method

Table 3.3 Intraday Precision of the Method

Table 3.4 Interday Precision of the Method

Table 3.5 Volume of 0.01 M Na₂EDTA Solution Required for Different Amounts of Calcium Chloride

Table 3.6 Accuracy of Method

Table 3.7 Intraday Precision of the Method

Table 3.8 Interday Precision of the Method

Table 3.9 Gel Electrophoresis – Relative Band Densities at Different siRNA Concentrations

Table 4.1 Various Liposomal Formulations with Their Composition

Table 4.2 Selection of Process Parameters for Pre-formed Liposomes

Table 4.3 Selection of Process Parameters for Pre-Formed Liposomes

Table 4.4 Formulation Development of D Liposomes

Table 4.5 Formulation development of DD Liposomes

Table 4.6 Formulation development of DDH liposomes

Table 4.7 Formulation development of DDC Liposomes

Table 4.8 Formulation development of DDHC liposomes

Table 4.9 Formulation development of DDHCP liposomes

Table 4.10 Optimized Formulations

Table 4.11 Lyophilization Optimization

Table 4.12 Lyophilization Optimization

Table 4.13 Characterization of siRNA loaded liposomes

Table 4.14 siRNA Entrapment of Various Liposomes

Table 4.15 Effect of siRNA Complexation on Particle Size

Table 4.16 Effect of siRNA Complexation on Zeta Potential

Table 4.18 Methods for Calcium Phosphate Mediated siRNA Loading in Liposomes

Table 4.19 Various Variables and Responses Involved in Optimization

Table 4.20 Coded and Actual Values of the formulation parameters for step-1

Table 4.21 Coded and Actual Values of the formulation parameters for step-2

Table 4.22 Design Matrix for Calcium Chloride Loaded Liposome Optimization

Table 4.23 Summary of ANOVA results for Different Models

Table 4.24 ANOVA Table for Response Surface Quadratic Model

Table 4.25 Summary of ANOVA results for Quadratic Model

Table 4.26 Summary of ANOVA results for Different Models

Table 4.27 ANOVA table for Response Surface Quadratic Model

Table 4.28 Summary of ANOVA results for Quadratic Model

Table 4.29 Constraints Applied for Selection of Optimized Batch

Table 4.30 Optimized Batch Parameters Based on Desirability

Table 4.31 Predicted Responses of the Optimized Batch

Table 4.32 Experimental Confirmation of the Predicted Responses

Table 4.33 Effect of incubation time on siRNA Entrapment

Table 4.34 Effect of Incubation Temperature on siRNA Entrapment

Table 4.36 Summary of ANOVA results for Different Models

Table 4.37 ANOVA table for Response Surface Quadratic Model

Table 4.38 Summary of ANOVA results for Quadratic Model

Table 4.39 Summary of ANOVA results for Different Models

Table 4.40 ANOVA table for Response Surface Quadratic Model

Table 4.41 Summary of ANOVA results for Quadratic Model

Table 4.42 Constraints Applied for Selection of Optimized Batch

Table 4.43 Optimized Batch Parameters Based on Desirability

Table 4.44 Predicted Responses of the Optimized Batch

Table 4.45 Experimental Confirmation of the Predicted Responses

Table 4.46 Effect of RGD Levels on siRNA Entrapment and Particle Size

Table 4.47 Calcium Entrapment Efficiency of Optimized Liposomes

Table 4.48 Results of Assay of Various siRNA formulations

Table 4.49 siRNA Efficiency of Various RGD Grafted Liposomes (as Determined by Various Methods)

Table 4.50 Effect of incorporation of siRNA on Particle Size of Liposomes

Table 5.1 Cell-line Treatment Parameters for MTT Assay

Table 5.2 Cell-Line Treatment Parameters for Flow-Cytometry

Table 5.3 Cell-Line Treatment Parameters for Confocal Microscopy

Table 5.4 Details of Primers

Table 5.5 RNA to cDNA Conversion Parameters

Table 5.6 PCR Cycle Steps

Table 5.7 mRNA Quantification – Reaction Parameters

Table 5.8 RT-PCR Cycle Steps

Table 5.9 Viability of A549 Cells on Exposure to Cationic Liposomes

Table 5.10 Viability of H1299 Cells on Exposure to Cationic Liposomes

Table 5.11 Viability of H1299 Cells on Exposure to CPE Liposomes

Table 5.12 Viability of H1299 Cells on Exposure to Various CPE Liposomes

Table 5.13 Uptake of Liposomes in A549 Cells

Table 5.14 Uptake of Cationic Liposomes in A549 Cells

Table 5.15 Uptake of Liposomes in H1299 Cells

Table 5.16 Transfection in A549 Cells

Table 5.17 Transfection in H1299 Cells

Table 5.18 Chemosensitization of Gemcitabine HCl in A549 Cells

Table 5.19 Chemosensitization of Gemcitabine HCl in H1299 Cells

Table 5.20 IC₅₀ values of Various Formulations with or without siRNA

Table 5.21 Change in IC₅₀ of Gemcitabine HCl after Chemosensitization by RGD-DDHC Liposomes(2%)

Table 5.22 Change in IC₅₀ of Gemcitabine HCl After Chemosensitization by RGD-CPE Liposomes(2%)

Table 5.23 Change in IC₅₀ of Gemcitabine HCl After Chemosensitization by Lipofectamine 2000

Table 5.24 Comparison of Change in IC₅₀ Value of Various Formulation

Table 5.25 Serum Stability of Liposomes

Table 5.26 Serum Stability of Naked siRNA

Table 5.27 In vitro Release in Serum at pH 7.4

Table 5.28 Haemolysis by Cationic Liposomes

Table 5.29 Haemolysis in CP liposomes

Table 5.30 Electrolyte Induced Flocculation of DDHC Liposomes

Table 5.31 Electrolyte Induced Flocculation of CPE Liposomes

Table 6.1 Sighting Study: Dosing protocol

Table 6.2 Results of Sighting Study

Table 6.3 MTD Study: Dosing Protocol

Table 6.4 Results for MTD study

Table 7.1 Stability Testing Data of RGD-DDHC Liposomes (2%)

Table 7.2 Stability Testing Data of RGD-CPE Liposomes(2%)

List of Figures

Figure 1.1 RNA interference

Figure 2.1 Mechanism of action of Gemcitabine Hydrochloride

Figure 2.2 The structure of Multilamellar Vesicles Showing the Organization of Phospholipid Bilayers and the Encapsulation of Lipophilic and Hydrophilic Compounds

Figure 2.3 Seven-step Ladder for Optimizing Drug Delivery Systems

Figure 2.4 Quantitative Factors and Factor Space

Figure 2.5 Different Types of Responses as Functions of Factor Settings; (a) Linear; (b) Quadratic; (c) Cubic

Figure 2.6 (a) A Typical Response Surface Plotted Between A Response Variable, Release Exponent, and Two Factors, HPMC And Sodium CMC, In Case of Mucoadhesive Compressed Matrices; (b) The Corresponding Contour Plot

Figure 2.7 Approaches for Knockdown of Target Gene Or mRNA

Figure 2.8 Cellular Mechanisms of RNAi

Figure 3.1 Calibration Plot of siRNA

Figure 3.2 Volume of 0.01 M Na₂EDTA Solution Required for Different Amounts of Calcium Chloride

Figure 3.3 Determination of Quantifiable Range of siRNA - Gel Electrophoresis Band Densities at different siRNA Concentraions

Figure 3.4 Relative Quantification of siRNA - Gel Electrophoresis Band Densities at Different siRNA Concentrations

Figure 3.5 Calibration Plot of siRNA Gel Retardation

Figure 3.6 Accuracy and Precision of Gel Electrophoresis Method for siRNA Quantificati

Figure 4.1 MALDI Analysis

Figure 4.2 CGE Analysis

Figure 4.3 MALDI Analysis

Figure 4.4 CGE Analysis

Figure 4.5 Gel Electrophoresis of siRNA

Figure 4.6 Effect of temperature on siRNA A-vertical view B-3D view

Figure 4.7 Effect of pH on siRNA A-vertical view B- 3D view

Figure 4.8 Formation of siRNA Encapsulated Cationic Liposomes

Figure 4.9 Lyophilization Cycle Recipe

Figure 4.10 Lyophilization Plot

Figure 4.11 Gel Electrophoresis of DD liposomes

Figure 4.12 Gel Electrophoresis of DDH Liposomes

Figure 4.13 Gel Electrophoresis of DDH Liposomes

Figure 4.14 Gel Electrophoresis of DDC liposomes at N/Chol=0.77

Figure 4.15 Gel Electrophoresis of DDC liposomes at N/Chol=0.38

Figure 4.16 Gel Electrophoresis of DDHC liposomes

Figure 4.17 Gel Electrophoresis of DDHC liposomes prepared with 2 mol% mPEG2000-DSPE

Figure 4.18 Gel Electrophoresis of DDHCP liposomes

Figure 4.19 Particle size of RGD-DDHC Liposomes (2%) after Complexation

Figure 4.20 Zeta potential of RGD-DDHC liposomes (2%) after Complexation

Figure 4.21 Transmission Electron Micrograph of RGD-DDHC liposomes (2%) after Complexation

Figure 4.22 Effect of Lipid: Calcium on Calcium Entrapment

Figure 4.23 Effect of DPPC: Chol on Calcium Entrapment

Figure 4.24 Effect of Concentration of Calcium on Calcium Entrapment

Figure 4.25 Response Surface Showing Combined Effect of Lipid:Calcium and DPPC:Chol on Calcium Entrapment

Figure 4.26 Response Surface Showing Combined Effect of Lipid:Caclium and Concentraion of Calcium on Calcium Entrapment

Figure 4.27 Response Surface Showing Combined Effect of Lipid:Caclium and Concentraion of Calcium on Calcium Entrapment

Figure 4.28 Effect of Lipid:Caclium on Particle Size

Figure 4.29 Effect of DPPC:Chol on Particle Size

Figure 4.30 Effect of Concentration of Calcium on Particle Size

Figure 4.31 Response Surface Showing Combined Effect of Lipid:Calcium and DPPC:Chol on Particle Size

Figure 4.32 Response Surface Showing Combined Effect of Lipid:Calcium and Concentration of Calcium on Particle Size

Figure 4.33 Response Surface Showing Combined effect of DPPC:Chol and Concentration of Calcium on Particle Size

Figure 4.34 Desirability Plot for Selection of Optimized Batch

Figure 4.35 Effect of Calcium: siRNA on siRNA Entrapment

Figure 4.36 Effect of Lipid:Ethanol on siRNA Entrapment

Figure 4.37 Effect of siRNA Concentration on siRNA Entrapment

Figure 4.40 Response Surface Showing Combined Effect of Lipid:Ethanol and siRNA Concentration on siRNA Entrapment

Figure 4.39 Response Surface Showing Combined Effect of Calcium:siRNA and Concentration of Calcium on siRNA Entrapment

Figure 4.38 Response Surface Showing Combined Effect of lipid: ethanol and Calcium: siRNA on siRNA Entrapment

Figure 4.41 Gel electrophoresis for siRNA concentration (Calcium:siRNA = 5)

Figure 4.42 Gel electrophoresis for siRNA concentration (Calcium:siRNA = 7)

Figure 4.43 Gel electrophoresis for siRNA concentration (Calcium:siRNA = 9)

Figure 4.44 Gel electrophoresis for siRNA concentration (Calcium:siRNA = 5)

Figure 4.45 Gel electrophoresis for siRNA concentration (Calcium:siRNA = 7)

Figure 4.46 Gel electrophoresis for siRNA Concentration (Calcium:siRNA = 9)

Figure 4.47 Gel electrophoresis for siRNA Concentration (Calcium:siRNA = 5)

Figure 4.48 Gel electrophoresis for siRNA Concentration (Calcium:siRNA = 7)

Figure 4.49 Gel electrophoresis for siRNA Concentration (Calcium:siRNA = 9)

Figure 4.50 Effect of Calcium: siRNA on Particle Size

Figure 4.51 Effect of Lipid: Ethanol on Particle Size

Figure 4.52 Effect of siRNA Concentration on Particle Size

Figure 4.55 Response Surface Showing Combined Effect of Lipid:Ethanol and siRNA Concentration on Particle Size

Figure 4.54 Response Surface Showing Combined Effect of Calcium:siRNA and siRNA Concentration on Particle Size

Figure 4.53 Response Surface Showing Combined Effect of Calcium:siRNA and Lipid:Ethanol on Particle Size

Figure 4.56 Desirability Plot for Selection of Optimized Batch

Figure 4.57 Malvern Particle Size Report of One of the RGD-CPE Liposome(2%) Batches

Figure 4.58 Malvern Zeta Potential Report of One of the RGD-CPE Liposome(2%) Batches

Figure 4.59 TEM Micrograph of Calcium Phosphate Loaded Liposomes

Figure 5.1 Cytotoxicity of Different Cationic Liposomes in A549 Cell-line

Figure 5.2 Cytotoxicity of Different Cationic Liposomes in H1299 Cell-line.

Figure 5.3 Cytotoxicity of Different CPE Liposomes in A549 Cell-line
Figure 5.4 Cytotoxicity of Different CPE Liposomes in H1299 Cell-line
Figure 5.5 Uptake of Liposomes in A549 Cells
Figure 5.6 Quantification of Mean Fluorescence Intensity in A549 Cells
Figure 5.7 Uptake of Liposomes in A549 Cells
Figure 5.8 Quantification of Mean Fluorescence Intensity in H1299 Cells
Figure 5.9 Uptake of Liposomes in H1299 Cells
Figure 5.10 Cell Uptake in A549 Cell Line
Figure 5.11 Cell Uptake in H1299 Cell Line
Figure 5.12 Live Uptake of Naked siRNA in A549 Cells
Figure 5.13 Live uptake of DDHC liposomes in A549 cells
Figure 5.14 Live uptake of CPE liposomes in A549 cells
Figure 5.15 Live uptake of RGD-DDHC liposomes in A549 cells
Figure 5.16 Live Uptake of RGD-CPE Liposomes in A549 cells
Figure 5.17 3D Z-stack image for DDHC liposomes uptake
Figure 5.18 3D Z-stack image for CPE liposomes uptake
Figure 5.19 3D Z-stack Image for RGD-DDHC Liposomes Uptake
Figure 5.20 3D Z-stack Image for RGD-CPE Liposomes Uptake
Figure 5.21 Cell Growth Inhibition in A549 Cells
Figure 5.22 Cell Growth Inhibition in H1299 Cells
Figure 5.23 Amplification Plot for RRM1 and GAPDH mRNA
Figure 5.24 High Resolution Melt Curve for RRM1
Figure 5.25 High Resolution Melt Curve for GAPDH
Figure 5.26 High Resolution Melt Curve for RRM1 and GAPDH
Figure 5.27 Transfection in A549 Cells
Figure 5.28 Transfection in H1299 Cells
Figure 5.29 Chemosensitization of Gemcitabine in A549 Cells by siRNA
Figure 5.30 Chemosensitization of Gemcitabine in H1299 Cells by siRNA
Figure 5.31 Gel Electrophoresis of Naked siRNA
Figure 5.32 *In vitro* Release of siRNA from Liposomes
Figure 5.33 Haemolytic Potential of Cationic Liposomes
Figure 5.34 Haemolytic potential of calcium phosphate loaded liposomes
Figure 5.35 Electrolyte Induced Flocculation of DDHC Liposomes
Figure 5.36 Electrolyte Induced Flocculation of CPE Liposomes

Materials & Chemicals

Materials and Chemicals	Source
Nuclease free water	Ambion, USA
DEPC- diethylpyrocarbonate	Himedia lab. Pvt. Ltd., Mumbai, India
Ethylene Diamine Tetraacetic Acid (EDTA)	Himedia lab. Pvt. Ltd., Mumbai, India
Ammonia	Sigma-Aldrich, USA
Ammonium Chloride	Sigma-Aldrich, USA
Calcium Chloride	Sigma-Aldrich, USA
Solochrome Black-T	Sigma-Aldrich, USA
Potassium nitrate	Sigma-Aldrich, USA
Ethidium Bromide	Sigma-Aldrich, USA
Agarose (electrophoresis grade)	Himedia lab. Pvt. Ltd., Mumbai, India
TBE (Tris-Borate-EDTA)	Himedia lab. Pvt. Ltd., Mumbai, India
Sucrose	Merck Bioscience, India
Bromophenol blue	Himedia lab. Pvt. Ltd., Mumbai, India
Boric Acid	Himedia lab. Pvt. Ltd., Mumbai, India
FBS	Himedia lab. Pvt. Ltd., Mumbai, India
Penicillin	Himedia lab. Pvt. Ltd., Mumbai, India
Streptomycin	Himedia lab. Pvt. Ltd., Mumbai, India
Sodium Phosphate	Sigma-Aldrich, USA
Rebonucleotide reductase subunit-1 siRNA	Eurofins MWG Operons Ltd, Germany
glyceraldehyde-3-phosphate dehydrogenase (GAPDH) Primers	IDT, India
siRNA	Eurofins MWG Operons Ltd, Germany
(FAM) labelled negative control siRNA (FAM-NC-siRNA)	GenePharma, Shanghai, China
Negative control (scramble) siRNA	GenePharma, Shanghai, China
Gemcitabine HCl	Sun Pharma Ltd., India
Didioleoyl Trimethylammoniumpropane (DOTAP)	Lipoid GmbH, Germany
Phosphatidyl Glycerol (PG)	Lipoid GmbH, Germany
Dimyristoyl Phosphatidyl glycerol (DMPG)	Lipoid GmbH, Germany
Dioleoyl Phosphatidylethanolamine (DOPE)	Lipoid GmbH, Germany
Phosphatidyl Choline (PC)	Lipoid GmbH, Germany
Hydrogenated Soya Phosphatidyl Choline (HSPC)	Lipoid GmbH, Germany
Cholesterol	Sigma-Aldrich, USA
mPEG-DSPE-2000	Lipoid GmbH, Germany
DOTMA	Lipoid GmbH, Germany
Polycarbonate Membranes	Whatman, USA
Polyethylene drain disk	Whatman, USA
Diethylpyrocarbonate treated H ₂ O	Sigma, USA
6X DNA gel loading buffer	Fermentas Life Sciences, USA
Karl-Fischer reagents	Sigma, USA
RGDmPEG-DSPE ₂₀₀₀	Peptide International, USA
Lactose	Merck, India
Mannitol	Merck, India
Sephadex G-50	Sigma Aldrich, USA

Disodium Hydrogen Phosphate	Merck, India
human lung carcinoma cell line (A549)	NCCS, Pune
Dulbecco's Modified Eagle Medium (DMEM)	Himedia lab. Pvt. Ltd., Mumbai, India
3-(4, 5-dimethylthiazole-2-yl)-2,5- di-phenyl tetrazolium bromide (MTT)	Himedia lab. Pvt. Ltd., Mumbai, India
Lipofectamine-2000	Invitrogen, USA
Phenol	SD Fine chemicals Ltd., Mumbai, India
Chloroform	SD Fine chemicals Ltd., Mumbai, India
Methanol	SD Fine chemicals Ltd., Mumbai, India
DMSO	Sigma, USA
TRIzol reagent	Invitrogen, USA
RNA to cDNA conversion kit	Invitrogen, USA
SYBR Green Master mix	Applied Biosciences, USA
Dialysis Membrane	Sigma, USA

Equipments

Equipments	Source
Dual beam spectrophotometer (UV-1800)	Shimadzu, Japan
Electrophoresis chamber	Genet Electrophoresis Powerpack, Bangalore, India
GelDoc™ XR ⁺ Imaging System	BioRad, USA
Gel electrophoresis system	GeNei, India
rotary evaporator, IKA RV-10	Cole-Parmer, USA
high-pressure extruder	Avestin, Canada
lyophilizer	Virtis-Advantage plus, USA
Laboratory Centrifuge	Remi Sci. Equipment, India
Malvern Zetasizer Nano ZS	Malvern Instruments, Malvern, UK
Cryo-TEM	TECNAI G2 Spirit BioT WIN, FEI-Netherlands
Glow Discharge to perform cryo TEM	Emitech K100X, Quoram Technologies, UK
JouanIGO150 5% CO2 incubator	Thermo-Fischer, Germany
enzyme-linked immunosorbent assay plate reader	Bio-Rad, USA
Fluorescence activated cell sorter (FACS-BD-AriaIII)	BD, USA
confocal laser scanning microscope, LSM 710	Carl-Zeiss Inc., USA
Step One real time PCR	Applied Biosciences, USA
Weighing balance, ATX224	Unibloc, Shimadzu
Probe sonicator (Labsonic M)	Sartorius, India
Bath sonicator	Sartorius, Inida
Ultra Centrifuge (Beckman-Coulter Optima 100 xp)	Beckman, Germany
Orbitek Shaker incubator	Scigenics, India
pH meter	Labindia Inst Pvt. Ltd., India
Magnetic Stirrer	Remi Sci. Equipment, India
Weiber vertical Laminar Air Flow	Weiber, India
Inverted microscope	Nikon, Japan
Optical Microscope with polarizer	Olympus Co. Pvt. Ltd., Japan
Nikon H600L Microscope	Nikon, Japan
Deep freezer	EIE Inst. Ltd., Ahmedabad
Karl-Fischer Auto titrator	Toshiwal Inst. Pvt. Ltd., India

Abbreviations

RNAi: RNA interference

dsRNA: double stranded RNA

siRNA: small interfering RNA

FAM-NC-siRNA: FAM labelled negative control siRNA

RGD: Arginine-Glycine-D-Aspartate

DOTAP: Dioleoyl-trimethylammoniumpropane

DOPE: Dioleoyl-phosphatidylethanolamine

HSPC: Hydrogenated soya phosphatidylcholine

DMPG: Dimyristoyl Phosphatidyl glycerol

PC: Phosphatidyl Choline

DPPC: Dipalmitoyl phosphatidylcholine

DSPG: Disteroyl phosphatidylglycerol

DSPE-mPEG₂₀₀₀: 1,2-Distearoyl-phosphatidylethanolamine-methyl-polyethyleneglycol conjugate-2000 (Na⁺ salt)

DEPC: Diethyl Pyrocarbonate

FBS: Fetal bovine serum

RRM1: Ribonucleotide reductase Subunit

MTT: 13-(4, 5-dimethylthiazole-2-yl)-2,5- di-phenyl tetrazolium bromide

DMSO: Dimethyl sulfoxide

L2K: Lipofectamine

GAPDH: glyceraldehyde-3-phosphate dehydrogenase

DMEM: Dulbecco's Modified Eagle Medium

EDTA: Ethylene Diamine Tetraacetic Acid

EtBr: ethidium bromide

TBE: Tris-Borate-EDTA

CGE: Capillary Gel Electrophoresis

MALDI: Matrix assisted laser desorption ionization

PG: Phosphatidyl Glycerol

asODN: antisense oligodeoxynucleotides

Cryo-TEM: Cryo-Transmission Electron Microscopy

RBF: Round bottom Flask

ANOVA: Analysis of Variance

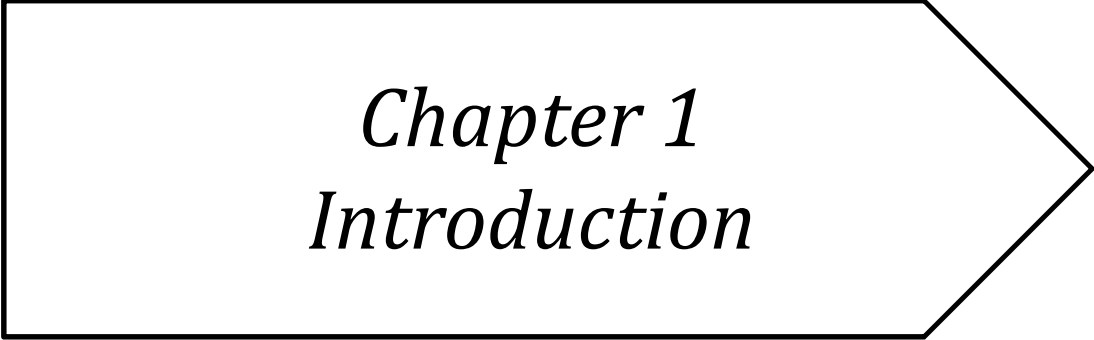
CPE liposomes: Calcium Phosphate Encapsulated Liposomes

NSCLC: Non-small cell lung carcinoma

SCLC: small-cell lung carcinoma

PBS: phosphate buffer solution

PDI: Polydispersity Index



Chapter 1
Introduction

1.1. Introduction

Lung cancer is the most common cancer in the world for several decades and the most common cause of death from cancer with 1.38 million deaths (18.2% of the total) [1]. Lung cancer is currently treated with intravenous administration of chemotherapeutic agents but is nonselective as it cannot differentiate between host cells and cancer cells leading to normal cell toxicity [2]. Further, the diagnostic tools available currently can inadequately detect the tumors and hence render the condition dejected [2]. This provides impetus to pursue the research for effectively treating the lung cancer.

Lung cancer is the most common cancer in developed and developing nations like India [3]. One million of the current 5 million deaths in world, and 2.41 million in developing countries is contributed by India and, in 2020, this figure is projected at 1.5 million [4, 5]. The most common etiological factor for the cause of lung cancer is smoking, which is on the rise in India. In India smoking is prevalent in 29% of adult males, 2.5% of adult females, 11.7% of male collegians and 8.1% among school children and adolescents [5]. Against this backdrop, the proposed project will significantly impact effective treatment of lung cancer.

Lung cancers are classified according to their histological type [6]. This classification has important implications for clinical management and prognosis of the disease. The vast majority of lung cancers are carcinomas—malignancies that arise from epithelial cells. The two most prevalent histological types of lung carcinoma, categorized by the size and appearance of the malignant cells seen by a histopathologist under a microscope: *non-small cell* and *small-cell* lung carcinoma.

The non-small cell lung carcinomas are grouped together because their prognosis and management are similar. There are three main sub-types: squamous cell lung carcinoma, adenocarcinoma, and large cell lung carcinoma. Accounting for 25% of lung cancers, squamous cell lung carcinoma usually starts near a central bronchus. A hollow cavity and associated necrosis are commonly found at the center of the tumor. Well-differentiated squamous cell lung cancers often grow more slowly than other cancer types. Adenocarcinoma accounts for 40% of non-small cell lung cancers. It usually originates in peripheral lung tissue. Most cases of adenocarcinoma are associated with smoking; however, among people who have never smoked ("never-smokers"), adenocarcinoma is the most common form of lung cancer. A subtype of adenocarcinoma, the bronchioloalveolar

carcinoma, is more common in female never-smokers, and may have different responses to treatment.

Small cell lung carcinoma is less common. It was formerly referred to as "oat cell" carcinoma. Most cases arise in the larger airways (primary and secondary bronchi) and grow rapidly, becoming quite large. The small cells contain dense neurosecretory granules (vesicles containing neuroendocrine hormones), which give this tumor an endocrine/paraneoplastic syndrome association. While initially more sensitive to chemotherapy and radiation, it is often metastatic at presentation, and ultimately carries a worse prognosis. Small cell lung cancers have long been dichotomously staged into limited and extensive stage disease. This type of lung cancer is strongly associated with smoking.

If investigations confirm lung cancer, CT scan and often positron emission tomography (PET) are used to determine whether the disease is localized and amenable to surgery or whether it has spread to the point where it cannot be cured surgically [2].

Surgery itself has an operative death rate of about 4.4%, depending on the patient's lung function and other risk factors [7]. Surgery is usually only an option in non-small cell lung carcinoma limited to one lung, up to stage IIIA. This is assessed with medical imaging (computed tomography, positron emission tomography). A sufficient preoperative respiratory reserve must be present to allow adequate lung function after the tissue is removed.

The combination regimen depends on the tumor type [6]. Non-small cell lung carcinoma is often treated with cisplatin or carboplatin, in combination with gemcitabine, paclitaxel, docetaxel, etoposide, or vinorelbine. In small cell lung carcinoma, cisplatin and etoposide are most commonly used. Combinations with carboplatin, gemcitabine, paclitaxel, vinorelbine, topotecan, and irinotecan are also used. In extensive-stage small-cell lung cancer celecoxib may safely be combined with etoposide, this combination showed improve outcomes.

Radiotherapy is often given together with chemotherapy, and may be used with curative intent in patients with non-small cell lung carcinoma who are not eligible for surgery. This form of high intensity radiotherapy is called *radical radiotherapy*. For both non-small cell lung carcinoma and small cell lung carcinoma patients, smaller doses of radiation to the chest may be used for symptom control (palliative radiotherapy).

In recent years, various molecular targeted therapies have been developed for the treatment of advanced lung cancer [2, 6]. Gefitinib (Iressa) is one such drug, which targets the tyrosine

kinase domain of the epidermal growth factor receptor (EGFR), expressed in many cases of non-small cell lung carcinoma. It was not shown to increase survival, although females, Asians, nonsmokers, and those with bronchioloalveolar carcinoma appear to derive the most benefit from gefitinib.

The angiogenesis inhibitor bevacizumab, (in combination with paclitaxel and carboplatin), improves the survival of patients with advanced non-small cell lung carcinoma [2, 6]. Advances in cytotoxic drugs, pharmacogenetics and targeted drug design have showed promise in treatment of lung cancer. A number of targeted agents are at the early stages of clinical research, such as cyclo-oxygenase-2 inhibitors, the apoptosis promoter exisulind, proteasome inhibitors, bexarotene, the epidermal growth factor receptor inhibitor cetuximab, and vaccines.

Currently camptothecin, paclitaxel, carboplatin, cisplatin, docetaxel, topotecan, etoposide and gemcitabine are the most widely used anticancer agents in treatment of lung cancer with their known reported toxicities. The medications are available as injections for systemic use and result in hazardous side effects due to their non-specificity on the dividing cells in the body.

Intracellular transport of different biologically active molecules is one of the key problems in drug delivery in general. Currently the anticancer agents have poor intracellular concentration in the cancer cells.

Lung cancer prevalence in western countries and its treatment has drawn significant attention from NIH and other medical agencies. Prevalence of lung cancer in western countries has drawn attention of National Institute of Health and other medical agencies. As a result number of new drugs, formulations and techniques are being employed in research and clinical trials for therapy of lung cancer. Various drugs like camptothecin, docetaxel, paclitaxel, carboplatin, cisplatin, gemcitabine, etoposide, single or in combination with other drugs are in clinical trials for NSCLC and SCLC. These drugs are available in injection form while direct lung targeting through aerosolization may be a viable alternative. Recently Liposomal Camptothecin formulation has been tested clinically in Phase II clinical trials with successful results.

Recent research on targeted drug nanoparticles, liposomes, micellar formulations encapsulating these anticancer drugs after attaching with cancer cell over expressed receptor specific ligand is gaining high impetus owing to its very high selectivity and sensitivity

towards cancer cells. Use of apoptotic genes like p53, mdm inhibitor genes and the siRNAs is also a topic of current research and yielding good outcomes. However the realities of marketing these targeted products is still a mile away. The recent success of CFTR gene delivery using liposomes has been a great impetus to the nanocarrier based gene delivery and it further improves the chance for viral and non-viral p53 gene delivery entering into the market.

Lung cancer research in India is comparatively in infancy compared to the research in western countries. Currently the focus is on drug encapsulating anticancer nanocarriers. Research is going on at laboratory scale by Misra et al. at M.S.University of baroda on pulmonary delivery and they have developed liposomal gene (p53) and drug (Etoposide and Docetaxel) formulations for their anticancer action in lung cancer and have obtained good results in lung cancer treatment in human lung cell lines (Unpublished data).

In spite of the recent developments in lung cancer research in India there is still a wide gap in research, diagnosis and therapy of lung cancer. The lung cancer targeted drug and gene therapy is still to be well explored and has lot of potential for betterment of lung cancer research and therapy.

RNA interference (RNAi) is the process of mRNA degradation that is induced by double-stranded RNA in a sequence-specific manner [8]. RNAi has been observed in all eukaryotes, from yeast to mammals. The power and utility of RNAi for specifically silencing the expression of any gene for which sequence is available has driven its incredibly rapid adoption as a tool for reverse genetics in eukaryotic systems.

The cell has a specific enzyme (in *Drosophila*; it is called Dicer) that recognizes the double stranded RNA and chops it up into small fragments between 21-25 base pairs in length. These short RNA fragments (called small interfering RNA, or siRNA) bind to the RNA-induced silencing complex (RISC). The RISC is activated when the siRNA unwinds and the activated complex binds to the corresponding mRNA using the antisense RNA. The RISC contains an enzyme to cleave the bound mRNA (called Slicer in *Drosophila*) and therefore cause gene suppression. Once the mRNA has been cleaved, it can no longer be translated into functional protein.

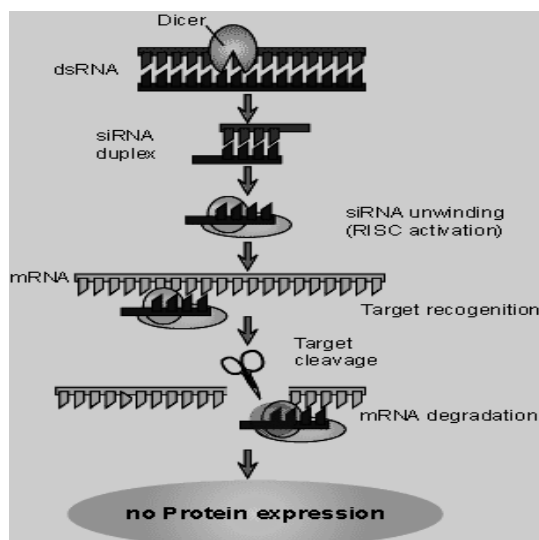


Figure 1.1 RNA Interference

The structure of siRNA is highly specific to prevent erroneous gene silencing. siRNA molecules are 21-23 nucleotide double stranded RNA (dsRNA) duplexes with symmetric 2-3 nucleotide 3' overhangs and 5' phosphate and 3' hydroxyl groups [8].

RNA interference (RNAi) is a conserved cellular mechanism by which a small double stranded RNA (dsRNA) directs the degradation of complementary mRNA and therefore inhibits the expression of a specific gene [8]. Since its discovery, RNAi has become a powerful tool to study gene functions in biological processes.[9-11] The ability to induce RNAi in mammalian cells using synthetic small interfering RNA (siRNA) has stimulated great interest in therapeutic applications of RNAi [12-14]. In numerous studies, siRNAs have shown promise for treating a variety of diseases, including influenza and HIV infection, cancer and genetic defects [15-17]. The double stranded RNA-based molecule, siRNA, has a high potential as biopharmaceutical therapeutics. As RNAi interferes with translation, and not with DNA transcription, siRNA may not interact with chromosomal DNA. This lack of DNA interaction greatly reduces concerns about possible adverse gene alteration that might result from DNA-based gene therapy. The interaction of siRNA with mRNA, not protein, also makes it possible to reduce the production of harmful proteins before synthesis.

A key challenge of RNAi-based therapeutic application is the efficient delivery of siRNA into target cells. Various challenges for siRNA deliveries are described below. siRNA is usually 21 nucleotides in length and highly charged and therefore cannot cross the cytoplasmic membrane by free diffusion. In the circulation and interstitial space, siRNA is vulnerable to degradation by nucleases [18]. Although siRNA can be delivered directly and

locally to the target sites in limited applications [19, 20], a carrier system is required in most applications to protect siRNA from degradation and to facilitate its uptake by target cells [21, 22]. The proposed carrier system contains a key cationic component, such as a cationic lipid, a cationic polymer or a cationic peptide, in order to bind siRNA effectively along with other neutral lipids.

So far, the most successful strategies against cancer have been the destructive ones. At the cellular level, this implies the elimination, as selectively as possible, of the neoplastic cells. However, not all oncogenes and oncosuppressors contribute equally to cancer development [23]. The plasticity of the cell with a network of signal-transducing pathways makes it difficult to pinpoint the key genes whose blockage would irreversibly lead to self-destruction. RNAi technology can help to discover genes essential for viability in cancer cells that can be then used as targets for suicide. Inhibiting overexpressed oncogenes, such as ras or myc, should block pathways that cancer cells depend on. In most cancers, however, it may be necessary to block pathways at several points, or even to target several pathways. Identifying the genes that are altered in the stepwise progression to malignancy has become one of the central goals of cancer research; automation of data generation (robotics) and computer analysis (bioinformatics) have significantly accelerated the process of discovering cancer-linked genes [23]. Once an oncogene that is highly represented in a particular type of cancer (melanoma or glioblastoma, for example) is identified, there is the hope that this will lead to clinically useful targeted therapies.

siRNA is of inherent potency because it exploits the endogenous RNAi pathway, allows specific reduction of disease associated genes, and is applicable to any gene with a complementary sequence [24]. As cancer belongs to the category of genetic diseases, many important genes associated with various cancers have been discovered, their mutations precisely identified, and the pathways through which they act characterized [25]. The genetic nature of cancer provides solid support for the rationale of siRNA-mediated gene therapy. Indeed, a number of siRNAs have been designed to target dominant oncogenes, malfunctionally regulated oncogenes, or viral oncogenes involved in carcinogenesis. Moreover, therapeutic siRNAs have been investigated for silencing target molecules crucial for tumor–host interactions and tumor resistance to chemo- or radiotherapy. The silencing of critical cancer-associated target proteins by siRNAs has resulted in significant antiproliferative and/or apoptotic effects [26].

Table 1.1 Some putative siRNA targets against cancer [23]

Gene–protein target*	Cellular function	Type of cancer tested
B-raf	Serine/threonine kinase	Malignant melanoma
Nox1	Superoxide-generating oxidase	Transformed NRK cells**
FAS/Her2	Fatty acid synthase	Breast-MDA-MB-231
Cyclin E	Cell-cycle control	Hepatocarcinoma
Hec1	Chromosomal segregation	-
Gp210	Nuclear pore assembly	Adenocarcinoma (Hela cells)
c-Kit	Signal transduction	Gastrointestinal
MDR	Multidrug resistance	Adenocarcinoma (Hela cells)
bcl-2	Antiapoptotic	Esophageal adenocarcinoma
livin	Antiapoptotic	Adenocarcinoma
survivin	Antiapoptotic	Adenocarcinoma (Hela cells)
Philadelphia chromosome	-	Chronic myeloid leukemia
Ribonucleotide reductase	Gemcitabine resistance	Hepatic metastasis
Rho C	Cell motility	Metastasis

**Normal rat kidney cells. *Genes are written in italics and lower case letters while proteins begin with a capital letter and are written in roman letters.

In gemcitabine metabolism, where 13 genes are involved, the first step in phosphorylation is catalyzed by dCK (deoxycytosine kinase), which is the rate-limiting step for further phosphorylation to active metabolites, and thus is essential for the activation of gemcitabine. Alternatively, gemcitabine is inactivated by DCTD into its inactive form. RRM1 is the rate-limiting step of DNA synthesis and is inhibited by diphosphorylated gemcitabine (dFdCDP). The RRM1 gene encodes the regulatory subunit of ribonucleotide reductase, an essential enzyme that catalyses the reduction of ribonucleotide di-phosphates to the corresponding deoxyribonucleotides. It is the molecular target of gemcitabine (2', 2'-difluorodeoxycytidine), an antimetabolite with activity in several malignancies including NSCLC [27]. dCK deficiency, increased DCTD, and increased RRM1 activity are the main mechanisms of gemcitabine resistance. Earlier work had suggested that patients with low as compared with high levels of tumoral RRM1 expression had improved survival when treated with

gemcitabine-based therapy [28]. In addition, continuous exposure of lung cancer cell lines to increasing amounts of gemcitabine resulted in increased RRM1 expression. A recent report suggested that gemcitabine resistance, generated in vitro through exposure of two NSCLC cell lines (H358 and H460) to increasing concentrations of the drug, was primarily a function of increased expression of RRM1 [29]. Thus, RRM1 is a major cellular determinant of cytotoxic efficacy of gemcitabine. Therefore, the rate limiting step involving RRM1 was chosen as an siRNA target for improving therapy of lung cancer using gemcitabine.

RGD-targeted nanocarriers may specifically address drugs to angiogenic endothelial cells and/or cancer cells by the binding of the RGD peptide to $\alpha_v\beta_3$ overexpressed by these cells, allowing the “active targeting” of the tumors [30]. RGD-targeted nanocarriers can be internalized via receptor-mediated endocytosis, which is not possible with single peptide constructs or with non-targeted nanocarriers; this is particularly interesting for the intracellular delivery of drugs to cancer cells [31]. RGD-targeted nanocarriers have recently proven advantageous in delivering chemotherapeutics, peptides and proteins, nucleic acids, and irradiation. The rationale behind the design of RGD-targeted nanocarriers is the delivery of various pharmacological agents to the $\alpha_v\beta_3$ -expressing tumor vasculature. The cytotoxic drug destroys the tumor vasculature, resulting in the indirect killing of tumor cells induced by the lack of oxygen and nutrients. The tumor growth might be inhibited by preventing tumors from recruiting new blood vessels. $\alpha_v\beta_3$ integrin is up regulated in angiogenic endothelial cells but also in several tumor cells, leading RGD-targeted nanocarriers to a potential double targeting.

1.2. Objective of the Proposed Work

The objective of the proposed investigation was to enhance the chemosensitization effect of the anticancer agent by pre exposure of lung cancer cells with siRNA encapsulated in a liposomal forms.

1.3. Rationale

To achieve success rate in cure of lung cancer having second highest incidence and mortality rate in India. The current cure chemotherapy for lung cancer has limitation being non-selective and manifests in dose related toxicity.

1.4. Hypothesis

It is hypothesized that the pre exposure to nanoconstructs encapsulating siRNA will enhance the chemosensitization effect of the anticancer drugs.

1.5. Research Design and Method

1. Development and characterization of liposomes encapsulating chemotherapeutic agent.
2. Development of siRNA liposomal formulations using different lipid excipients.
3. *In vitro* characterization of developed formulations by cell line studies and to assess chemosensitization potential.
4. *In vivo* toxicity studies for developed liposomal formulations.

1.6. Expected Results

The scientific literature refers to the enhanced chemosensitization effects of anticancer agents after initial siRNA exposure. The exposure of the tumor cells sensitive to siRNA may show anticancer effect at lower doses of the drug after their exposure to siRNA containing liposomes.

1.7. Work Plan

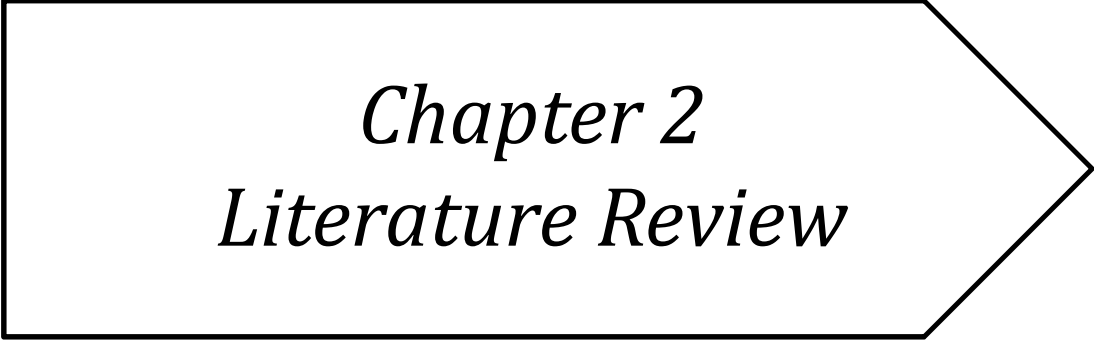
1. Development of liposomes encapsulating siRNA.
2. Characterization of liposomes encapsulating siRNA to find out particle size, zeta potential, % siRNA encapsulated, stability etc.
3. Cell line studies including intracellular uptake studies, cytotoxicity study, transfection study, cell cycle analysis in lung cancer cell lines.
4. Further *in vitro* characterization of developed formulations for serum stability of siRNA in liposomal form, hemolytic potential and electrolyte induced flocculation.
5. *In vivo* toxicity studies to assess safety profile of developed liposomal carriers.
6. Stability studies of developed formulations at storage and accelerated conditions.
7. Statistical Analyses of data.

1.8. References

1. Lung Cancer Incidence and Mortality Worldwide in 2008 [database on the Internet]. GLOBACON 2008 (IARC), Section of Cancer Information. 2008.
2. Lung Cancer (Non-Small Cell) [database on the Internet]. American Cancer Society. 2012. Available from:
<http://www.cancer.org/acs/groups/cid/documents/webcontent/003115-pdf.pdf>.
3. Moore MA, Ariyaratne Y, Badar F, Bhurgri Y, Datta K, Mathew A, et al. Cancer epidemiology in South Asia - past, present and future. *Asian Pac J Cancer Prev*. 2010;11 Suppl 2:49-66.
4. Pai SA. Gutkha banned in Indian states. *Lancet Oncol*. 2002 Sep;3(9):521.
5. Thankappan KR, Thresia CU. Tobacco use & social status in Kerala. *Indian J Med Res*. 2007 Oct;126(4):300-8.
6. Horn L, Pao W, Johnson DH. Neoplasms of the Lung. In: Longo D, Fauci A, Kasper D, Hauser S, Jameson J, Loscalzo J, editors. *Harrison's Principles of Internal Medicine*, 18th Edition. United States: McGraw-Hill; 2011.
7. Tyson JJ. The coordination of cell growth and division — intentional or Incidental? *BioEssays*. 1985;2(2):72-7.
8. Fire A, Xu S, Montgomery MK, Kostas SA, Driver SE, Mello CC. Potent and specific genetic interference by double-stranded RNA in *Caenorhabditis elegans*. *Nature*. 1998 Feb 19;391(6669):806-11.
9. Novina CD, Sharp PA. The RNAi revolution. *Nature*. 2004 Jul 8;430(6996):161-4.
10. Kittler R, Buchholz F. Functional genomic analysis of cell division by endoribonuclease-prepared siRNAs. *Cell cycle*. 2005 Apr;4(4):564-7.
11. Leung RK, Whittaker PA. RNA interference: from gene silencing to gene-specific therapeutics. *Pharmacology & therapeutics*. 2005 Aug;107(2):222-39.
12. Benallaoua M, Francois M, Batteux F, Thelier N, Shyy JY, Fitting C, et al. Pharmacologic induction of heme oxygenase 1 reduces acute inflammatory arthritis in mice. *Arthritis and rheumatism*. 2007 Aug;56(8):2585-94.
13. Kong X, Zhang W, Lockey RF, Auais A, Piedimonte G, Mohapatra SS. Respiratory syncytial virus infection in Fischer 344 rats is attenuated by short interfering RNA against the RSV-NS1 gene. *Genetic vaccines and therapy*. 2007;5:4.

14. Zimmermann TS, Lee AC, Akinc A, Bramlage B, Bumcrot D, Fedoruk MN, et al. RNAi-mediated gene silencing in non-human primates. *Nature*. 2006 May 4;441(7089):111-4.
15. Lau TS, Li Y, Kameoka M, Ng TB, Wan DC. Suppression of HIV replication using RNA interference against HIV-1 integrase. *FEBS letters*. 2007 Jul 10;581(17):3253-9.
16. Thomas M, Ge Q, Lu JJ, Klibanov AM, Chen J. Polycation-mediated delivery of siRNAs for prophylaxis and treatment of influenza virus infection. *Expert opinion on biological therapy*. 2005 Apr;5(4):495-505.
17. Yuan Z, Wong S, Borrelli A, Chung MA. Down-regulation of MUC1 in cancer cells inhibits cell migration by promoting E-cadherin/catenin complex formation. *Biochemical and biophysical research communications*. 2007 Oct 26;362(3):740-6.
18. Larson SD, Jackson LN, Chen LA, Rychahou PG, Evers BM. Effectiveness of siRNA uptake in target tissues by various delivery methods. *Surgery*. 2007 Aug;142(2):262-9.
19. Fountaine TM, Wood MJ, Wade-Martins R. Delivering RNA interference to the mammalian brain. *Current gene therapy*. 2005 Aug;5(4):399-410.
20. Kumar P, Wu H, McBride JL, Jung KE, Kim MH, Davidson BL, et al. Transvascular delivery of small interfering RNA to the central nervous system. *Nature*. 2007 Jul 5;448(7149):39-43.
21. Veldhoen S, Laufer SD, Trampe A, Restle T. Cellular delivery of small interfering RNA by a non-covalently attached cell-penetrating peptide: quantitative analysis of uptake and biological effect. *Nucleic acids research*. 2006;34(22):6561-73.
22. Yadava P, Roura D, Hughes JA. Evaluation of two cationic delivery systems for siRNA. *Oligonucleotides*. 2007 Summer;17(2):213-22.
23. Izquierdo M. Short interfering RNAs as a tool for cancer gene therapy. *Cancer Gene Ther*. 2004 11/19/online;12(3):217-27.
24. Leung RK, Whittaker PA. RNA interference: from gene silencing to gene-specific therapeutics. *Pharmacology & therapeutics*. 2005 Aug;107(2):222-39.
25. Vogelstein B, Kinzler KW. Cancer genes and the pathways they control. *Nat Med*. 2004 Aug;10(8):789-99.
26. Pai SI, Lin YY, Macaes B, Meneshian A, Hung CF, Wu TC. Prospects of RNA interference therapy for cancer. *Gene Ther*. 2006 Mar;13(6):464-77.
27. Johnson DH. Gemcitabine for the treatment of non-small-cell lung cancer. *Oncology (Williston Park)*. 2001 Mar;15(3 Suppl 6):33-9.

28. Rosell R, Danenberg KD, Alberola V, Bepler G, Sanchez JJ, Camps C, et al. Ribonucleotide reductase messenger RNA expression and survival in gemcitabine/cisplatin-treated advanced non-small cell lung cancer patients. *Clin Cancer Res.* 2004 Feb 15;10(4):1318-25.
29. Davidson JD, Ma L, Flagella M, Geeganage S, Gelbert LM, Slapak CA. An increase in the expression of ribonucleotide reductase large subunit 1 is associated with gemcitabine resistance in non-small cell lung cancer cell lines. *Cancer Res.* 2004 Jun 1;64(11):3761-6.
30. Byrne JD, Betancourt T, Brannon-Peppas L. Active targeting schemes for nanoparticle systems in cancer therapeutics. *Adv Drug Deliv Rev.* 2008 Dec 14;60(15):1615-26.
31. Folkman J. Tumor angiogenesis: therapeutic implications. *N Engl J Med.* 1971 Nov 18;285(21):1182-6.



Chapter 2
Literature Review

2.1. Lung Cancer

The lungs are located in the chest. They help you breathe. When you breathe, air goes through your nose, down your windpipe (trachea), and into the lungs, where it spreads through tubes called bronchi. Most lung cancer begins in the cells that line these tubes. Lung cancer, the most common cause of cancer-related death in men and women, is responsible for 1.3 million deaths worldwide annually, as of 2004 [1].

There are two main types of lung cancer:

- Non-small cell lung cancer (NSCLC) is the most common type of lung cancer.
- Small cell lung cancer makes up about 20% of all lung cancer cases.

If the lung cancer is made up of both types, it is called mixed small cell/large cell cancer. If the cancer started somewhere else in the body and spread to the lungs, it is called metastatic cancer to the lung.

2.1.1. Causes of the Lung Cancer

The most common cause of lung cancer is long-term exposure to tobacco smoke [1-3]. The occurrence of lung cancer in nonsmokers, who account for as many as 15% of cases, is often attributed to a combination of genetic factors, radon gas [4], asbestos [5], and air pollution including secondhand smoke [7].

2.1.2. Symptoms that Suggest Lung Cancer Include [1, 2, 4]

- dyspnea (shortness of breath)
- hemoptysis (coughing up blood)
- chronic coughing or change in regular coughing pattern
- wheezing
- chest pain or pain in the abdomen
- cachexia (weight loss), fatigue, and loss of appetite
- dysphonia (hoarse voice)
- clubbing of the fingernails (uncommon)

- dysphagia (difficulty swallowing).

2.1.3. Pathogenesis

Similar to many other cancers, lung cancer is initiated by activation of oncogenes or inactivation of tumor suppressor genes. Oncogenes are genes that are believed to make people more susceptible to cancer. Proto-oncogenes are believed to turn into oncogenes when exposed to particular carcinogens. Mutations in the K-ras proto-oncogene are responsible for 10–30% of lung adenocarcinomas. The epidermal growth factor receptor (EGFR) regulates cell proliferation, apoptosis, angiogenesis, and tumor invasion. Mutations and amplification of EGFR are common in non-small-cell lung cancer and provide the basis for treatment with EGFR-inhibitors. Her2/neu is affected less frequently. Chromosomal damage can lead to loss of heterozygosity. This can cause inactivation of tumor suppressor genes. Damage to chromosomes 3p, 5q, 13q, and 17p are particularly common in small-cell lung carcinoma. The p53 tumor suppressor gene, located on chromosome 17p, is affected in 60-75% of cases. Other genes that are often mutated or amplified are c-MET, NKX2-1, LKB1, PIK3CA, and BRAF.

Several genetic polymorphisms are associated with lung cancer. These include polymorphisms in genes coding for interleukin-1, cytochrome P450, apoptosis promoters such as caspase-8, and DNA repair molecules such as XRCC1. People with these polymorphisms are more likely to develop lung cancer after exposure to carcinogens. A recent study suggested that the MDM2 309G allele is a low-penetrant risk factor for developing lung cancer in Asians.

2.1.4. Prevention and Treatment

Eliminating tobacco smoking is a primary goal in the prevention of lung cancer, and smoking cessation is an important preventive tool in this process.

- **Surgery:** Positron emission tomography (PET) is used to determine whether the disease is localized and amenable to surgery or whether it has spread to the point where it cannot be cured surgically. Video-assisted thoracoscopic surgery and VATS lobectomy have allowed

for minimally invasive approaches to lung cancer surgery that may have the advantages of quicker recovery,

- **Radiotherapy:** Radiotherapy is often given together with chemotherapy, and may be used with curative intent in patients with non-small-cell lung carcinoma who are not eligible for surgery. This form of high intensity radiotherapy is called radical radiotherapy.^[11] A refinement of this technique is continuous hyperfractionated accelerated radiotherapy (CHART), in which a high dose of radiotherapy is given in a short time period. For small-cell lung carcinoma cases that are potentially curable, chest radiation is often recommended in addition to chemotherapy. The use of adjuvant thoracic radiotherapy following curative intent surgery for non-small-cell lung carcinoma is not well established and is controversial. Benefits, if any, may only be limited to those in whom the tumor has spread to the mediastinal lymph nodes. For both non-small-cell lung carcinoma and small-cell lung carcinoma patients, smaller doses of radiation to the chest may be used for symptom control (palliative radiotherapy). Brachytherapy (localized radiotherapy) may be given directly inside the airway when cancer affects a short section of bronchus. It is used when inoperable lung cancer causes blockage of a large airway. Patients with limited-stage small-cell lung carcinoma are usually given prophylactic cranial irradiation (PCI). This is a type of radiotherapy to the brain, used to reduce the risk of metastasis. More recently, PCI has also been shown to be beneficial in those with extensive small-cell lung cancer. In patients whose cancer has improved following a course of chemotherapy, PCI has been shown to reduce the cumulative risk of brain metastases within one year from 40.4% to 14.6%. Recent improvements in targeting and imaging have led to the development of extracranial stereotactic radiation in the treatment of early-stage lung cancer. In this form of radiation therapy, very high doses are delivered in a small number of sessions using stereotactic targeting techniques. Its use is primarily in patients who are not surgical candidates due to medical comorbidities.

- **Chemotherapy:** The chemotherapy regimen depends on the tumor type.

- **Small-cell lung carcinoma:** Even if relatively early stage, small-cell lung carcinoma is treated primarily with chemotherapy and radiation. In small-cell lung carcinoma, cisplatin and etoposide are most commonly used. Combinations with carboplatin, gemcitabine, paclitaxel, vinorelbine, topotecan, and irinotecan are also used [1]. Celecoxib showed a potential signal of response in a small study [6].

- **Non-small-cell lung carcinoma:** Primary chemotherapy is also given in advanced and metastatic non-small-cell lung carcinoma. Testing for the molecular genetic subtype of non-small-cell lung cancer may be of assistance in selecting the most appropriate initial therapy. For example, mutation of the epidermal growth factor receptor gene may predict whether initial treatment with a specific inhibitor or with chemotherapy is more advantageous [7]. Advanced non-small-cell lung carcinoma is often treated with cisplatin or carboplatin, in combination with gemcitabine, paclitaxel, docetaxel, etoposide, or vinorelbine. Bevacizumab improves results in non-squamous cancers treated with paclitaxel and carboplatin in patients less than 70 years old who have reasonable general performance status. Pemetrexed has been studied extensively in non-small-cell lung cancer, with numerous studies since 1995. For adenocarcinoma and large-cell lung cancer, cisplatin with pemetrexed was more beneficial than cisplatin and gemcitabine; squamous cancer had the opposite results. As a consequence, subtyping of non-small lung cancer histology has become more important. Bronchoalveolar carcinoma is a subtype of non-small-cell lung carcinoma that may respond to gefitinib and erlotinib [8].

- **Maintenance therapy:** In advanced non-small-cell lung cancer there are several approaches for continuing treatment after an initial response to therapy. Switch maintenance changes to different medications than the initial therapy and can use pemetrexed, erlotinib, and docetaxel, although pemetrexed is only used in non-squamous NSCLC [9].

- **Adjuvant chemotherapy:** Adjuvant chemotherapy refers to the use of chemotherapy after apparently curative surgery to improve the outcome. In non-small-cell lung cancer, samples are taken during surgery of nearby lymph nodes. If these samples contain cancer, the patient has stage II or III disease. In this situation, adjuvant chemotherapy may improve survival by

up to 15%. Standard practice has often been to offer platinum-based chemotherapy (including either cisplatin or carboplatin). However, the benefit of platinum-based adjuvant chemotherapy was confined to patients who had tumors with low ERCC1 (excision repair cross-complementing 1) activity. Adjuvant chemotherapy for patients with stage IB cancer is controversial, as clinical trials have not clearly demonstrated a survival benefit [10]. Trials of preoperative chemotherapy (neoadjuvant chemotherapy) in resectable non-small-cell lung carcinoma have been inconclusive.

2.2. Drug Profile

Gemcitabine Hydrochloride: Gemcitabine Hydrochloride is a cytidine analogue. Gemcitabine (2,2 difluorodeoxycytidine; dFdC), a difluoro analog of deoxycytidine, has become an important drug for patients with metastatic pancreatic cancer, non-small cell lung cancer, ovarian, bladder, esophageal, and head and neck cancer .

2.2.1. Mechanism of Action

Gemcitabine enters cells via active nucleoside transporters [11]. Intracellularly, deoxycytidine kinase phosphorylates gemcitabine to produce difluorodeoxycytidine monophosphate (dFdCMP), from which point it is converted to difluorodeoxycytidine di- and triphosphate (dFdCDP and dFdCTP). While its anabolism and effects on DNA in general mimic those of cytarabine, there are differences in kinetics of inhibition, additional sites of action, effects of incorporation into DNA, and spectrum of clinical activity. Unlike cytarabine, the cytotoxicity of gemcitabine is not confined to the S phase of the cell cycle, and the drug is equally effective against confluent cells and cells in logarithmic growth phase. The cytotoxic activity may be a result of several actions on DNA synthesis: dFdCTP competes with dCTP as a weak inhibitor of DNA polymerase; dFdCDP is a potent inhibitor of ribonucleotide reductase, resulting in depletion of deoxyribonucleotide pools necessary for DNA synthesis; and dFdCTP is incorporated into DNA and after the incorporation of one more additional nucleotide leads to DNA strand termination. This "extra" nucleotide may be important in hiding the dFdCTP from DNA repair enzymes, as the incorporated dFdCMP appears to be resistant to repair. The ability of cells to incorporate dFdCTP into DNA is critical for gemcitabine-induced apoptosis [12].

2.2.3. Therapeutic Uses

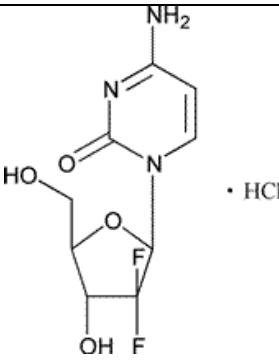
The standard dosing schedule for gemcitabine (GEMZAR) is a 30-minute intravenous infusion of 1 to 1.2 g/m² on days 1, 8, and 15 of each 28-day cycle [13].

2.2.4. Clinical Toxicities [13]

The principal toxicity of gemcitabine is myelosuppression. In general, the longer-duration infusions lead to greater myelosuppression. Nonhematologic toxicities including a flu-like syndrome, asthenia, and mild elevation in liver transaminases may occur in 40% or more of patients. Although severe nonhematologic toxicities are rare, interstitial pneumonitis may occur and is responsive to steroids. Rarely, patients on gemcitabine treatment for many months may develop a slowly progressive hemolytic uremic syndrome, necessitating drug discontinuation. Gemcitabine is a very potent radiosensitizer [14] and should not be used with radiotherapy except in closely monitored clinical trials.

Table 1 Drug Profile

Name	Gemcitabine hydrochloride
Category	Anticancer (anti metabolite)
Chemical name(IUPAC)	4-amino-1-[(2R,4R,5R)-3,3-difluoro-4-hydroxy-5-(hydroxymethyl)oxolan-2-yl]pyrimidin-2-one
Proprietary name	DDFC , DFDC , GEO , Gemcin , Gemcitabina (INN – Spanish) , Gemcitabine HCl , Gemcitabinum (INN – Latin) , Gemtro , Gemzar
Molecular formula	$C_9H_{11}F_2N_2O_4 \cdot HCl$
Molecular weight	299.7 g / mole
Physicochemical properties	
Physical state and appearance	White to off white solid powder
Melting point	168.64 c
Log P	- 1.4
pka value	3.6

Solubility	Freely soluble in water , sparingly soluble in methanol , particularly insoluble in organic solvent
Half life	42 to 49 minute
Dose	1000 to 1200 mg / m ²
Structure	

2.2.5. Problem Associated with Gemcitabine Hydrochloride

- Major limit for the use of gemcitabine is represented by its rapid metabolic inactivation (deamination operated by deoxycytidine deaminase) responsible for its short half-life together with its low but still important systemic toxicity
- The half-life and volume of distribution depends on age, gender and duration for infusion.
- the development of multidrug resistance in cells exposed to gemcitabine can limit its effectiveness. Gemcitabine hydrochloride is efflux by the Pgp (P glycol protein) and resistance is observed by MDR gene (multi drug resistance gene).
- Dose of Gemcitabine Hydrochloride 1000 to 1200 mg/m².

2.2.6. Chemoresistance with Gemcitabine Hydrochloride :

dCK is cellular enzyme required to metabolize Gemcitabine Hydrochloride to active metabolite. Decreased dCK (deoxycytidine kinase) expression is associated with acquired resistance to gemcitabine in NSCLC cells.

Several members of the ATP-binding cassette (ABC) transporter superfamily, such as multidrug resistance protein 1 (ABCC1), confer drug resistance to drug-sensitive cells by effluxing

anticancer or antiviral agents or their metabolites from cells when expressed at high levels [15]. Recently, ABCC5, which lacks a transmembrane domain that is present in another family member, ABCC1, was shown to mediate the ATP-dependent transport of several anticancer agents and antiviral nucleosides and confer resistance to gemcitabine.

2.2.7. Chemosensitization

Despite a reasonable response rate after initial chemotherapy in patients with metastatic bladder cancer, 60–70% of responding patients relapse within the first year, with a median survival of 12–14 months drug-resistant phenotype during treatment. Experimental models have helped clarify mechanisms associated with acquisition of chemotherapeutic agents in cancer cells. However, no study has focused on the resistant phenotype of bladder cancer to gemcitabine; therefore, the application of gemcitabine-resistant bladder cancer cells to preclinical experimental model may uncover novel findings for elucidating molecular mechanism of drug-resistance resulting in the development of novel strategies for advanced bladder cancer. This limited efficacy may be due to de novo drug resistance and/or the development of cellular mechanisms of resistance. In gemcitabine metabolism, where 13 genes are involved, the first step in phosphorylation is catalyzed by dCK, which is the rate-limiting step for further phosphorylation to active metabolites, and thus is essential for the activation of gemcitabine. Alternatively, gemcitabine is inactivated by DCTD into its inactive form. RRM1 is the rate-limiting step of DNA synthesis and is inhibited by diphosphorylated gemcitabine (dFdCDP). The RRM1 gene encodes the regulatory subunit of ribonucleotide reductase, an essential enzyme that catalyses the reduction of ribonucleotide di-phosphates to the corresponding deoxyribonucleotides. It is the molecular target of gemcitabine (2', 2'-difluorodeoxycytidine), an antimetabolite with activity in several malignancies including NSCLC [16]. dCK deficiency, increased DCTD, and increased RRM1 activity are the main mechanisms of gemcitabine resistance. Earlier work had suggested that patients with low as compared with high levels of tumoral RRM1 expression had improved survival when treated with gemcitabine-based therapy [17]. In addition, continuous exposure of lung cancer cell lines to increasing amounts of gemcitabine resulted in increased RRM1 expression. A recent report suggested that gemcitabine resistance, generated in vitro through exposure of two NSCLC cell lines (H358 and H460) to

increasing concentrations of the drug, was primarily a function of increased expression of RRM1 [18]. These data were confirmed in a subcutaneous murine colon tumor model (Colon 26) where gemcitabine resistance had been generated through prolonged gemcitabine exposure and serial transplantation [18]. However, induction of drug resistance through continuous exposure results in alterations in multiple genes as demonstrated by these authors. Thus, these results in genetically modified lung cancer cell lines demonstrate directly that RRM1 is a major cellular determinant of cytotoxic efficacy of gemcitabine. In addition data demonstrate that RRM1 is a minor determinant of platinum efficacy.

2.3. Liposomes

Liposomes are synthetic, single or multi-compartmental vesicles having lipid membranes enclosing aqueous chambers. Liposomes are vesicles composed of phospholipids bilayers surrounding aqueous compartments as described by Bangham et al [19]. They consist of one or more bilayers. The driving force for bilayer assembly is the amphiphilic nature of phospholipid molecules. Liposomes are composed of phospholipid/s or lipids or and glycerides with or without sterols. Phospholipid typically consists of a hydrophilic head group attached to two hydrophobic fatty acid chains. When suspended in an excess of aqueous solution, phospholipid molecules orient themselves in ordered bilayers so that the polar heads are hydrated and hydrophobic tails are excluded from the aqueous environment. Although suspended phospholipids may also assume other geometric(s) such as micelles and tubular aggregates in hexagonal phases, this can be controlled by several factors including lipid composition and method of preparation. Entrapment of compounds is highly influenced by their physiochemical properties. Generally hydrophobic molecules are incorporated into the lipid bilayers whereas hydrophilic compounds are entrapped in the internal aqueous volume [20].

2.3.1. Composition of Liposomes

2.3.1.1. Phospholipids

Glycerol containing phospholipids are by far, the most commonly used component of liposome formulations and represent more than 50% of the weight of lipid present in biological membranes [21]. As examples of potentially useful lipids can be mentioned natural lipids such as egg lecithin, soya lecithin, and synthetic lipids such as phosphoglycerolipids, sphingolipids, and digalactosylglycerolipids. Amongst natural lipids may be mentioned sphingolipids such as sphingomyelin, ceramide and cerebroside; galactosylglycerolipids such as digalactosyldiacylglycerol; phosphoglycerolipids such as egg-yolk phosphatidylcholine and soya-bean phosphatidylcholine ; and lecithins such as egg-yolk lecithin and soya-bean lecithin. Amongst synthetic lipids may be mentioned dimyristoyl phosphatidylcholine, dipalmitoyl phosphatidylcholine (DPPC), distearoyl phosphatidylcholine, dilauryl phosphatidylcholine, 1-myristoyl-2-palmitoyl phosphatidylcholine, 1-palmitoyl-2-myristoyl phosphatidylcholine, dioleoyl phosphatidylcholine, hydrogenated soyaphosphatidylcholines (HSPC), and the like.

Some naturally occurring phospholipids include phosphatidylcholine (PC), phosphatidylinositol (PI) and phosphatidylglycerol (PG) while dipalmitoyl phosphatidylcholine (DPPC), dipalmitoyl phosphatidylserine (DPPS), dipalmitoyl phosphatidylethanolamine (DPPE), dipalmitoyl phosphatidic acid (DPPA), dipalmitoyl phosphatidylglycerol (DPPG), dioleoyl phosphatidylcholine (DOPC) and dioleoyl phosphatidylglycerol (DOPG) are some synthetic phospholipids.

2.3.1.2. Sterols

Sterols such as cholesterol, ergosterol, lanosterol, or its derivatives are often included as components of liposomal membrane. Cholesterol has been called the “mortar” of bilayer because by virtue of its molecular shape and solubility properties, it fills in empty spaces among the phospholipid molecules, anchoring them more strongly into the structure. Its inclusion in liposomal membranes has 3 effects (i) increasing the fluidity or microviscosity of the bilayer (ii) reducing the permeability of the membrane to water-soluble molecules and (iii) solubilizing the membrane in the presence of biological fluids such as plasma.

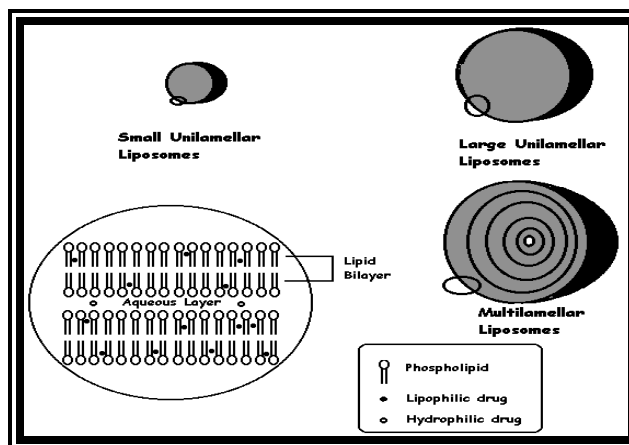


Figure 2.2 The structure of multilamellar vesicles showing the organization of phospholipid bilayers and the encapsulation of lipophilic and hydrophilic compounds.

2.3.1.3. Other Non-Structural Components

Charge inducer materials which provides a negative charge, for example phosphatidic acid, dicetyl phosphate or beef brain ganglioside etc, or one which provides a positive charge for example stearylamine acetate or cetylpyridinium chloride etc. have been incorporated into liposomes so as to impart either a negative or a positive surface charge to these structures. Many

single chain surfactants of number of single and double chain lipids having fluorocarbon chains and also compounds like quaternary ammonium salts and dialkyl phosphates can also be used to form liposomes [22].

2.3.2. Types of Liposomes

Different types of liposomes can be prepared and are classified by the size and structure. Different types of liposomes are small unilamellar vesicles (SUV), large unilamellar vesicles (LUV), oligolamellar vesicles (OLV), and multi-lamellar vesicles (MLVs). MLVs consist of numerous concentric bilayers separated by aqueous spaces and range up to 15 μm in diameter. Vesicles consisting of a single bilayer encompassing a central aqueous compartment are referred to as small unilamellar vesicles (SUVs), which range upto 100 nm in diameter and large unilamellar vesicles (LUVs) ranging from 100 to 500 nm in diameter (**Figure 2.2**).

2.3.3. Methods of Preparation of Liposomes

Numerous procedures have been developed to prepare liposomes. There are at least fourteen major published methods for making liposomes. The seven, most commonly employed methods are, Lipid film hydration method [19], Ethanol injection method [23] Ether infusion method [24], Detergent dialysis method [25], French press method [26], Rehydration-dehydration techniques [27] and Reverse phase evaporation method [28].

2.3.4. Characterization of Liposomes

The behavior of liposomes in both physical and biological systems is determined to a large extent by factors such as physical size, chemical composition, quantity of entrapped solutes etc. Hence, liposomes are characterized with respect to the following parameters:

2.3.4.1. Size and Size Distribution

There are number of methods reported in the literature to determine size and its distribution of the vesicles [29, 30]. The most commonly used ones are light microscopy preferably using electron microscope, laser light scattering or cryoelectron microscopy.

2.3.4.2. Lamellarity

The lamellarity, the average number of bilayers present in liposomes, can be determined either by ^{31}P -NMR spectroscopy or freeze fracture electron microscopy.

2.3.4.3. Determination of Percentage Capture

The quantity of material entrapped inside liposomes can be determined more commonly by mini-column centrifugation method, protamine aggregation method, dialysis technique or by gel chromatography.

2.3.5. Stability of Liposomes

A prerequisite for the successful introduction of liposomes in therapy is the long-term stability of the formulation. The stability of drug-laden liposome dispersions preferably should meet the standards of conventional pharmaceutical product. A 1-year shelf life is considered to be an absolute minimum. Both chemical and physical determines the shelf life of a product.

In the literature, on the physical stability of liposomes, attention has been focused on two processes affecting the quality and therefore acceptability of liposomes [31]. First, the encapsulated drug can leak from the vesicles into the extra-liposomal compartment (reduced retention). Second, liposomes can aggregate and/or fuse, forming larger particles. Both these processes change the disposition of the drug in vivo and thereby presumably affect the therapeutic index of the drug involved. Besides, other physical parameters may also change during storage. For instance, hydrolysis of phospholipids causes the formation of fatty acids and lysophospholipids. These compounds considerably affect the physical properties of the bilayer [31]. Apart from this, chemical degradation process may influence the safety of liposomes. Solid experimental data on the safety of partially hydrolyzed liposomes are not yet available; lysophospholipids alone have been reported to be toxic.

Several approaches have been developed to ensure the physical stability of liposomes on storage.

1. For storage of aqueous dispersions, the lipid composition of the bilayer and the aqueous solvent can be adjusted to induce optimum stability by reducing permeability/leakage. Phospholipids

with long and saturated alkyl chains (distearoyl phosphatidyl choline and dipalmitoyl phosphatidyl choline or saturated hydrogenated soyabean or egg phosphatidyl choline) provide rigid bilayers with low permeabilities for small, non-bilayer-interacting compounds [31]. The incorporation of the bovine serum albumin in the liposomal membrane and treatment with glutaraldehyde has been reported to prevent leakage of the entrapped contents [32]. Crommelin has reported the effect of bilayer composition on permeability of carboxyfluorescein [33].

To formulate drugs in liposomes it is necessary to reduce the leakage of an entrapped drug. The rate of leakage of a molecule from liposomes is governed by the physio-chemical properties of a molecule. Liposomes are freely permeable to water, but cations are released at a slower rate than anions [19], whereas aqueous hydrogen bonding may determine the leakage rate of non-electrolytes [34].

Phospholipids in the liquid-crystalline state are more permeable to entrapped material than when they are in the gel state. Thus, loss of entrapped material is temperature dependent, generally being greatest around the phospholipid phase transition temperature (T_c) [35]. The stability of liposomes in terms of retention of dideoxyinosine triphosphate (ddITP) was measured by Betageri [36] at 4°, 25°, and 37°C. He observed that retention of ddITP in liposomes was maximum when stored at 4°C followed by 25°C and 37°C.

Another way to control stability is to incorporate cholesterol into the lipid structure, since it is known to reduce leakage of various solutes through the lipid bilayer when the membrane is in a fluid-like state [36, 37], or by polymerization of phospholipid molecules [38, 39]. The introduction of cholesterol in liposomes of 5,6-carboxyfluorescein (CF) has been reported to reduce the rate of leakage during storage [40]. He also observed that CF retention was greater in liposomes stored at 4°C in the presence of O₂ than those of room temperature, although liposomes stored at room temperature but in O₂-free atmosphere were more stable than those stored at room temperature in the presence of O₂.

2. Freezing the liposome dispersion is also an approach to achieve prolonged liposome shelf-life [41]. Lyophilization and rehydration, which include a freezing and thawing cycle, represent another method, used by many laboratories for better stability of liposomal formulations [42].

Several groups have published reports on freezing, drying [43] or freeze-drying of liposomes. Cryoprotectants play an important role in the physical stabilization of liposomes during freezing, drying or freeze-drying. The 100% CF retention could be found using cryoprotectant after a full freezing-thawing cycle [31]. Studies made on the stability of liposomes with time, when they were either freeze-dried or in solution have been reported [33].

3. In addition, two other techniques can solve the problem of drug leakage during storage, proliposomes and remote loading [31] that permit liposome dispersion preparation in situ. Several reports have been published in this context. Chemical analysis mainly concerns hydrolysis of the ester bonds in phospholipids and oxidation of their unsaturated acyl chains if present. Hydrolysis of phospholipid to free fatty acid and lysophospholipids can disturb the phospholipid bilayer structure and may disrupt it, leading to leakage of encapsulated products. Oxidation of unsaturated phospholipids and cholesterol may be initiated by the action of light and heavy metals [44]. According to Hernandez-caselles [40], the presence of A-tocopherol decreased the breakdown of phosphatidyl choline to lysophosphatidyl choline and also reduced the level of peroxidation. Although the mechanism of the action of α -tocopherol is not clear, it is suggested that this may happen through specific binding to the phospholipid molecule [45]. α -tocopherol acetate was found to be much less effective than α -tocopherol in preventing lipid peroxidation [46]. Further information about chemical stability can be found in reviews of hydrolytic and oxidation reactions in phospholipids [31].

2.3.6. Liposomes as Drug Delivery Systems

In the recent past, controlled release concept and technology have received increasing attention in the face of growing awareness to toxicity and ineffectiveness of drugs when administered or applied by conventional methods. Liposomes as drug delivery systems are among research topics that are being vigorously investigated in both academic and industrial laboratories, with different outlooks and common goals and end products. The scientific literature is rich with comprehensive review of liposomes as drug delivery systems [47, 48].

Over the last twenty years, the liposome has changed its status from being a novel plaything for the laboratory worker to a powerful tool for an industrialist with the gap between the ideal

desired characteristics of liposomes and what is technically feasible becoming narrower all the time. Vastly improved technology in terms of drug capture, vesicle stability on storage, scale-up production and the design of formulations for special tasks has facilitated the application of a wide range of drugs in the treatment and prevention of diseases in experimental animals and clinically.

Liposomes may prove to be efficient carrier for targeting the drug to the site of action because of the following properties: Amphiphilic nature, flexibility in structural characteristics, localized drug effect, controllability of drug release rate, stability in vivo, direct cell liposome interaction, sterilizability, ability to protect drug and body from each other, non-toxicity, non-immunogenicity, biocompatibility and biodegradability and accommodation of molecules with wide range of solubility and molecular weight. At the same time, there are certain problems associated with liposome as drug delivery such as difficulty in procuring pure phospholipids, difficulty in scale-up, poor stability over a long shelf-life, expensive, batch to batch variation in performance, low drug loading, difficulty in avoiding the reticulo-endothelial system and possibility of unwanted vascular obstruction caused by large liposomes [49]. However, research into the use of liposomes in drug delivery has led to vastly improved technology in terms of drug capture, vesicle stability, storage, scaled up production and the design of formulations for specialized tasks. **Table 2.2** shows the liposome application according to their mode of action.

Due to their high degree of biocompatibility, liposomes were initially considered as delivery systems for intravenous administration. The first parenterally applied formulation Ambisome (Vestar Inc., San Dimas, CA), a liposomal amphotericin formulation for the treatment of disseminated fungal infections that frequently occur in immunosuppressed patients, was launched in Ireland in 1990 that showed both high therapeutic activity and reduced toxicity as compared to the original product [50]. More recently in 1995, a sterically stabilized liposomal formulation containing the anticancer drug, doxorubicin has been launched in United States [51].

It has since become apparent that liposomes can also serve as an effective tool for other delivery systems that include oral [52], ophthalmic [53], aerosol [54], dermal/transdermal [55, 56] applications, as immunological adjuvants [57, 58], as carriers of antigens [57, 58], leishmaniasis,

lysosomal storage diseases, cell biological application [59] etc. The recent research is concentrated on the use of liposomes to deliver hemoglobin and act as red blood cell substitutes. The scientists are also engaged in designing of liposomal prodrug using principle of specific enzyme cleavage and facilitated spontaneous hydrolysis. Another field of liposomal research in producing sterically stabilized liposomes for prolonged circulation in blood stream. Liposomes are currently being studied as drug carriers for a variety of drugs that include recombinant proteins [60], gene transfer and immuno diagnostic applications [61]. Of these, non-invasive route of administration continuously demands significant efforts in designing the liposomes that will no doubt continue to contribute significantly to more efficient use of "old drugs" with better and established therapeutic index vis-à-vis minimum side effects.

Table 2.2 Major Modes of Liposomal Action and Related Applications

Mode of action	Application
Intracellular uptake (lysosomes, endosomes/cytoplasm)	Microbial disease, Metal storage disease, Gene manipulation, uptake by some tumour, cells, macrophage activation to a tumoricidal/microcidal state, efficient antigen presentation by antigen presenting cells (vaccines).
Slow release of drugs near the target area	Tumors near fixed macrophages.
Avoidance of tissue, sensitive to drugs	Cardio toxicity of doxorubicin
Circulating reservoirs	Blood surrogates
Facilitation of drug uptake by certain routes	Drug delivery to skin, lungs, eyes, mucosal tissues.

2.4. Formulation Optimization

An experimental approach to Design of Experiment (DoE) optimization of drug delivery systems (DDS) comprises several phases [62-65]. Broadly, these phases can be sequentially summed up in seven salient steps. **Figure 2.3** delineates these steps pictographically.

The optimization study begins with **Step I**, where an endeavor is made to ascertain the initial drug delivery objective(s) in an explicit manner. Various main response parameters, which closely and pragmatically epitomize the objective(s), are chosen for the purpose.

• In **Step II**, the experimenter has several potential independent product and/or process variables to choose from. By executing a set of suitable screening techniques and designs, the formulator selects the “vital few” influential factors among the possible “so many” input variables. Following selection of these factors, a factor influence study is carried out to quantitatively estimate the main effects and interactions. Before going to the more detailed study, experimental studies are undertaken to define the broad range of factor levels as well.

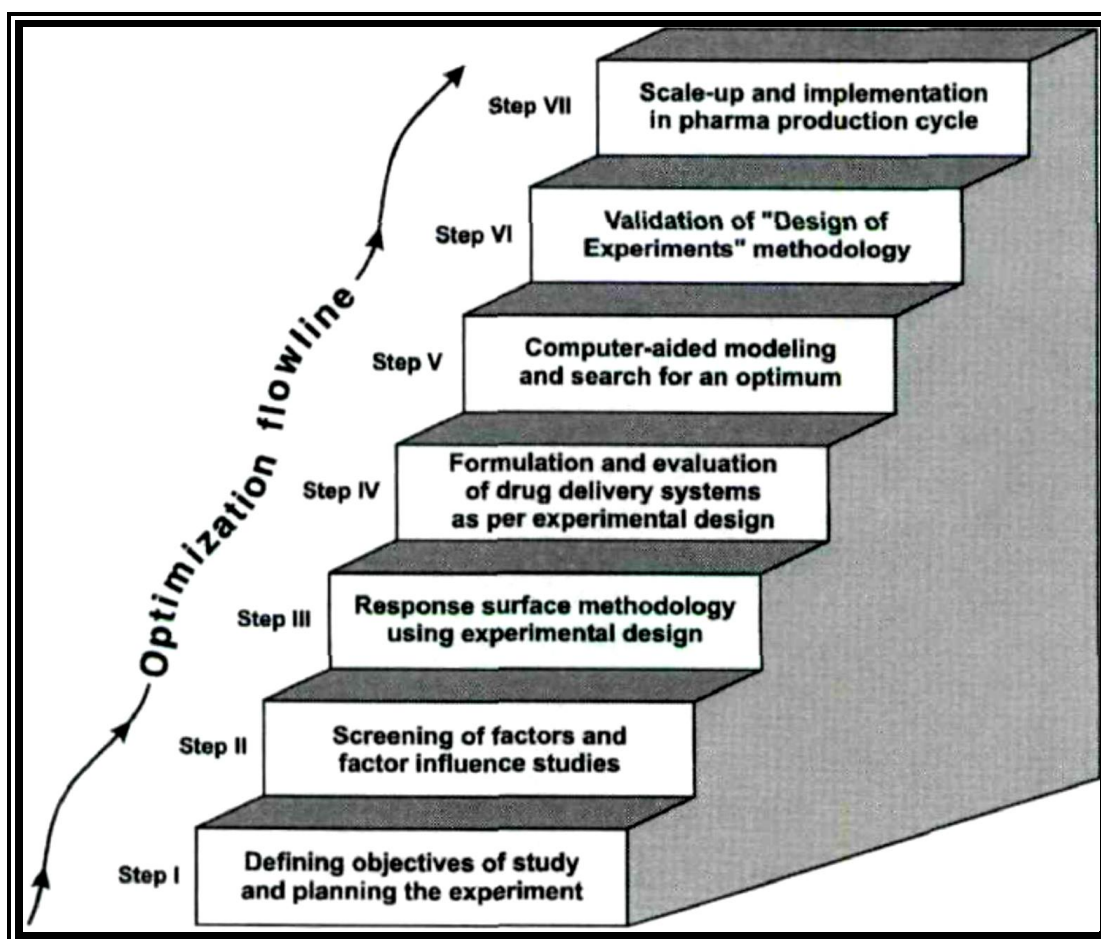


Figure 2.3 Seven-step Ladder for Optimizing Drug Delivery Systems

• During **Step III**, an opposite experimental design is worked out on the basis of the study objective(s), and the number and the type of factors, factor levels, and responses being explored. Working details on variegated vistas of the experimental designs, customarily required to implement DoE optimization of drug delivery, have been elucidated in the subsequent section.

Afterwards, response surface modeling (RSM) is characteristically employed to relate a response variable to the levels of input variables, and a design matrix is generated to guide the drug delivery scientist to choose optimal formulations.

- In **Step IV**, the drug delivery formulations are experimentally prepared according to the approved experimental design, and the chosen responses are evaluated.
- Later in **Step V**, a suitable mathematical model for the objective(s) under exploration is proposed, the experimental data thus obtained are analyzed accordingly, and the statistical significance of the proposed model discerned. Optimal formulation compositions are searched within the experimental domain, employing graphical or numerical techniques. This entire exercise is invariably executed with the help of pertinent computer software.
- **Step VI** is the penultimate phase of the optimization exercise, involving validation of response prognostic ability of the model put forward. Drug delivery performance of some studies, taken as the checkpoints, is assessed vis-a-vis that predicted using RSM, and the results are critically compared.
- Finally, during **Step VII**, which is carried out in the industrial milieu, the process is scaled up and set forth ultimately for the production cycle.

The niceties of the significance and execution of each of these seven steps is discussed in greater detail below.

The foremost step while executing systematic DoE methodology is to understand the deliverables of the finished product. This step is not merely confined to understanding the process performance and the product composition, but it usually goes beyond to enfold the concepts of economics, quality control, packaging, market research, etc.

The term objective (also called criterion) has been used to indicate either the goal of an optimization experiment or the property of interest [64, 66]. The objectives for an experiment should be clearly determined after discussion among the project team members having sound expertise and empiricism on product development, optimization, production, and/or quality

control. The group of scientists contemplates the key objectives and identifies the trivial ones. Prioritizing the objectives helps in determining the direction to proceed with regard to the selection of the factors, the responses, and the particular design [62, 65]. This step can be very time consuming and may not furnish rapid results. However, unless the objectives are accurately defined, it may be necessary to repeat the entire work that is to follow. The response variables, selected with dexterity, should be such that they provide maximal information with the minimal experimental effort and time. Such response variables are usually the performance objectives, such as the extent and rate of drug release, or are occasionally related to the visual aesthetics, such as chipping, grittiness, or mottling [63].

The word ‘optimize’ simply means to make as perfect, effective, or functional as possible [66, 67]. The term optimized has been used in the past to suggest that a product has been improved to accomplish the objectives of a development scientist. However, today the term implies that DoE and computers have been used to achieve the objective(s). With respect to drug formulations or pharmaceutical processes, optimization is a phenomenon of finding the best possible composition or operating conditions [67, 68]. Accordingly, optimization has been defined as the implementation of systematic approaches to achieve the best combination of product and/or process characteristics under a given set of conditions [63].

2.4.1. Experimental Designs

The conduct of an experiment and the subsequent interpretation of its experimental outcome are the twin essential features of the general scientific methodology [67, 69]. This can be accomplished only if the experiments are carried out in a systematic way and the inferences are drawn accordingly.

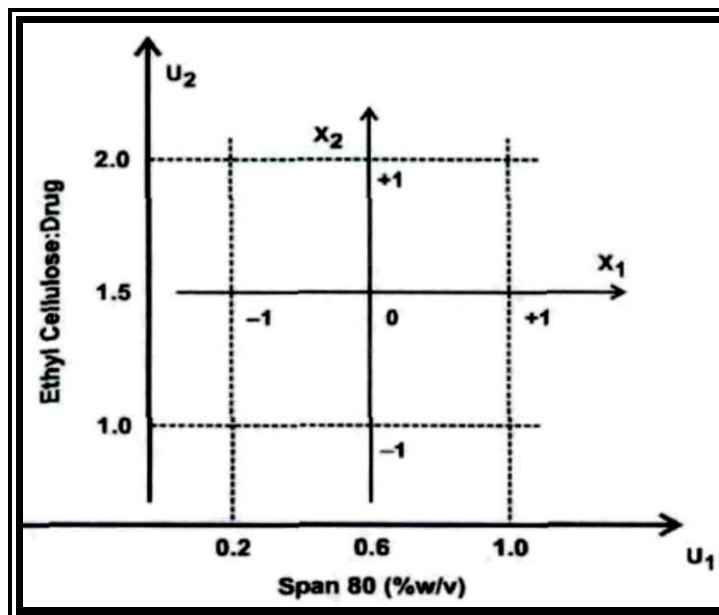


Figure 2.4 Quantitative factors and factor space. The axes for the natural variables, ethyl cellulose:drug ratio and Span 80 are labeled U_1 and U_2 and those of the corresponding coded variables X_1 and X_2

An experimental design is the statistical strategy for organizing the experiments in such a manner that the required information is obtained as efficiently and precisely as possible [70-73]. Runs or trials are the experiments conducted according to the selected experimental design [64, 68]. Such DoE trials are arranged in the design space so that the reliable and consistent information is attainable with minimum experimentation. The layout of the experimental runs in a matrix form, according to the experimental design, is known as the design matrix [68]. The choice of design depends upon the proposed model, the shape of the domain, and the objective of the study. Primarily, the experimental (or statistical) designs are based on the principles of randomization (i.e., the manner of allocations of treatments to the experimental units), replication (i.e., the number of units employed for each treatment), and error control or local control (i.e., the grouping of specific types of experiments to increase the precision) [73-75]. DoE is an efficient procedure for planning experiments in such a way that the data obtained can be analyzed to yield valid and unbiased conclusions [76, 77]. An experimental design is a strategy for laying out a detailed experimental plan in advance to the conduct of the experimental studies [69, 71, 78]. Before the selection of experimental design, it is essential to demarcate the experimental domain within the factor space - i.e., the broad range of factor studies. To accomplish this task, first a

pragmatic range of experimental domain is embarked upon and the levels and their number are selected so that the optimum lies within its realm [79]. While selecting the levels, one must see that the increments between them should be realistic. Too wide increments may miss finding the useful information between the levels, while a too narrow range may not yield accurate results [63]. There are numerous types of experimental designs. Various commonly employed experimental designs for RSM, screening, and factor-influence studies in pharmaceutical product development are

- a. factorial designs
- b. fractional factorial designs
- c. Plackett-Burman designs
- d. star designs
- e. central composite designs
- f. Box-Behnken designs
- g. center of gravity designs
- h. equiradial designs
- i. mixture designs
- j. Taguchi designs
- k. optimal designs
- l. Rechtschaffner designs
- m. Cotter designs

For a three-factor study, an experimental design can invariably be envisaged as a "cube," with the possible combinations of the factor levels (low or high) represented at its respective corners [77]. The cube thus can be the most appropriate representation of the experimental region being explored. Most design types discussed in the current article are, therefore, being depicted pictorially using this cubic model, with experimental points at the corners, centers of faces, centers of edges, and so forth. Such depiction facilitates easier comprehension of various designs and comparisons among them. For designs in which more than three factors are adjusted, the same concept is applicable except that a hypercube represents the experimental region. Such cubic designs are popular because they are symmetrical and straightforward for conceptualizing and envisioning the model.

2.4.1.1. Factorial Designs

Factorial designs (FDs) are very frequently used response surface designs [78, 80, 81]. A factorial experiment is one in which all levels of a given factor are combined with all levels of every other factor in the experiment [68, 81, 82]. These are generally based upon first-degree mathematical models. Full FDs involve studying the effect of all the factors (k) at various levels (x), including the interactions among them, with the total number of experiments being xr . FDs can be investigated at either two levels (2^k FD) or more than two levels. If the number of levels is the same for each factor in the optimization study, the FDs are said to be symmetric, whereas in cases of a different number of levels for different factors, FDs are termed asymmetric [68].

2.4.1.2. Design Augmentation

In the whole DoE endeavor, a situation sometimes arrives in which a study, conducted at some stage, is found to be inadequate and needs to be investigated further, or when the study carried out during the initial stages needs to be “reused” [63]. In either situation, more design points can be added systematically to the erstwhile design. Thus, the erstwhile primitive design can be enhanced to a more advanced design furnishing more information, better reliability, and higher resolution. This process of extension of a statistical design, by adding some more rational design points, is known as design augmentation [83]. For instance, a design involving study at two levels can be augmented to a three-level design by adding some more design points. A design can be augmented in a number of ways, such as by replicating, adding center points to two-level designs, adding axial points (i.e., design points at various axes of the experimental domain), or by folding over.

2.4.2. Response Surfaces

During this crucial stage in DoE, one or more selected experimental responses are recorded for a set of experiments carried out in a systematic way to develop a mathematical model [70, 71, 74, 78, 81, 84]. These approaches comprise the postulation of an empirical mathematical model for each response, which adequately represents change in the response within the zone of interest. Rather than estimating the effects of each variable directly, response surface modeling (RSM) involves fitting the coefficients into the model equation of a particular response variable and

mapping the response over the whole of the experimental domain in the form of a surface [62, 64, 68, 79].

Principally, RSM is a group of statistical techniques for empirical model building and model exploitation [62, 85]. By careful design and analysis of experiments, it seeks to relate a response to a number of predictors affecting it by generating a response surface, which is an area of space defined within upper and lower limits of the independent variables depicting the relationship of these variables to the measured response.

Experimental designs, which allow the estimation of main effects, interaction effects, and even quadratic effects, and, hence, provide an idea of the (local) shape of the response surface being investigated, are termed response surface designs [64, 68, 70, 86]. Under some circumstances, a model involving only main effects and interactions may be appropriate to describe a response surface. Such circumstances arise when analysis of the results reveals no evidence of "pure quadratic" curvature in the response of interest - i.e., the response at the center approximately equals the average of the responses at the two extreme levels, +1 and - 1.

In each part of **Figure 2.5**, the value of the response increases from the bottom of the figure to the top and those of the factor settings increase from left to right. If a response behaves as in **Figure 2.5**, the design matrix to quantify that behavior needs only to contain factors with two levels - low and high. This model is a basic assumption of simple two-level screening or factor-influence designs. If a response behaves as in **Figure 2.5(b)**, the minimum number of levels required for a factor to quantify that behavior is three.

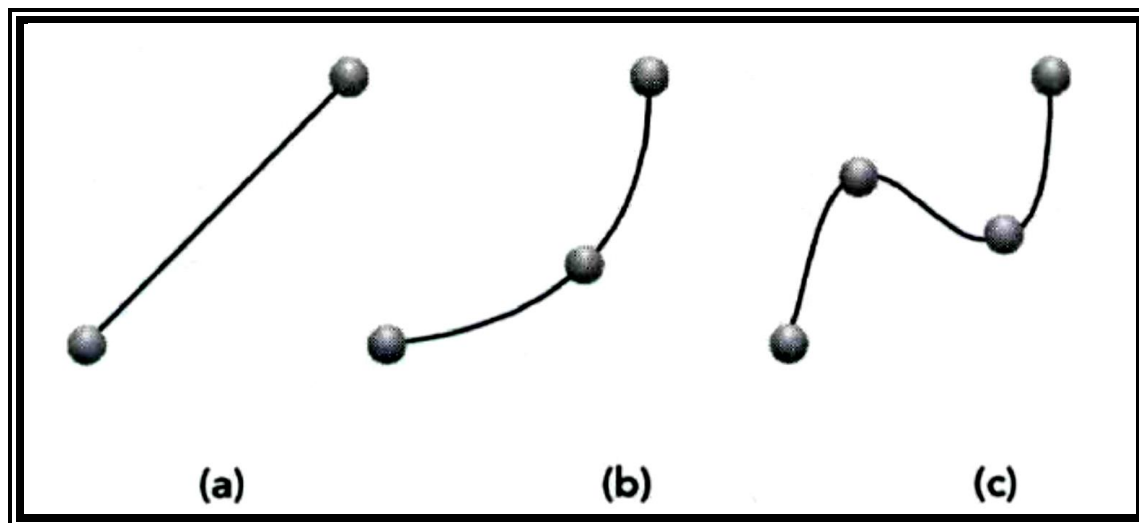


Figure 2.5 Different types of responses as functions of factor settings; (a) linear; (b) quadratic; (c) cubic

Addition of center points to a two-level design appears to be a logical step at this point, but the arrangement of the treatments in such a matrix may confound all the quadratic effects with each other [85, 86]. A two-level design with center points can only detect the quadratic nature of the response, but not estimate the individual pure quadratic effects. Generally, the quadratic models are proposed for optimization of drug delivery devices [67-69]. Therefore, response surface designs involving studies at three or more than three levels are employed for DoE optimization purposes. These response surface designs are used to find improved or optimal process settings, troubleshoot the process problems and weak points, and make a formulation or process more robust (i.e., less variable) against external and non-controllable influences [86]. Relatively more complicated cubic responses (**Figure 2.5(c)**) are quite infrequent in pharmaceutical practice [68, 69].

The prediction ability of response surface designs can be determined by prediction variance, which is a function of experimental variance (σ^2) and variance function (d) as described by Eq. (1) [68, 75, 86].

$$\text{var}(\hat{y}) = d \cdot \sigma^2 \text{_____} (1)$$

where $\text{var}(\hat{y})$ is the prediction variance. The variance function (d) further depends upon the levels of a factor and the experimental design. When the prediction variance of a response is

constant in all the directions at a given distance from the center point of the domain, the design is termed rotatable [75, 78]. Ideally, all response surface designs should possess the characteristic of rotatability - i.e., the ability' of a design to be run in any direction without any change in response prediction variance.

Conduct of DoE trials, according to the chosen statistical design, yields a series of data on the response variables explored. Such data can be suitably modeled to generate mathematical relationships between the independent variables and the dependent variables. Graphical depiction of the mathematical relationship is known as a response surface [70, 79, 86]. A response surface plot is a 3-D graphical representation of a response plotted between two independent variables and one response variable. The use of 3-D response surface plots allows us to understand the behavior of the system by demonstrating the contribution of the independent variables.

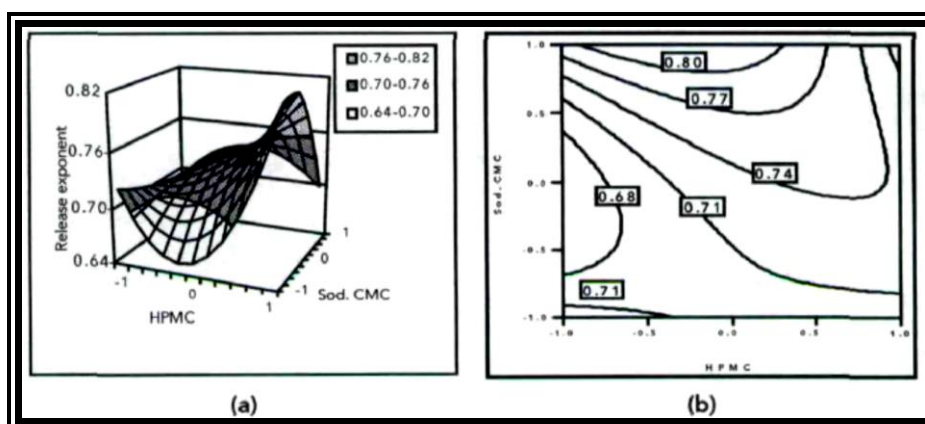


Figure 2.6 (a) A Typical Response Surface Plotted Between A Response Variable, Release Exponent, and Two Factors, HPMC And Sodium CMC, In Case of Mucoadhesive Compressed Matrices; (b) The Corresponding Contour Plot

The geometric illustration of a response obtained by plotting one independent variable against another, while holding the magnitude of response and other variables as constant, is known as a contour plot [64]. Such contour plots represent the 2-D slices of the corresponding 3-D response surfaces. The resulting curves are called contour lines. **Figure 2.6** depicts a typical response surface and contour plot for a diffusional release exponent (proposed by Korsmeyer et al. [87]) as the response variable, reported with mucoadhesive compressed matrices of atenolol[88]. For complete response depiction among k independent variables, a total of kC_2 number of response surfaces and contour plots may be required. In other words, 1, 3, 6, or 10 number of 3-D and 2-D

plots are needed to provide depiction of each response for 2, 3, 4, or 5 number of variables, respectively [63].

2.4.3. Mathematical Models

The mathematical model, simply referred to as the model, is an algebraic expression defining the dependence of a response variable on the independent variable(s) [89, 90]. Mathematical models can either be empirical or theoretical [64]. An empirical model provides a way to describe the factor/response relationship. It is most frequently, but not invariably, a set of polynomial equations of a given order [75]. Most commonly used linear models are shown in Eqs. (2)-(4):

$$Y = \beta_0 + \beta_1 X_1 + \beta_2 X_2 + \dots + \varepsilon \text{_____} (2)$$

$$Y = \beta_0 + \beta_1 X_1 + \beta_2 X_2 + \beta_{12} X_1 X_2 + \dots + \varepsilon \text{_____} (3)$$

$$Y = \beta_0 + \beta_1 X_1 + \beta_2 X_2 + \beta_{12} X_1 X_2 + \beta_{11} X_1^2 + \beta_{22} X_2^2 \dots + \varepsilon \text{_____} (4)$$

where y represents the estimated response, sometimes also denoted as $E(y)$. The symbols X , represent the value of the factors, and β_0 , β_i , β_{ii} and β_{ij} are the constants representing the intercept, coefficients of first-order (first-degree) terms, coefficients of second-order quadratic terms, and coefficients of second-order interaction terms, respectively. The symbol ε implies pure error. Equations (2) and (3) are linear in variables, representing a flat surface and a twisted plane in 3-D space, respectively. Equation (4) represents a linear second-order model that describes a twisted plane with curvature, arising from the quadratic terms. A theoretical model or mechanistic model may also exist or be proposed. It is most often a nonlinear model, where transformation to a linear function is not usually possible [64]. Such theoretical relationships are, however, rarely employed in pharmaceutical product development.

2.5. RNA Interference

In the last decade, 'RNA Interference' (RNAi) has been termed as one of the most important innovations in the field of biology and it is utilized to manipulate gene expression within cells for the treatment of number of diseases and as powerful tool to study gene function. Various carrier systems were utilized in this approach to fight against diseases by regulating expression of a specific factor or gene, which actually responsible for a particular disease.[91] RNAi was principally demonstrated by Fire et al. in 1998 for potent target-specific gene silencing in the nematode *Caenorhabditis elegans*. [92] However, in the last decade endogenous small RNAs were identified and found to modulate gene expression with control over accurate cell function. MicroRNAs (miRNA) (endogenous) short interfering RNAs (siRNAs, endo-siRNAs) and piwi interacting RNAs (piRNAs) are identified as basic controllers of various endogenous processes such as apoptosis, stem cell self-renewal, differentiation and maintenance of cell integrity.[93, 94] In recent time, microRNA (miRNA) has come out as a new approach for the treatment of cancer and various neurodegenerative diseases. Therapy by miRNA involves re-introduction of a synthetic version of a natural miRNA which gets depleted in the diseased tissue.[95] Proper knowledge of target mRNA sequence and designing of its complementary anti sense sequence may lead effective silencing of a specific gene responsible for disease conditions. Hence, these strategies being extensively investigated for personalized therapy of cancer, HIV and other mutate viral diseases.[96-99] Resistance of a chemotherapeutic can also be modified using these approaches.[100] miRNA technique controls the production disease specific protein or gene by down-regulating its expression rather than relieving the symptoms of the disease. This approach can be differentiated from other genetic approaches by its action on the mRNA, expressing the disease producing protein, rather than acting on a particular faulty gene. The success of this approach depends on the understanding of the correct sequence of mRNA carrying the message of protein responsible for the disease. Due to colossal number of completed human genome projects lots of information on target genes for the rational design of antisense drugs is available within hours for research and clinical trials. Currently, different RNAi therapeutics are under clinical trials and many others at preclinical stage are in queue to enter the clinics for various applications like cancer, HIV, age-related macular degeneration, respiratory syncytial virus as

well as rare diseases like pachyonychia congenita. Unfortunately, Sirna-027 from Sirna Therapeutics has recently been terminated which were in phase II respectively of clinical trials. Constraints in regulatory approval of these molecules is inefficient delivery to target site but this can be resolved by better understanding of barriers encountered from the site of administration to the site of action. These barriers can be overcome by designing the delivery systems involving either chemical modifications like structural changes or using nanocarriers or surface modification by specific ligand attachment targeting at particular receptors. Combinations of these methods may also prove beneficial.[101, 102]

But for all its potential, RNAi therapy is a long way from entering the clinic. In this review, we concisely describe how RNAi is accomplished, with a focus on various carrier systems for both modified and unmodified RNA molecules like siRNA, ShRNA and miRNA and their potential therapeutic applications in various human diseases.

2.5.1. Development of RNAi Technology:

Since its discovery, the constant development in the RNAi therapy and its applications as a therapeutic agent has been attained. In 1992, the unfolded mechanism of action of antisense therapeutics was first elucidated by Fire *et al.* In 1998, he identified the RNAi a key factor for the knock down of targeted mRNA responsible for the target protein synthesis [103]. A major breakthrough in RNAi technology was an identification of the dsRNA processing enzyme Dicer [104] and the RNA induced silencing complex (RISC) [105], which trigger RNAi by using the small dsRNA species generated by Dicer as assistant fragments to target mRNA for degradation [106-108]. In 2001, Thomas Tuschla et al defined the basic conditions for siRNA that initiates RNAi in mammalian cells, which involves between 19 and 23 nucleotides (19 to 23mer) with 2 nucleotide overhangs on each 3' end [106, 109]. With the above findings the invasion of siRNA, a 20-23 nucleotide was investigated for its antiviral activity to inhibit disease related gene expression. Currently, based on the knowledge gained and continuous development in the area of RNAi therapy it became a central target to the scientist and pharmaceutical industries. At present, research is not merely confined to the development of an RNAi therapeutics having target orientation, affinity and *in vitro*, *in vivo* activities in different cell lines and animal models

but also to formulate this technology for its therapeutic applications considering its pharmacological and toxicological profile and to get through in all stages of clinical trials is most significant. A lot can be done in design, development and optimization of transfection carriers, its formulations for RNAi agents and to evaluate their doses and dosage frequency for therapeutic activity both at preclinical and clinical levels [110-112]. Presently, gene silencing is accomplished by using small molecules such as dsRNA (double stranded RNA), shRNA (short hairpin RNA), siRNA (small interfering RNA), microRNAs (miRNA) and piwi interacting RNAs (piRNAs). Furthermore, the therapeutic and biopharmaceutical profile of these therapeutics is improved by modifying physical and chemical properties like sugars, bases or by conjugating with different novel carriers [101, 102, 110-112]. The amount of antisense agent, concentration of mRNA produced, production and degradation rate of mRNA and the type of knock down mechanism involved were identified as crucial factors in monitoring therapeutic and biopharmaceutical parameters of these therapeutics. The challenges in delivery of RNAi therapeutics is becoming quite uncomplicated with development of novel RNAi agents and their efficient carrier systems which knock down the targeted mRNA in cytoplasm itself instead of the nucleus [113]. Since, discovery of RNAi technology, its development and conceptual understanding are achieving newer heights day by day which make use of these agents at therapeutic level very easy and such a progress also helps to achieve an improved success rate later at all stages of clinical trials.

2.5.2. Targets of RNAi

The different approaches available for gene silencing are as follows:

- 1) Blocking transcription process (i.e. synthesis of complementary mRNA from the targeted DNA molecule). This is done by two different strategies - strand invasion and triple-strand formation. Out of these, strategies triple-strand formation was used most commonly which includes formation hydrogen bonds between the third strand and the complementary strand of dsDNA molecule [114] e.g. Homopyrimidine oligonucleotides.[115-120]

- 2) Blocking of post transcriptional gene silencing (PTGS) phenomenon which includes the knock down or knock-out of transcribed target mRNA to inhibit the protein synthesis

Gene therapy targets a particular gene which gets either knock-out or knock down by antisense molecules such as RNAi but to achieve effective knock-down or knock-out has always remained a huge challenge in development and formulation aspects of RNAi technology. Better clinical and therapeutic profile of RNAi agents can be achieved with more knowledge and better understanding of different pharmaceutical and pharmacological parameters [110, 111].

2.5.3. Challenges to RNAi Delivery

The objective of RNAi therapy is to bring out the therapeutic outcome by reaching at the target site in amount greater than minimum effective concentration. The path from the site of administration to the target site comprises of many hurdles like physiological, cellular and immunological barriers. In addition, large size and ionic nature of RNAi nanoconstructs affect the transfection capacity of these molecules [110]. Here, the focus of this review is to understand structure, function and physiological role of these barriers in therapy and to reflect the probable approaches for effective RNAi therapy.

2.5.3.1. Physiological Barriers

This is the first barrier coming across the effective delivery of RNAi molecules. This barrier comprises of many check points like glomerular filtration, hepatic metabolism, RES uptake, endothelial barrier and degradation by nucleases. Nucleases degrade the RNAi molecules within a minute after their administration and lower the potency and therapeutic profile of these molecules by 70% [121]. To overcome this hurdle, approaches like chemical modification or use of non-viral carriers were used to deliver and to prevent the cleavage of the RNAi agents [113, 122-125]. The probable approaches which will improve the stability of RNAi agents towards nucleases are stated below:

- 1) Alteration can be possible in pentose sugars at the 2'-OH position and 3' half of the siRNA molecule.[123]

- 2) Formation of phosphorothioate oligonucleotides by replacing the oxygen with sulphur.[123]
- 3) Hexitol nucleic acids (HNAs), morpholino compounds, locked nucleic acids (LNAs) and peptide nucleic acids (PNAs) can also be modified at 2'-OH position.
- 4) Substituting 6-carbon sugar for ribose, 2'-F and 2'-OMe group along with the gapmers helps to sustain the therapeutic activity of these molecules.[113, 123]
- 5) Formulating the anionic molecules into cationic nanoparticles, liposomes, lipoplex or polyplex prevents the cleavage from nucleases by virtue of the electrostatic interaction.[126, 127]

Delivery of various formulation of RNAi molecules like nanoparticles, liposomes, lipoplex or polyplex having particle size (PS) more than 200nm are prone to the phagocytosis by reticuloendothelial system (RES) system [128] whereas, PS less than 100nm get caught at the hepatic Kupffer cells. The rate and extent of clearance of these nanoconstructs from the systemic circulation is depends on the size and charge of the complex formed between RNAi nanoconstructs and serum proteins [129-132]. The clearance can be lowered by coating these nanoconstructs with hydrophilic agents like polyethylene glycol, which compensate the surface charge of these nanoconstructs and make them long circulating [133, 134]. Hence, control on PS and charge of the final formulation may help to improve its therapeutic activity. Development of the delivery system targeting to the tissues of liver, spleen is beneficial due to opsonisation of RNAi nanoconstructs at these organs [113].

To elicit the pharmacological action antisense molecules has to reach at parenchymal cells which are highly protected by the layer of endothelial cells. These endothelial cells hold their position at the extracellular matrix in association with various adhering molecules like integrins. Only the small molecules can get through this paracellular route [135]. In certain organs like liver and spleen the space at the junction allows the larger molecule to travel across the barrier. In addition, the RNAi molecules may travel to target site via caveolin based transcytosis [136]. Due to flexibility in entry of various size particles the molecules such as cell penetrating peptides, targeting ligands or molecular conjugates can be used to deliver the RNAi therapeutics [113].

2.5.3.2. Cellular Barriers

Next to physiological barrier, the antisense molecule has to overcome cellular barrier which comprise of different check points like cell entry, endosomal escape, nuclear localization and knock-down of protein expression. Rigorous toxicity is an outcome of non-viral carriers which non-specifically get inside the non-targeting cells. The non-specific uptake is an outcome of interaction between negatively charged cell membranes and cationic carriers [137] which can be minimized by coating with hydrophilic molecules like polyethylene glycol or conjugating with ligand motif such as transferrin [138], folate [139], surface receptor-specific antibodies [140], etc which will increase their cellular entry [141] and reduce RES uptake. The transfection efficacy of carrier system is based on rate of cellular internalization and endosomal escape [142, 143]. The endosomal degradation is achieved using various approaches like use of fusogenic lipids or peptides to rupture lysosomal membranes and by forming pores in membranes [144, 145]. Literature reveals that lipofectin and DOPE (1, 2-dioleoyl-*sn*-glycero-3-phosphoethanolamine) were used to formulate a pH-sensitive liposomes encapsulating antisense agent for delivering active at low pH surroundings [146]. DOPE present inside the liposomes destabilized the endosomal membrane by forming pores inside it [147, 148]. The structure of endosomal membrane can be disturbed using high buffering capacity polymers like polyethylenimine which prevent acidification of endosomes [149, 150]. In addition, the endosomal membrane can be osmolysed by using osmotic agents like glycerol, sucrose, PVP etc.

Nuclear localization of RNAi molecules is required for knock down of the related protein synthesis. It has been reported in literature that the anionic lipid competes for the anionic RNAi molecules and displace it from the complex of cationic lipid/polymer-antisense molecules [151, 152]. Nuclear localization of RNAi molecules can be enhanced by conjugating them with cationic polymers like polyethyleneimine (PEI) or poly-L-lysine (PLL). The duration of action of RNAi agents is depends on many steps such as cellular uptake, intracellular trafficking, endosomal release and nuclear entry. The molecules like cell penetrating signal peptides, endosomal release signal peptides or nuclear localization signal peptides along with antisense agent has been reported to direct all these steps.[119, 153] Inhibition or down regulation of the protein or gene expression is an outcome of an interaction between RNAi agent and its

complementary mRNA. Transfection efficiency of antisense carrier governs strength of interaction between them. The lipid/polymer to oligonucleotide ratio is a key factor in deciding the transfection efficiency of the carrier [142]. Hence, knowledge and conceptual understanding of these barriers and carriers leads to the efficient delivery of RNAi molecules at the target site. Moreover, the better understanding of bio-distribution and physiochemical properties of RNAi molecules also helps to enhance the success of RNAi therapy.

2.5.4. Cellular Mechanisms of RNAi

The main objective of RNAi therapy is knocking down or knocking out target gene or mRNA to elicit its pharmacological effect. Matured complementary target mRNA produced from DNA undergoes the process of protein synthesis i.e. translation or PTGS which can be a potential target for RNAi molecules to exert their therapeutic action (**Figure 2.7**). Translation comprises of three steps such as initiation, elongation and termination.

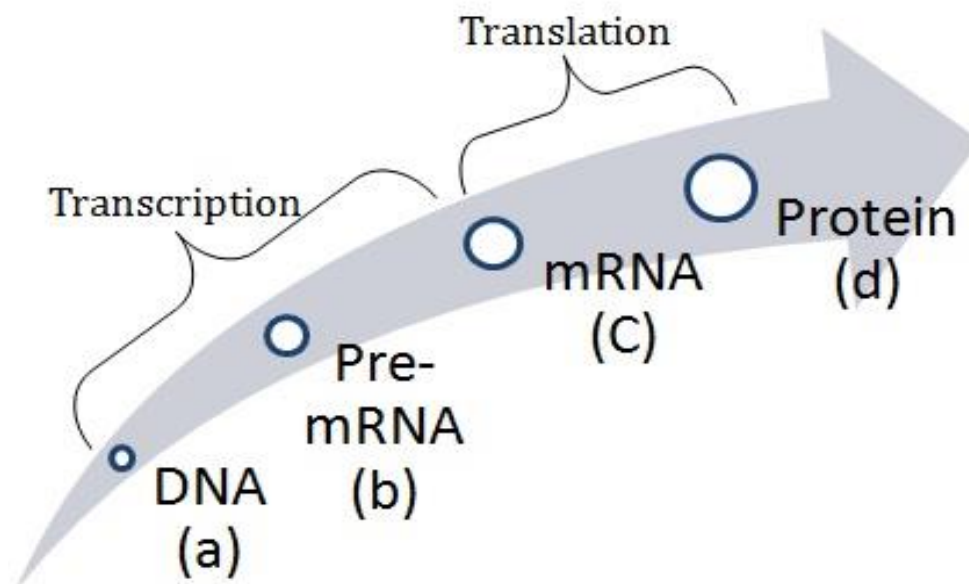


Figure 2.7 Approaches for Knockdown of Target Gene Or mRNA: (A) Transcription Inhibition: DNA Targeting (B) Preventing mRNA Formation: Pre-mRNA Targeting (C) Translation Inhibition: Protein Targeting

RNA interference (RNAi), monitor activity and potency of genes within mortal cells. RNA interference was also called as co-suppression, post transcriptional gene silencing (PTGS), and quelling. The RNAi pathway is divided into two phases such as initiation phase and execution phase. The initiation phase is triggered in the presence of dsDNA precursor which subsequently gets cleaved at 11 nucleotide interval by the enzyme dicer with C-terminal dsRNA binding domain, an N-terminal RNA helicase as well as two RNaseIII-like domains,[104] into short fragments of 20-23 nucleotides with over-hanging 3'ends that are known as siRNA.[154] In execution phase each siRNA so formed is uncoiled into two single strands i.e. passenger strand and guide strand. Out of these two strands of uncoiled siRNA the passenger strand get degraded and guide strand couples with RNA induced silencing complex (RISC) forming a large multiprotein complex which brings out the post transcriptional gene silencing (PTGS). PTGS implicates sequence specific base coupling between the guide strand of the siRNA and the target mRNA followed by endonucleolytic cleavage of the mRNA strand across the middle of the siRNA strand[106, 155] and later degradation of the targeted unprotected mRNA. Due to the potency, maximal effectiveness, duration of action, and sequence specificity of small interfering RNA (siRNA) it becomes an important tool of RNAi therapy both *in-vitro* and *in-vivo* [119, 156, 157]. The cellular mechanism of RNAi involves several complicated steps which are depicted in (Figure 2.8).

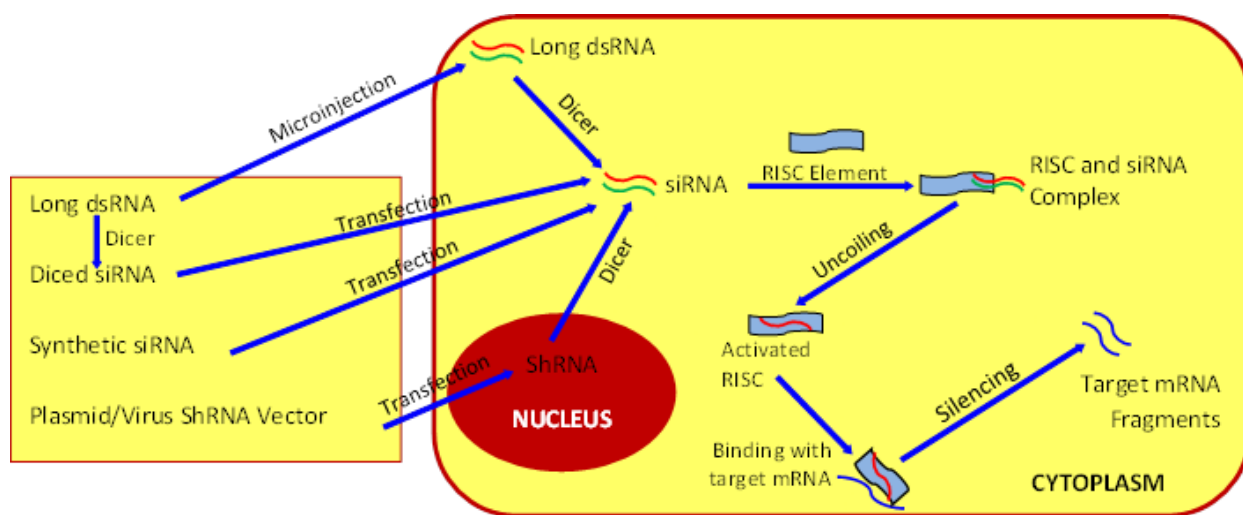


Figure 2.8 Cellular mechanisms of RNAi

2.5.5. Small Interfering RNA (siRNA)

Knockdown or silencing of targeted genes in most of the cells can be done by small interfering RNA (siRNA) which belongs to a class of double stranded RNA. siRNA is a double stranded RNA molecules which are 19–23 base pair (bp) in length with the molecular weight of about 13 to 15 kd and have 38 to 46 negative charges. The structure of siRNA is well defined, which contains a two-nucleotide overhang on the 3' end of both strands, phosphate group on the 5' end and a hydroxyl group on the 3' end [106]. siRNAs are double-stranded duplexes which need to be unwound before they assembled into a RISC. siRNAs is divided into two classes and is depend on the thermodynamic stabilities at the two ends,; symmetric siRNAs and asymmetric siRNAs. A symmetric siRNA contains two equally stable ends and thus, both the strands of the siRNA are assembled into the RISC with equivalent efficiency. An asymmetric siRNA contains one end with less stability than the other. siRNA can be unwind easily from the less stable end and one strand of the siRNA can be process referred to as the asymmetric assembly of RISCs [158]. Gene silencing by siRNA includes it's binding to corresponding mRNA and degradation of target mRNA. In mammalian cells, synthetic siRNA duplexes can activate RNAi which knock down target mRNA sequence and hence, corresponding protein production. A specific endogenous siRNA is originated either from a long double-stranded RNA (dsRNA ~ 200 nucleotides) coded by a certain gene, or from an exogenous source such as non-viral and viral vectors. This long dsRNA is then fragmented into the 19 – 23 base pair siRNAs by RNase-III like enzyme called Dicer and then this siRNA forms complex known as the RNA-inducing silencing complex (RISC). The sense strand of siRNA guides the RISC to the appropriate target mRNA molecule, where it cleaves and destroys the complementary mRNA. The broken mRNA is rapidly degraded and protein expression is reduced or abolished [106, 159]. Principle of antisense oligonucleotide therapy helps in the development of RNA interference RNAi by using siRNA. Antisense oligonucleotides contain the single strands of DNA or RNA that are complementary to a specific sequence of mRNA. It inhibits translation of a complementary mRNA molecule by binding to it and physically obstructing the translation machinery. However, antisense RNA often lacks effective design, biological activity, and an efficient route of administration and because of that it has been replaced by the new technology of RNAi. Specific siRNA sequences for many target mRNAs can be predicted by using current bioinformatics

technologies. These artificial siRNAs are capable of silencing their complementary mRNAs by mechanisms similar to those of endogenous siRNA. These artificial siRNAs can either be synthesized chemically as oligos (siRNAs) or cloned into a plasmid or virus vector like adenovirus, retrovirus or lentivirus as short hairpin RNAs (shRNAs). To block gene expression by using siRNA have many advantages over other methods, like chemical inhibitors and dominant negative mutants. Knockdown the expression of any class of genes including both protein-encoding genes and non-coding RNAs can be targeted by siRNA. On the other hand, there are only a limited number of chemical inhibitors available against certain proteins or pathways, and many of them are not specific. siRNA have number of advantages like is highly specific, can be easily synthesized or cloned into expression vectors, siRNA-mediated silencing is more specific and less toxic compared with both chemical inhibitors and dominant negative mutants. Therefore, siRNA silencing is overall an excellent tool in various diseases to knock down the overexpressed genes involved in it, where conventional treatment often fails.

2.5.6. RNAi as Therapeutics

RNAi technology is also currently being evaluated as a potentially useful method to develop highly specific RNA-based gene-silencing therapeutics. As a new therapeutic approach, RNAi might be specific enough to allow the use of multiple RNAi targets at the same time, without the toxic effects often observed during chemotherapy and the sequence-independent toxic effects of antisense therapy. Gene expression is silenced by fundamental cellular mechanism of RNAi. Overexpression of pathological proteins is suppressed through RNAi and is applicable to all classes of molecular targets, including those which are difficult to modulate selectively with traditional pharmaceutical approaches. The target mRNA is enzymatically cleaved by RNAi which leads to suppression of the overexpressed protein. RNAi therapeutics as a drug class has the potential to exert a transformational effect on modern medicine [160]. RNAi is used in analysis of the biological function of individual genes or genes known to be associated with diseases [161]. RNAi is an emerging field for basic and biomedical research that may lead to a number of clinical applications. Various studies have been published demonstrating efficacious silencing of disease genes by local and systemic administration of RNAi in animal models of human disease. Both exogenous and endogenous genes have been silenced, and promising *in*

vivo results have been obtained across multiple organs and tissues. Efficacy has been demonstrated for viral infection (respiratory and vaginal), ocular disease, disorders of the nervous system, cancer and inflammatory bowel disease.

Table 2.3 Modes of Rnai Delivery and Potential Targets In Various Diseases

Sr. No.	Route of Administration	Potential organ target	Disease Target
1.	Local/Direct	Eye	Macular degeneration, Diabetic macular oedema
		Skin	Atopic dermatitis
		Vagina	Herpes simplex virus
		Rectum	Inflammatory Bowel disease
		Lung	SARS, RSV, Flu
		Brain	Huntington's disease, Depression, Alzheimer's disease, Spinocerebral ataxia, ALS, Encephalitis, Neuropathic pain
		Spinal cord	Chronic pain
		Vagina	HSV
		Isolated tumour	Glioblastoma multiforme, Prostate, Adenocarcinoma, Human papillomavirus
2.	Systemic	Digestive system	Irritable Bowel disease
		Liver	Hypercholesterolemia, HBV
		Heart	Myocardial infarction
		Kidney	Acute kidney injury
		Metastasized tumours	Ewing's sarcoma
	Joints	Rheumatoid arthritis	

Now a day, several researchers have explored the use of RNAi to limit infection by viruses in cultured cells. Jacque et al. directed siRNAs against the HIV-1 genome, including the viral long terminal repeat (LTR), vif and nef [162]. Gitlin et al. attenuated poliovirus infection after transfection with siRNAs that targeted either a capsid-protein mRNA or the viral polymerase mRNA.[163] Similarly, RNAi has been used to attenuate infection by Rous sarcoma virus in chick embryos, and sequences within the hepatitis C virus have been successfully targeted in living mice when present as a fusion with a reporter construct [92]. HIV-resistant progeny T cells and macrophages were produced by transplanting hematopoietic stem cells transduced with a lentivirus expressing an anti-HIV shRNA [164]. Intravenous injection of shRNA-encoding DNA vectors as well as intratracheal administration of shRNA vectors, have provided possible approaches to treat respiratory viruses such as influenza or respiratory syncytial virus [165]. shRNAs directed against the structural protein 1D (Ad5-NT21) or polymerase 3D (Ad5-POL) of foot and mouth disease virus (FMDV), delivered by adenovirus are capable of inhibiting virus replication in both cultured porcine cells and in guinea pigs [166]. The LNA-antimiR against miR-122 decreases total plasma cholesterol level without hepatotoxicity in African green monkeys [109]. Anti-miR-126 antagonizes to miR-126 and suppresses the asthmatic phenotype in mice model of allergic asthma [167]. SPC3649 (LNA-antimiRTM-122) is being developed as a new potential approach in treatment of Hepatitis C infection [168].

Devastating problems may be arising due to many neurological diseases which are progressive and untreatable. RNAi-based gene silencing which is having high-order of specificity is more beneficial than other therapeutic approaches in the treatment of neurological disorders. Diseases like neurodegenerative disorders (Huntington's disease, spinobulbar muscular atrophy, frontotemporal dementia with parkinsonism, dystonia, and slow channel congenital myasthenic syndrome), CNS tumors, chronic pain, prion diseases, trinucleotide repeat diseases, infectious diseases, are likely candidates to benefit from RNAi.[92] Silencing of mutant SOD1 expression possibly treats Familial Amyotrophic Lateral Sclerosis (FALS) and allele-specific silencing of mutant SOD1 using siRNA has been demonstrated by Ding *et al.* [169]. Potential therapeutic targets for siRNA-mediated gene silencing in Alzheimer's disease (AD) are the β - and γ - secretases. These enzymes help in the cleavage of APP to β - amyloid and thus provide logical targets for AD therapy by either direct inhibition or down regulation of expression using siRNA.

Various researchers have shown that siRNAs can be used against viral targets [170]. Equine Infectious Anemia Virus (EIAV) mediated silencing of mutant SOD1 expression in vulnerable motor neuron populations using shRNA causes reversal of a dominantly inherited form of Amyotrophic lateral sclerosis (ALS) in a transgenic mouse model [171]. Long-term *in vivo* expression of two different rAAV5-shRNA vectors led to significant reduction in striatal mHtt mRNA and protein levels which can ameliorate the Huntington's disease (HD) phenotype of R6/1 mice [172]. There are some important problems which have to be solved before clinical use of RNAi. For successful therapeutic application of RNAi in humans, refinement of delivery methods seems to be the major barrier. Efficient and suitable delivery system should be used for successful therapeutic application of RNAi.

Cancers are often caused by deregulated expression of genes that lead to uninhibited cell growth. Bcl-2 and p53 are the particular interest of genes which involved in apoptotic pathways. A study showed that siRNAs directed against BCR/ABL transcripts induced apoptosis [173]. siRNAs have been used to target K-RAS^{V112} which constitutively activates RAS leading to pancreatic and colon cancer. Knockdown of K-RAS^{V112} resulted in specific degradation of K-RAS^{V112} and inhibition of colony growth in soft agar [174]. Many diseases like cancer and angiogenesis-related diseases are characterized by the uncontrolled growth of new blood vessels because of the overexpression of multiple endogenous and exogenous pathogenic genes. Combination of multiple drugs is used when disease progression and the development of drug resistance stop the effect of single-drug treatments. Combination of multiple-siRNA to target multiple disease-causing genes provide a unique advantage for combination therapy. Improved anti-angiogenesis potency has been observed in combination of siRNAs targeting VEGF-A, VEGFR1 and VEGFR2 when compared with siRNAs targeting only one factor [175, 176]. Combination of multiple siRNAs targeting to angiogenic factors in each category may enable the identification of potent anti-angiogenic agents for potential therapeutic applications. Several attractive siRNA targets are available to fight against cancer and angiogenesis. Intratumoral injection of an adenoviral vector encoding a shRNA to target S phase kinase-associated protein 2, effectively inhibited a small cell lung carcinoma in mice [177]. Plasmid vectors of shRNA specific against STAT6 gene induced apoptosis in colon cancer cells [178, 179]. Inhibition of p16 expression in squamous cell carcinoma using shRNA and integrated these shRNA into adenoviral and

retroviral vectors for transient and integrated expression in human cells [178]. Antisense inhibitor to miR-27a, miR-96 and miR-182 leads to a significant increase in endogenous FOXO1 expression in breast cancer cells [180]. Fluiter et al., demonstrated that *in vitro* H-Ras knockdown and *in vivo* tumor growth inhibition in prostate tumor xenografts by anti-H-Ras ODN containing alpha-L-LNA.[181] p53 gene upregulate the mammalian miR-34 in response to radiation. miR-34 is responsible for a normal cellular response to DNA damage *in vivo* and it points to a potential therapeutic use for anti-miR-34 as a radio- sensitizing agent in p53-mutant breast cancer [182]. Delivery of vessel-targeted nanoparticle containing anti-miR-132 restored p120RasGAP expression in the tumor endothelium which results into suppression of angiogenesis and decreased tumor burden in human breast carcinoma [183]. Transfection of anti-miR-146a OND into balloon-injured rat carotid arteries markedly decreased neointimal hyperplasia [184]. Inhibition of the formation of capillary-like structures stimulated by hypoxia and decreased cell migration in response to VEGF (vascular endothelial growth factor) was achieved through miR-210 blockade via anti-miRNA transfection [185].

Table 2.4 Therapeutic intervention using siRNA

Sr. No.	Disease	Type	Target
1.	Viral	HIV-1	LTR, <i>vif</i> , <i>nef</i> , <i>Tat</i> , <i>Rev</i> , Gag, CD4, CCR5, p24, Pol
		Poliovirus	Capsid, viral polymerase
		Hepatitis B	Core region (3.5 kb RNA), Pregenomic RNA
		Rous sarcoma virus	Gag
		Hepatitis C	EMCV-IRE5, NS3, NS5B, NA, Core, NS4B, 5' UTR, NS5A
		Respiratory Syncytial Virus	Phosphoprotein (P), Fusion protein (F)
		Influenza A	NP, PA, PB1, PB2, M, NS
		Rotavirus	VP4
		Adenovirus (group B)	CD46 (cellular coreceptor)
		γ herpes virus	Rta, ORF45
2.	Cancer	Leukemia	c-raf, bcl-2
		Cervical carcinoma	E6, E7 (HPV)
		Pancreatic carcinoma	K-RAS ^{V112}
		Melanoma	ATF2, BRAF ^{V599E}

		Ovarian carcinoma	H-Ras, mVEGF, COX-2
		Prostate cancer	P110a, p110B of PI 3 kinase
		Wilms' tumor	Wt1, Pax2, Wnt4
3.	Angiogenesis	Tumor angiogenesis	VEGF
		Ocular neovascularization	VEGF, VEGFR1 and VEGFR2
		Rheumatoid arthritis	Akt, GG2-1, ASC
4.	Neurological Disorders	Alzheimer's disease	β -, γ -Secretase, Protein kinases (GSK-3, Cdk-5)
		Parkinson's disease	α -Synuclein, LRRK2
		Huntington's disease	Huntington
		Familial amyotrophic lateral sclerosis	SOD-1
		Spinocerebral ataxia	SCA-1, SCA-2
		DYT1 dystonia	TOR 1A

2.5.7. *In Vivo* Delivery Vectors

Most challenging task in the RNAi delivery is efficient intracellular accumulation of RNA macromolecule. Variety of approaches, including viral and nonviral delivery vectors, administration through local and systemic route, has been utilized to down regulate target protein. Different formulations ranging from saline solution of naked siRNA to lipid, protein or cholesterol conjugates, aptamers etc have been used to elicit the RNAi response *in vivo*.

Each of these has distinct merits and demerits to use them in clinical application. RNAi molecules require a delivery vector for many reasons. These include high negative charge, molecular weight, and degradation by nucleases [102]. Viral vectors are more beneficial when transfection efficiency is in a question. However, non-viral vectors own substantial advantages i.e. less *in-vivo* toxicity, immunogenicity and insertional mutagenesis [186]. An ideal RNAi delivery vector should be equipped with a cationic group for effective transfection, an endosomolytic group for endosomal escape, a surface modifier to decrease steric hindrance that ultimately enhances circulation time in blood, and a targeting moiety to direct a delivery system at target cells or tissue [112]. As far as systemic delivery is concerned, size of delivery vectors plays an enormous role in biological system. To avoid glomerular filtration, size of the delivery vector should not be less than 5 nm. At the same time, delivery system should be big enough to

avoid leakage to interstitial spaces of hepatic sinusoid and entrapment by hepatic Kuffer cells, which requires particle size greater than 100 nm [112]. Further, to avoid macrophage uptake in to systemic circulation, size should not be more than 200nm. Hence, ideal size of deliver vectors for systemic delivery should lie between 100-200 nm.

Viral vectors usually elicit long term inhibition of target protein in a single administration, but these vectors suffer from a major risk of immune response in host, which has been highlighted recently [187]. Earlier with the use of AAV mediated shRNA delivery in to mice, diversion of RNAi mechanism was observed that ultimately manifested in marked toxicity.

While working with viral vectors, it is extremely difficult to forecast RNAi exposure with respect to its amount and duration. Furthermore, it may be possible that viral vector encoded with high level of shRNA interfere with endogenous miRNA pathway. Non-viral delivery vectors have been extensively utilized for the delivery of nucleic acids, locally and systemically. These mainly include lipids, polymers, and peptides. Various lipid complexes, liposomes, polymers, proteins and antibodies have been used to deliver RNAi to target site. Cationic lipids and polymers have shown some cytotoxic effects that might limit the use of these carriers in RNAi delivery for particular disease indications and dosing paradigms [159]. Ultimately, one should go ahead with a carrier system, which is having least in-vivo toxicity with enhanced transfection efficacy [188, 189].

Some of the marketed lipid based non-viral RNAi vectors for transfection are Oligofectamin [190], Lipofectamine, TransIT-TKO and DharmFECT [191], all of which have been employed delivering RNAi macromolecules in-vivo. Usually, positively charged lipids are employed for complexation and delivery of RNAi; however, few of the neutral and anionic lipids have also been tried [192]. According to few reports, in vivo, these Cationic lipids possess poor *in vivo* stability and reproducibility with cytotoxicity [193]. For efficient delivery of RNAi, with minimum side effects, optimization of a charge ration between vector and nucleic acid is must, because it is the negative charge of RNAi molecule which complexes with cationic group of the vector. Cationic lipids or liposomes made up from these lipids are normally more toxic than their neutral counterparts. In contrast to lipid based vectors, polymer vectors possess relatively less

immune response, though not much safer in unmodified form [194]. Polymers give flexibility for use in terms of its physical and chemical properties that might be the major cause for extensive investigation on polymeric delivery of RNAi therapeutics. Charge density, molecular weight, and pH markedly affect the complex formation between polycations and RNAi, also known as polyplex. Polycations interacts weakly with RNAi as contrast to DNA molecule and hence, finally leads to the formation of loose polyplex. However, increment in charge ratio can overcome this drawback but, ultimately increased charge density results into decreased margin of safety with respect to cytotoxicity [195]. Cationic polymer Polyethylenimine (PEI) is one of the most extensively investigated non-viral delivery vector to transfer RNAi intracellularly for systemic and local applications [159]. PEI has also been utilized as a reference standard for many in-vitro and in-vivo studies. A proton sponge effect of this cationic polymer results into endosomal release of RNAi into cytoplasm and assures high efficiency of transported RNAi [149]. However, in-vivo toxicity of PEI has forced researchers to develop newer modified polymers and polycations for safe and effective RNAi delivery. Apart from this, nanoparticles made up of hydrophobic polymeric matrix encapsulating RNAi macromolecule is one of the alternate means for delivering RNAi. This system offers appreciable protection of RNAi against nucleases but negotiates with loading capacity of genomic materials [196]. Peptide vectors have also been utilized to transfect RNAi in-vivo. Various cell penetrating peptides and its modifications which are studied for in-vivo intracellular delivery of nucleic acids are TAT, transportan, penetratin, CADY, MPG and VP22 [159].

Many times small molecules, proteins and antibodies are used as conjugates with RNAi for efficient targeted delivery, which should also be focused with regard to the biological activity. Alteration may occur in normal physiology if a specific receptor or other endogenous molecule is used, which has a potential role in normal body functions. This finally causes undesired side effects. Conclusively, non-RNAi part in to delivery system increases intricacy during manufacturing, especially at commercial scale. However, non-RNAi part is much essential to balance a well-recognized transfection to toxicity poser. Development of novel biodegradable polymers and less cytotoxic lipids may come out with more efficient and less immune active delivery vectors [160, 197].

2.5.8. *In Vivo* Delivery of RNAi

Delivery of RNA macromolecules *in vivo* can be achieved by two ways, systemic and local. Larger amount of nucleic acids is required when administered systematically into biological system to achieve down regulation of target gene. In contrary, local delivery of these macromolecules at desired sites is more preferable, as therapeutic effect can be governed at low dose with reduced systemic side effects [170, 198, 199]. Vast numbers of studies have been conducted for delivering RNAi therapeutics *in-vivo*. These includes direct injection of macromolecules, pulmonary administration via inhalers and nebulizers, intravenous injection using naked or vector mediated delivery approaches etc [200-202]. Many researchers have utilized vector mediated delivery for RNA macromolecules which includes delivery by using lipids, peptid, and polymers. These further can be surface modified with suitable ligand molecules [203, 204]. Recently, aptamer approach has also been employed to deliver siRNA intracellularly [205, 206].

A key concept behind considering a selection between local and systemic RNAi administration is the frequency and amount of doses required to accomplish adequate nucleic acid concentration in the target site and the probable unwanted effects due to exposure of non-targeted tissues to these RNAi molecules. Current scenario in silencing technology suggests that so far efficacy has only been shown by local RNAi application when local and systemic exposure come to the same platform. However, systemic administration has a defiant advantage when tissue like a liver is considered, where majority of systemically administered drug molecules get localized [160].

2.5.8.1. *Systemic Delivery of RNAi Therapeutics*

After numerous successes in mammalian cell culture system, RNAi therapeutics were successfully tried in animal models to elicit desired down regulation of target protein. Previously, *in-vivo* delivery of RNAi was attained by giving hydrodynamic injection into the tail vein of the mice, which resulted in significant suppression of a Luciferase gene [207]. In continuation of this, studies were also conducted in using high-pressure intravenous tail injection of siRNA and shRNA in adult as well as postnatal mice. This caused marked reduction of gene expression, up to 90%, in the liver and also in other organs such as lung, kidney, spleen and pancreas [208, 209]. Accumulation of large amount of the siRNA in to the liver prompted

researcher to think about application of RNAi therapeutics in the treatment of liver diseases. One such study involved RNAi administration in to acute liver failure induced mice model. This involved endogenous genes expressing FAS cell death receptor and caspase 8, both are involved in apoptosis during hepatic injury that is initiated by viruses or transplant rejection [174, 210]. It was observed that significant liver protection was obtained following pretreatment with FAS and caspase-8 targeting siRNAs, where liver failure was induced using different chemicals. Further, expression of FAS was found to be inhibited upto 10 days, which suggests in-vivo stability of siRNA in mice.

Liver is readily targeted via systemic RNAi delivery as compared to other organs. Recently, systemic administration of adenoviral vector expressing siRNA against HBV demonstrated reduction in viral load and almost restricted the replication of HBV for 26 days. Even though liver is assumed to be port of systemically delivered molecules, findings from this study put forward the application of RNAi in liver diseases [211]. Efforts have also been made to deliver RNAi across the BBB but it remained the most challenging task because, RNAi macromolecules cannot cross BBB. However, several researchers tried different strategies to deliver RNAi into the CNS including “Trojan Horse” technique using liposomes [212]. In this technique, RNAi macromolecules are encapsulated within the liposomes, which may be surface modified using polyethylene glycol (PEG). The PEG surface modification serves to protect liposomes, and so as RNAi, against macrophage uptake to impart long systemic circulation. This PEG can also help to graft cell specific monoclonal antibodies which can target a definite tissue or cells. Moreover, more than one targeting ligands can also be grafted onto liposomal surface for multiple targeting. For example, two distinct monoclonal antibodies or aptamers attached onto liposomal surface helps to target specific site into the CNS, since one targeting moiety can be distinct to BBB and thus allow transport across it and other one can be distinct to a cell type receptor inside the CNS [213]. In recent times, Alvarez-Erviti et al. have showed the application of exosomes to deliver RNAi across the BBB. Exosomes are biological nanovesicles, which help in transportation of RNAs and proteins [214]. Exosomes were obtained from dendritic cells and purified to reduce immunogenicity. To attain higher concentration inside the brain, dendritic cells were bioengineered to express an exosomal membrane protein known as Lamp2b fused to CNS rabies viral glycoprotein (RVG). RVG selectively binds to acetylcholine receptors in the CNS [215].

Finally, intravenous injection of RVG attached exosomes containing siRNA caused marked accumulation of siRNA in to the neurons and oligodendrocytes without having any immune response.[216] Efforts have also been made to target HIV using RNAi strategies and this has been promoted by decreased viral load following RNAi application against HIV infection [217]. However, pathogenesis of HIV limits the use of RNAi macromolecule in the treatment of this disease. HIV can mutate to run away from RNAi trap. HIV may escape RNAi through recently recognized function of its Tat protein, which interferes with dicer activity [218]. Thus, betterment in the formulation, encoding RNAi molecule, may overcome these situations in near future.

Recent advancement in systemic RNAi delivery is the targeting to specific cells or tissue by cell surface receptor. This strategy helps to provide maximum therapeutic benefit at least adverse events. Many targeting moieties including aptamers, monoclonal antibodies, and peptides in conjugation with RNAi, have been investigated to target specific cell surface receptor and thus to the desired site into the body [124, 219, 220]. Systemic administration of targeted RNAi was first time utilized in human during phase I clinical trial, which involved targeted RRM2 (Ribonucleotide reductase subunit M2) siRNA nanoparticles via intravenous route to the patients bearing solid tumor). Results demonstrated significant inhibition of RRM2 gene at both mRNA and protein stages [221].

Monoclonal antibody grafted liposomes, immunoliposomes, have been utilized to overcome barriers of BBB and transfer RNAi molecule into the brain.[222] RNAi expressed plasmid has been entrapped into the immunoliposomes, having particle size less than 100 nm. Further, surface of these liposomes was sterically stabilized to impart longer circulation into the blood. Results demonstrated that intravenous administration of RNAi immunoliposomes silenced significant gene expression in the brain. More specifically, intracranial brain cancer induced rats were administered plasmid DNA encoded with shRNA targeting Luciferase gene, which were expressed in brain tumor, by intravenous route. Results showed that 90% of Luciferase gene silencing was attained for not less than 5 days. In addition to this, mice bearing human brain cancer were also regressed and life span of the mice was increased by 90% after administering shRNA encoded plasmid containing immunoliposomes [223]. Despite of these tremendous efforts, RNAi requires repeated administration to achieve long term effect because, in-vivo

distribution of RNAi throughout the tissue and into the targeted cells is much heterogeneous. Hence, future approach to deliver sustained RNAi therapeutics may help to solve this issue and application of this novel technology in to clinical practice.

2.5.8.2. Clinical Trials and RNAi

The discovery of RNAi has been widely acknowledged as a major breakthrough in biology. This exciting technology has the potential to make a broad and significant impact in therapeutics. Much important scientific and clinical advancement are being made at a very rapid pace. Major companies demonstrating significant impact in clinical development of RNAi platform worldwide include Silence therapeutics, Alnylam therapeutics, Quark, Calando pharmaceuticals, Sirna, Allergan, Gradalis inc., Santaris Pharma A/S and Pfizer and Acuity as in collaborative research [145-150]. Alnylam is supporting the development of Direct RNAi™ therapeutics. These products are designed to be administered directly to sites of diseases in various parts of the body, such as the eye, the brain or the lungs. Calando is a clinical stage nano-biotechnology company at the forefront of RNAi therapeutics and develops nanoparticle therapeutics that use sugar (cyclodextrin)-based polymer technologies as a drug delivery system for siRNA. CALAA-01, the company's leading drug candidate for treating cancer, is in phase II trial. Silence Therapeutics has several RNAi drugs in phase I and II trials for treating diabetic macular edema, age-related macular degeneration, acute kidney injury, and cancers. Quark pharmaceuticals has focused on diseases of the eye (e.g., wet, diabetic macular edema, diabetic retinopathy, NAION, glaucoma etc.), lung (e.g., acute lung injury, primary graft dysfunction in lung transplantation), kidney (acute kidney injury, delayed graft function), inner ear (e.g. acute hearing loss, ototoxicity and Ménière's disease), and spinal cord (spinal cord injury). These companies are concentrating majorly on siRNA therapeutics whereas Gradalis, inc. has made an effort to move shRNA base therapeutics into clinics including anti-cancer pbi-shRNA™ STMN1 LP to phase I and FANG™ autologous tumor cell vaccine to phase II. Miravirsen is the first microRNA-targeted drug to receive Investigational New Drug (IND) acceptance from FDA, paving the way to conduct Phase 2 trials for treatment of hepatitis C in the United States [6]. Santaris Pharma A/S advances Miravirsen, the first miRNA-Targeted Drug to enter clinical trials, into Phase 2 to treat patients infected with hepatitis C virus. Further research is in progress to understand the roles of miRNAs

in cancer and the potential for manipulating miRNAs for cancer therapy as these molecules make their way towards clinical trials [224].

Table 2.5 siRNA – Clinical Trials [145-150, 224] (<http://clinicaltrials.gov/>)

Sr. No.	Product Details	Company and Strategic Alliance	Target tissue	Indication	Type and route of delivery	Status
1.	SiRNA TD101	TransDerm, Inc./Pachyonychia Congenital Project	Thick calluses, non-specific topical keratolytics, and oral retinoids	Pachyonychia Congenita	Injection into a callus	Phase Ib
2.	SiRNA Sirna-027/AGN211745	Allergan/ Sirna Therapeutics Inc	Retina	Age-Related Macular Degeneration, Choroidal Neovascularization	Naked siRNA Intravitreal Injection	Phase I and II
3.	SiRNA AGN211745	Allergan	Retina	Choroid Neovascularization Age-Related Macular Degeneration	Injection	Phase II terminated
4.	SiRNA CALAA-01	Calando Pharmaceuticals	Cancer cells	Cancer/ Solid Tumor	Intravenous	Phase I
5.	Atu027	Silence Therapeutics AG	Targets PKN3 molecule in cancer cells.	Advanced Solid Tumors	Intravenous infusion	Phase I
6.	QPI-1007	Quark Pharmaceuticals	Eye	Optic Atrophy, Non-arteritic Anterior Ischemic Optic Neuropathy	Intravitreal Injection	Phase I
7.	SiRNA Cand5/bevasiranib	Acuity/ later licensed by Opko	Eye	Age-Related Macular Degeneration	Naked siRNA Intravitreal	Terminated at Phase-III

8.	Akli-5	Silence Therapeutics, AtuRNAi technology sublicensed to Pfizer via Quark's license.	Kidney	Acute kidney injury in kidney transplantation	Chemically modified siRNA with AtuRNAi technology, IV	Phase I/II
9.	PF-655 (formerly REDD14NP)		Eye	Age-Related Macular Degeneration	Naked siRNA Intravitreal	Phase II
10.	DGF _i		Kidney	Delayed graft function in kidney.	Chemically modified siRNA with AtuRNAi technology, IV	Phase I/II
11.	TKM-080301	National Cancer Institute (NCI)/National Institutes of Health Clinical Center	Liver	Colorectal, Pancreas, Gastric, Breast and Ovarian cancer with Hepatic Metastase.	Intra-Arterial	Phase I
12.	SYL1001	Sylentis, S.A.	cornea and conjunctival sac	Ocular Pain, Dry Eye	Eye drops: Topical administration	Phase I
13.	QPI-1002 (I5NP)	Quark Pharmaceuticals	Temporarily inhibit expression of the pro-apoptotic protein, p53	Injury of Kidney, Acute renal failure.	IV injection	Phase I
14.	SYL040012	Sylentis, S.A.	Eye	Glaucoma, Ocular Hypertension	Ophthalmic drops	Phase I/II
15.	PF-04523655 (Stratum I) and PF-04523655 With/Without Ranibizumab	Quark Pharmaceuticals	Eye	Choroidal Neovascularization Diabetic Retinopathy and macular edema.	intravitreal (IVT)	Phase II

16.	ALN-TTR01	Anylam pharmaceuticals	Wild type and all mutant forms of TTR, Hepatocyte specific gene silencing	TTR amyloidosis	IV bolus	Phase I
17.	ALN-VSP	Anylam pharmaceuticals	kinesin spindle protein, or KSP and VEGF	Liver cancer	IV bolus	Phase II
18.	ALN-PCS	Anylam pharmaceuticals	subtilisin/kexin type 9, or PCSK9	Hypercholesterolemia	Intravenous	Phase I
19.	ALN-RSV01	Anylam pharmaceuticals	nucleocapsid "N" gene of the RSV genome	Respiratory syncytial virus infection	Intravenous	Phase I

2.5.9. Delivery of Therapeutic siRNA in cancer

The RNAi phenomenon and siRNA have provided new opportunities for the development of innovative medicine to treat previously incurable diseases such as cancer. siRNA is of inherent potency because it exploits the endogenous RNAi pathway, allows specific reduction of disease-associated genes, and is applicable to any gene with a complementary sequence [225]. As cancer belongs to the category of genetic diseases, many important genes associated with various cancers have been discovered, their mutations precisely identified, and the pathways through which they act characterized [226]. The genetic nature of cancer provides solid support for the rationale of siRNA-mediated gene therapy. Indeed, a number of siRNAs have been designed to target dominant oncogenes, malfunctionally regulated oncogenes, or viral oncogenes involved in carcinogenesis. Moreover, therapeutic siRNAs have been investigated for silencing target molecules crucial for tumor-host interactions and tumor resistance to chemo- or

radiotherapy. The silencing of critical cancer-associated target proteins by siRNAs has resulted in significant antiproliferative and/or apoptotic effects [227].

Nevertheless, most approaches to RNAi-mediated gene silencing for cancer therapy have been with cell cultures in the laboratory, and key impediments in the transition to the bedside due to delivery considerations still remain. Delivery systems that can improve siRNA stability and cancer cell-specificity need to be developed, involving the minimizing of off-target and nonspecific immune stimulatory effects. As the route of administration may differ depending on the nature of the cancer, the delivery systems must be optimized for specific cancers. The current status of siRNA delivery systems for various cancers is summarized in **Table 2.6**, and its particular application in lung cancer is discussed below.

Table 2.6 Examples of siRNA delivery systems for treatment of cancers

Delivery systems	Property	Targeted gene	Animal model	Route	Ref.
Liposomes	SNALP	HBV	HBV vector-based mouse	i.v.	[228]
	Cationic liposome	Bcl-2	Liver metastasis mouse model	i.v.	[229]
	Cationic liposome	Integrin α_v	Prostate cancer xenograft	i.t.	[230]
	Cationic liposome	CD31	Prostate cancer xenograft	i.v.	[231]
	Cationic liposome	Bcl-2	Prostate cancer xenograft	i.t.	[229]
	Cationic cardiolipin liposome	Raf-1	Prostate cancer xenograft	i.v.	[232]
	Cationic cardiolipin analogue-based liposomes	c-raf	Breast cancer xenograft	i.v.	[233]
	Neutral liposomes (DOPC)	EphA2	Ovarian cancer xenograft	i.v./i.p.	[234, 235]
	Neutral liposomes (DOPC)	FAK	Ovarian cancer xenograft	i.p.	[236]

Delivery systems	Property	Targeted gene	Animal model	Route	Ref.
	Neutral liposomes (DOPC)	ADRB2	Ovarian cancer xenograft	i.p.	[237]
	Neutral liposomes (DOPC)	IL-8	Ovarian cancer xenograft	i.p.	[238]
	Liposome-polycation-DNA	EGFR	Lung cancer xenograft	i.v.	[239]
	Cationic immunoliposome		Lung metastasis	i.v.	[240]
	Immunoliposome	Her-2	Breast cancer xenograft	i.v.	[241]
Nanoparticles	CaCO ₃ nanoparticle	VEGF	Gastric cancer xenograft	i.t.	[242]
	Chitosan-coated nanoparticle	RhoA	Breast cancer xenograft	i.v.	[243]
	Folated lipid nanoparticle	Her-2	Nasopharyngeal cancer xenograft	i.t.	[244]
Polymers	PEI	Her-2	Ovarian cancer xenograft	i.p.	[245]
	PEI	PTN	Orthotopic glioblastoma	i.c.	[246]
	Poly (ester amine)	Akt1	Urethane-induced lung cancer	Inhalation	[247]
Others	Atelocollagen	HPV18 type E6 and E7	Cervical cancer xenograft	i.t.	[248]
	Chemical modification	HBV	HBV vector-based mouse	i.v.	[249]
	Carbon nanotube	TERT	Lewis lung tumor	i.t.	[196]
	Cyclodextrin-containing polycation	EWS-FLI1	Metastatic Ewing's sarcoma	i.v.	[250]
	Fusion protein (Protamine, HIV-1 envelop Ab)	c-myc, MDM2, VEGF	Subcutaneous B16 melanoma tumor	i.t./i.v.	[251]
	Electroporation	EGFP	Subcutaneous B16F10	i.t.	[252]

Delivery systems	Property	Targeted gene	Animal model	Route	Ref.
			expressing EGFP		
i.v.: intravenous injection, i.p.: intraperitoneal injection, i.t.: intratumoral injection, i.c.: intracerebral injection.					

2.5.10. siRNA Application in Lung Cancer

Lung cancer is the most common cause of cancer-related death in men and the second most common cause of lethality in women. The main types of lung cancer are divided into small cell lung carcinoma and non-small cell lung carcinoma. The treatment modalities for these two types of cancer are different, so it is important to distinguish the two types. Recently, various new molecular targets for lung cancer therapies have been developed; for example, gefitinib (Iressa), which targets the tyrosine kinase domain of the epidermal growth factor receptor, another tyrosine kinase inhibitor known as erlotinib (Tarceva), and the angiogenesis inhibitor bevacizumab. For delivery into lung cancer cell lines, liposomes with arginine octamers on their surface were used for encapsulation of human double-minute gene 2-specific siRNA. The siRNA-loaded arginine octamer-liposomes showed a high stability in blood after 24 h of incubation and showed good transfection efficiencies into several lung cancer cell lines [253].

In another approach, LPD nanoparticles were developed for delivery of siRNA to lung cancer cells. siRNA targeting survivin in PEGylated LPD nanoparticles showed steric stabilization in the presence of serum and exerted antitumor effects by down-regulation of survivin expression, as measured by initiation of apoptosis, inhibition of tumor cell growth, and sensitization of tumor cells to anticancer drug treatment [254]. In an *in vivo* study, LPD nanoparticle formulations provided significant growth inhibition in a lung cancer xenograft mouse model.

LPD nanoparticle-mediated intravenous injection (1.2 mg/kg; 3 daily injections) of siRNAs specific for the epidermal growth factor receptor induced silencing of the target gene, and showed a synergistic effect on anti-lung cancer tumor activity when combined with cisplatin [239]. In a B16F10 lung metastatic mouse model, the LPD nanoparticles and siRNA complexes

afforded silencing of the target gene, and showed little immunotoxicity or development of organ defects after intravenous administration [255].

Cationic immunoliposomes have been used for systemic delivery of siRNA in an animal lung cancer metastasis model induced by the intravenous inoculation of MDA435/LCC6 cells. Cationic liposomes composed of DOTAP and DOPE were modified by conjugation with an anti-transferrin receptor single-chain antibody fragment. The complexes of cationic immunoliposomes with fluorescent siRNA were intravenously injected at a dose of 9 mg/kg into mice. A distribution of fluorescent siRNA was observed in the tumor-metastasized lung tissues, but not in the liver [240]. Polymer-based delivery systems have been studied in lung cancer models. Positively charged single-walled carbon nanotubes (-CONH- (CH₂)₆-NH₃⁺) were used to carry siRNA targeting telomerase reverse transcriptase into cancer cells in vitro and in a lung tumor model. The siRNA coupled to single-walled cationic carbon nanotubes was shown to be internalized to tumor cells in vitro, and suppressed the expression of the target gene. The intratumoral injection of siRNA and the positively charged carbon nanotube complexes into subcutaneous Lewis lung tumors has been reported to reduce tumor growth in mice [256].

Recently, noninvasive aerosolized siRNA delivery systems were developed for lung cancer treatment. Poly(ester amine), a degradable PEI-alt-PEG copolymer, was synthesized by reaction of low-molecularweight PEI with PEG diacrylate [196]. An aerosol of poly(ester amine)/ Akt1-targeting siRNA complex was delivered into mice with urethane-induced lung cancer through a nose-only inhalation system. Following aerosol delivery twice weekly for 4 weeks, Akt1 siRNA delivered in complexes with poly(ester amine) showed down-regulation of Akt related signals and inhibited the progression of tumors in the lung cancer model of K-rasLA1 mice [247].

2.6. RGD Peptide for Targeting

RGD-based strategies include RGD antagonists, RGD conjugates, and RGD nanoparticles. Because of the expression of integrins in various cell types and their role in tumor angiogenesis and progression, integrins have become important therapeutic targets. Integrin antagonists currently preclinically studied or in clinical trials include (i) monoclonal antibodies (such as etaracizumab, Abegrin), (ii) RGD-based antagonists (peptidic or peptidomimetic), (iii) non – RGD antagonists (such as ATN-161, a non-RGD-based peptide inhibitor of integrin $\alpha_5\beta_1$), and (iv) integrin-targeted therapeutics. A cyclic RGD peptide antagonist of $\alpha_v\beta_3$ and $\alpha_v\beta_5$, cilengitide (EMD 121974) showed favorable safety profiles and no-dose-limiting toxicities in phase I clinical trials. Cilengitide is currently being tested in phase II trials in patients with lung and prostate cancer and glioblastomas. In addition, cilengitide has been shown to enhance radiotherapy efficiency in endothelial cell and non-small-cell lung cancer models. Nanocarriers like liposomes, nanoparticles, micelles, etc. can be grafted at their surface with a targeting ligand such as an RGD-based sequence. Several advantages are attributable to these nanocarriers: (i) the size of these nanocarriers (20 – 400 nm) leads to the “passive targeting” of tumors via the so-called enhanced permeability and retention (EPR) effect [257]; (ii) because of the size of these systems, renal filtration is avoided, leading to prolonged blood circulation times and longer accessibility of the ligand to target receptors within the tissue [258]; (iii) RGD-targeted nanocarriers may specifically address drugs to angiogenic endothelial cells and/or cancer cells by the binding of the RGD peptide to $\alpha_v\beta_3$ overexpressed by these cells, allowing the “active targeting” of the tumors [259]; (iv) RGD-targeted nanocarriers can be internalized via receptor-mediated endocytosis, which is not possible with single peptide constructs or with non-targeted nanocarriers; this is particularly interesting for the intracellular delivery of drugs to cancer cells [260]. RGD-targeted nanocarriers have recently proven advantageous in delivering chemotherapeutics, peptides and proteins, nucleic acids, and irradiation. The rationale behind the design of RGD-targeted nanocarriers is the delivery of various pharmacological agents to the $\alpha_v\beta_3$ -expressing tumor vasculature. The cytotoxic drug destroys the tumor vasculature, resulting in the indirect killing of tumor cells induced by the lack of oxygen and nutrients. The tumor growth might be inhibited by preventing tumors from recruiting new blood vessels as suggested by Judah Folkman. $\alpha_v\beta_3$ integrin is up regulated in angiogenic endothelial cells but also in

several tumor cells, leading RGD-targeted nanocarriers to a potential double targeting. However, this double targeting is not yet exploited by systems delivering chemotherapeutics while it is described for integrin antagonists as etaracizumab or for RGD peptides.

2.7. References

1. Tsao AS. Tumors of the Lungs. In: Porter RS, Kaplan JL, editors. *The Merck Manual - for The Healthcare Professionals*. US: MERCK PUBLISHING GROUP; 2010.
2. Horn L, Pao W, Johnson DH. Neoplasms of the Lung. In: Longo D, Fauci A, Kasper D, Hauser S, Jameson J, Loscalzo J, editors. *Harrison's Principles of Internal Medicine*, 18th Edition. United States: McGraw-Hill; 2011.
3. Thun MJ, Hannan LM, Adams-Campbell LL, Boffetta P, Buring JE, Feskanich D, et al. Lung Cancer Occurrence in Never-Smokers: An Analysis of 13 Cohorts and 22 Cancer Registry Studies. *PLoS Med*. 2008;5(9):e185.
4. Mason RJ, V. Courtney Broaddus MD, Murray JJF, Martin TR, Nadel JA. Murray and Nadel's Textbook of Respiratory Medicine: 2-Volume Set: Saunders/Elsevier; 2010.
5. O'Reilly KM, McLaughlin AM, Beckett WS, Sime PJ. Asbestos-related lung disease. *Am Fam Physician*. 2007 Mar 1;75(5):683-8.
6. Aruajo AM, Mendez JC, Coelho AL, Sousa B, Barata F, Figueiredo A, et al. Phase II study of celecoxib with cisplatin plus etoposide in extensive-stage small cell lung cancer. *Cancer Invest*. 2009 May;27(4):391-6.
7. Subramanian J, Govindan R. Lung Cancer in Never Smokers: A Review. *Journal of Clinical Oncology*. 2007 February 10, 2007;25(5):561-70.
8. Raz DJ, He B, Rosell R, Jablons DM. Bronchioloalveolar carcinoma: a review. *Clin Lung Cancer*. 2006 Mar;7(5):313-22.
9. Rosti G, Bevilacqua G, Bidoli P, Portalone L, Santo A, Genestreti G. Small cell lung cancer. *Ann Oncol*. 2006 Mar;17 Suppl 2:ii5-10.
10. Seo JB, Im J-G, Goo JM, Chung MJ, Kim M-Y. Atypical Pulmonary Metastases: Spectrum of Radiologic Findings¹. *Radiographics*. 2001 March 1, 2001;21(2):403-17.
11. Hammond JR, Lee S, Ferguson PJ. [³H]gemcitabine uptake by nucleoside transporters in a human head and neck squamous carcinoma cell line. *J Pharmacol Exp Ther*. 1999 Mar;288(3):1185-91.
12. Brunton L, Lazo J, Parker K. Goodman & Gilman's *The Pharmacological Basis of Therapeutics*: McGraw-Hill Education; 2005.

13. Leung RK, Whittaker PA. RNA interference: from gene silencing to gene-specific therapeutics. *Pharmacology & therapeutics*. 2005 Aug;107(2):222-39.
14. Doyle TH, Mornex F, McKenna WG. The Clinical Implications of Gemcitabine Radiosensitization. *Clinical Cancer Research*. 2001 February 1, 2001;7(2):226-8.
15. Oguri T, Achiwa H, Sato S, Bessho Y, Takano Y, Miyazaki M, et al. The determinants of sensitivity and acquired resistance to gemcitabine differ in non-small cell lung cancer: a role of ABCC5 in gemcitabine sensitivity. *Molecular Cancer Therapeutics*. 2006 July 1, 2006;5(7):1800-6.
16. Johnson DH. Gemcitabine for the treatment of non-small-cell lung cancer. *Oncology (Williston Park)*. 2001 Mar;15(3 Suppl 6):33-9.
17. Rosell R, Danenberg KD, Alberola V, Bepler G, Sanchez JJ, Camps C, et al. Ribonucleotide reductase messenger RNA expression and survival in gemcitabine/cisplatin-treated advanced non-small cell lung cancer patients. *Clin Cancer Res*. 2004 Feb 15;10(4):1318-25.
18. Davidson JD, Ma L, Flagella M, Geeganage S, Gelbert LM, Slapak CA. An increase in the expression of ribonucleotide reductase large subunit 1 is associated with gemcitabine resistance in non-small cell lung cancer cell lines. *Cancer Res*. 2004 Jun 1;64(11):3761-6.
19. Bangham AD, Standish MM, Watkins JC. Diffusion of univalent ions across the lamellae of swollen phospholipids. *Journal of Molecular Biology*. 1965 8//;13(1):238-IN27.
20. Stamp D, Juliano RL. Factors affecting the encapsulation of drugs within liposomes. *Can J Physiol Pharmacol*. 1979 May;57(5):535-9.
21. Riaz M, Weiner N, Martin F. *Pharmaceutical Dosage Forms: Disperse Systems*. Leiberman HA, Reiger MA, Banker GS, editors. New York: Marcel Dekker Inc.; 1988.
22. Ringdorf H, Schlarb B, Venzmer J. *Molecular Architecture and Function of Polymeric Oriented Systems: Models for the Study of Organization, Surface Recognition, and Dynamics of Biomembranes*. *Angewandte Chemie International Edition*. 1988;27(1):113-58.
23. Batzri S, Korn ED. Single bilayer liposomes prepared without sonication. *Biochimica et Biophysica Acta (BBA) - Biomembranes*. 1973 4/16//;298(4):1015-9.

-
24. Deamer D, Bangham AD. Large volume liposomes by an ether vaporization method. *Biochim Biophys Acta*. 1976 Sep 7;443(3):629-34.
 25. Kagawa Y, Racker E. Partial Resolution of the Enzymes Catalyzing Oxidative Phosphorylation: XXV. RECONSTITUTION OF VESICLES CATALYZING 32P_i —ADENOSINE TRIPHOSPHATE EXCHANGE. *Journal of Biological Chemistry*. 1971 September 10, 1971;246(17):5477-87.
 26. Barenholz Y, Amselem S, Lichtenberg D. A new method for preparation of phospholipid vesicles (liposomes) - French press. *FEBS Lett*. 1979 Mar 1;99(1):210-4.
 27. Shew RL, Deamer DW. A novel method for encapsulation of macromolecules in liposomes. *Biochim Biophys Acta*. 1985 Jun 11;816(1):1-8.
 28. Cortesi R, Esposito E, Gambarin S, Telloli P, Menegatti E, Nastruzzi C. Preparation of liposomes by reverse-phase evaporation using alternative organic solvents. *J Microencapsul*. 1999 Mar-Apr;16(2):251-6.
 29. Bangham AD, Hill MV, M.G.A. M. In: Korn ED, editor. *Methods in Membrane Biology*. New York: Plenum Press; 1974. p. 1-68.
 30. Meeren PVd, Laethem MV, Vanderdeelen J, Baert L. Particle Sizing of Liposomal Dispersions: A Critical Evaluation of Some Quasi-Elastic Light-Scattering Data-Analysis Software Programs. *Journal of Liposome Research*. 1992;2(1):23-42.
 31. Talsma H, Crommelin DJ. Liposome as drug delivery system Part-III Stabilization. *Pharm Tech*. 1993;16:48-59.
 32. Law SL, Lo WY, Lin M. Increase of Liposome Stability by Incorporation of Bovine Serum Albumin. *Drug Development and Industrial Pharmacy*. 1994;20(8):1411-23.
 33. Crommelin DJA, van Bommel EMG. Stability of Liposomes on Storage: Freeze Dried, Frozen or as an Aqueous Dispersion. *Pharmaceutical Research*. 1984 1984/07/01;1(4):159-63.
 34. Cohen BE. The permeability of liposomes to nonelectrolytes. I. Activation energies for permeation. *J Membr Biol*. 1975;20(3-4):205-34.

-
35. Papahadjopoulos D, Jacobson K, Nir S, Isac T. Phase transitions in phospholipid vesicles. Fluorescence polarization and permeability measurements concerning the effect of temperature and cholesterol. *Biochim Biophys Acta*. 1973 Jul 6;311(3):330-48.
 36. Betageri GV. Liposomal Encapsulation and Stability of Dideoxyinosine Triphosphate. *Drug Development and Industrial Pharmacy*. 1993;19(5):531-9.
 37. Scherphof G, Dame J, Wilschut J. Interaction of Liposomes with Plasma Proteins. In: Gregoriadis G, editor. *Liposome Technology*. Boca Raton, FL: CRC Press Inc.; 1984. p. 205.
 38. Johnson DH, Chapman D. Preparation of Liposomes. In: Gregoriadis G, editor. *Liposome Technology*. Boca Raton, FL: CRC Press Inc.; 1984. p. 205.
 39. Scherphof G, Dame J, Hoekstra D. In: Knight CG, editor. *Liposomes: From Physical Structure to Therapeutic Applications*. Amsterdam: Elsevier/North Holland Biomedical Press; 1981. p. 310.
 40. Hernandez-Caselles T, Villalain J, Gomez-Fernandez JC. Stability of liposomes on long term storage. *J Pharm Pharmacol*. 1990 Jun;42(6):397-400.
 41. Crommelin DJA, Storm G. Pharmaceutical Aspects of Liposome Preparation, Characterization and Stability. In: Muller BW, editor. *Controlled Drug Delivery*. Studgart: Wissenschaftliche Verlagsgesellschaft mbH; 1987. p. 80-91.
 42. Venkataram S, Awni WM, Jordan K, Rahman YE. Pharmacokinetics of two alternative dosage forms for cyclosporine: liposomes and intralipid. *J Pharm Sci*. 1990 Mar;79(3):216-9.
 43. Hauser H, Strauss G. Stabilization of small unilamellar phospholipid vesicles during spray-drying. *Biochim Biophys Acta*. 1987 Feb 26;897(2):331-4.
 44. Torchilin VP, Weissig V. *Liposomes: A Practical Approach*: OUP Oxford; 2003.
 45. Villalain J, Aranda FJ, Gomez-Fernandez JC. Calorimetric and infrared spectroscopic studies of the interaction of alpha-tocopherol and alpha-tocopheryl acetate with phospholipid vesicles. *Eur J Biochem*. 1986 Jul 1;158(1):141-7.

-
46. Fukuzawa K, Chida H, Tokumura A, Tsukatani H. Antioxidative effect of alpha-tocopherol incorporation into lecithin liposomes on ascorbic acid-Fe²⁺-induced lipid peroxidation. *Arch Biochem Biophys*. 1981 Jan;206(1):173-80.
 47. Gulati M, Grover M, Singh M, Singh S. Study of azathioprine encapsulation into liposomes. *J Microencapsul*. 1998 Jul-Aug;15(4):485-94.
 48. Perugini P, Pavanetto F. Liposomes containing boronophenylalanine for boron neutron capture therapy. *J Microencapsul*. 1998 Jul-Aug;15(4):473-83.
 49. Deasy PB, editor. *Microencapsulation and related drug Processes*. New York: Marcel Dekker Inc.; 1984.
 50. Talsma H, Crommelin DJ. Liposome as drug delivery system Part I: Preparation *Pharm Tech*. 1993;16:96-106.
 51. Lasic DD. *Liposomes: from physics to applications*: Elsevier; 1993.
 52. Sveinsson SJ, Peter Holbrook W. Oral mucosal adhesive ointment containing liposomal corticosteroid. *International Journal of Pharmaceutics*. 1993 6/30;95(1-3):105-9.
 53. Velpandian T, Gupta SK, Gupta YK, Biswas NR, Agarwal HC. Ocular drug targeting by liposomes and their corneal interactions. *J Microencapsul*. 1999 Mar-Apr;16(2):243-50.
 54. Conley J, Yang H, Wilson T, Blasetti K, Di Ninno V, Schnell G, et al. Aerosol delivery of liposome-encapsulated ciprofloxacin: aerosol characterization and efficacy against *Francisella tularensis* infection in mice. *Antimicrob Agents Chemother*. 1997 Jun;41(6):1288-92.
 55. Fresta M, Puglisi G. Corticosteroid dermal delivery with skin-lipid liposomes. *Journal of Controlled Release*. 1997 2/17;44(2-3):141-51.
 56. Trafny EA, Antos-Bielska M, Grzybowski J. Antibacterial activity of liposome-encapsulated antibiotics against *Pseudomonas aeruginosa* attached to the matrix of human dermis. *J Microencapsul*. 1999 Jul-Aug;16(4):419-29.
 57. Allison AC, Gregoriadis G. Liposomes as immunological adjuvants. *Nature*. 1974;252(5480):252-.

58. Gregoriadis G, McCormack B, Obrenovic M, Perrie Y, Saffie R. Liposomes As Immunological Adjuvants and Vaccine Carriers. In: O'Hagan D, editor. *Vaccine Adjuvants*: Springer New York; 2000. p. 137-50.
59. Pagano RE, Weinstein JN. Interactions of liposomes with mammalian cells. *Annu Rev Biophys Bioeng.* 1978;7:435-68.
60. Sugarman SM, Perez-Soler R. Liposomes in the treatment of malignancy: a clinical perspective. *Crit Rev Oncol Hematol.* 1992;12(3):231-42.
61. Tolstoshev P. Gene therapy, concepts, current trials and future directions. *Annu Rev Pharmacol Toxicol.* 1993;33:573-96.
62. Myers WR. Response surface methodology. In: Chow SC, editor. *Encyclopedia of Biopharmaceutical Statistics*. New York: Marcel Dekker; 2003.
63. Singh B, Gupta RK, Ahuja N. Computer-assisted optimization of pharmaceutical formulations. In: Jain NK, editor. *Pharmaceutical Product Development*. New Delhi: CBS Publishers; 2004.
64. Doornbos DA, P. d. Optimization techniques in formulation and processing. In: Swarbrick J, Boylan JC, editors. *Encyclopedia of Pharmaceutical Technology*. New York: Marcel Dekker; 1995.
65. Kannan V, Kandarapu S, Garg S. Optimization techniques for the design and development of novel drug delivery systems Part II. *Pharm Tech.* 2003:102-18.
66. Schwartz JB, Connor RE. Optimization techniques in pharmaceutical formulation and processing. In: Banker GS, Rhodes CT, editors. *Modern Pharmaceutics 3rd Ed.* New York: Marcel Dekker; 1996.
67. Lewis GA. Optimization techniques in formulation and processing. In: Swarbrick J, Boylan JC, editors. *Encyclopedia of Pharmaceutical Technology 2nd Ed.* New York: Marcel Dekker; 2002.
68. Lewis GA, Mathieu D, Phan-Tan-Luu R. *Pharmaceutical Experimental Design 1st Ed.* New York: Marcel Dekker; 1999.
69. Armstrong NA, James KC. *Understanding Experimental Designs and Interpretation in Pharmaceutics.* London: Ellis Horwood; 1990.

-
70. Wehrlé P, Stamm A. Statistical Tools for Process Control and Quality Improvement in the Pharmaceutical Industry. *Drug Development and Industrial Pharmacy*. 1994;20(2):141-64.
 71. Haaland PD. *Experimental Design in Biotechnology*. New York: Marcel Dekker; 1989.
 72. Kettaneh-Wold N. Use of experimental design in the pharmaceutical industry. *J Pharm Biomed Anal*. 1991;9(8):605-10.
 73. Cochran WC, Cox GM. *Experimental Design* 2nd Ed. New York: Marcel Dekker; 1992.
 74. Das MN, Giri NC. *Design and Analysis of Experiments* 2nd Ed. New Delhi: Wiley Eastern Limited; 1994.
 75. Montgomery DC. *Design and Analysis of Experiments* 5th Ed. New York: Wiley; 2001.
 76. Porter SC, Verseput RP, Cunningham CR. Process optimization using design of experiments. *Pharm Tech*. 1997:1-7.
 77. Tye H. Application of statistical "design of experiment" methods in drug discovery. *Drug Discov Today*. 2004;9:485-91.
 78. Araujo PW, Brereton RG. Experimental Design II. Optimization. *Trends in Anal Chem*. 1996;15:63-70.
 79. Singh B, Ahuja N. Response Surface Optimization of Drug Delivery Systems. In: Jain NK, editor. *Progress in Controlled and Novel Drug Delivery Systems* 1st Ed. New Delhi: CBS Publishers; 2004.
 80. Li J. Factorial Designs. In: Chow SC, editor. *Encyclopedia of Biopharmaceutical Statistics*. New York: Marcel Dekker; 2003.
 81. Bolton S. *Pharmaceutical Statistics: Practical and Clinical Applications* 3rd Ed. New York: Marcel Dekker; 1997.
 82. Acikgoz M, Kas HS, Orman M, Hincal AA. Chitosan microspheres of diclofenac sodium: I. application of factorial design and evaluation of release kinetics. *J Microencapsul*. 1996 Mar-Apr;13(2):141-59.
 83. Anderson M, Kraber S, Hansel H, Klick S, Beckenbach R, H. C-B. *Design Expert® Software Version 6 User's Guide*. StatEase Inc. 2002.

-
84. Abu-Izza KA, Garcia-Contreras L, Lu DR. Preparation and evaluation of sustained release AZT-loaded microspheres: optimization of the release characteristics using response surface methodology. *J Pharm Sci.* 1996 Feb;85(2):144-9.
 85. Box GEP, Connor LR, Cousins WR, Davies OL, Hunsworth FR, Sulitto GP, editors. *The Design and Analysis of Industrial Experiments* 2nd Ed. London: Oliver and Boyd; 1960.
 86. Myers RH, Montgomery DC. *Response Surface Methodology: Process and Product Optimization using Design Experiments.* New York: Wiley; 1995.
 87. Korsmeyer RW, Gurny R, Doelker E, Buri P, Peppas NA. Mechanisms of solute release from porous hydrophilic polymers. *International Journal of Pharmaceutics.* 1983 5//;15(1):25-35.
 88. Singh B, Chakkal SK, Ahuja N, editors. *Computer-aided design, development and optimization of controlled release mucoadhesive formulations of atenolol* Proceedings of National Seminar on Pharmaceutics in the Light of Drug Delivery Challenges; 2003; Chandigarh, India.
 89. Box GEP, Hunter WG, Hunger JS. *Statistics for Experimenters.* New York: Wiley; 1978.
 90. Box GEP, Draper NR. *Empirical Model-Building and Response Surfaces.* New York: Wiley; 1987.
 91. Fire A, Xu S, Montgomery MK, Kostas SA, Driver SE, Mello CC. Potent and specific genetic interference by double-stranded RNA in *Caenorhabditis elegans.* *Nature.* 1998 Feb 19;391(6669):806-11.
 92. Jana S, Chakraborty C, Nandi S, Deb JK. RNA interference: potential therapeutic targets. *Applied microbiology and biotechnology.* 2004 Nov;65(6):649-57.
 93. Carninci P, Yasuda J, Hayashizaki Y. Multifaceted mammalian transcriptome. *Current opinion in cell biology.* 2008 Jun;20(3):274-80.
 94. Costa FF. Non-coding RNAs: Meet thy masters. *BioEssays : news and reviews in molecular, cellular and developmental biology.* 2010 Jul;32(7):599-608.
 95. Roshan R, Ghosh T, Scaria V, Pillai B. MicroRNAs: novel therapeutic targets in neurodegenerative diseases. *Drug discovery today.* 2009 Dec;14(23-24):1123-9.

-
96. Bitko V, Musiyenko A, Shulyayeva O, Barik S. Inhibition of respiratory viruses by nasally administered siRNA. *Nature medicine*. 2005 Jan;11(1):50-5.
 97. Dowdy S. The future of personalized cancer treatment: An entirely new direction for RNAi delivery. *Nature biotechnology*. 2009.
 98. Morrissey DV, Lockridge JA, Shaw L, Blanchard K, Jensen K, Breen W, et al. Potent and persistent in vivo anti-HBV activity of chemically modified siRNAs. *Nature biotechnology*. 2005 Aug;23(8):1002-7.
 99. Palliser D, Chowdhury D, Wang QY, Lee SJ, Bronson RT, Knipe DM, et al. An siRNA-based microbicide protects mice from lethal herpes simplex virus 2 infection. *Nature*. 2006 Jan 5;439(7072):89-94.
 100. MacDiarmid JA, Amaro-Mugridge NB, Madrid-Weiss J, Sedliarou I, Wetzel S, Kochar K, et al. Sequential treatment of drug-resistant tumors with targeted minicells containing siRNA or a cytotoxic drug. *Nature biotechnology*. 2009 Jul;27(7):643-51.
 101. Gao K, Huang L. Nonviral methods for siRNA delivery. *Molecular pharmaceuticals*. 2009 May-Jun;6(3):651-8.
 102. Jeong JH, Mok H, Oh YK, Park TG. siRNA conjugate delivery systems. *Bioconjugate chemistry*. 2009 Jan;20(1):5-14.
 103. Hajeri PB, Singh SK. siRNAs: their potential as therapeutic agents--Part I. Designing of siRNAs. *Drug discovery today*. 2009 Sep;14(17-18):851-8.
 104. Bernstein E, Caudy AA, Hammond SM, Hannon GJ. Role for a bidentate ribonuclease in the initiation step of RNA interference. *Nature*. 2001 Jan 18;409(6818):363-6.
 105. Hammond SM, Bernstein E, Beach D, Hannon GJ. An RNA-directed nuclease mediates post-transcriptional gene silencing in *Drosophila* cells. *Nature*. 2000 Mar 16;404(6775):293-6.
 106. Elbashir SM, Lendeckel W, Tuschl T. RNA interference is mediated by 21- and 22-nucleotide RNAs. *Genes & development*. 2001 Jan 15;15(2):188-200.
 107. Elbashir SM, Martinez J, Patkaniowska A, Lendeckel W, Tuschl T. Functional anatomy of siRNAs for mediating efficient RNAi in *Drosophila melanogaster* embryo lysate. *The EMBO journal*. 2001 Dec 3;20(23):6877-88.
-

-
108. Zamore PD, Tuschl T, Sharp PA, Bartel DP. RNAi: double-stranded RNA directs the ATP-dependent cleavage of mRNA at 21 to 23 nucleotide intervals. *Cell*. 2000 Mar 31;101(1):25-33.
 109. Elmen J, Lindow M, Schutz S, Lawrence M, Petri A, Obad S, et al. LNA-mediated microRNA silencing in non-human primates. *Nature*. 2008 Apr 17;452(7189):896-9.
 110. Juliano R, Bauman J, Kang H, Ming X. Biological barriers to therapy with antisense and siRNA oligonucleotides. *Molecular pharmaceuticals*. 2009 May-Jun;6(3):686-95.
 111. Urakami T, Oku N. Current status of siRNA delivery technology and siRNA drug development. *Open Drug Delivery J*. 2007;1:20-7.
 112. Whitehead KA, Langer R, Anderson DG. Knocking down barriers: advances in siRNA delivery. *Nature reviews Drug discovery*. 2009 Feb;8(2):129-38.
 113. Juliano R, Alam MR, Dixit V, Kang H. Mechanisms and strategies for effective delivery of antisense and siRNA oligonucleotides. *Nucleic acids research*. 2008 Jul;36(12):4158-71.
 114. Helene C, Thuong NT, Harel-Bellan A. Control of gene expression by triple helix-forming oligonucleotides. The antigene strategy. *Annals of the New York Academy of Sciences*. 1992 Oct 28;660:27-36.
 115. Blommers MJ, Natt F, Jahnke W, Cuenoud B. Dual recognition of double-stranded DNA by 2'-aminoethoxy-modified oligonucleotides: the solution structure of an intramolecular triplex obtained by NMR spectroscopy. *Biochemistry*. 1998 Dec 22;37(51):17714-25.
 116. Cooney M, Czernuszewicz G, Postel EH, Flint SJ, Hogan ME. Site-specific oligonucleotide binding represses transcription of the human c-myc gene in vitro. *Science*. 1988 Jul 22;241(4864):456-9.
 117. Faruqi AF, Egholm M, Glazer PM. Peptide nucleic acid-targeted mutagenesis of a chromosomal gene in mouse cells. *Proceedings of the National Academy of Sciences*. 1998;95(4):1398.
 118. Faruqi AF, Krawczyk SH, Matteucci MD, Glazer PM. Potassium-resistant triple helix formation and improved intracellular gene targeting by oligodeoxyribonucleotides containing 7-deazaxanthine. *Nucleic acids research*. 1997 Feb 1;25(3):633-40.

-
119. Kher G, Trehan S, Misra A. 7 - Antisense Oligonucleotides and RNA Interference. In: Ambikanandan M, editor. *Challenges in Delivery of Therapeutic Genomics and Proteomics*. London: Elsevier; 2011. p. 325-86.
 120. Moser HE, Dervan PB. Sequence-specific cleavage of double helical DNA by triple helix formation. *Science*. 1987 Oct 30;238(4827):645-50.
 121. Mahato RI, Kawabata K, Takakura Y, Hashida M. In vivo disposition characteristics of plasmid DNA complexed with cationic liposomes. *Journal of drug targeting*. 1995;3(2):149-57.
 122. Borchard G. Chitosans for gene delivery. *Advanced drug delivery reviews*. 2001 Nov 5;52(2):145-50.
 123. Crooke ST. Progress in antisense technology. *Annual review of medicine*. 2004;55:61-95.
 124. Juliano RL. Peptide-oligonucleotide conjugates for the delivery of antisense and siRNA. *Curr Opin Mol Ther*. 2005 Apr;7(2):132-6.
 125. Wang J, Zhang PC, Lu HF, Ma N, Wang S, Mao HQ, et al. New polyphosphoramidate with a spermidine side chain as a gene carrier. *Journal of controlled release : official journal of the Controlled Release Society*. 2002 Sep 18;83(1):157-68.
 126. Sternberg B, Sorgi FL, Huang L. New structures in complex formation between DNA and cationic liposomes visualized by freeze-fracture electron microscopy. *FEBS Lett*. 1994 Dec 19;356(2-3):361-6.
 127. Yi SW, Yune TY, Kim TW, Chung H, Choi YW, Kwon IC, et al. A cationic lipid emulsion/DNA complex as a physically stable and serum-resistant gene delivery system. *Pharmaceutical Research*. 2000 Mar;17(3):314-20.
 128. Alexis F, Pridgen E, Molnar LK, Farokhzad OC. Factors affecting the clearance and biodistribution of polymeric nanoparticles. *Molecular pharmaceutics*. 2008 Jul-Aug;5(4):505-15.
 129. Lasic DD, Martin F. *Stealth liposomes*: CRC; 1995.
 130. Litzinger DC, Brown JM, Wala I, Kaufman SA, Van GY, Farrell CL, et al. Fate of cationic liposomes and their complex with oligonucleotide in vivo. *Biochim Biophys Acta*. 1996 Jun 11;1281(2):139-49.

-
131. Mahato RI, Kawabata K, Nomura T, Takakura Y, Hashida M. Physicochemical and pharmacokinetic characteristics of plasmid DNA/cationic liposome complexes. *Journal of Pharmaceutical Sciences*. 1995 Nov;84(11):1267-71.
 132. Thierry AR, Lunardi-Iskandar Y, Bryant JL, Rabinovich P, Gallo RC, Mahan LC. Systemic gene therapy: biodistribution and long-term expression of a transgene in mice. *Proceedings of the National Academy of Sciences of the United States of America*. 1995 Oct 10;92(21):9742-6.
 133. Bailon P, Won CY. PEG-modified biopharmaceuticals. *Expert opinion on drug delivery*. 2009 Jan;6(1):1-16.
 134. Martin C. Woodle FJM, Annie Yau-Young, Carl T. Redemann, inventor Liposome Technology, Inc., assignee. Liposomes with enhanced circulation time patent 5013556. May 7, 1991.
 135. Rippe B, Rosengren BI, Carlsson O, Venturoli D. Transendothelial transport: the vesicle controversy. *Journal of vascular research*. 2002 Sep-Oct;39(5):375-90.
 136. Schubert W, Frank PG, Razani B, Park DS, Chow CW, Lisanti MP. Caveolae-deficient endothelial cells show defects in the uptake and transport of albumin in vivo. *The Journal of biological chemistry*. 2001 Dec 28;276(52):48619-22.
 137. Uyechi LS, Gagne L, Thurston G, Szoka FC, Jr. Mechanism of lipoplex gene delivery in mouse lung: binding and internalization of fluorescent lipid and DNA components. *Gene therapy*. 2001 Jun;8(11):828-36.
 138. Kircheis R, Wightman L, Schreiber A, Robitza B, Rossler V, Kursa M, et al. Polyethylenimine/DNA complexes shielded by transferrin target gene expression to tumors after systemic application. *Gene therapy*. 2001 Jan;8(1):28-40.
 139. Reddy JA, Abburi C, Hofland H, Howard SJ, Vlahov I, Wils P, et al. Folate-targeted, cationic liposome-mediated gene transfer into disseminated peritoneal tumors. *Gene therapy*. 2002 Nov;9(22):1542-50.
 140. Balyasnikova IV, Yeomans DC, McDonald TB, Danilov SM. Antibody-mediated lung endothelium targeting: in vivo model on primates. *Gene therapy*. 2002 Feb;9(4):282-90.

-
141. Abes R, Arzumanov AA, Moulton HM, Abes S, Ivanova GD, Iversen PL, et al. Cell-penetrating-peptide-based delivery of oligonucleotides: an overview. *Biochemical Society transactions*. 2007 Aug;35(Pt 4):775-9.
 142. Lechardeur D, Lukacs GL. Intracellular barriers to non-viral gene transfer. *Current gene therapy*. 2002 May;2(2):183-94.
 143. Zabner J, Fasbender AJ, Moninger T, Poellinger KA, Welsh MJ. Cellular and molecular barriers to gene transfer by a cationic lipid. *The Journal of biological chemistry*. 1995 Aug 11;270(32):18997-9007.
 144. de Lima MC, Simoes S, Pires P, Gaspar R, Slepushkin V, Duzgunes N. Gene delivery mediated by cationic liposomes: from biophysical aspects to enhancement of transfection. *Molecular membrane biology*. 1999 Jan-Mar;16(1):103-9.
 145. Pereira FB, Goni FM, Nieva JL. Liposome destabilization induced by the HIV-1 fusion peptide effect of a single amino acid substitution. *FEBS Lett*. 1995 Apr 3;362(2):243-6.
 146. Kaneda Y, Uchida T, Kim J, Ishiura M, Okada Y. The improved efficient method for introducing macromolecules into cells using HVJ (Sendai virus) liposomes with gangliosides. *Experimental cell research*. 1987 Nov;173(1):56-69.
 147. Farhood H, Serbina N, Huang L. The role of dioleoyl phosphatidylethanolamine in cationic liposome mediated gene transfer. *Biochim Biophys Acta*. 1995 May 4;1235(2):289-95.
 148. Litzinger DC, Huang L. Phosphatidylethanolamine liposomes: drug delivery, gene transfer and immunodiagnostic applications. *Biochim Biophys Acta*. 1992 Aug 14;1113(2):201-27.
 149. Boussif O, Lezoualc'h F, Zanta MA, Mergny MD, Scherman D, Demeneix B, et al. A versatile vector for gene and oligonucleotide transfer into cells in culture and in vivo: polyethylenimine. *Proceedings of the National Academy of Sciences of the United States of America*. 1995 Aug 1;92(16):7297-301.
 150. Remy JS, Sirlin C, Vierling P, Behr JP. Gene transfer with a series of lipophilic DNA-binding molecules. *Bioconjugate chemistry*. 1994 Nov-Dec;5(6):647-54.
 151. Johnson-Saliba M, Jans DA. Gene therapy: optimising DNA delivery to the nucleus. *Current drug targets*. 2001 Dec;2(4):371-99.

-
152. Xu Y, Szoka FC, Jr. Mechanism of DNA release from cationic liposome/DNA complexes used in cell transfection. *Biochemistry*. 1996 May 7;35(18):5616-23.
 153. Jere D, Arote R, Jiang HL, Kim YK, Cho MH, Cho CS. Bioreducible polymers for efficient gene and siRNA delivery. *Biomedical materials*. 2009 Apr;4(2):025020.
 154. Blaszczyk J, Tropea JE, Bubunenko M, Routzahn KM, Waugh DS, Court DL, et al. Crystallographic and modeling studies of RNase III suggest a mechanism for double-stranded RNA cleavage. *Structure*. 2001 Dec;9(12):1225-36.
 155. Martinez J, Patkaniowska A, Urlaub H, Luhrmann R, Tuschl T. Single-stranded antisense siRNAs guide target RNA cleavage in RNAi. *Cell*. 2002 Sep 6;110(5):563-74.
 156. Meister G, Tuschl T. Mechanisms of gene silencing by double-stranded RNA. *Nature*. 2004 Sep 16;431(7006):343-9.
 157. Vickers TA, Koo S, Bennett CF, Crooke ST, Dean NM, Baker BF. Efficient reduction of target RNAs by small interfering RNA and RNase H-dependent antisense agents. A comparative analysis. *The Journal of biological chemistry*. 2003 Feb 28;278(9):7108-18.
 158. Tang G. siRNA and miRNA: an insight into RISCs. *Trends Biochem Sci*. 2005 Feb;30(2):106-14.
 159. Khatri NI, Rathi MN, Kolte AA, Kore GG, Lalan MS, Trehan S, et al. Patents Review in siRNA Delivery for Pulmonary Disorders. *Recent Pat Drug Deliv Formul*. 2012 Apr 1;6(1):45-65.
 160. Bumcrot D, Manoharan M, Koteliansky V, Sah DW. RNAi therapeutics: a potential new class of pharmaceutical drugs. *Nat Chem Biol*. 2006 Dec;2(12):711-9.
 161. Seyhan AA. RNAi: a potential new class of therapeutic for human genetic disease. *Hum Genet*. 2011 Nov;130(5):583-605.
 162. Lai EC. Micro RNAs are complementary to 3' UTR sequence motifs that mediate negative post-transcriptional regulation. *Nat Genet*. 2002 Apr;30(4):363-4.
 163. Gitlin L, Karelsky S, Andino R. Short interfering RNA confers intracellular antiviral immunity in human cells. *Nature*. 2002 Jul 25;418(6896):430-4.

-
164. Banerjea A, Li MJ, Bauer G, Remling L, Lee NS, Rossi J, et al. Inhibition of HIV-1 by lentiviral vector-transduced siRNAs in T lymphocytes differentiated in SCID-hu mice and CD34+ progenitor cell-derived macrophages. *Mol Ther*. 2003 Jul;8(1):62-71.
 165. Ge Q, Filip L, Bai A, Nguyen T, Eisen HN, Chen J. Inhibition of influenza virus production in virus-infected mice by RNA interference. *Proceedings of the National Academy of Sciences of the United States of America*. 2004 Jun 8;101(23):8676-81.
 166. Chen W, Liu M, Jiao Y, Yan W, Wei X, Chen J, et al. Adenovirus-mediated RNA interference against foot-and-mouth disease virus infection both in vitro and in vivo. *J Virol*. 2006 Apr;80(7):3559-66.
 167. Mattes J, Collison A, Plank M, Phipps S, Foster PS. Antagonism of microRNA-126 suppresses the effector function of TH2 cells and the development of allergic airways disease. *Proceedings of the National Academy of Sciences of the United States of America*. 2009 Nov 3;106(44):18704-9.
 168. Lanford RE, Hildebrandt-Eriksen ES, Petri A, Persson R, Lindow M, Munk ME, et al. Therapeutic silencing of microRNA-122 in primates with chronic hepatitis C virus infection. *Science*. 2010 Jan 8;327(5962):198-201.
 169. Ding H, Schwarz DS, Keene A, Affar el B, Fenton L, Xia X, et al. Selective silencing by RNAi of a dominant allele that causes amyotrophic lateral sclerosis. *Aging Cell*. 2003 Aug;2(4):209-17.
 170. Pushparaj PN, Aarthi JJ, Manikandan J, Kumar SD. siRNA, miRNA, and shRNA: in vivo applications. *J Dent Res*. 2008 Nov;87(11):992-1003.
 171. Ralph GS, Radcliffe PA, Day DM, Carthy JM, Leroux MA, Lee DC, et al. Silencing mutant SOD1 using RNAi protects against neurodegeneration and extends survival in an ALS model. *Nature medicine*. 2005 Apr;11(4):429-33.
 172. Rodriguez-Lebron E, Denovan-Wright EM, Nash K, Lewin AS, Mandel RJ. Intrastratial rAAV-mediated delivery of anti-huntingtin shRNAs induces partial reversal of disease progression in R6/1 Huntington's disease transgenic mice. *Mol Ther*. 2005 Oct;12(4):618-33.

-
173. Wilda M, Fuchs U, Wossmann W, Borkhardt A. Killing of leukemic cells with a BCR/ABL fusion gene by RNA interference (RNAi). *Oncogene*. 2002 Aug 22;21(37):5716-24.
 174. Brummelkamp TR, Bernards R, Agami R. Stable suppression of tumorigenicity by virus-mediated RNA interference. *Cancer Cell*. 2002 Sep;2(3):243-7.
 175. Ryther RC, Flynt AS, Phillips JA, 3rd, Patton JG. siRNA therapeutics: big potential from small RNAs. *Gene therapy*. 2005 Jan;12(1):5-11.
 176. Kim B, Tang Q, Biswas PS, Xu J, Schiffelers RM, Xie FY, et al. Inhibition of ocular angiogenesis by siRNA targeting vascular endothelial growth factor pathway genes: therapeutic strategy for herpetic stromal keratitis. *Am J Pathol*. 2004 Dec;165(6):2177-85.
 177. Sumimoto H, Yamagata S, Shimizu A, Miyoshi H, Mizuguchi H, Hayakawa T, et al. Gene therapy for human small-cell lung carcinoma by inactivation of Skp-2 with virally mediated RNA interference. *Gene therapy*. 2005 Jan;12(1):95-100.
 178. Shin JJ, Katayama T, Michaud WA, Rocco JW. Short hairpin RNA system to inhibit human p16 in squamous cell carcinoma. *Arch Otolaryngol Head Neck Surg*. 2004 Jan;130(1):68-73.
 179. Zhang MS, Zhou YF, Zhang WJ, Zhang XL, Pan Q, Ji XM, et al. Apoptosis induced by short hairpin RNA-mediated STAT6 gene silencing in human colon cancer cells. *Chin Med J (Engl)*. 2006 May 20;119(10):801-8.
 180. Guttilla IK, White BA. Coordinate regulation of FOXO1 by miR-27a, miR-96, and miR-182 in breast cancer cells. *The Journal of biological chemistry*. 2009 Aug 28;284(35):23204-16.
 181. Fluiter K, Frieden M, Vreijling J, Rosenbohm C, De Wissel MB, Christensen SM, et al. On the in vitro and in vivo properties of four locked nucleic acid nucleotides incorporated into an anti-H-Ras antisense oligonucleotide. *Chembiochem*. 2005 Jun;6(6):1104-9.
 182. Kato M, Paranjape T, Muller RU, Nallur S, Gillespie E, Keane K, et al. The mir-34 microRNA is required for the DNA damage response in vivo in *C. elegans* and in vitro in human breast cancer cells. *Oncogene*. 2009 Jun 25;28(25):2419-24.

-
183. Anand S, Majeti BK, Acevedo LM, Murphy EA, Mukthavaram R, Scheppke L, et al. MicroRNA-132-mediated loss of p120RasGAP activates the endothelium to facilitate pathological angiogenesis. *Nature medicine*. 2010 Aug;16(8):909-14.
 184. Sun SG, Zheng B, Han M, Fang XM, Li HX, Miao SB, et al. miR-146a and Kruppel-like factor 4 form a feedback loop to participate in vascular smooth muscle cell proliferation. *EMBO Rep*. 2011 Jan;12(1):56-62.
 185. Fasanaro P, D'Alessandra Y, Di Stefano V, Melchionna R, Romani S, Pompilio G, et al. MicroRNA-210 modulates endothelial cell response to hypoxia and inhibits the receptor tyrosine kinase ligand Ephrin-A3. *The Journal of biological chemistry*. 2008 Jun 6;283(23):15878-83.
 186. Li SD, Huang L. Non-viral is superior to viral gene delivery. *Journal of controlled release : official journal of the Controlled Release Society*. 2007 Nov 20;123(3):181-3.
 187. Grimm D, Streetz KL, Jopling CL, Storm TA, Pandey K, Davis CR, et al. Fatality in mice due to oversaturation of cellular microRNA/short hairpin RNA pathways. *Nature*. 2006 May 25;441(7092):537-41.
 188. Tan PH, Yang LC, Shih HC, Lan KC, Cheng JT. Gene knockdown with intrathecal siRNA of NMDA receptor NR2B subunit reduces formalin-induced nociception in the rat. *Gene therapy*. 2005 Jan;12(1):59-66.
 189. Luo MC, Zhang DQ, Ma SW, Huang YY, Shuster SJ, Porreca F, et al. An efficient intrathecal delivery of small interfering RNA to the spinal cord and peripheral neurons. *Mol Pain*. 2005;1:29.
 190. Qing G. MK, James A. M. , inventor Qing G., Mukesh K., James A. M. , assignee. RNAi therapeutic for respiratory virus infection patent US20100254945. 2010.
 191. Wang JC, Lai S, Guo X, Zhang X, de Crombrughe B, Sonnylal S, et al. Attenuation of fibrosis in vitro and in vivo with SPARC siRNA. *Arthritis Res Ther*. 2010;12(2):R60.
 192. Anil K.S. GLB, Charles N.L., Arturo C.R., inventor Delivery of siRNA by neutral lipid compositions 2009.
 193. de Fougerolles AR. Delivery vehicles for small interfering RNA in vivo. *Hum Gene Ther*. 2008 Feb;19(2):125-32.

-
194. Brower V. RNA interference advances to early-stage clinical trials. *J Natl Cancer Inst.* 2010 Oct 6;102(19):1459-61.
 195. Katas H, Alpar HO. Development and characterisation of chitosan nanoparticles for siRNA delivery. *Journal of controlled release : official journal of the Controlled Release Society.* 2006 Oct 10;115(2):216-25.
 196. Park MR, Han KO, Han IK, Cho MH, Nah JW, Choi YJ, et al. Degradable polyethylenimine-alt-poly(ethylene glycol) copolymers as novel gene carriers. *Journal of controlled release : official journal of the Controlled Release Society.* 2005 Jul 20;105(3):367-80.
 197. Rao DD, Vorhies JS, Senzer N, Nemunaitis J. siRNA vs. shRNA: similarities and differences. *Advanced drug delivery reviews.* 2009 Jul 25;61(9):746-59.
 198. Pardridge WM. shRNA and siRNA delivery to the brain. *Advanced drug delivery reviews.* 2007 Mar 30;59(2-3):141-52.
 199. Shen Y. Advances in the development of siRNA-based therapeutics for cancer. *IDrugs.* 2008 Aug;11(8):572-8.
 200. Alshamsan A, Haddadi A, Incani V, Samuel J, Lavasanifar A, Uludag H. Formulation and delivery of siRNA by oleic acid and stearic acid modified polyethylenimine. *Molecular pharmaceutics.* 2009 Jan-Feb;6(1):121-33.
 201. Watts JK, Deleavey GF, Damha MJ. Chemically modified siRNA: tools and applications. *Drug Discov Today.* 2008 Oct;13(19-20):842-55.
 202. Zhang C, Newsome JT, Mewani R, Pei J, Gokhale PC, Kasid UN. Systemic delivery and pre-clinical evaluation of nanoparticles containing antisense oligonucleotides and siRNAs. *Methods Mol Biol.* 2009;480:65-83.
 203. Aigner A. Cellular delivery in vivo of siRNA-based therapeutics. *Curr Pharm Des.* 2008;14(34):3603-19.
 204. Law M, Jafari M, Chen P. Physicochemical characterization of siRNA-peptide complexes. *Biotechnol Prog.* 2008 Jul-Aug;24(4):957-63.
 205. Neidhardt J, Wycisk K, Klockener-Gruissem B. [Viral and nonviral gene therapy for treatment of retinal diseases]. *Ophthalmologe.* 2005 Aug;102(8):764-71.

-
206. Turner JJ, Jones S, Fabani MM, Ivanova G, Arzumanov AA, Gait MJ. RNA targeting with peptide conjugates of oligonucleotides, siRNA and PNA. *Blood Cells Mol Dis.* 2007 Jan-Feb;38(1):1-7.
 207. McCaffrey AP, Meuse L, Pham TT, Conklin DS, Hannon GJ, Kay MA. RNA interference in adult mice. *Nature.* 2002 Jul 4;418(6893):38-9.
 208. Layzer JM, McCaffrey AP, Tanner AK, Huang Z, Kay MA, Sullenger BA. In vivo activity of nuclease-resistant siRNAs. *RNA.* 2004 May;10(5):766-71.
 209. Matsuda T, Cepko CL. Electroporation and RNA interference in the rodent retina in vivo and in vitro. *Proceedings of the National Academy of Sciences of the United States of America.* 2004 Jan 6;101(1):16-22.
 210. Zender L, Hutker S, Liedtke C, Tillmann HL, Zender S, Mundt B, et al. Caspase 8 small interfering RNA prevents acute liver failure in mice. *Proceedings of the National Academy of Sciences of the United States of America.* 2003 Jun 24;100(13):7797-802.
 211. Uprichard SL, Boyd B, Althage A, Chisari FV. Clearance of hepatitis B virus from the liver of transgenic mice by short hairpin RNAs. *Proceedings of the National Academy of Sciences of the United States of America.* 2005 Jan 18;102(3):773-8.
 212. Boado RJ, Zhang Y, Xia CF, Pardridge WM. Fusion antibody for Alzheimer's disease with bidirectional transport across the blood-brain barrier and abeta fibril disaggregation. *Bioconjugate chemistry.* 2007 Mar-Apr;18(2):447-55.
 213. Lovett-Racke AE, Cravens PD, Gocke AR, Racke MK, Stuve O. Therapeutic potential of small interfering RNA for central nervous system diseases. *Arch Neurol.* 2005 Dec;62(12):1810-3.
 214. Valadi H, Ekstrom K, Bossios A, Sjostrand M, Lee JJ, Lotvall JO. Exosome-mediated transfer of mRNAs and microRNAs is a novel mechanism of genetic exchange between cells. *Nat Cell Biol.* 2007 Jun;9(6):654-9.
 215. Kumar P, Wu H, McBride JL, Jung KE, Kim MH, Davidson BL, et al. Transvascular delivery of small interfering RNA to the central nervous system. *Nature.* 2007 Jul 5;448(7149):39-43.

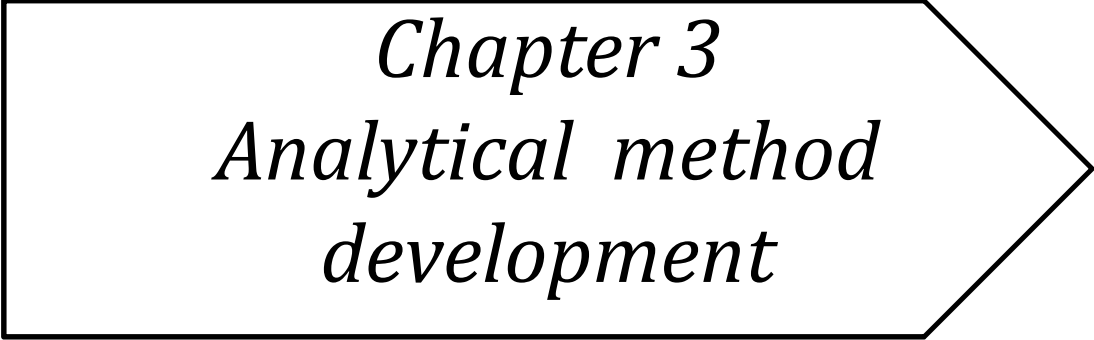
-
216. Alvarez-Erviti L, Seow Y, Yin H, Betts C, Lakhali S, Wood MJ. Delivery of siRNA to the mouse brain by systemic injection of targeted exosomes. *Nat Biotechnol*. 2011 Apr;29(4):341-5.
217. Boden D, Pusch O, Ramratnam B. HIV-1-specific RNA interference. *Curr Opin Mol Ther*. 2004 Aug;6(4):373-80.
218. Bennasser Y, Le SY, Benkirane M, Jeang KT. Evidence that HIV-1 encodes an siRNA and a suppressor of RNA silencing. *Immunity*. 2005 May;22(5):607-19.
219. Chu TC, Twu KY, Ellington AD, Levy M. Aptamer mediated siRNA delivery. *Nucleic acids research*. 2006;34(10):e73.
220. Kumar P, Ban HS, Kim SS, Wu H, Pearson T, Greiner DL, et al. T cell-specific siRNA delivery suppresses HIV-1 infection in humanized mice. *Cell*. 2008 Aug 22;134(4):577-86.
221. Davis ME, Zuckerman JE, Choi CH, Seligson D, Tolcher A, Alabi CA, et al. Evidence of RNAi in humans from systemically administered siRNA via targeted nanoparticles. *Nature*. 2010 Apr 15;464(7291):1067-70.
222. Shi N, Pardridge WM. Noninvasive gene targeting to the brain. *Proceedings of the National Academy of Sciences of the United States of America*. 2000 Jun 20;97(13):7567-72.
223. Xia CF, Zhang Y, Boado RJ, Pardridge WM. Intravenous siRNA of brain cancer with receptor targeting and avidin-biotin technology. *Pharmaceutical Research*. 2007 Dec;24(12):2309-16.
224. Kasinski AL, Slack FJ. Epigenetics and genetics. MicroRNAs en route to the clinic: progress in validating and targeting microRNAs for cancer therapy. *Nat Rev Cancer*. 2011 Dec;11(12):849-64.
225. Leung RK, Whittaker PA. RNA interference: from gene silencing to gene-specific therapeutics. *Pharmacol Ther*. 2005 Aug;107(2):222-39.
226. Vogelstein B, Kinzler KW. Cancer genes and the pathways they control. *Nature medicine*. 2004 08//print;10(8):789-99.
227. Pai SI, Lin YY, Macaes B, Meneshian A, Hung CF, Wu TC. Prospects of RNA interference therapy for cancer. *Gene Ther*. 2006 Mar;13(6):464-77.
-

-
228. Morrissey DV, Lockridge JA, Shaw L, Blanchard K, Jensen K, Breen W, et al. Potent and persistent in vivo anti-HBV activity of chemically modified siRNAs. *Nat Biotechnol.* 2005 Aug;23(8):1002-7.
229. Yano J, Hirabayashi K, Nakagawa S, Yamaguchi T, Nogawa M, Kashimori I, et al. Antitumor activity of small interfering RNA/cationic liposome complex in mouse models of cancer. *Clin Cancer Res.* 2004 Nov 15;10(22):7721-6.
230. Bisanz K, Yu J, Edlund M, Spohn B, Hung MC, Chung LW, et al. Targeting ECM-integrin interaction with liposome-encapsulated small interfering RNAs inhibits the growth of human prostate cancer in a bone xenograft imaging model. *Mol Ther.* 2005 Oct;12(4):634-43.
231. Santel A, Aleku M, Keil O, Endruschat J, Esche V, Durieux B, et al. RNA interference in the mouse vascular endothelium by systemic administration of siRNA-lipoplexes for cancer therapy. *Gene therapy.* 2006 Sep;13(18):1360-70.
232. Pal A, Ahmad A, Khan S, Sakabe I, Zhang C, Kasid UN, et al. Systemic delivery of RafsiRNA using cationic cardiolipin liposomes silences Raf-1 expression and inhibits tumor growth in xenograft model of human prostate cancer. *Int J Oncol.* 2005 Apr;26(4):1087-91.
233. Chien PY, Wang J, Carbonaro D, Lei S, Miller B, Sheikh S, et al. Novel cationic cardiolipin analogue-based liposome for efficient DNA and small interfering RNA delivery in vitro and in vivo. *Cancer Gene Ther.* 2005 Mar;12(3):321-8.
234. Landen CN, Jr., Chavez-Reyes A, Bucana C, Schmandt R, Deavers MT, Lopez-Berestein G, et al. Therapeutic EphA2 gene targeting in vivo using neutral liposomal small interfering RNA delivery. *Cancer Res.* 2005 Aug 1;65(15):6910-8.
235. Landen CN, Merritt WM, Mangala LS, Sanguino AM, Bucana C, Lu C, et al. Intraperitoneal delivery of liposomal siRNA for therapy of advanced ovarian cancer. *Cancer Biol Ther.* 2006 Dec;5(12):1708-13.
236. Halder J, Kamat AA, Landen CN, Jr., Han LY, Lutgendorf SK, Lin YG, et al. Focal adhesion kinase targeting using in vivo short interfering RNA delivery in neutral liposomes for ovarian carcinoma therapy. *Clin Cancer Res.* 2006 Aug 15;12(16):4916-24.
-

-
237. Thaker PH, Han LY, Kamat AA, Arevalo JM, Takahashi R, Lu C, et al. Chronic stress promotes tumor growth and angiogenesis in a mouse model of ovarian carcinoma. *Nature medicine*. 2006 Aug;12(8):939-44.
238. Merritt WM, Lin YG, Spannuth WA, Fletcher MS, Kamat AA, Han LY, et al. Effect of interleukin-8 gene silencing with liposome-encapsulated small interfering RNA on ovarian cancer cell growth. *J Natl Cancer Inst*. 2008 Mar 5;100(5):359-72.
239. Li SD, Chen YC, Hackett MJ, Huang L. Tumor-targeted delivery of siRNA by self-assembled nanoparticles. *Mol Ther*. 2008 Jan;16(1):163-9.
240. Pirollo KF, Zon G, Rait A, Zhou Q, Yu W, Hogrefe R, et al. Tumor-targeting nanoimmunoliposome complex for short interfering RNA delivery. *Hum Gene Ther*. 2006 Jan;17(1):117-24.
241. Hogrefe RI, Lebedev AV, Zon G, Pirollo KF, Rait A, Zhou Q, et al. Chemically modified short interfering hybrids (siHYBRIDS): nanoimmunoliposome delivery in vitro and in vivo for RNAi of HER-2. *Nucleosides Nucleotides Nucleic Acids*. 2006;25(8):889-907.
242. He XW, Liu T, Chen YX, Cheng DJ, Li XR, Xiao Y, et al. Calcium carbonate nanoparticle delivering vascular endothelial growth factor-C siRNA effectively inhibits lymphangiogenesis and growth of gastric cancer in vivo. *Cancer Gene Ther*. 2008 Mar;15(3):193-202.
243. Pille JY, Li H, Blot E, Bertrand JR, Pritchard LL, Opolon P, et al. Intravenous delivery of anti-RhoA small interfering RNA loaded in nanoparticles of chitosan in mice: safety and efficacy in xenografted aggressive breast cancer. *Hum Gene Ther*. 2006 Oct;17(10):1019-26.
244. Yoshizawa T, Hattori Y, Hakoshima M, Koga K, Maitani Y. Folate-linked lipid-based nanoparticles for synthetic siRNA delivery in KB tumor xenografts. *Eur J Pharm Biopharm*. 2008 Nov;70(3):718-25.
245. Urban-Klein B, Werth S, Abuharbeid S, Czubayko F, Aigner A. RNAi-mediated gene-targeting through systemic application of polyethylenimine (PEI)-complexed siRNA in vivo. *Gene therapy*. 2005 Mar;12(5):461-6.
-

-
246. Grzelinski M, Urban-Klein B, Martens T, Lamszus K, Bakowsky U, Hobel S, et al. RNA interference-mediated gene silencing of pleiotrophin through polyethylenimine-complexed small interfering RNAs in vivo exerts antitumoral effects in glioblastoma xenografts. *Hum Gene Ther.* 2006 Jul;17(7):751-66.
247. Xu CX, Jere D, Jin H, Chang SH, Chung YS, Shin JY, et al. Poly(ester amine)-mediated, aerosol-delivered Akt1 small interfering RNA suppresses lung tumorigenesis. *Am J Respir Crit Care Med.* 2008 Jul 1;178(1):60-73.
248. Fujii T, Saito M, Iwasaki E, Ochiya T, Takei Y, Hayashi S, et al. Intratumor injection of small interfering RNA-targeting human papillomavirus 18 E6 and E7 successfully inhibits the growth of cervical cancer. *Int J Oncol.* 2006 Sep;29(3):541-8.
249. Morrissey DV, Blanchard K, Shaw L, Jensen K, Lockridge JA, Dickinson B, et al. Activity of stabilized short interfering RNA in a mouse model of hepatitis B virus replication. *Hepatology.* 2005 Jun;41(6):1349-56.
250. Hu-Lieskovan S, Heidel JD, Bartlett DW, Davis ME, Triche TJ. Sequence-specific knockdown of EWS-FLI1 by targeted, nonviral delivery of small interfering RNA inhibits tumor growth in a murine model of metastatic Ewing's sarcoma. *Cancer Res.* 2005 Oct 1;65(19):8984-92.
251. Song E, Zhu P, Lee SK, Chowdhury D, Kussman S, Dykxhoorn DM, et al. Antibody mediated in vivo delivery of small interfering RNAs via cell-surface receptors. *Nat Biotechnol.* 2005 Jun;23(6):709-17.
252. Golzio M, Mazzolini L, Ledoux A, Paganin A, Izard M, Hellaudais L, et al. In vivo gene silencing in solid tumors by targeted electrically mediated siRNA delivery. *Gene therapy.* 2007 May;14(9):752-9.
253. Zhang C, Tang N, Liu X, Liang W, Xu W, Torchilin VP. siRNA-containing liposomes modified with polyarginine effectively silence the targeted gene. *Journal of controlled release : official journal of the Controlled Release Society.* 2006 May 15;112(2):229-39.
254. Li SD, Huang L. Targeted delivery of antisense oligodeoxynucleotide and small interference RNA into lung cancer cells. *Molecular pharmaceutics.* 2006 Sep-Oct;3(5):579-88.
-

255. Li SD, Chono S, Huang L. Efficient gene silencing in metastatic tumor by siRNA formulated in surface-modified nanoparticles. *Journal of controlled release : official journal of the Controlled Release Society*. 2008 Feb 18;126(1):77-84.
256. Zhang Z, Yang X, Zhang Y, Zeng B, Wang S, Zhu T, et al. Delivery of telomerase reverse transcriptase small interfering RNA in complex with positively charged single-walled carbon nanotubes suppresses tumor growth. *Clin Cancer Res*. 2006 Aug 15;12(16):4933-9.
257. Maeda H, Sawa T, Konno T. Mechanism of tumor-targeted delivery of macromolecular drugs, including the EPR effect in solid tumor and clinical overview of the prototype polymeric drug SMANCS. *Journal of controlled release : official journal of the Controlled Release Society*. 2001 Jul 6;74(1-3):47-61.
258. Malam Y, Loizidou M, Seifalian AM. Liposomes and nanoparticles: nanosized vehicles for drug delivery in cancer. *Trends Pharmacol Sci*. 2009 Nov;30(11):592-9.
259. Byrne JD, Betancourt T, Brannon-Peppas L. Active targeting schemes for nanoparticle systems in cancer therapeutics. *Adv Drug Deliv Rev*. 2008 Dec 14;60(15):1615-26.
260. Folkman J. Tumor angiogenesis: therapeutic implications. *N Engl J Med*. 1971 Nov 18;285(21):1182-6.



Chapter 3
Analytical method
development

3.1. Preparation of Calibration Plot of siRNA

Spectrophotometric method was used for determination of siRNA content of the formulation. The determination was based on the zero order UV spectra of siRNA at the λ_{max} of 260 nm in nuclease-free water [1, 2].

3.1.1 Reagents

- i. Nuclease Free Water
- ii. DEPC- diethylpyrocarbonate water

3.1.2 Method of Analysis

Every apparatus was washed with DEPC water for removing any DNAses and RNAses. High-purity reference standard (single-use vials of lyophilized siRNA) was used for construction of calibration curve. Standard solution of siRNA was prepared by dissolving 0.4 mg of siRNA in 10 ml of nuclease-free water to get concentration of 40 ppm. Secondary Standard solutions were prepared by diluting appropriate quantities of standard stock solution with nuclease-free water to obtain concentrations of 8, 16, 24 and 32 ppm. Absorbances of secondary standard as well as standard stock solutions were recorded at 260 nm using a dual beam spectrophotometer (UV-1800, Shimadzu, JAPAN). Absorbance of each dilute solution was recorded in triplicate.

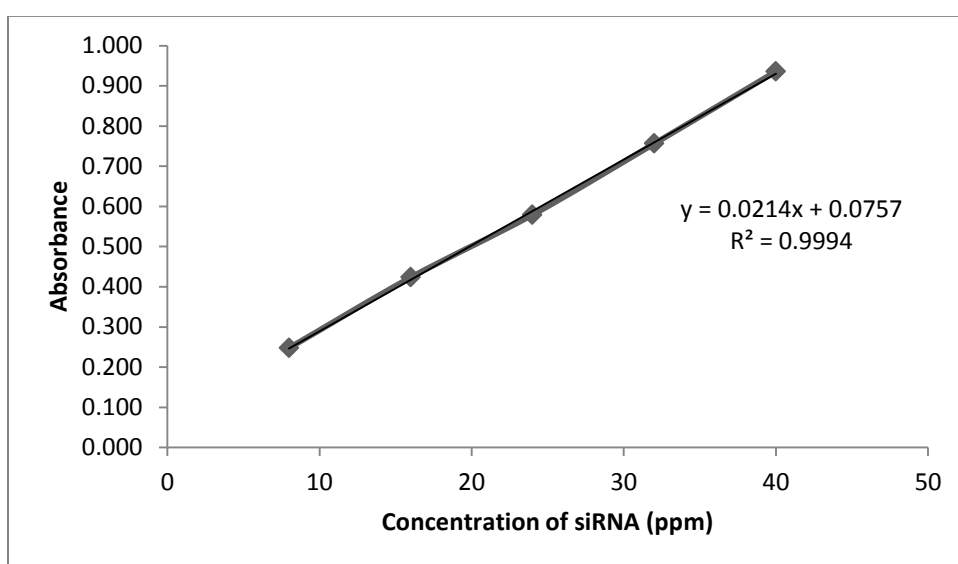
Mean values of absorbance along with their standard deviations (SD) are shown in **Table 3.1**. Calibration plot of siRNA has shown in **Figure 3.1**. Calibration plot showed a straight line expressed by the equation, $y = 0.0217x + 0.0537$, with regression coefficient of 0.9991.

The concentrations of the stock standards were calculated from molecular weights of siRNA and its absorptivity.

Table 3.1 UV Spectrophotometric Absorbance of siRNA

Concentration of siRNA (ppm)	Mean Absorbance (n=3)*	Standard Deviation
8	0.246	0.003
16	0.417	0.002
24	0.579	0.004
32	0.756	0.003
40	0.936	0.006

*Experiments were performed in triplicate.

**Figure 3.1 Calibration Plot of siRNA**

3.1.3 Accuracy and Precision of Method

UV-spectrophotometric method was evaluated for precision and accuracy by determining % recovery and relative standard deviation (%RSD) respectively. siRNA sample solutions of 8, 24 and 40 ppm were prepared using nuclease-free water. Absorbance of each solution was recorded and % recovery was calculated to determine accuracy. Precision was determined by measuring absorbance of each sample at different time periods and calculating % relative standard deviation. All the measurements were made in triplicate.

Table 3.2, Table 3.3 and **Table 3.4** represents accuracy, intraday and interday precision of the method respectively. As it can be seen, the % recovery was found to be between 99.5% to

100.5% and %RSD of interday and intraday measurements below 1%, the method was found to comply the FDA and ICH guidelines on accuracy and precision of an analytical method validation [3, 4].

Table 3.2 Accuracy of the Method

Concentration (ppm)	Obtained Concentration* (n=3) (ppm)	Standard Deviation(SD)	%Recovery
8	8.020	0.072	100.25
24	23.940	0.085	99.75
40	40.074	0.057	100.19

*Experiment was performed in triplicate.

Table 3.3 Intraday Precision of the Method

Concentration (ppm)	Obtained Concentration* (n=3) (ppm)	Standard Deviation(SD)	%Relative Standard Deviation
8	8.020	0.072	0.904
24	23.940	0.085	0.356
40	40.074	0.057	0.142

*Experiment was performed in triplicate.

Table 3.4 Interday Precision of the Method

	Concentration (ppm)	Obtained Concentration (n=3) (ppm)	Standard Deviation(SD)	%Relative Standard Deviation
Day 1	8	8.014	0.069	0.865
	24	24.016	0.011	0.046
	40	40.033	0.060	0.151
Day 2	8	7.986	0.037	0.462
	24	24.034	0.050	0.206
	40	40.039	0.066	0.164
Day 3	8	8.040	0.050	0.621
	24	24.018	0.024	0.102
	40	40.041	0.059	0.148

*Experiments were performed in triplicate.

3.2. Analysis of Calcium Content of Liposomes

Direct complexometric titration method was used for analysis of calcium content of liposomes. The determination was based on the formation of 1:1 complex between calcium and ethylene diamine tetraacetic acid (EDTA) [5-7].

3.2.1. Introduction

The complexometric titration involves titrating metal ions with a complexing agent or chelating agent (Ligand) and is commonly referred to as complexometric titration. In this method, a simple ion is transformed into a complex ion and the equivalence point is determined by using metal indicators or electrometrically. Various other names such as chilometric titrations, chilometry, chilatometric titrations and EDTA titrations have been used to describe this method. All these terms refer to same analytical method and they have resulted from the use of EDTA (Ethylene diamine tetra acetic acid) and other chilons. These chilons react with metal ions to form a special type of complex known as chelate.

Metal ions in solution are always solvated, i.e. a definite number of solvent molecules (usually 2, 4 or 6) are firmly bound to the metal ion. However, these bound solvent molecules are replaced by other solvent molecules or ions during the formation of a metal complex or metal co-ordination compound.

The molecules or ions which displace the solvent molecules are called Ligands. Ligands or complexing agents or chelating agents can be any electron donating entity, which has the ability to bind to the metal ion and produce a complex ion.

Ligands having more than one electron donating groups are called chelating agents. The most effective complexing agent in ligands are amino and carboxylate ions. The solubility of metal chelates in water depends upon the presence of hydrophilic groups such as COOH, SO₃H, NH₂ and OH. When both acidic and basic groups are present, the complex will be soluble over a wide range of pH. When hydrophilic groups are absent, the solubilities of both the chelating agent and the metal chelate will be low, but they will be soluble in organic solvents. The term sequestering agent is generally applied to chelating agents that form water-soluble complexes with bi- or poly-valent metal ions. Thus, although the metals remain in solution, they fail to give normal ionic

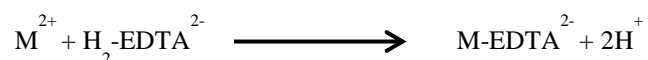
reactions. Ethylenediaminetetra-acetic acid is a typical sequestering agent, whereas, dimethylglyoxime and salicylaldehyde are chelating agents, forming insoluble complexes.

Disodium EDTA: Disodium salt of EDTA is a water soluble chelating agent and is always preferred. It is non-hygroscopic and a very stable sequestering agent (Ligands which form water soluble chelates are called sequestering agents). EDTA has the widest general application in analyses because of the following important properties:

- It has low price.
- The special structure of its anion which has 6 ligand atoms.
- It forms strainless five-membered rings.

Ethylenediamine tetra-acetic acid ionizes in four stages ($pK_1=2.0$, $pK_2=2.67$, $pK_3=6.16$ and $pK_4=10.26$) and, since the actual complexing species is H_2-EDTA^{2-} , complexes will form more efficiently and be more stable in alkaline solution. If, however, the solubility product of the metal hydroxide is low, it may be precipitated if the hydroxyl ion concentration is increased too much. On the other hand, at lower pH values when the concentration of H_2-EDTA^{2-} is lower, the stability constant of the complexes will not be so high. Complexes of most divalent metals are stable in ammoniacal solution.

Equation below shows complexation between metal ion and H^+ ion for ligand:



Thus, stability of metal complex is pH dependent. Lower the pH of the solution, lesser would be the stability of complex (because more H^+ ions are available to compete with the metal ions for ligand). Only metals that form very stable complexes can be titrated in acidic solution, and metals forming weak complexes can only be effectively titrated in alkaline solution.

Principle: In EDTA titration, if we plot pM (negative log of metal ion concentration) v/s volume of titrant, we will find that at the end point, the pM rapidly increases. This sudden pM raise results from removal of traces of metal ions from solution by EDTA.

Any method, which can determine this disappearance of free metal ions, can be used to detect end point in complexometric titrations. End point can be detected usually with an indicator or instrumentally by potentiometric or conductometric (electrometric) method.

Indicators: The end point in complexometric titrations is shown by means of pM indicators. The concept of pM arises as follows:

If K is the stability constant,

$$K = \frac{[MX]}{[M][X]}$$

$$\text{then, } [M] = \frac{[MX]}{[X]K}$$

$$\text{or } \log [M] = \log \frac{[MX]}{[X]} - \log K$$

$$\text{and } pM = \log \frac{[X]}{[MX]} - pK$$

Therefore, if a solution is made such that $[X] = [MX]$, $pM = -pK$ (or $pM = pK'$, where $K' =$ dissociation constant). This means that, in a solution containing equal activities of metal complex and free chelating agent, the concentration of metal ions will remain roughly constant and will be buffered in the same way as hydrogen ions in a pH buffer. Since, however, chelating agents are also bases; equilibrium in a metal-buffer solution is often greatly affected by a change in pH. In general, for chelating agents of the amino acid type (e.g., edetic acid and ammonia triacetic acid), it may be said that when $[X] = [MX]$, pM increases with pH until about pH 10, when it attains a constant value. This pH is, therefore, usually chosen for carrying out titrations of metals with chelating agents in buffered solutions.

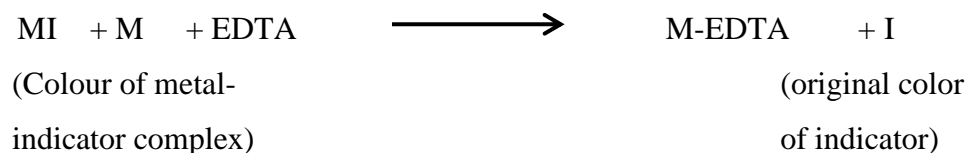
The pM indicator is a dye which is capable of acting as a chelating agent to give a dye-metal complex. The latter is different in colour from the dye itself and also has a low stability constant than the chelate-metal complex. The colour of the solution, therefore, remains that of the dye complex until the end point, when an equivalent amount of sodium EDTA has been added. As soon as there is the slightest excess of EDTA, the metal-dye complex decomposes to produce free dye; this is accomplished by a change in colour.

Over 200 organic compounds form colored chelates with ions in a pM range that is unique to the cation and the dye selected. To be useful, the dye-metal chelates usually will be visible at 10^{-6} - 10^{-7} M concentration $\{(39 \text{ g/mol}) \cdot 10^{-7} \text{ M} = 39 \times 10^{-7} \text{ g/L of calcium}\}$. Many of these indicators also have the typical properties of acid-base indicators and the colour changes are the result of

the displacement of the H^+ by a metal ion. Metal indicators must comply with the following requirements-

- Compound must be chemically stable throughout the titration.
- It should form 1:1 complex which must be weaker than the metal chelate complex.
- Colour of the indicator and the metal complexed indicator must be sufficiently different.
- Colour reaction should be selective for the metal being titrated.
- The indicator should not compete with the EDTA.

Mechanism of action of indicator: Let the metal be denoted by M, indicator by I and chelate by EDTA. At the onset of the titration, the reaction medium contains the metal-indicator complex (MI) and excess of metal ion. When EDTA titrant is added to the system, a competitive reaction takes place between the free metal ions and EDTA. Since the metal-indicator complex (MI) is weaker than the metal-EDTA chelate, the EDTA which is being added during the course of the titration is chelating the free metal ions in solution at the expense of the MI complex. Finally, at the end point, EDTA removes the last traces of the metal from the indicator and the indicator changes from its complexed colour to its metal free colour. The overall reaction is given by:



Many compounds have been used as indicators, like:

- Triphenyl methane dyes
- Phthalein and substituted phthaleins
- Azo dyes
- Phenolic compounds

Types of Complexometric Titrations : Complexometric titrations are of 4 types:

a. Direct Titration: It is the simplest and the most convenient method used in chelometry. In this method, the standard chelon solution is added to the metal ion solution until the end point is

detected. This method is analogous to simple acid-base titrations. E.g.-calcium gluconate injection, calcium lactate tablets and compound sodium lactate injection for the assay of calcium chloride ($\text{CaCl}_2 \cdot 6\text{H}_2\text{O}$).

Limitations -Slow complexation reaction
 -Interference due to presence of other ions

b. Back Titration: In this method, excess of a standard EDTA solution is added to the metal solution, which is to be analyzed, and the excess is back titrated with a standard solution of a second metal ion, e.g. determination of Mn. This metal cannot be directly titrated with EDTA because of precipitation of $\text{Mn}(\text{OH})_2$. An excess of known volume of EDTA is added to an acidic solution of Mn salt and then ammonia buffer is used to adjust the pH to 10 and the excess EDTA remaining after chelation, is back titrated with a standard Zn solution kept in burette using Eriochrome blackT as indicator. This method is analogous to back titration method in acidimetry. e.g.- ZnO

c. Replacement Titration: In this method the metal, which is to be analyzed, displaces quantitatively the metal from the complex. When direct or back titrations do not give sharp end points, the metal may be determined by the displacement of an equivalent amount of Mg or Zn from a less stable EDTA complex.



Mn displaces Mg from Mn EDTA solution. The freed Mg metal is then directly titrated with a standard EDTA solution. In this method, excess quantity of Mg EDTA chelate is added to Mn solution. Mn quantitatively displaces Mg from Mg EDTA chelate. This displacement takes place because Mn forms a more stable complex with EDTA. By this method Ca, Pb, Hg may be determined using Eriochrome blackT indicator.

d. Indirect Titration: This is also known as Alkalimetric titration. It is used for the determination of ions such as anions, which do not react with EDTA chelate. Protons from disodium EDTA are displaced by a heavy metal and titrated with sodium alkali.



e.g. - Barbiturates do not react with EDTA but are quantitatively precipitated from alkaline solution by mercuric ions as 1:1 complex.

3.2.2. Reagents

- i. Disodium EDTA solution (0.001 M): 0.372 g of disodium EDTA was dissolved in water and volume was made up to 1000 ml.
- ii. Ammonia-Ammonium chloride buffer pH 10: 17.5 g ammonium chloride was weighed and 142 mL concentrated ammonia solution was added to it and diluted to 250 mL with de-ionized water.
- iii. Calcium Chloride stock solution (1 mg/mL): Dissolve 100 mg of calcium chloride and dissolve in 100 mL de-ionized water to obtain 10 mg/mL solution of calcium chloride.
- iv. Solochrome black/potassium nitrate solution (indicator solution): 10 mg of solochrome black/potassium nitrate mixture was dissolved in 10 mL of water to get 1 mg/mL indicator solution.

3.2.3. Method of Analysis

0.25, 0.50, 0.75, 1.00, 1.25 and 1.50 mL of calcium chloride stock solution were taken in separate volumetric flasks and volume was made up to 10 mL with de-ionized water to obtain 25 to 150 μg of calcium chloride in solution. Each solution was sampled out in a beaker and 0.5 mL of ammonia buffer and 0.6-0.8 mL of indicator solution were added to it. Each solution was then titrated slowly with EDTA solution until color of solution was changed from wine red to clear blue. Each titration was performed in triplicate.

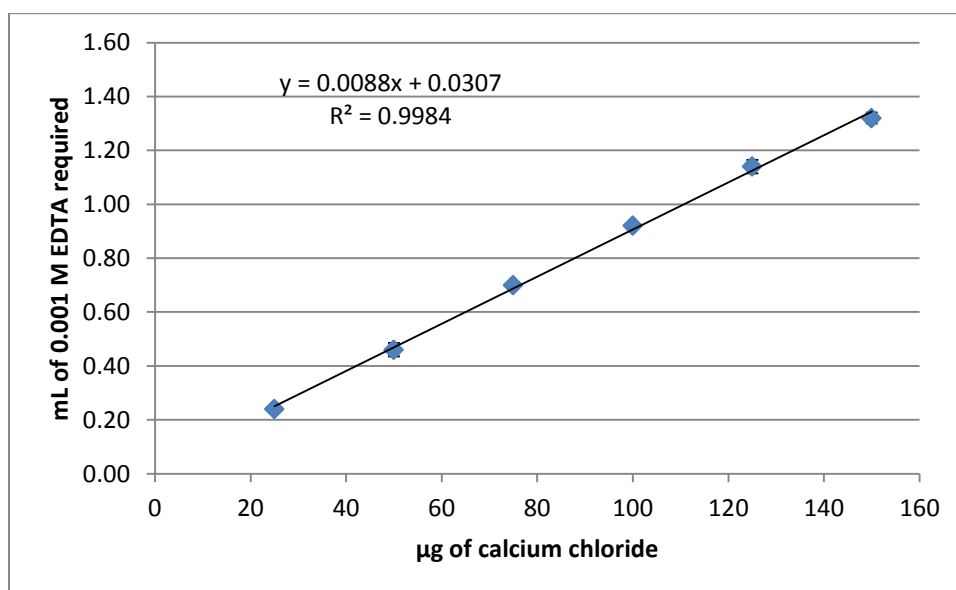
The volume of EDTA solution required for different concentrations of calcium chloride were determined (**Table 3.5**). The plot of volume of EDTA solution required against the amount of calcium chloride in solution is shown in **Figure 3.2**. Calibration plot showed a straight line expressed by the equation $y = 0.0088x + 0.0307$, with regression coefficient of 0.9984.

Table 3.5 Volume of 0.001 M Na₂EDTA Solution Required for Different Amounts of Calcium Chloride*

µg of Calcium Chloride in solution	ml of 0.001 M Na₂EDTA solution (n=3)	Standard Deviation
25	0.24	0.010
50	0.46	0.025
75	0.70	0.010
100	0.92	0.010
125	1.14	0.025
150	1.32	0.020

*Experiments were performed in triplicate.

Figure 3.2 Volume of 0.01 M Na₂EDTA Solution Required for Different Amounts of Calcium Chloride



3.2.4. Accuracy and Precision of Method:

Complexometric titration method was evaluated for precision and accuracy by determining % recovery and %relative standard deviation (%RSD) respectively. Calcium chloride sample solutions containing 50, 100 and 150 µg were prepared using de-ionized water. Titrations were carried out for each sample and % recovery was calculated to determine accuracy. And precision

was determined by carrying out titrations of each sample at different time periods and calculating % relative standard deviation. All the measurements were made in triplicate.

Table 3.6, Table 3.7 and **Table 3.8** represent accuracy, intraday and interday precision of the method respectively. As it can be seen, the % recovery was found to be between 99.5 % to 100.5% and %RSD of interday and intraday measurements below 1%, the method was found to comply the FDA and ICH guidelines on accuracy and precision of an analytical method validation [3, 4].

Table 3.6 Accuracy of Method*

Concentration of CaCl₂ (µg)	Obtained Concentration (µg)	Standard Deviation (SD)	%Recovery
250	50.250	0.395	100.500
100	100.383	0.460	100.383
150	149.973	0.300	99.982

*Experiments were performed in triplicate.

Table 3.7 Intraday Precision of the Method*

Concentration of CaCl₂ (µg)	Obtained Concentration (µg)	Standard Deviation (SD)	%Relative Standard Deviation
50	50.250	0.395	0.786
100	100.383	0.460	0.458
150	149.973	0.300	0.200

*Experiments were performed in triplicate.

Table 3.8 Interday Precision of the Method*

	Concentration of CaCl ₂ (µg)	Obtained Concentration (µg)	Standard Deviation (SD)	%Relative Standard Deviation
Day 1	50	50.540	0.217	0.429
	100	101.093	0.773	0.764
	150	150.113	0.451	0.300
Day 2	50	50.523	0.401	0.793
	100	49.544	44.155	89.124
	150	77.013	63.988	83.087
Day 3	50	50.197	0.427	0.850
	100	100.117	0.378	0.378
	150	150.090	0.256	0.171

*Experiments were performed in triplicate.

3.3. siRNA Gel Electrophoresis: Gel Retardation Assay

Agarose gel electrophoresis was used for relative quantification of free siRNA migrated on the gel due to differences in the surface charge.

3.3.1. Introduction

Liposomes for siRNA delivery need to be able to strongly complex and encapsulate siRNA for an effective siRNA delivery. Liposomes with calcium encapsulated inside should also encapsulate siRNA effectively to make them useful for successful delivery of siRNA. To test the complexation capacity of cationic lipids or siRNA encapsulation efficiency of calcium loaded liposomes, ethidium bromide agarose gel electrophoresis assay was used. This is a molecular biological technique that separates a mixed population of nucleic acids by size. Negatively charged DNA or RNA moves through an agarose gel matrix towards the positive end of an electric field. The smaller the molecules are, the farther they migrate through the pores of the gel.

To make nucleic acid visible in the gel, dyes such as ethidium bromide (EtBr) are commonly used. Ethidium bromide intercalates into minor grooves of double-stranded nucleic acids and fluoresces under UV light.

Based on these fundamentals, if the siRNA is encapsulated in liposomes, the migration of the siRNA would be retarded. Moreover, the degree of retardation would be directly proportional to the strength of complexation. Therefore, if the migration of complexed siRNA was not as far as that of naked siRNAs, we concluded that this is the liposomes, holding the siRNA molecules and interfering with its migration.

3.3.2. Method of Analysis

Agarose (2 g, electrophoresis grade, Gibco) was added to 100 ml of 1x TBE (Tris-Borate-EDTA, 89 mM Tris-Borate and 2 mM EDTA) buffer. The mixture was then heated in a heating mantle with shaking the flask 3 to 4 times while boiling to dissolve the agarose. When the agarose was completely dissolved, the solution was then allowed to cool to a consistency that can be poured. The gel tray was securely sealed at the ends with tape strips to form a fluid-tight seal. The comb was placed over the gel tray. After that, when the agarose had been cooled to about 60 °C, ethidium bromide was added (0.5 µg/mL), and it was poured into the gel tray to a depth of 4-8 mm. Then the gel was allowed to set at 20 °C for 30 min. followed by refrigeration for further 15 mins for complete solidification of the gel. The comb was removed from the solidified gel as well as the tape from the edges of the gel tray. The gel was then transferred to the electrophoresis chamber (Genet Electrophoresis Powerpack, Bangalore, India), and submerged into the electrophoresis buffer (1x TBE buffer).

3.3.3. Determination of Quantifiable Range of siRNA for Gel Retardation Assay

siRNA solutions of different concentrations (1, 5, 10, 20, 40, 60, 80, and 100 pmole) were prepared. Solutions were mixed with gel loading buffer (sucrose 50% w/v + bromophenol blue 0.25% w/v) by using a vortex mixture in 0.5 mL microcentrifuge tubes. siRNA samples (15 µL each) were loaded (volume) into the wells. Electrophoresis at 100 V/cm (Genet Electrophoresis Powerpack, Bangalore, India) was carried out for 1 h. The gel was removed and the siRNA in the agarose gel was visualized under UV light using GelDoc™ XR⁺ Imaging System (BioRad, USA).

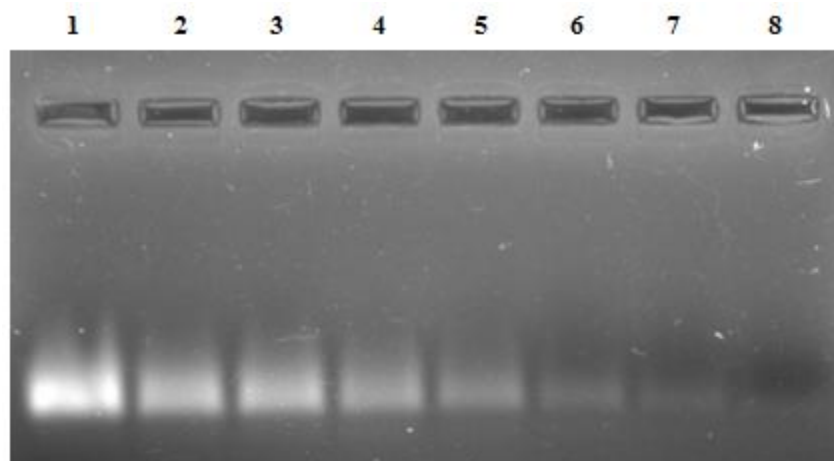


Figure 3.3 Determination of Quantifiable Range of siRNA - Gel Electrophoresis Band Densities at different siRNA Concentraions

*1- 100 pmole, 2- 80 pmole, 3- 60 pmole, 4- 40 pmole,
5- 20 pmole, 6- 10 pmole, 7- 5 pmole, 8- 1 pmole*

The gel electrophoresis data (**Figure 3.3**) showed that siRNA can be quantified at a minimum of 20 pmole concentration. At lower concentrations (below 20 pmole) the bands were not accurately quantifiable.

3.3.4. Relative Quantification

To develop a calibration curve for the quantitation of siRNA, relative quantification was used i.e., the band density at highest siRNA concentration (50 pmole) being taken as 1 and evaluating band density of lower concentrations relative to the former.

For relative quantification, siRNA solutions of different concentrations (20 pmole-50 pmole) were prepared. Solutions were mixed with gel loading buffer by using a vortex mixture in 0.5 mL microcentrifuge tubes. siRNA samples (15 μ L each) were loaded (volume) into the wells. Electrophoresis at 100 V/cm was carried out for 1 h. The gel was removed and the siRNA in the agarose gel was visualized under UV light using GelDoc™ XR⁺ Imaging System (BioRad, USA).

Multiple analysis (n=5) was carried out to allow for the quantification of probable errors in the measurements and improve the prediction of the analysis. **Figure 3.4** shows one of the agarose gels with band-densities. **Table 3.9** shows the relative mean band densities at different siRNA concentrations with standard deviation. The calibration plot is given in **Figure 3.5**. The results

were found to be linear with regression coefficient of 0.9952 and the equation representing line was $y = 0.1703x + 0.133$.

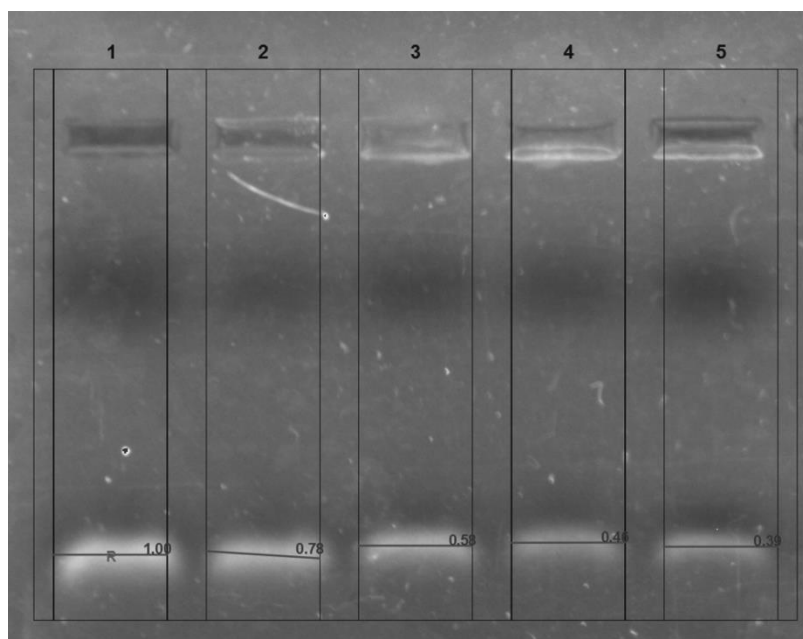


Figure 3.4 Relative Quantification of siRNA - Gel Electrophoresis Band Densities at Different siRNA Concentrations

1-50 pmole, 2- 40 pmole, 3- 30 pmole, 4- 25 pmole, 5- 20 pmole

Table 3.9 Gel Electrophoresis – Relative Band Densities at Different siRNA Concentration

Concentration of siRNA (pmole)	Relative Band Density* (n=3)	Std. Dev.
20	0.323	0.015
25	0.450	0.010
30	0.647	0.025
40	0.800	0.020
50	1.000	0.000

*Experiments were performed in triplicate.

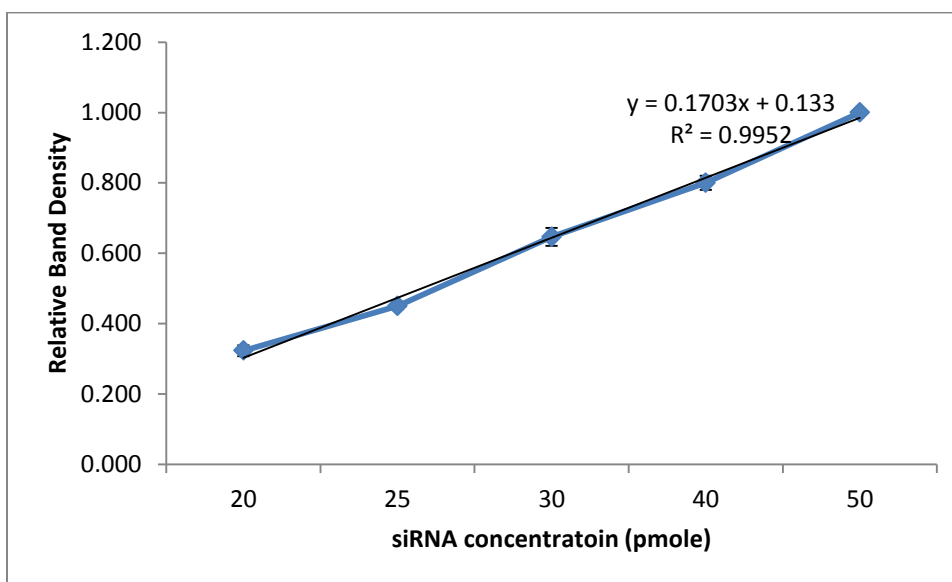


Figure 3.5 Calibration Plot of siRNA Gel Retardation

3.3.5. Accuracy and Precision of the Method

Accuracy and Precision of the method were evaluated by running 100 pmole of siRNA concentration in 8 repeated experiments and determining the % recovery and Relative standard deviation. The band densities are shown in the **Figure 3.6**.

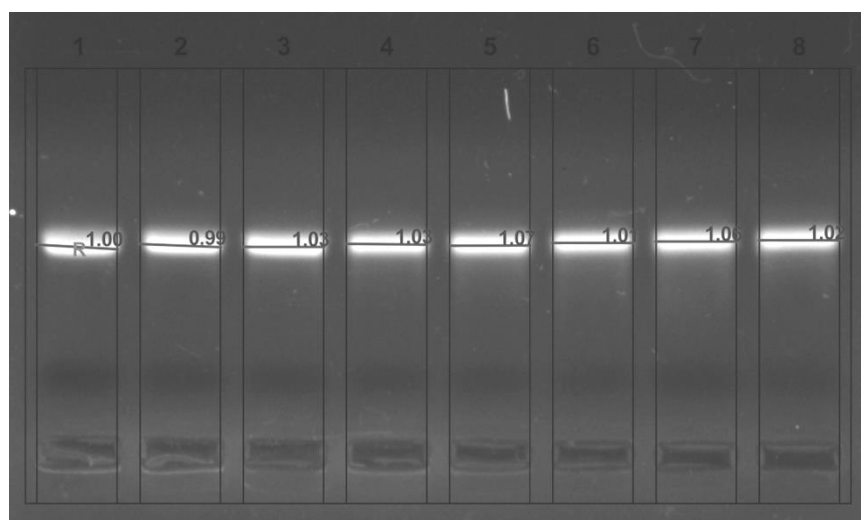
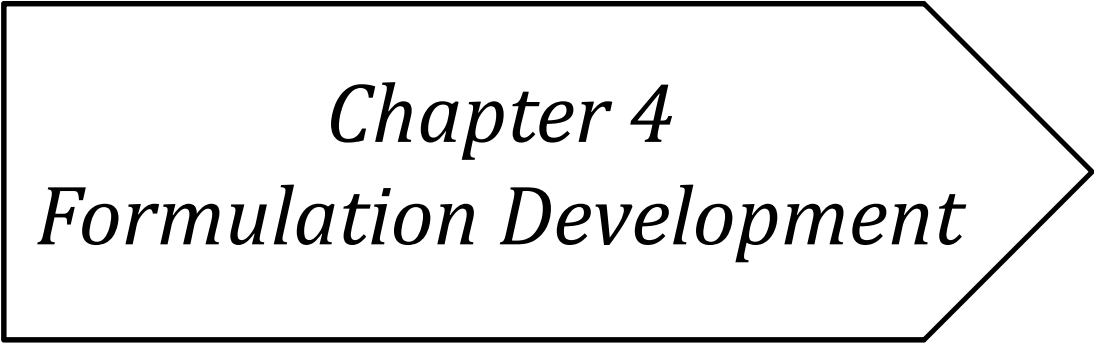


Figure 3.6 Accuracy and Precision of Gel Electrophoresis Method for siRNA Quantification

%recovery and %relative standard deviation of the method were found to be $102.7 \pm 2.6\%$ and 2.55% concluding the adequacy of the analytical method for quantification of siRNA.

3.4. References

1. Blackburn WH, Dickerson EB, Smith MH, McDonald JF, Lyon LA. Peptide-Functionalized Nanogels for Targeted siRNA Delivery. *Bioconjugate Chemistry*. 2009;20(5):960-8.
2. Katas H, Alpar HO. Development and characterisation of chitosan nanoparticles for siRNA delivery. *Journal of controlled release*. 2006;115(2):216-25.
3. Validation of analytical procedures: definitions and terminology. International Conference on Harmonization (ICH) of Technical Requirements for the Registration of Pharmaceuticals for Human Use, Geneva. 1996.
4. General Chapter 1225- Validation of compendial methods. United States Pharmacopeia 30, National Formulary 25, The United States Pharmacopeial Convention, Inc, Rockville, Md, USA. 2007.
5. Husain A. Theoretical Basis of Analysis: Complexometric Titrations. *Pharmaceutical Analysis*. New Delhi, INDIA: Jamia Hamdard; 2007.
6. Kim J, Vipulnandan C. Effect of pH on EDTA Method of Measuring Calcium. Houston, TX: University of Houston; Available from: http://cigmat.cive.uh.edu/content/conf_exhib/99_poster/4.htm.
7. Vogel AI, Mendham J. Vogel's textbook of quantitative chemical analysis: Prentice Hall; 2000.



Chapter 4
Formulation Development

4.1. Selection of siRNA

siRNA targeting Rebonucleotide reductase subunit-1 was selected to potentiate the chemotherapeutic action of Gemcitabine HCl. Gene responsible for the resistance of Gemcitabine is **Rebonucleotide reductase Subunit 1 (RRM1)**.

siRNA targeting RRM1

Guide strand sequences (5' → 3'): AGACGCUAGAGCGGUCUUA

- ✓ MW [g/mol]: 13315
- ✓ T_m [°C]: 57.9
- ✓ Purification: HPLC

GC-Content [%]: 47.6

4.1.1. Sense-strand Analysis

Sequence: 5'-AGA CGC UAG AGC GGU CUU A-3'

Sense: 5'- [AGACGCUAGAGCGGUCUUA] RNA [TT] DNA -3'

4.1.1.1. MALDI-Mass Spectrometry of siRNA

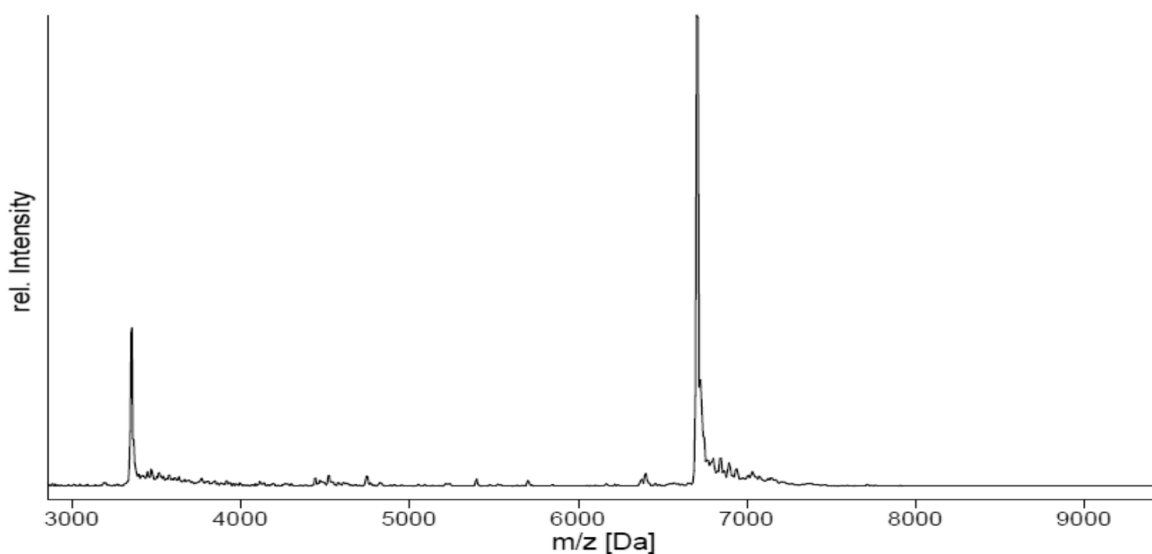


Figure 4.1 MALDI Analysis

Target Mass of the Single Sense Strand: 6709 Da

Detected Mass of the Single Sense Strand: 6708 Da

4.1.1.2. Capillary Gel Electrophoresis (CGE) Analysis of siRNA

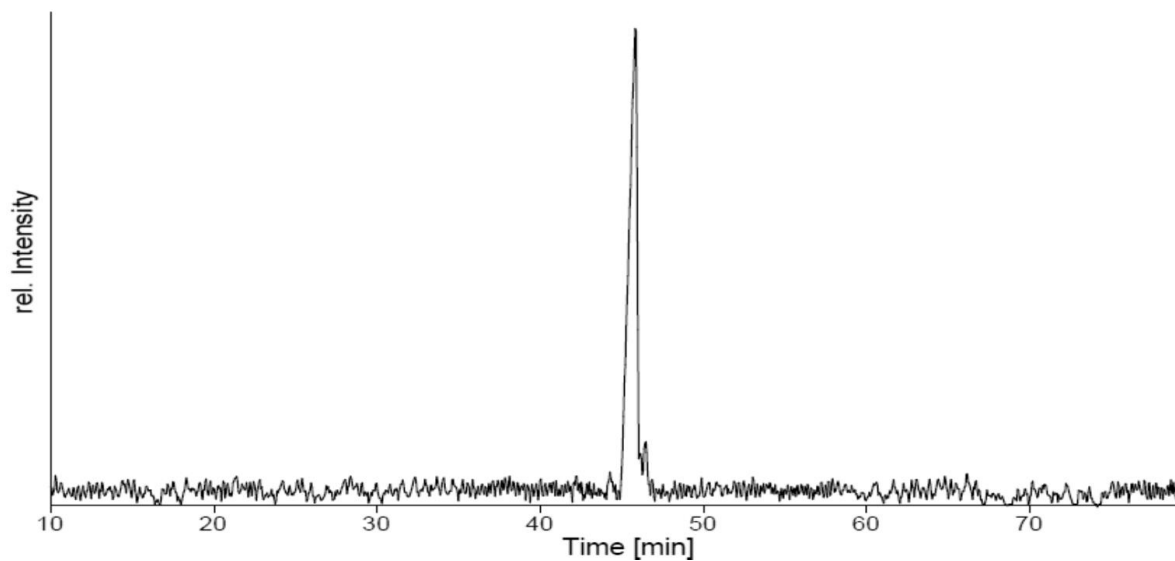


Figure 4.2 CGE Analysis

4.1.2. Antisense-strand Analysis

Sequence: 5'-AGA CGC UAG AGC GGU CUU A-3'

Antisense: 5'- [UAAGACCGCUCUAGCGUCU] RNA [TT] DNA -3'

4.1.2.1. MALDI mass Spectrometry of siRNA

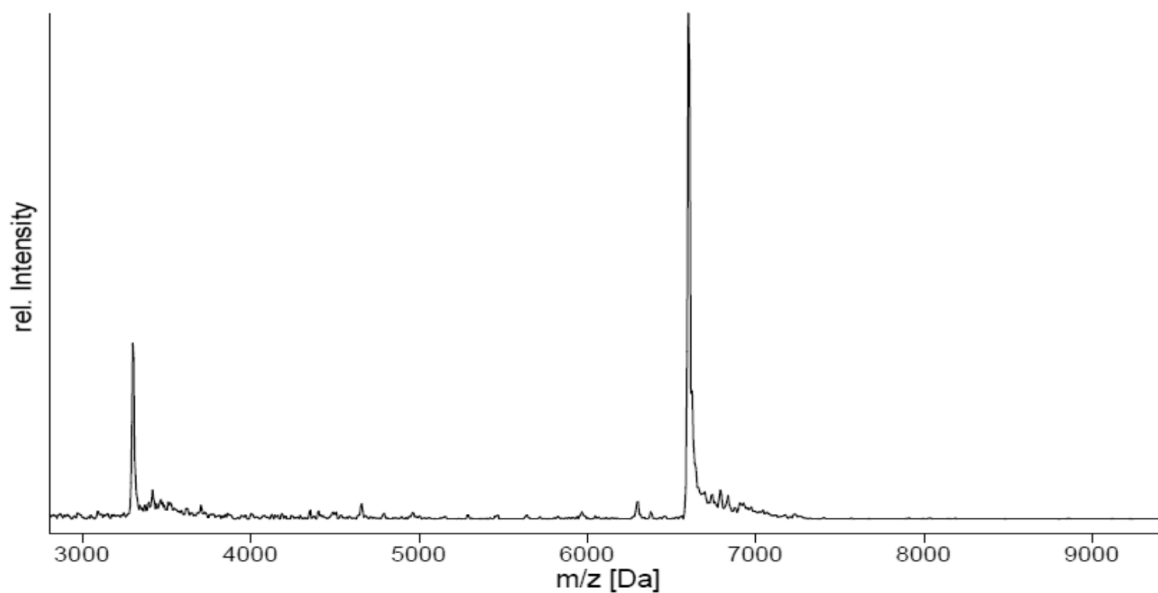


Figure 4.3 MALDI Analysis

Target Mass of the Single Antisense Strand: 6606 Da

Detected Mass of the Single Antisense Strand: 6605 Da

4.1.2.2. Capillary Gel Electrophoresis (CGE) analysis of siRNA

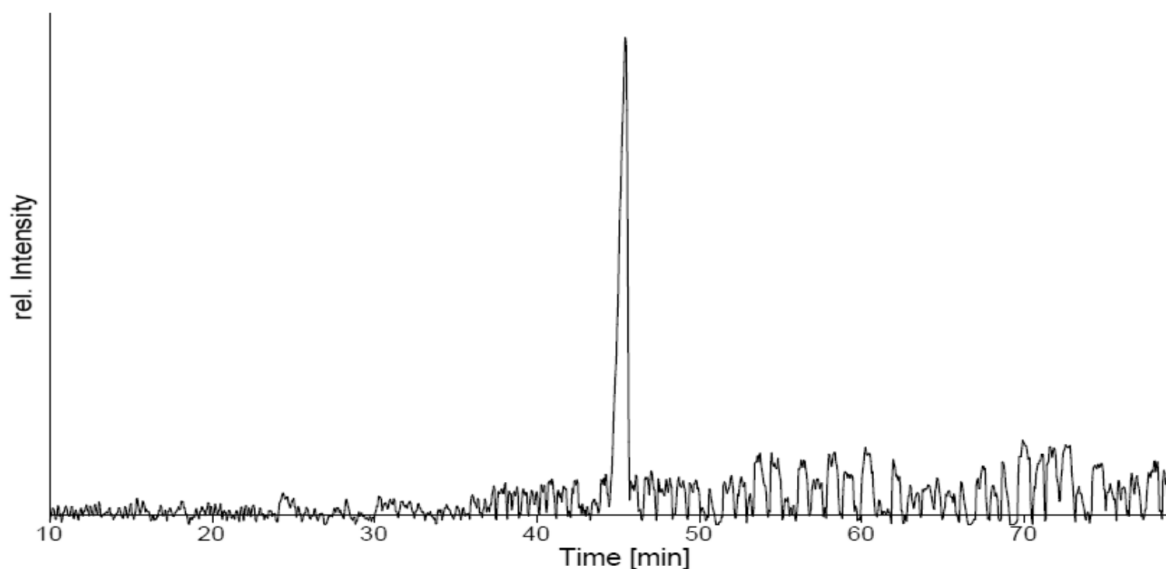


Figure 4.4 CGE Analysis

Figure 4.1 and **Figure 4.3** show molecular weight of the sense and anti-sense strands. Single intense peak corresponding molecular weight in both MALDI spectra was been detected. Purity of the sense and antisense strands were determined by CGE analysis.

4.1.3. Gel Electrophoresis of siRNA

- ❖ 2% Agarose gel
- ❖ Ethidium Bromide staining dye
- ❖ TBE buffer (Tris Borate EDTA)
- ❖ Gel loading buffer
 - Sucrose
 - Bromo-phenol Blue

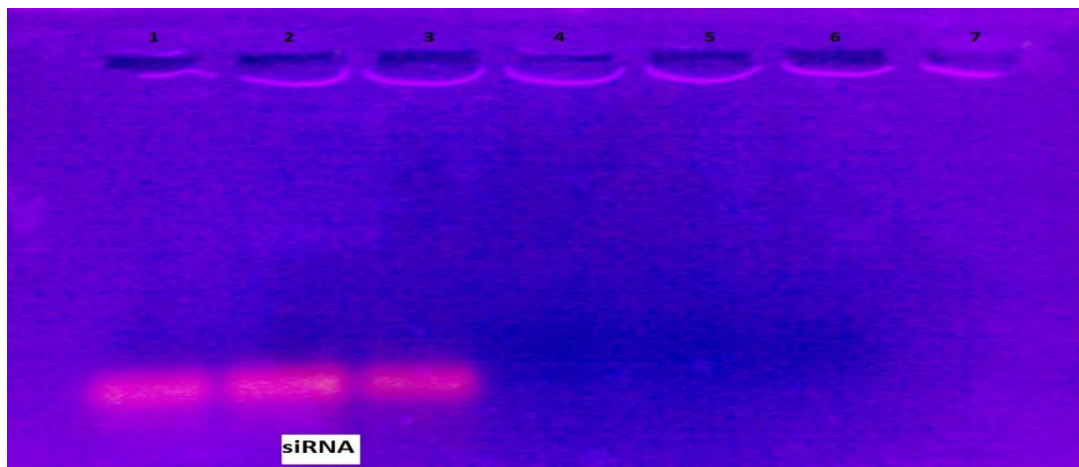


Figure 4.5 Gel Electrophoresis of siRNA

1, 2 & 3-siRNA 0.1nM, 4-siRNA+RNase (1mg/mL), 5-siRNA+RNase (1mg/mL), 6-DEPC (Diethyl pyrocarbonate) water & 7-Nuclease free water

As seen in above **Figure 4.5**, siRNA was clearly detected on to 2% agarose gel. Further, RNase completely degraded the siRNA. Thus, working with siRNA molecule needs RNA free exposure and hence, DEPC treatment was used to remove RNA from all materials used for the formulation.

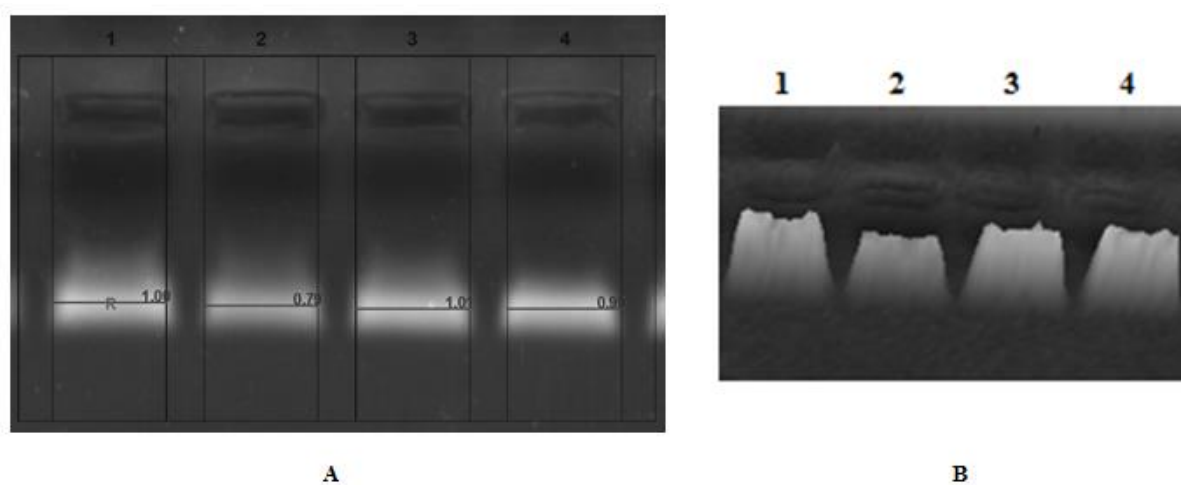


Figure 4.6 Effect of temperature on siRNA A-vertical view B-3D view

1= 25°C, 2= 60°C, 3= 40°C, 4=50°C

siRNA is prone to degrade with heating and the same was observed by incubating the siRNA at different temperature for fixed period of time i.e. 30 min. **Figure 4.6** shows that more than 20 % of siRNA degraded at 60°C and hence temperature above 50°C should not be used during processing of any operation where siRNA is involved. Same thing was taken care while formulation development.

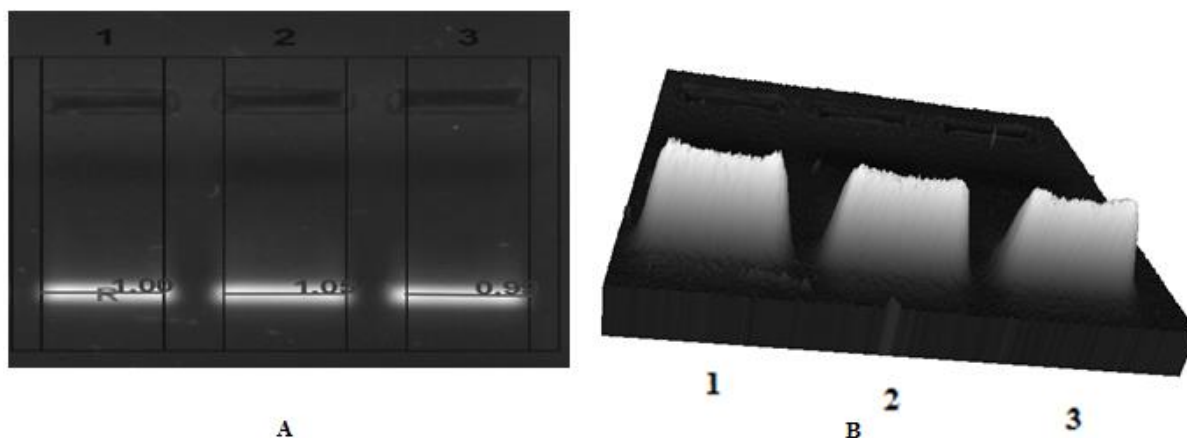


Figure 4.7 Effect of pH on siRNA A-vertical view B- 3D view

1=pH 6.5, 2=pH 7.5, 3=pH 8.5

Figure 4.7 shows the pH stability of selected siRNA at three different pH. Relative quantification shows that even at weak alkaline condition i.e. pH=8.5, siRNA is stable. Purpose to study pH stability was to confirm the integrity of siRNA at working pH i.e. pH= 7.5 and 8.5.

4.2. Development of Cationic siRNA loaded liposomes

4.2.1. Introduction

Different lipid based strategies were tried for the effective entrapment of siRNA into liposomes. Different kinds of lipids used are:

Phospholipids:

- Positively Charged- Didioleoyl Trimethylammoniumpropane (DOTAP)
- Negatively Charged- Phosphatidyl Glycerol (PG); Dimyristoyel Phosphatidyl glycerol (DMPG)
- Fusogenic- Dioleoyl Phosphatidylethanolamine (DOPE)
- Neutral – Phosphatidyl Choline (PC); Hydrogenated Soya Phosphatidyl Choline (HSPC)

Other lipid:

- Cholesterol
- mPEG-DSPE-2000 (methoxy Polyethylene Glycol Disteroyl Phosphatidyl Ethanolamine)

4.2.1.1. DOTAP

[1,2-bis(oleoyloxy)-3-(trimethylammonio)propane], or DOTAP, was first synthesized by Leventis and Silvius in 1990 [1]. The molecule consists of a quaternary amine head group coupled to a glycerol backbone with two oleoyl chains. The only differences between this molecule and DOTMA are that ester bonds link the chains to the backbone rather than ether bonds. It was originally hypothesized that ester bonds, which are hydrolysable, could render the lipid biodegradable and reduce cytotoxicity. This study showed that the transfection activities and levels of cytotoxicity associated with DOTAP/DOPE formulations are not statistically different from those associated with DOTMA/DOPE composites. Notably, this type of monovalent lipids also showed little to no cytotoxic effect on near-confluent cell monolayers [1].

The use of 100% DOTAP for gene delivery is inefficient due to the density of positive charges on the liposome surface, which possibly prevents counter ion exchange [2]. DOTAP is completely protonated at pH 7.4 (which is not the case for all other cationic lipids) [2], so it is possible that more energy is required to separate the DNA from the lipoplex for successful

transfection [3]. Thus, for DOTAP to be more effective in gene delivery, it should be combined with a helper lipid, as seems to be the case for most cationic lipid formulations.

High temperature and long incubation times have been used to create lipoplexes that exhibit resistance to serum interaction [4]. Interestingly, this approach was only observed to affect monovalent cationic lipids such as DOTMA, DOTAP, or DC-Chol, as opposed to multivalent cationic lipids. The specific reasons for this phenomenon remain unclear. In fact, the specific mechanism behind serum inactivation of lipoplexes in general is as yet unexplained. Several hypotheses have been offered as to the mechanism, including the prevention of lipoplex binding to cell membranes by serum proteins [4], the prevention of structural complex maturation by serum proteins binding to cationic charges on the lipoplexes [4], and the disparity of endocytosis pathways-which have varying kinetics-that are used for lipoplex endocytosis, with the method of endocytosis being regulated by the size of the lipoplexes or aggregates of lipoplexes plus serum proteins.

4.2.1.2. DOPE

DOPE often presents a super synergistic effect when used in cationic liposomes, because DOPE destabilized lipid bilayers, and it was believed to be involved in endosomal disruption, allowing the release of DNA into the cytosol [5] and leading to mixed bilayers [6]. Most studies have shown that lipoplexes containing the non-bilayer-phase-preferring lipid DOPE or cholesterol would promote HC_{II} organization [7]. A transition from the LC_{α} phase to the HC_{II} phase could be expected by increasing weight fraction of DOPE, via controlling the spontaneous radius of curvature “ R_o ” of the lipid layers, favoured by the elastic free energy [8]. Another helper lipid, cholesterol, could also promote HC_{II} organization as DOPE. It has been proved that *in vivo* applications cholesterol was a more effective helper lipid than DOPE [9]. Koltover et al. disclosed the reason in the level of phase transition through synchrotron small-angle X-ray scattering (SAXS) and optical microscopy to show the phase transition from $L_{\alpha}C$ to HC_{II} induced by DOPE via controlling the spontaneous curvature $C_o = 1/R_o$ of the lipid monolayer [10]. It has been concluded that DOPE facilitates endosomal escape by forming an unstable inverted hexagonal phase at the endosomal pH that destabilizes both the complex and the endosomal membrane. But in a recent study, they developed CL-siRNA complexes with a novel

cubic phase nanostructure exhibiting efficient silencing at low toxicity by using glycerol monooleate other than DOPE as the helper lipid [11].

The inverse bicontinuous gyroid cubic nanostructure was unequivocally established from synchrotron X-ray scattering data, while fluorescence microscopy revealed co-localization of lipid and siRNA in complexes. Tubes of lipoplexes containing DOTAP/MOG, DOTAP or DOTAP/PC, and DOTAP/DOPE were observed in freeze-fracture electron micrographs. The tubes were extremely short and appeared bead-like in lipoplexes containing DOTAP/MOG, slightly longer in those containing DOTAP or DOTAP/PC, and extensively elongated in DOTAP/DOPE lipoplexes [12]. The spaghetti-like structures, occurring at DNA: lipid concentrations which were used during transfection and their diameter came closest to the diameter of the nuclear pores, may be the active cationic lipoplexes [13]. In the study of the structure and morphology of DC-Chol-DOPE/DNA complexes it was found the existence of cluster-like aggregates made of multilamellar DNA/lipid domains coexisting with other multilamellar lipoplexes or, alternatively, with DNA-coated vesicles [14]. The further study showed that DC-Chol-DOPE/DNA lipoplexes preferentially used a raft mediated endocytosis, while DOTAP-DOPC/DNA systems were mainly internalized by not specific fluid phase macropinocytosis. Most efficient multicomponent lipoplexes, incorporating different lipid species in their lipid bilayer, can use multiple endocytic pathways to enter cells. Their data demonstrated that efficiency of endocytosis was Non-Viral Gene Therapy regulated by shape coupling between lipoplex and membrane lipids to suggest that such a shape-dependent coupling regulated efficient formation of endocytic vesicles thus determining the success of internalization [15].

4.2.1.3. Negatively Charged Lipid- DMPG

Dimyristoyl phosphatidylglycerol (DMPG), anionic and a saturated lipid with 14-C atoms in each hydrophobic chain, under physiological conditions presents a gel/fluid transition at 23⁰C. Due to the presence of an ionizable phosphate group, the thermo-structural properties of PG-lipids are not only dependent on the hydrocarbon chain length, but also strongly reliant on the pH of the medium and the presence of ions. In general, gene delivery by anionic lipids is not very efficient. The negatively charged head group prevents efficient DNA compaction due to

repulsive electrostatic forces that occur between the phosphate backbone of DNA and the anionic head groups of the lipids. However, due to the fact that cationic liposomes can be inactivated in the presence of serum, are unstable upon storage, and exhibit some cytotoxicity both *in vitro* and *in vivo*, anionic liposomes have been studied as potential gene delivery vehicles [16-18].

Formation of DNA-containing liposomes using anionic lipids can be brought about through the use of divalent cations to negate the mutual electrostatic repulsion and facilitate lipoplex assembly. Anionic lipoplexes are composed of physiologically safe components including anionic lipids, cations, and plasmid DNA [19]. Commonly used lipids in this category are phospholipids that can be found naturally in cellular membranes such as phosphatidic acid, phosphatidylglycerol, and phosphatidylserine. As with the lipids presented earlier, anionic lipids can contain any of a wide range of fatty acid chains in the hydrophobic region. The specific fatty acids incorporated are responsible for the fluidic characteristics of the liposome in terms of phase behavior and elasticity. Perhaps due to the natural presence of these specific phospholipids in the host cell membrane, gene delivery via lipoplexes with net negative surface potentials has been associated with lower clearance and phagocytosis by macrophages, which is consistent with favorable biocompatibility [20].

Various anionic liposomes have been characterized for gene delivery in a small number of cell types including CHO cells and primary hippocampal neurons [21, 22]. While such investigations are novel, overall knowledge regarding anionic lipofection is as yet limited due to a lack of extensive testing; DNA entrapment in anionic liposomes is still inefficient, and cytotoxicity data remain inadequate.

Divalent cations can be incorporated into the system to enable the condensation of nucleic acids prior to envelopment by anionic lipids. Several divalent cations have been tested for use in anionic lipoplexes such as Ca^{2+} , Mg^{2+} , Mn^{2+} and Ba^{2+} , but it has been observed that the use of Ca^{2+} yielded the highest transfection efficiency due to its higher DNA binding affinity [23, 24]. An investigation conducted by Srinivasan and Burgess confirmed that Ca^{2+} was the most effective cation for DNA compaction as compared to Na^+ and Mg^{2+} [19]. This affinity is potentially a result of the smaller hydrodynamic radius of calcium which gives a larger charge

per unit surface area. The use of Ca^{2+} not only overcame the strong electrostatic repulsion between the DNA and the lipids, but also promoted uptake of the lipoplexes by the cell. However, the use of high concentrations of calcium (in excess of 25 mM) was shown to be detrimental to transfection efficiency because of the creation of aggregate lipoplexes, having particle sizes of 500 nm and higher [19]. Optimum transfection efficiency is achieved with particles sizes of about 200 nm due to factors thought to be related to clathrin-mediated uptake [25].

4.2.1.4. mPEG₂₀₀₀-DSPE

Numerous biotech drugs have been discovered, some of which have been successfully applied in clinical use along with the development of biotechnology. Many chronic diseases such as cancer and cardiovascular dysfunction can be effectively prevented and treated utilizing biotech drugs. Nucleic acids, RNA, and DNA show huge potential in the treatment of cancer, the delivery of which would be inefficient to the target sites, though. Therefore, a delivery system is required to boost the therapeutic efficacy of labile macromolecular drugs. Currently used nanocarriers, such as liposomes, polymeric NPs, nanoemulsions, and SLNs, have proven useful to deliver nucleic acids [26-28]. Also, PEG-DSPE has been widely applied in the preparation of nanocarriers for the delivery of nucleic acids as drug-carrier material.

Liposome-mediated nucleic acid delivery has been in the spotlight recently, but hurdles still exist, such as low blood stability and RES absorption, and the poor targeting of liposome seriously prevents the nucleic acid from exerting a treatment effect [29]. The end group of PEG-DSPE has been modified with ligands and then inserted into the liposomes for targeted delivery, which can significantly prolong the circulation time in blood, reduce the RES absorption, increase the bioavailability of target organs, target tissues, target cells, or intracellular parts [26, 30].

A small, stable, long-circulating liposomal carrier for antisense oligodeoxynucleotides (asODN) was developed by Stuart et al [31]. The ligand of anti-CD19 coupled with butyrate-PEG-DSPE was included in the liposomal carrier. The result showed that the majority of the asODN was cleared from blood with a half-life of more than 10 sec compared to a time of less than 1 hr for the free asODN. Anti-CD19 liposomes were also effective in delivering an MDR1 asODN to a

multidrug-resistant human B-lymphoma cell line *in vitro* and decreasing the activity of P-glycoprotein. But the nontargeted liposomes and the free asODN did not display any inhibition.

Gene therapy has become a crucial strategy for treating a variety of human diseases including cancer but its safety and effectiveness need to be improved [32, 33]. Thus, the development of suitable carriers for delivering therapeutic genes to target cells or tissues is meaningful and valuable.

Hayes et al. constructed a cationic lipid–nucleic acid NP from a liquid monophasic containing water and a water-miscible organic solvent where both lipid and DNA components are separately soluble prior to their combination. Then, an antibody lipopolymer (anti-HER2 scFv-PEG-DSPE) conjugate was inserted into the NPs. The result showed that PEGylation could reduce the aggregation levels of these cationic NPs in human plasma, and selectively target and transfect HER2 overexpressing cells *in vitro* without losing activity at higher PEG-lipid content. Also, the NPs are relatively small in size, can protect nucleic acids, and can be easily stored under a variety of conditions [34].

According to the poor stability of nucleic acids in the physiological fluids, selective gene inhibition by nucleic acid therapeutics realizes the treatment of diseases that cannot be cured by conventional drug carriers. Li and Huang developed anisamide ligand–modified sterically stabilized NPs for loading antisense oligodeoxynucleotide and siRNA into lung cancer cells. Thus, they prepared stable NPs in the presence of serum. It has been verified that anisamide ligand increased the delivery efficiency of nanoparticles by four- to sevenfold for sigma receptor overexpressing cells and provided strong antisense efficacy for downregulating surviving mRNA and protein, which inhibited tumor cell growth and sensitized tumor cells to anticancer drugs as a result [35].

4.2.1.5. Cholesterol

Cholesterol, from the Greek chole- (bile) and stereos (solid) followed by the chemical suffix -ol for an alcohol, is an organic molecule. It is a sterol and is an essential structural component of animal cell membranes that is required to establish proper membrane permeability and fluidity. In addition to its importance within cells, cholesterol also serves as a precursor for the

biosynthesis of steroid hormones, bile acids, and vitamin D. Cholesterol is the principal sterol synthesized by animals; in vertebrates it is formed predominantly in the liver. It is almost completely absent among prokaryotes (i.e., bacteria). The hydroxyl group on cholesterol interacts with the polar head groups of the membrane phospholipids and sphingolipids, while the bulky steroid and the hydrocarbon chain are embedded in the membrane, alongside the nonpolar fatty-acid chain of the other lipids. Through the interaction with the phospholipid fatty-acid chains, cholesterol increases membrane packing, which reduces membrane fluidity.

DOPE and cholesterol are often used as neutral lipids. On its own, DOPE forms inverted hexagonal H_{III} (non-bilayer) phase structures at neutral pH and physiologic temperatures. When combined with a cationic lipid, however, it can participate in bilayer formation. When the cationic lipid is laterally phase-separated by interaction with negatively charged molecules or macromolecules, the DOPE may form non-bilayer structures. The latter may facilitate the destabilization of the cellular membranes with which the cationic lipid interacts, possibly mediating the cytoplasmic delivery of nucleic acids. Cholesterol-containing cationic liposomes were found to be structurally more stable in physiologic media, thereby enabling the lipoplexes to reach their target tissue intact, thereby protecting the DNA from degradation, and eventually facilitating transfection.

In mixed phospholipid systems containing anionic lipids, not only DOPE, but also cholesterol, has similar abilities to promote H_{II} phase organization. n. Lipids such as DOPC would hinder the ability of cationic lipids to induce H_{II} or non-bilayer structures (Hafez et al., 2001). Aqueous dispersions of DOPS/DOPC (1:1; molar ratio) adopt the bilayer structure (Hafez et al., 2001). In a lipid dispersion containing DODAC/DOPS/DOPC (1:1:1; molar ratio), the presence of an equimolar amount of DODAC (with respect to DOPS) does not result in an H_{II} phase structure. A complete transition to an H_{II} phase structure occurs in DODAC/DOPS/DOPE (1:1:1; molar ratio) dispersions [36]. The addition of DOPE to the DOPC-containing lipid dispersion of results in a transition to the H_{II} phase organization in a DODAC/DOPS/DOPC/DOPE (1:1:1:1; molar ratio) lipid dispersion [36]. In a DODAC/DOPS/DOPC/cholesterol (1:1:1:1; molar ratio) lipid dispersion, the inclusion of cholesterol induces the H_{II} phase structure.

Li et al. (1998) developed a formulation (termed “LPD1”) composed of protamine sulfate, DNA, and 1,2-dioleoyl-3-trimethylammonium-propane (DOTAP)/cholesterol liposomes, producing condensed particles with a relatively small diameter [35]. These gene carriers were stable over time and produced high levels of gene expression *in vivo*. Many current *in vivo* gene transfection protocols utilize vectors containing cholesterol as the neutral-lipid component (leading to L phase complexes), and are more stable in blood.

The biochemistry of life establishes rigid proportions of chemical elements in key molecules: exactly one P atom is in each DNA and RNA nucleotide [37], and each type of amino acid and nucleotide has a specific number of N atoms. The high biological demand for these two chemical elements manifests itself globally – N and P largely limit the world’s primary productivity [38]. But do the fixed proportions of these elements at the molecular scale themselves have a global imprint? The oceanographer A.C. Redfield himself suspected as much, writing: the relative proportion of phosphate and nitrate must tend to approach that characteristic of protoplasm in general and invoking nitrogen fixation and denitrification as mechanisms that can maintain the pattern [39]. We are now gaining a better understanding of the relative contributions of various macromolecules such as DNA, ATP, phospholipids, chlorophyll, free amino acids, surface-adsorbed nutrients and vacuoles to the overall cellular N:P [40]. Most significantly, it has been shown that the largest contributors to cellular N:P ratios in most living things are proteins and RNAs [41].

4.2.2. Development of Cationic Liposomes:

siRNA containing cationic liposomes were prepared using lipid based non-viral delivery vectors. Bilayer forming lipids were utilized to prepare siRNA liposomes containing cationic and neutral phospholipids, cholesterol and mPEG₂₀₀₀-DSPE. These liposomes were developed in two stages:

1. Preparation of blank cationic liposomes
2. Incubation of pre-formed liposomes with siRNA

siRNA encapsulated liposomes were prepared by incubating siRNA with preformed liposomes (**Figure 4.8**).

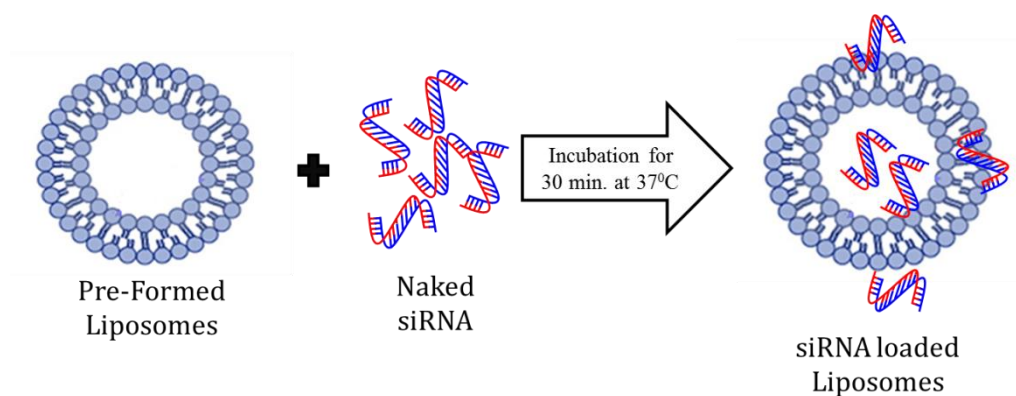


Figure 4.8 Formation of siRNA Encapsulated Cationic Liposomes

4.2.2.1. Preparation of pre-formed liposomes

Various types of formulations containing different lipids as described in **Table 4.1** were developed. All formulations were optimized based on complexation efficiency of preformed liposomes with naked siRNA. Pre-formed cationic liposomes were prepared by thin film hydration method [42] and described below.

Table 4.1 Various Liposomal Formulations with Their Composition

Sr.No.	Formulation	Composition
1	D liposomes	DOTAP
2	DD liposomes	DOTAP:DOPE
3	DDH liposomes	DOTAP:DOPE:PC
4	DDC liposomes	DOTAP:DOPE:Chol
5	DDHC liposomes	DOTAP:DOPE:PC:Chol
6	DDHCP liposomes	DOTAP:DOPE:PC:Chol:PG

Combinations of lipids (as per **Table 4.1**) viz. DOTAP, DOPE, PC, Cholesterol and mPEG-DSPE₂₀₀₀ at different molar ratio, were dissolved in chloroform and added to 50 mL round bottom flask. Organic solvent was evaporated under vacuum (600 mmHg) and temperature (45°C) using rotary evaporator (IKA RV-10, USA). Nitrogen was purged gently for removal of trace amount of solvent, if any. The thin lipid film was hydrated by DEPC treated nuclease free water above glass transition temperature of most rigid phospholipid used. After 1 hr of hydration, liposomal dispersion was collected from RBF and transferred to a glass container. Particle size of liposomes was reduced using successively passing through 1, 0.4, 0.2 and 0.1 µm polycarbonate membranes (Whatman, USA) using high-pressure extruder (Avestin, USA). Polyethylene drain disk (Whatman, USA) was used to support the polycarbonate membrane and hence to potentiate the extrusion process. Prepared liposomes were stored in a glass container at 2-8°C till further processing.

4.2.2.2. Development of siRNA Liposomes

siRNA containing cationic liposomes were prepared by incubating naked siRNA with preformed liposomes at different N/P (Nitrogen/Phosphate) charge ratio, ranging from 0 to 2.0, at optimal time and temperature under constant moderate stirring. Various combinations of lipids were utilized to optimize the formulation with regard to encapsulation of siRNA. Prepared liposomes were filled in to a glass container and further processed for lyophilization.

4.2.2.3. Optimization of Parameters

In above given methods, various process and formulation parameters were involved and all were optimized to achieve best suited formulation for siRNA incorporation.

4.2.2.4. RGD Grafting on the Surface of Liposomes

Optimal formulation containing HSPC, cholesterol, DOTAP, DOPE and mPEG₂₀₀₀-DSPE was further improved by incorporation cyclic RGD peptide due to its capability to target tumor cells. RGD-mPEG₂₀₀₀-DSPE was also added along with above listed lipids in the initial phase during thin film formation to incorporate RGD into the liposomes. Hydration and rest procedure was same as followed earlier in section **4.2.2.1**.

4.2.2.5. Lyophilization of siRNA Liposomes

Prepared cationic liposomes were lyophilized to impart physical stability to the liposomes. Various types of cryoprotectants are used at different ratio to optimize the lyophilization and to preserve particle size during freeze drying. Liposomes were diluted with nuclease free water, containing optimized amount of cryoprotectant, upto 1.0 mL and filled into the 2 mL glass vial (Schott, USA) having 13 mm neck diameter. Vials were half stoppered with grey bromo butyl slotted rubber stoppers (Helvoet, Belgium) and kept on the shelf of lyophilizer (Virtis-Advantage plus, USA). Liposomes were freezed upto -40°C and dried under vacuum for next 44 hr. Complete lyocycle describing freezing time, primary and secondary drying time, ramp and hold duration, vacuum level are given below in **Figure 4.9**.

Recipe Number <input type="text" value="16"/>				Primary Drying				
Thermal Treatment				Temp	Time	Vacuum	R/H	
	Temp	Time	R/H					
Step 1	5	10	H	Step 1	-40	60	200	H
Step 2	-5	20	R	Step 2	-20	40	100	R
Step 3	-5	30	H	Step 3	-20	120	100	H
Step 4	-40	70	R	Step 4	-15	50	100	R
Step 5	-40	300	H	Step 5	-15	300	100	H
Step 6	0	0	H	Step 6	-10	50	100	R
Step 7	0	0	H	Step 7	-10	600	100	H
Step 8	0	0	H	Step 8	10	200	100	R
Step 9	0	0	H	Step 9	10	600	100	H
Step 10	0	0	H	Step 10	20	50	100	R
Step 11	0	0	H	Step 11	20	180	100	H
Step 12	0	0	H	Step 12	0	0	0	H
				Step 13	0	0	0	H
				Step 14	0	0	0	H
				Step 15	0	0	0	H
				Step 16	0	0	0	H
Freeze	<input type="text" value="-40"/>			Secondary SP	<input type="text" value="50"/>			
Extra Freeze	<input type="text" value="10"/>			Post Ht	<input type="text" value="20"/>	<input type="text" value="900"/>	<input type="text" value="200"/>	
Condenser	<input type="text" value="-40"/>							
Vacuum	<input type="text" value="200"/>							

Figure 4.9 Lyophilization Cycle Recipe

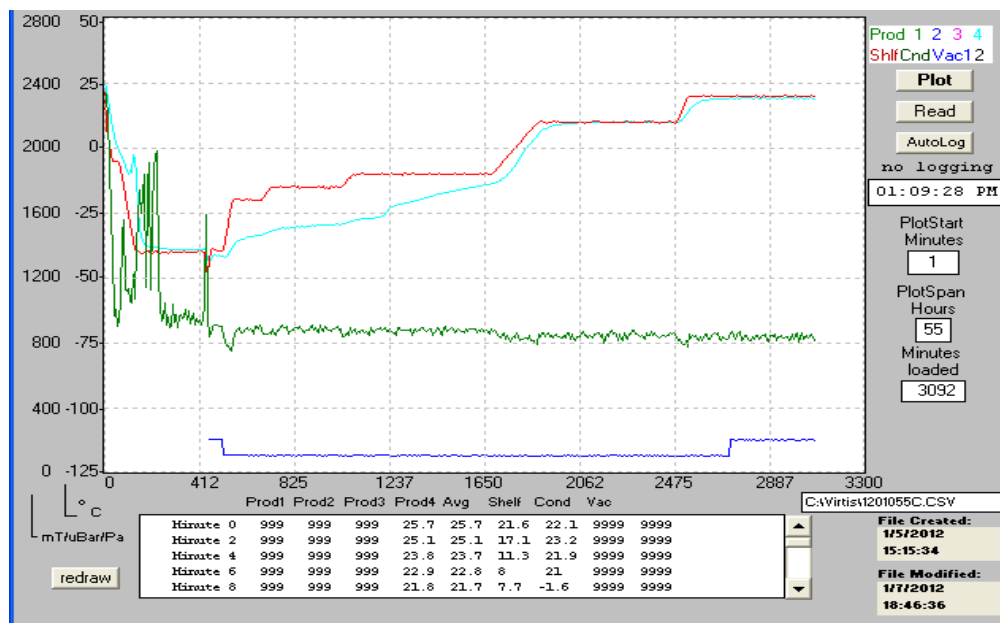


Figure 4.10 Lyophilization Plot

4.2.2.6. Assay

Assay of the prepared formulation was carried out to confirm the amount of siRNA loaded as compared to added siRNA. Assay is important parameter to determine whether any degradation is there or not in final formulations and based on that further potency calculations can be carried out for the *in vitro* and *in vivo* studies. Below given procedure was followed for the assay of the prepared formulations:

Nano-constructs were diluted with Diethylpyrocarbonate (DEPC; Sigma)-treated H₂O to give a final volume of 100 μ L (if required). The samples were then vortexed with 200 μ L of phenol/chloroform (1:1 v/v) and were subsequently spun at 14,000 rpm at 4°C for 10 min. From this centrifuged samples, aqueous layer was separated out and quantified using below given two methods:

1. 5 μ L of the sample was diluted with DEPC treated water up to 25 μ L and mixed with 5 μ L loading buffer and was loaded onto 2% agarose gel. Afterwards, siRNA was visualized by UV transillumination and gel photography using a Gel Doc System (Bio-Rad Lab., USA).
2. Aqueous layer was mixed further with DEPC treated water up to 1 mL and absorbance was taken at 260 nm. Concentration of siRNA was determined as follow:

1 OD = 43.27 $\mu\text{g/mL}$.

4.2.2.7. Entrapment Efficiency

i. Gel Retardation Assay

Following incubation period, siRNA nano-constructs were subjected to gel electrophoresis to assess encapsulation of siRNA within preformed liposomes. siRNA nano-constructs were mixed with 2 μL of 6X DNA gel loading buffer (Fermentas Life Sciences, USA) and loaded onto a 2% agarose gel containing 0.5 $\mu\text{g/mL}$ ethidium bromide, and separated by electrophoresis for 20 min at 100 V in TBE buffer (10.8 g/L Tris base, 5.5 g/L boric acid and 0.58 g/L EDTA). Afterwards, siRNA was visualized by UV trans-illumination and gel photography using a Gel Doc System (Bio-Rad Lab., USA). Amount of free siRNA was visualizes onto the gel.

$$\% \text{ Entrapment} = \frac{\text{Total amount of siRNA added} - \text{Free siRNA}}{\text{Total amount of siRNA added}}$$

ii. Ultracentrifugation

siRNA liposomes were added to the centrifuge tube and centrifuged at 70000 x g for 4 hr at 4°C. Pellet was vortexed with 200 μL of phenol/chloroform (1:1 v/v) and was subsequently spun at 14,000 rpm at 4°C for 10 min. From these centrifuged samples, aqueous layer was separated out and quantified using methods described in the Assay section (**Section 4.2.2.6.**) above.

4.2.2.8. Particle Size and Zeta Potential

The average particle size and zeta potential of siRNA nano-constructs were determined by differential light scattering with a Malvern Zetasizer Nano ZS (Malvern Instruments, Malvern, UK). Prior to the measurement siRNA nano-constructs were diluted with nuclease free water and measurements were carried out at 25°C. Zeta potential was calculated by Smoluchowski's equation from the electrophoretic mobility. Each sample was measured three times and the mean values were calculated.

4.2.2.9. Residual Water content:

The residual water content of lyophilized liposomes was determined by Karl-Fischer titration [43]. Commercially available pyridine free reagent was used for analysis. The reagent was

standardized with addition and determination of known quantity of water (250 mg). Firstly, 40 mL of methanol was added into the titration vessel and titrated with the reagent to determine the amount of water present in the samples. Following this, samples were added and water content was determined.

4.2.2.10. Cryo-Transmission Electron Microscopy (Cryo-TEM)

Morphology and lamellarity of the lipoplex were studied using Cryo-TEM (TECNAI G2 Spirit BioT WIN, FEI-Netherlands) operating at 200 kV with resolution of 0.27 nm and magnifications of the order of 750,000X. Hydrophobic carbon grid was converted to hydrophilic nature by using Glow Discharge to perform cryo TEM (Emitech K100X, Quoram Technologies, UK). Formulation was evenly dispersed on prepared grid and the grid was cryo-frozen in liquid ethane at -180°C . Cryo-frozen grid was transferred to cryo-holder maintained at -175°C using Liquid Nitrogen storage box. The cryo-holder was then inserted in the microscope for imaging the sample. Combination of bright field imaging at increasing magnification and of diffraction modes was used to reveal the form, lamellarity and vesicle size of the prepared formulation.

4.2.2.11. Statistical Analysis

All the experiments were performed in triplicates unless otherwise specified. Statistical analysis of data was performed using an ANOVA and Student-t test. GraphPad Prism (version 5, USA) was used for all analyses and P value < 0.05 was considered significant.

4.2.3. Result and Discussion

4.2.3.1. Preparation of Pre-formed liposomes

Various formulations with different compositions are listed in **Table 4.4**, **Table 4.5**, **Table 4.6**, **Table 4.7**, **Table 4.8** and **Table 4.9**. All formulated pre-formed liposomes were below or near to 100 nm in particle size.

i. Process optimization

Process parameter optimization such as vacuum conditions for dry film formation, hydration time, and speed of rotation of flask were optimized for desired results. The effect of one variable was studied at a time keeping other variables constant. The results are recorded in **Table 4.2** from which the following conclusions are drawn:

1. The vacuum required for solvent evaporation to form a uniform thin film was raised from 400 mm Hg to 650 mm Hg. The low vacuum (400 mm Hg) was found to be insufficient for the complete removal of the solvent. The presence of residual solvent may lead to physical destabilization of liposomes by interfering with the co-operative hydrophobic interactions among the phospholipid methylene groups that hold the structure together [44]. The vacuum of 600 mm of Hg for 60 min was found to be optimum for complete evaporation of solvent and producing more translucent and thin lipid film. However, for complete solvent removal of residual solvent (post film formation) the flask was purged with nitrogen for 4 hr. Higher vacuum (650 mm Hg) resulted in rapid evaporation of the solvent system leading to crystallization and hence resulted in poor orientation of liposomes. This is in agreement with the findings of Martin et al (1990) that differential solubilities of amphiphilic components of bilayer and drug in organic solvents are often encountered and must be taken into consideration in order to avoid crystallization of a single component during solvent-stripping operations.
2. Speed of rotation: The speed of rotation of flask was increased from 50 rpm to 150 rpm. Rotation of 50 rpm resulted in thick incompletely dried film and presence of residual solvents. While at 150 rpm speed, a dry film with varying thickness was produced with a thicker film at periphery and thinner film at the centre. A speed of 100 rpm was found to be adequate to give thin, uniform and completely dry film. Hence, 100 rpm speed of rotation of flask was selected to be optimum for liposomal preparations.
3. Hydration time: The lipid film was hydrated from 30 min to 2 hr before size reduction. An optimal hydration time was required for complete conversion of planner bilayers to spherical liposomes. Lower hydration time led to a non-uniform shape and size of the liposomes and also the un-hydrated part posed difficulty in size reduction. The hydration time beyond 1 hr resulted in no further improvement. Hence, 1 hr hydration time was found to be optimum for all preparations.

Table 4.2 Selection of Process Parameters for Pre-formed Liposomes*

COMPOSITION OF SOLVENT SYSTEM	
CHLOROFORM	Observation
	Suitable
SOLVENT EVAPORATION TIME	
Time (min)	Observation
45 min	Not proper hydration
60 min	Suitable (Solvent is completely removed)
90 min	No further improvement
SPEED OF ROTATION	
rpm	Observation
50 rpm	Non Uniform distribution
100 rpm	Suitable
150 rpm	Non Uniform distribution
HYDRATION TIME	
Time (min)	Observation
30 min	Not properly hydrated
60 min	Suitable hydration
90 min	No further improvement but decrease in PDE
VACUUM APPLIED	
vacuum (mm of Hg)	Observation
400	Flecking during hydration
500	Flecking during hydration
600	Uniform film and uniform liposomal dispersion
650	Un-uniform film

*Experiments were performed in triplicate.

4.2.3.2. Preparation of cationic siRNA liposomes:

Formulation of this phase was further to be complexed with siRNA and formulation parameters i.e. types of lipids and amount to be used is dependent on encapsulation of siRNA. Optimization of each lipid composition against encapsulation of siRNA is described below in section (4.2.3.2.ii).

i. Process optimization

Process parameter optimization such as incubation time and temperature were optimized for desired results. The effect of one variable was studied at a time keeping other variables constant. The results are recorded in **Table 4.3** from which the following conclusions are drawn:

Incubation Time: Incubation time for the complexation between siRNA and pre-formed liposomes is very vital. Many reports suggest that incubation should be between 20-30 min at

ambient temperature. Three different levels were studied as variables i.e. 15 min, 30 min and 45 min. At 15 min less than 70 % of siRNA were complexed with liposomes, confirmed by gel electrophoresis. Incubation at 30 and 45 min generated same results and showed more than 90 % of complexation.

Table 4.3 Selection of Process Parameters for Pre-Formed Liposomes#

Incubation Time	
Time (min)	% siRNA entrapped*
15 min	< 70
30 min	> 90
45 min	> 90
Incubation temperature	
Temperature (°C)	% siRNA entrapped*
25	< 80
37	> 90
45	> 90
*N/P =2 for all formulation.	

#Experiments were performed in triplicate.

ii. Formulation Optimization

The cationic pre-formed liposomes were used to complex negatively charged siRNA. Various lipids were used to prepare liposomes. A positively charged lipid DOTAP was a key lipid for encapsulation of siRNA. Combinations of lipids were tried to complex siRNA as given in **Table 4.1**. The gel retardation pattern of siRNA was affected mainly by N/P ratios. N is the nitrogen of the cationic lipid, DOTAP. This N is the quaternary nitrogen and hence, responsible for the positive charge for the cationic lipid. P in the N/P ratio is the phosphate group of nucleic acid base of siRNA. Apart from N/P incorporation of other lipids is also crucial for siRNA complexation. For siRNA complexation, formulations containing varying ratio of N/PC (phosphatidyl choline) and N/Chol are studied thoroughly.

Below N/P ratio of 1.0, a considerable amount of the siRNA migrated as free siRNA on agarose gels towards positive electrode. In both cases of D liposomes and DD liposomes, above N/P of

1.25 complexation occurred but obtained complex was very loose. As seen in **Figure 4.11**, complex occurred at N/P of 1.25 and very soon at N/P of 1.5 complexation was very low. However, by repeating the same formulation complexation was found to occur at 1.5 and again free siRNA was seen at N/P of 1.75 and 2.0. These results suggest the inability of D and DD liposomes for complete complexation of siRNA. This loose complex may release siRNA before entering inside the cell and certainly can lead to toxicity. Complexation of siRNA at different N/P ratio (0 to 2.0) for D liposomes and DD liposomes are given in **Table 4.4** and **Table 4.5** respectively.

Table 4.4 Formulation Development of D Liposomes*

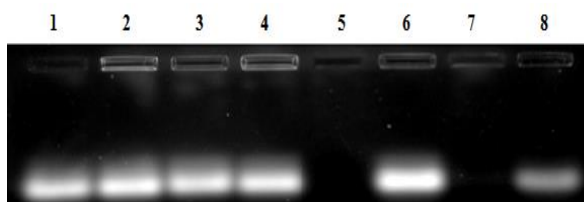
Formulation	Lipids	Lipid Ratio	N/P	Observation	% siRNA complexed	Remarks
D liposomes	DOTAP	1	0	Free siRNA	0	Loosely bound complex formed at N/P = 1.25 and above
		1	0.5	Partially complexed siRNA	22.2±0.53	
		1	0.75	Partially complexed siRNA	40.7±1.22	
		1	1.0	Partially complexed siRNA	62.5±1.32	
		1	1.25	Partially complexed siRNA	95.7±0.98	
		1	1.5	Partially complexed siRNA	96.9±1.06	
		1	1.75	Partially complexed siRNA	96.5±0.79	
		1	2.0	Partially complexed siRNA	96.3±1.09	

*Experiments were performed in triplicate.

Table 4.5 Formulation development of DD Liposomes*

Formulation	Lipids	Lipid Ratio	N/P	Observation	% siRNA complexed	Remarks
DD liposomes	DOTAP : DOPE	1:1	0	Free siRNA	0	Loosely bound complex formed at N/P=1.25 and above.
		1:1	0.5	Partially complexed siRNA	25.5±1.63	
		1:1	0.75	Partially complexed siRNA	43.2±0.89	
		1:1	1.0	Partially complexed siRNA	66.7±1.01	
		1:1	1.25	Completely complexed siRNA	96.4±1.08	
		1:1	1.5	Partially complexed siRNA	97.5±0.87	
		1:1	1.75	Completely complexed siRNA	96.2±1.35	
		1:1	2.0	Partially complexed siRNA	97.5±1.32	

*Experiments were performed in triplicate.

**Figure 4.11 Gel Electrophoresis of DD liposomes**

1=Naked siRNA, 2=N/p-0.5, 3=N/p-0.75, 4=N/p-1.0,
5=N/P-1.25, 6=N/P-1.5, 7=N/P-1.75, 8=N/p-2.0

PC was incorporated at different molar ratio with DOTAP viz, N/PC of 0.3, 0.38 and 0.75. HSPC was used as PC due to its higher rigidity ($T_g = 55\text{ }^\circ\text{C}$). Complete complexation (> 95%) was achieved at higher concentration of PC (N/PC=0.3). HSPC was used as a PC. Complexation was increased by increasing the amount of HSPC. **Table 4.6** summarizes the complexation efficiency of DDH liposomes by varying the amount of HSPC.

Table 4.6 Formulation development of DDH liposomes*

Formulation	Lipids	Lipid Ratio	N/P	Observation	% siRNA complexed	Remark
DDH Liposomes	DOTAP :DOPE: PC	1:1:1.3	1.0	Partially complexed siRNA	52.2±1.68	N/PC= 0.3 gives complete complexation at N/P=2.0.
		1:1:1.3	1.5	Partially complexed siRNA	60.5±1.45	
		1:1:1.3	2.0	Partially complexed siRNA	69.3±0.98	
		1:1:2.6	1.0	Partially complexed siRNA	55.5±2.63	
		1:1:2.6	1.5	Partially complexed siRNA	63.3±2.40	
		1:1:2.6	2.0	Partially complexed siRNA	73.3±1.86	
		1:1:3.9	1.0	Partially complexed siRNA	70.3±1.56	
		1:1:3.9	1.5	Partially complexed siRNA	85.2±2.23	
		1:1:3.9	2.0	Completely complexed siRNA	98.4±1.53	

*Experiments were performed in triplicate.

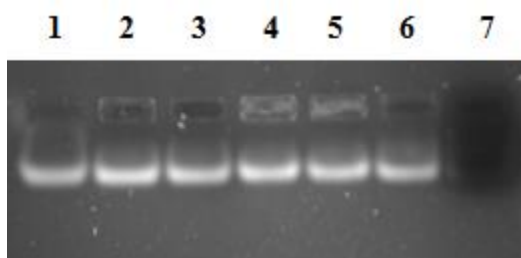


Figure 4.12 Gel Electrophoresis of DDH Liposomes

1=Naked siRNA, 2=N/P-1.0, 3=N/P-1.5, 4=N/P-2.0, 5=N/P-1.0, 6=N/P-1.5, 7=N/P-2.0

2,3,4=N/PC-0.75, 5,6,7=N/PC-0.3

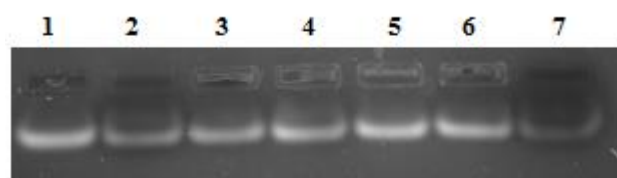


Figure 4.13 Gel Electrophoresis of DDH Liposomes

1=Naked siRNA, 2=N/P-1.0, 3=N/P-1.5, 4=N/P-2.0, 5=N/P-1.0, 6=N/P-1.5, 7=N/P-2.0
2,3,4=N/PC-0.5, 5,6,7=N/PC-0.38

- N/PC= 0.5 & 0.3 gives complete complexation at N/P=2.0.

Cholesterol has always been believed to be an unavoidable excipient for the liposomal preparation due to its membrane rigidizing capacity [45, 46]. In present work also same phenomenon was observed. Incorporation of cholesterol led to an increment in siRNA encapsulation as seen in **Table 4.7**. Three levels of cholesterol were used i.e. N/Chol = 0.77, 0.38 and 0.25. Complete incorporation of siRNA was detected at N/Chol ratio of 0.38. However, at lower concentration also, 90.5 % of complexation was observed. At higher concentration, cholesterol incorporation into the liposomes seemed to be dramatic and improper liposome formation was observed. Hence, restricted further increment in cholesterol amount more than N/Chol = 0.38 in DDC liposomes. **Figure 4.7** summarizes the effect of addition of cholesterol in DDC liposomes with respect to siRNA complexation. **Figure 4.14** and **Figure 4.15** shows gel-electrophoresis of DDC liposomes at different N/Chol ratios.

Table 4.7 Formulation development of DDC Liposomes

Formulation	Lipids	Lipid Ratio	N/P	Observation	% siRNA complexed	Remark
DDC liposomes	DOTAP :DOPE: Chol	1:1:1.3	1.0	Partially complexed siRNA	40.2±0.68	At N/Chol=0.38 siRNA complexation occurred at N/P=2.
		1:1:1.3	1.5	Partially complexed siRNA	52.3±1.48	
		1:1:1.3	2.0	Completely complexed siRNA	90.5±1.23	
		1:1:2.6	1.0	Partially complexed siRNA	43.2±1.02	
		1:1:2.6	1.5	Partially complexed siRNA	55.3±1.63	
		1:1:2.6	2.0	Partially complexed siRNA	97.5±1.24	
		1:1:3.9	-	Improper Liposome formation	-NA-	

*Experiments were performed in triplicate.

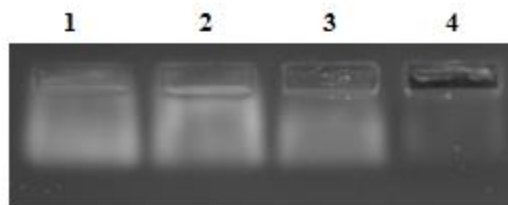


Figure 4.14 Gel Electrophoresis of DDC liposomes at N/Chol=0.77
 1=Naked siRNA, 2=N/p-1.0, 3=N/p-1.5, 4=N/p-2.0
N/Chol=0.77

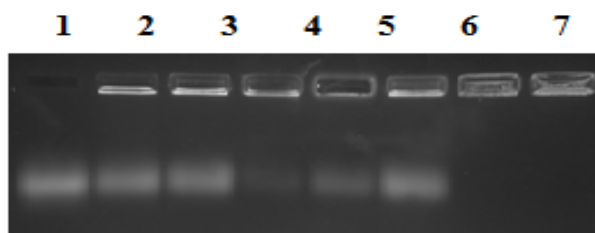


Figure 4.15 Gel Electrophoresis of DDC liposomes at N/Chol=0.38
 1=Naked siRNA, 2=N/p-0.5, 3=N/p-0.75, 4=N/p-1.0,
 5=N/P-1.25, 6=N/P-1.5, 7=N/P-1.75, 8=N/p-2.0; *N/Chol=0.38*

By keeping the N/PC ratio to 0.3, again cholesterol was incorporated and siRNA complexation was measured by agarose gel electrophoresis. Three concentrations of cholesterol were used i.e. N/Chol= 0.77, 0.3 and 0.25. There was no problem in liposome formation at higher concentration as seen with DDC liposomes at N/Chol = 0.25. This was due to membrane forming phospholipid, HSPC. It provided space for the cholesterol incorporation. However, complexation was again found to be complete (98.2) at N/Chol = 0.38 (**Table 4.8**).

Table 4.8 Formulation development of DDHC liposomes*

Formulation	Lipids	Lipid Ratio	N/P	Observation	% siRNA complexed	Remark
DDHC Liposomes	DOTAP : DOPE : PC: Chol (N/PC= 0.30)	1:1:3.3:1.3	1.0	Partially complexed siRNA	45.3±1.65	Complete complexation was achieved using combination of DOTAP, DOPE, PC and cholesterol at N/P < 2.0. <u>1:1:3.3:2.6</u>
		1:1:3.3:1.3	1.5	Partially complexed siRNA	58.3±1.06	
		1:1:3.3:1.3	2.0	Partially complexed siRNA	87.5±1.26	
		1:1:3.3:2.6	1.0	Partially complexed siRNA	55.3±1.09	
		1:1:3.3:2.6	1.5	Partially complexed siRNA	85.6±0.79	
		1:1:3.3:2.6	2.0	Completely complexed siRNA	98.2±1.57	
		1:1:3.3:3.9	1.0	Partially complexed siRNA	33.3±2.04	
		1:1:3.3:3.9	1.5	Partially complexed siRNA	49.7±1.63	
		1:1:3.3:3.9	2.0	Partially complexed siRNA	63.2±1.96	

*Experiments were performed in triplicate.



Figure 4.16 Gel Electrophoresis of DDHC liposomes

(a) 1: Naked siRNA, 2: N/P=0.50, 3: N/P=0.75, 4: N/P=1.00, 5: N/P=1.25, 6: N/P=1.50, 7: N/P=1.75, 8: N/P=2.00 (b) 3D image

Above figure shows that liposomes formed by incubating pre-liposomes made up of DOTAP, DOPE, HSPC, Cholesterol and mPEG₂₀₀₀-DSPE completely inhibited the electrophoretic mobility of siRNA at N/P ratio of 2.0. Further, RGD-mPEG₂₀₀₀-DSPE was incorporated for targeting of prepared liposomes to the tumor cell surface. There was no change in complexation efficacy by RGD grafting on liposomal surface (**Figure 4.17**). mPEG₂₀₀₀-DSPE linked RGD was used to graft RGD peptide onto the liposomal surface. Incorporation of 1 mol%, 2 mol% and 3 mol% of RGD-mPEG₂₀₀₀-DSPE into DDHC liposomes (RGD-DDHC liposomes) showed same result for siRNA encapsulation.

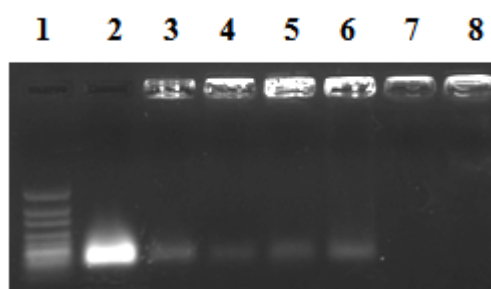


Figure 4.17 Gel Electrophoresis of DDHC liposomes prepared with 2 mol% mPEG₂₀₀₀-DSPE

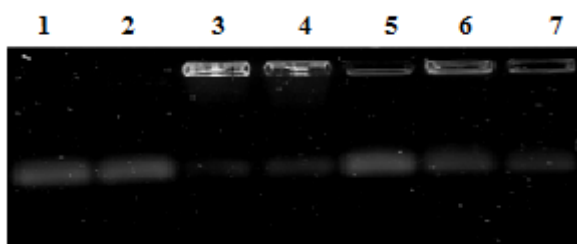
1: Ladder 10 bp, 2: Naked siRNA, 3: N/P=0.50, 4: N/P=1.0, 5: N/P=1.25, 6: N/P=1.50, 7: N/P=1.75, 8: N/P=2.00

All prepared cationic liposomes showed strong positive zeta potential value due to the use of positively charged lipid, DOTAP. This positive charge at the surface may lead to cytotoxicity as reported by many scientists. To neutralize the surface charge, DDHC liposomes were incubated with increasing amount of DMPG, a negatively charge phospholipid. Four levels of DMPG were used, i.e. N/PG= 3.33, 2.0, 1.25 and 1.0. These all led to removal of complexed siRNA from the DDHC liposomes (**Table 4.9** and **Figure 4.18**). Hence, this strategy was not used for further work.

Table 4.9 Formulation development of DDHCP liposomes

Formulation	Lipids	Lipid Ratio	N/P	N/PG	% siRNA complexed	Remark
DDHCP liposomes	DOTAP :DOPE : PC: Chol : PG (N/PC=0.30) (N/Chol=0.38)	1:1:3.3:2.6:0	2.0	0.0	98.2±0.86	Complexed siRNA
		1:1:3.3:2.6:0.3	2.0	3.33	90.4±1.21	Complexed siRNA
		1:1:3.3:2.6:0.5	2.0	2.0	74.5±1.66	Partially complexed siRNA
		1:1:3.3:2.6:0.8	2.0	1.25	56.4±2.13	Partially complexed siRNA
		1:1:3.3:2.6:1.0	2.0	1.0	37.5±1.65	Partially complexed siRNA

*Experiments were performed in triplicate.

**Figure 4.18 Gel Electrophoresis of DDHCP liposomes**

1=Naked siRNA, 2=Naked siRNA + Naked PG, 3=N/P-2.0, 4=N/P-2.0&N/PG-3.33, 5=N/P-2.0 &N/PG-2, 6=N/P-2.0 &N/PG-1.25, 7=N/P-2.0&N/PG-1.0

- PG affects the complexation of siRNA with cationic lipid.

4.2.3.3. Optimized formulations

From the results summarized in **Table 4.10** given below following points was summarized:

- D liposomes and DD liposomes did not form tightly bound complex with siRNA and hence, cannot be considered as an optimal formulations.
- DDH liposomes could form tight complex with siRNA but there was significant increase in particle size as compared to other formulation during complexation.
- DDC and DDHC formed very stable tightly bound complex with siRNA. Further, particle size was also below 200 nm after complexation. In case of the DDHC liposomes, particle

size after complexation was below 150 nm and hence, RGD was grafted on the surface of the DDHC liposomes.

Table 4.10 Optimized Formulations

Formulation	Lipid ratio	N/P	Particle size Before complexation	Particle size After complexation	Remarks
D liposomes	1*	2	85.6±2.6	504.6±7.5	Loosely bound complex
DD liposomes	1:1*	2	87.3±5.9	593.1±6.9	Loosely bound complex
DDH liposomes	1:1:3.3*	2	101.4±6.3	261.5±7.4	Tightly bound complex
DDC liposomes	1:1:2.6*	2	91.7±2.5	174.3±6.7	Tightly bound complex
DDHC liposomes	1:1:3.3:2.6*	2	104.5±4.6	145.9±8.7	Tightly bound complex
RGD-DDHC liposomes (1%)	1:1:3.3:2.6** (1 mol % RGD)	2	105.8±4.3	147.2±7.9	Tightly bound complex
RGD-DDHC liposomes (2%)	1:1:3.3:2.6** (2 mol % RGD)	2	106.3±7.9	147.5±8.9	Tightly bound complex
RGD-DDHC liposomes (3%)	1:1:3.3:2.6** (3 mol % RGD)	2	106.9±5.8	146.8±10.3	Tightly bound complex

* All formulations contain 5 mol% of mPEG₂₀₀₀-DSPE

** Contains 3 mol% of mPEG₂₀₀₀-DSPE

4.2.3.4. Lyophilization

The liposomal formulations were stabilized by lyophilization. As seen in the earlier results, that cationic liposomes are prone to increase in size with complexation and hence, on aging also size may increase. Thus, to provide physical stability lyophilization was carried out. Different cryoprotectants at various concentrations were added to the liposomal dispersion. The role of Cryoprotectant was to act as a bulking agent and hence, to provide physical structure to the lyophilized cake and secondly to preserve the particle size of the liposomes during thermal treatment i.e. freezing step of lyophilization. During freezing there is an ice formation from water molecules and this ice may rupture the morphology of prepared liposomes. Cryoprotectant

helps to stabilize the system by providing the protection against developed local effects during freezing and also prevent increase in local concentration of the precipitated solid during freezing. These all collectively stabilize the nanomaterial in its much possible original form. The lyophilized formulations were tested for particle size, zeta potential and physical appearance. There was no degradation of siRNA was observed after lyophilization and also complexation was much stable. Lactose, mannitol and sucrose were used at three different concentrations i.e. 25 g/mL, 50 mg/mL, 75 mg/mL in the final formulation (RGD-DDHC liposomes (2%)). Results for the lyophilization optimization are summarised in **Table 4.11** and **Table 4.12**.

Table 4.11 Lyophilization Optimization*

Cryoprotectants	Concentration (mg/mL)	Before lyophilization		After lyophilization	
		particle size (nm)	Zeta potential (mV)	particle size (nm)	Zeta potential (mV)
Lactose	25	147.5±2.89	12.26±0.54	300.5±7.7	11.32±1.20
Sucrose				176.3±6.9	11.84±0.65
Mannitol				246.2±10.3	12.47±0.84
Lactose	50			254.3±7.3	11.52±0.45
Sucrose				152.8±8.6	12.03±0.68
Mannitol				220.4±9.5	12.26±0.94
Lactose	75			259.3±7.3	14.32±1.10
Sucrose				154.3±6.7	12.64±0.99
Mannitol				213.2±9.9	11.59±0.75

*Experiments were performed in triplicate.

Table 4.12 Lyophilization Optimization*

Cryoprotectants	Concentration (mg/mL)	Lyophilized cake Integrity	Reconstitution time	Water Content (%w/w)
Lactose	25	Poor	20 sec	1.13±0.05
Sucrose		Poor	30 sec	1.43±0.09
Mannitol		Poor	20 sec	1.61±0.03
Lactose	50	Good	30 sec	1.17±0.04
Sucrose		Good	40 sec	1.89±0.01
Mannitol		Good	30 sec	1.78±0.09
Lactose	75	Good	70 sec	3.27±0.12
Sucrose		Good	85 sec	3.65±0.08
Mannitol		Good	55 sec	3.01±0.05

*Experiments were performed in triplicate.

i. Effect on Particle size and zeta potential:

Lactose and mannitol did not preserve the particle size of liposomes. At all concentration these two sugars failed to maintain the particle size below 200 nm. Sucrose did perform the task by maintaining the size of liposomes at 50 mg/mL and 75 mg/L concentrations. At all concentrations the maintenance of particle size by these cryoprotectants followed below given order: Lactose < Mannitol < Sucrose.

At all concentrations of used cryoprotectants, the zeta potential value did not change significantly. This result suggest the stability of complex after lyophilization and hence preservation of siRNA in the intact form.

ii. Physical Integrity and Redispersion:

Lower concentration of cryoprotectant i.e. 25 mg/mL did not form physical good cake. Lyophilized material was not in an intact form and poor quality of cake was formed. However, at higher concentrations, 50 mg/mL and 75 mg/mL, this problem was solved.

Less than 30 sec were required to reconstitute the lyophilized formulations with all types of cryoprotectant. However, at higher concentration 75 mg/mL, more than 60 sec were required for the reconstitution. Water content at 25 mg/mL and 50 mg/mL concentrations were found below 2% w/w. As sucrose preserved the particle size within narrow range as compared to non-lyophilized liposomes, the concentration having minimum particle size, good cake property and good redispersion property was selected. Taking collectively these results, 50 mg/mL of sucrose as a cryoprotectant was chosen.

4.2.3.5. Assay

Assay was determined by Phenol/Chloroform extraction method. Extracted siRNA was collected in aqueous layer and quantified using gel densitometry and UV spectroscopy. All types of formulations showed no degradation of siRNA during processing and in all formulations, detected siRNA was within limit (95-105 %), which was confirmed by both methods. Results are summarized in **Table 4.13**.

Table 4.13 Characterization of siRNA loaded liposomes*

Sr.No.	Formulation	Assay	
		UV spectroscopy	Gel retardation assay
1.	D liposomes	99.09±3.26	98.78±2.63
2.	DD liposomes	102.51±2.86	100.32±3.02
3.	DDH liposomes	102.64±4.01	101.03±4.06
4.	DDC liposomes	99.90±2.63	99.01±3.56
5.	DDHC liposomes	101.31±2.41	100.52±4.09
6.	RGD-DDHC liposomes (1%)	99.86±3.45	98.60±3.68
7.	RGD-DDHC liposomes (2%)	102.67±3.74	99.87±3.98
8.	RGD-DDHC liposomes (3%)	101.42±2.96	100.25±3.20

*Experiments were performed in triplicate.

Assay results clearly suggest that there is no degradation of siRNA during processing and gel electrophoresis further proves retaining of intact form of liposomes in final formulations. These data are supported by the studies conducted earlier that no degradation of siRNA was found at 37°C incubation for half an hr.

4.2.3.6. Entrapment Efficiency

All formulations were subjected to study entrapment of siRNA, either encapsulated within liposomes or complexed to the surface. Gel retardation assay method provided amount of free siRNA migration and hence, entrapped siRNA was calculated by deducting the free siRNA from initially added siRNA. Optimized formulations were also subjected to ultracentrifuge method to determine siRNA entrapment by direct analysis of liposomal fraction only, because free siRNA was removed from the supernatant after centrifugation. Results are summarized in **Table 4.14**. As D liposomes and DD liposomes did form loose complex, they are not included in the table. More than 95% of entrapment was achieved in all the optimized formulations and that can be considered as complete complexation of siRNA with preformed liposomes. RGD grafting did not affect the entrapment efficacy and difference between with and without RGD grafting was insignificant. Effect of various process and formulation parameters on the entrapment efficacy of the cationic liposomes has already been discussed in this chapter in the section **4.2.3**.

Table 4.14 siRNA Entrapment of Various Liposomes*

Sr.No.	Formulation	siRNA entrapment (%)		
		Gel retardation assay	Ultracentrifugation	
			UV spectroscopy	Gel electrophoresis
1.	DDH liposomes	98.4±2.79	99.02±3.51	95.01±2.63
2.	DDC liposomes	97.5±3.60	97.14±2.32	96.58±1.98
3.	DDHC liposomes	98.2±1.89	97.73±2.84	97.41±3.26
4.	RGD-DDHC liposomes (1%)	97.82±2.06	96.10±3.01	98.34±3.72
5.	RGD-DDHC liposomes (2%)	98.20±3.34	99.56±2.94	96.53±2.63
6.	RGD-DDHC liposomes (3%)	97.94±3.13	98.07±2.61	96.60±2.42

*Experiments were performed in triplicate.

4.2.3.7. Particle size and Zeta potential

Particle size of the cationic liposomes after complexation was mainly dependent on the rigidity of pre-formed liposomes obtained in step-1. siRNA complexation drastically increased the particle size ($p < 0.05$) of the D, DD and DDH liposomes. This effect occurred mainly due to surface complexation of siRNA with pre-formed liposomes. Zeta potential was found to be decreased after siRNA complexation and further confirms the surface interaction between positively charged liposomes and negatively charged siRNA. **Table 4.15** and **Table 4.16** describe change in particle size and zeta potential of developed cationic liposomes. **Figure 4.19** and **Figure 4.20** show particle size and zeta potential reports of one of the RGD-DDHC liposomes (2%) batch after siRNA complexation.

Table 4.15 Effect of siRNA Complexation on Particle Size*

Sr.No.	Formulation	Particle size (nm)		Change in Mean Particle size (%)
		Before	After	
1.	D liposomes	85.6±2.6	504.6±7.5	489.5
2.	DD liposomes	87.3±5.9	593.1±6.9	579.4
3.	DDH liposomes	101.4±6.3	261.5±7.4	157.9
4.	DDC liposomes	91.7±2.5	174.3±6.7	90.1
5.	DDHC liposomes	104.5±4.6	145.9±8.7	39.6
6.	RGD-DDHC liposomes (1%)	105.8±4.3	147.2±7.9	39.1
7.	RGD-DDHC liposomes (2%)	106.3±7.9	147.5±8.9	38.8
8.	RGD-DDHC liposomes (3%)	106.9±5.8	146.8±10.3	37.3

*Experiments were performed in triplicate.

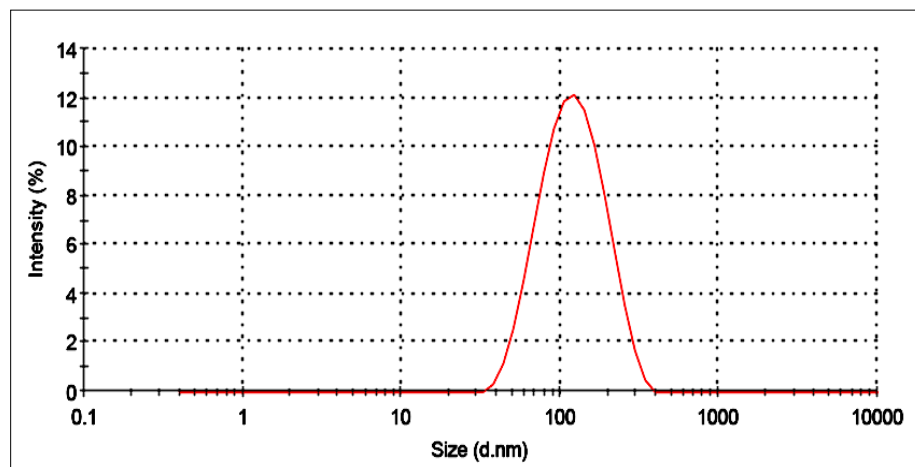


Figure 4.19 Particle size of RGD-DDHC Liposomes (2%) after Complexation

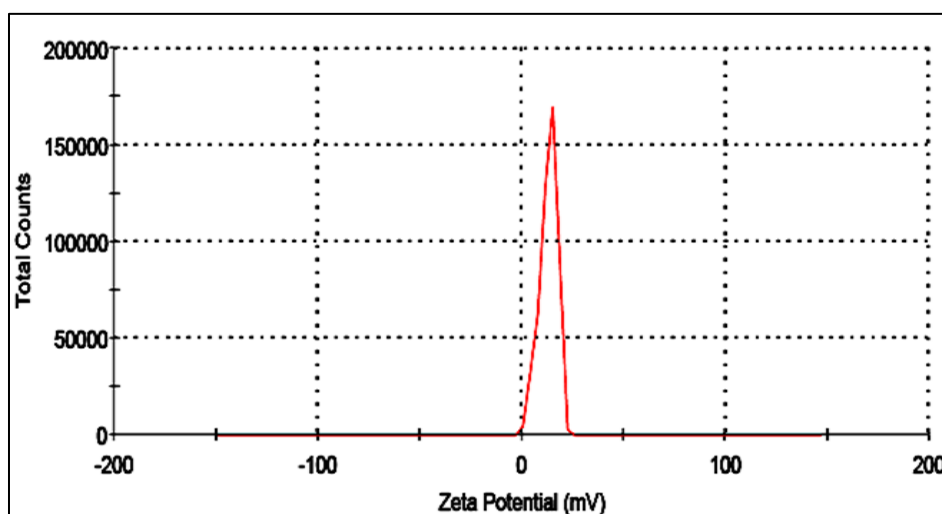


Figure 4.20 Zeta potential of RGD-DDHC liposomes (2%) after Complexation

Table 4.16 Effect of siRNA Complexation on Zeta Potential*

Sr.No.	Formulation	Zeta potential (mV)		Change in Mean Zeta Potential (%)
		Before	After	
1.	D liposomes	38.63±0.35	15.84±0.64	59.00
2.	DD liposomes	37.48±0.79	16.24±0.76	56.67
3.	DDH liposomes	34.42±1.36	13.39±0.87	61.10
4.	DDC liposomes	35.91±0.68	13.52±0.68	62.35
5.	DDHC liposomes	34.83±0.98	12.90±0.68	62.96
6.	RGD-DDHC liposomes (1%)	33.28±0.92	12.81±0.54	61.51
7.	RGD-DDHC liposomes (2%)	33.85±0.29	12.26±0.65	63.78
8.	RGD-DDHC liposomes (3%)	33.01±0.39	11.87±0.45	64.04

*Experiments were performed in triplicate.

4.2.3.8. Residual Water Content

Water content was well characterised by Karl fisher titration method. All lyophilized samples were found to contain less than 3% w/w of water content. Liposomes containing low Tg lipids, D liposomes and DD liposomes showed more than 2% of water content due to higher bound water in those lipids. DDHC liposomes and RGD-DDHC liposomes were found to contain below 2% of moisture after lyophilization. Residual water contents of lyophilized formulations are given below in **Table 4.17**.

Table 4.17 Residual Water Content of Various Lyophilized Products*

Sr.No.	Formulation	Water Content (%w/w)
1.	D liposomes	2.10±0.15
2.	DD liposomes	2.87±0.21
3.	DDH liposomes	1.96±0.16
4.	DDC liposomes	1.92±0.12
5.	DDHC liposomes	1.95±0.24
6.	RGD-DDHC liposomes (1%)	1.82±0.13
7.	RGD-DDHC liposomes (2%)	1.89±0.10
8.	RGD-DDHC liposomes (3%)	1.74±0.18

*Experiments were performed in triplicate.

4.2.3.9. Transmission Electron Microscopy

Images obtained by TEM revealed that prepared liposomes are spherical in shape as shown in **Figure 4.21**. All vesicles are unilamellar in structure and having particle size below 200 nm. This range can also help in EPR effect for tumor internalization of nano materials [47]. Bilayer thickness was also measured and found to be in-between 5-10 nm in size.

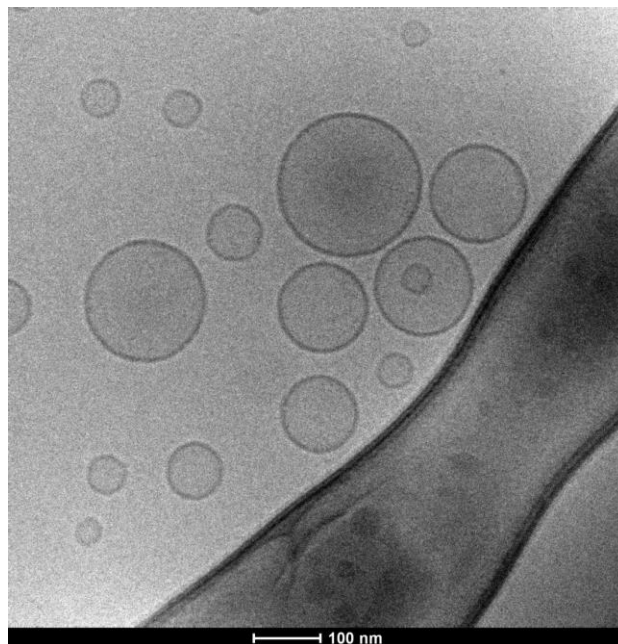


Figure 4.21 Transmission Electron Micrograph of RGD-DDHC liposomes (2%) after complexation

4.3 Development of Calcium Phosphate mediated siRNA Loaded in Liposomes

4.3.1. Methodology

Initially four different approaches were tried to screen best suited method to encapsulate siRNA within the liposomal core containing calcium phosphate precipitates. **Table 4.18** describes the brief procedure involved in each method.

Method-1: Incubation of siRNA with Calcium Phosphate encapsulated liposomes

Method-2: Incubation of Sodium phosphate and siRNA with calcium encapsulated liposomes

Method-3: Incubation of calcium with phosphate encapsulated liposomes and incubation with siRNA.

Method-4: Incubation of siRNA with liposomes hydrated using calcium phosphate precipitates.

Table 4.18 Methods for Calcium Phosphate Mediated siRNA Loading in Liposomes*

Sr.No.	Method	Description	Observation	Remarks
1.	Method-1	<ul style="list-style-type: none"> Preparation of calcium entrapped liposomes. Transport of phosphate inside the calcium entrapped liposomes to prepare calcium phosphate entrapped liposomes. Incubation of siRNA with above liposomes. 	Physically stable liposomes were obtained with more than 50% entrapment.	Method-1 was selected for further development
2.	Method-2	<ul style="list-style-type: none"> Preparation of calcium entrapped liposomes. Incubation of siRNA and phosphate with above liposomes to encapsulate siRNA inside the liposomes. 	Physically stable liposomes with less than 50% entrapment	-
3.	Method-3	<ul style="list-style-type: none"> Preparation of phosphate entrapped liposomes. Transport of calcium inside the phosphate entrapped liposomes to prepare calcium phosphate entrapped liposomes. 	Physically unstable liposomes	-

		<ul style="list-style-type: none"> • Incubation of siRNA with above liposomes. 		
4.	Method-4	<ul style="list-style-type: none"> • Hydration of lipid film with calcium phosphate precipitates to encapsulate calcium phosphate. • Incubation of siRNA with above liposomes. 	Physically unstable liposomes	-

*Experiments were performed in triplicate.

It was observed that method-3 and method-4 did not form physically stable liposomes and hence, were not further optimized. Method-2 formed stable liposomes before siRNA encapsulation but encapsulation was significantly less as compared to method-1. Thus, method-1 was taken further for optimization of siRNA entrapment using design of experiment concept.

4.3.2. Preparation of Calcium phosphate encapsulated siRNA liposomes (CPE liposomes)

In this method no cationic lipid was used in the formulation and all inactive ingredient used are approved as per IIG (Inactive Ingredient Guide) limit provided by USFDA. siRNA containing CPE liposomes were prepared in two steps:

Step-1: Preparation of calcium phosphate liposomes

Step-2: Loading of siRNA in calcium phosphate entrapped liposomes

4.3.2.1. Preparation of Calcium Phosphate Liposomes

Liposomes were prepared using thin film hydration method as described in the earlier formulation. Briefly, dipalmitoyl-*sn*-glycero-3-phosphocholine (DPPC), cholesterol, DOPE, and mPEG-DSPE, at different molar ratios, were dissolved in chloroform and added to 50 mL round bottom flask (RBF). Organic solvent was evaporated under vacuum (-600 mmHg) and temperature (45°C) using rotary evaporator (IKA RV-10, USA). Nitrogen was purged gently for removal of trace amount of solvent, if any. Thin film of these lipids was hydrated at 47°C using calcium chloride solution in DEPC treated nuclease free water (pH=8.5) for 1 hr. After 1 hr of hydration liposomal dispersion was collected from RBF and transferred to a glass container. Particle size of liposomes was reduced using successively passing through 1, 0.4, 0.2 and 0.1 μm

polycarbonate membranes (Whatman, USA) using high-pressure extruder (Avestin, USA). Polyethylene drain disk (Whatman, USA) was used to support the polycarbonate membrane and hence to potentiate the extrusion process. Untrapped salt was removed by passing through sephadex G-50 column. Liposomal fractions from the column were collected and this calcium entrapped liposomes were made permeable by addition of ethanol and finally incubated with disodium hydrogen phosphate solution having pH = 8.5 (prepared in nuclease free water). This addition allowed formation of calcium phosphate precipitates inside as well as outside of the liposomes. pH was adjusted between 7.0 - 7.5 and outer precipitates were removed by centrifugation (Remi, India) at 5000 g and 10°C temperature. Unreacted phosphate was removed by passing through sephadex G-50 column. Liposomal fractions were collected and stored at 2-8° C for further use.

4.3.2.2. RGD grafting on the surface of liposomes

Optimal formulation containing DPPC, cholesterol, DOPE, mPEG₂₀₀₀-DSPE was further improved by incorporation cyclic RGD peptide for its capability to target tumor cells. RGD-mPEG₂₀₀₀-DSPE was also added in the initial phase during thin film formation to incorporate RGD into the liposomes. Hydration and rest procedure was same as followed earlier in section 4.2.2.4.

4.3.2.3. Loading of siRNA in calcium phosphate entrapped liposomes

Calcium phosphate encapsulated liposomes were added with optimal amount of ethanol and incubated with siRNA at 48°C for next 20 min. Following incubation period, siRNA liposomes were cooled to room temperature and ethanol was removed by dialysis through dialysis membrane (10K) for 6 hr time period against 10% sucrose solution. siRNA liposomes were diluted to sufficient concentration to check entrapment on 2 % agarose gel electrophoresis. Prepared liposomes were filled in glass vials and stored at 2-8°C.

4.3.3. Formulation Optimization

CPE liposomal formulations were optimized using 3³ full factorial design (with 5 additional center points) in both steps as per variable given in **Table 4.19**, by keeping all other process and

formulation parameter invariant, to maximize siRNA entrapment and to minimize particle size [48-57]. Coded and actual values used in formulation optimization are tabulated here (**Table 4.20** and **Table 4.21**)

Table 4.19 Various Variables and Responses Involved in Optimization

Step-1	Variables	Lipid:Calcium
		DPPC:Cholesterol
		Concentration of Ca (mg/mL)
Response Parameters	Calcium entrapment	
	Particle size	
Step-2	Variables	Calcium: siRNA
		Lipid: Ethanol
		siRNA concentration (mg/mL)
	Response Parameters	siRNA entrapment
		Particle size

Table 4.20 Coded and Actual Values of the formulation parameters for step-1

Coded value	Actual value		
	Lipid:Calcium (mole ratio)	DPPC:Cholesterol (mole ratio)	Concentration of Ca (mg/mL)
-1	0.1	1	75
0	0.25	5	100
1	0.5	9	125

Table 4.21 Coded and Actual Values of the formulation parameters for step-2

Coded value	Actual value		
	Calcium:siRNA (mole ratio)	Lipid:Ethanol (mole ratio)	siRNA concentration (mg/mL)
-1	5.00	1.00	10.00
0	7.00	1.50	12.00
1	9.00	2.00	14.00

RSM was applied using comprehensive software, Design-Expert 8.0.4 (Stat-Ease Inc., MN) to fit second order polynomial equations, obtained by multiple linear regression analysis (MLRA) approach. A full and reduced model for all variables was established by putting the values of regression coefficients in polynomial equation. Statistical soundness of the polynomial equations was established on the basis of ANOVA statistics [58-64].

Two dimensional contour plots and three dimensional response surface plots were established by varying levels of two factors and keeping the third factor at fixed levels at a time [65-67]. In this way they are more helpful in understanding the actual interaction amongst the varying factors on the response parameter and are more meaningful. The 2-D contour plots and 3-D response surface graphs were constructed using the Design Expert software.

The experimental design and the derived polynomial equation for the optimization of liposomal formulations were validated for their utility by performing check point analysis. Eight optimum checkpoints were selected, prepared and evaluated for response parameters. Statistical comparison between the predicted values and average of three experimental values of the response parameters was performed to derive percentage error and to evaluate significant difference between these values.

Optimized formulation was derived by specifying goal and importance to the formulation variables and response parameters. Results obtained from the software are further verified by actual preparation of the batches and comparing the predicted and actual results.

4.3.4. Calcium Entrapment

Entrapment of calcium in CPE liposomes was determined using complexometry titration. The free calcium was titrated against EDTA solution as per the method described in Section 3.2.

Free calcium was separated from liposomes by two methods:

1) Sephadex Column Separation

CE liposomes were passed through sephadex G-50 column. 0.5 mL of CE liposomes was loaded onto 10 cm long sephadex G-50 column. Samples were eluted with DEPC treated nuclease free water. Initially liposomal fraction was collected and this was followed by free calcium fractions.

2) Ultracentrifugation

CPE liposomes were ultracentrifuged at 70000 x g for 4 hr at 4°C. Supernatant was collected and labelled as free calcium.

In both the cases free calcium was obtained and was titrated against 0.1M disodium EDTA solution using solochrome black/potassium nitrate indicator solution. End point was detected by color change from wine red to clear blue.

4.3.5. Particle Size and Zeta Potential

The average particle size and zeta potential of siRNA nano-constructs were determined by differential light scattering with a Malvern Zetasizer Nano ZS (Malvern Instruments, Malvern, UK). Prior to the measurement siRNA nano-constructs were diluted with nuclease free water and measurements were carried out at 25°C. Zeta potential was calculated by Smoluchowski's equation from the electrophoretic mobility. Each sample was measured three times and the mean values were calculated.

4.3.6. Assay

Assay of the prepared formulation was carried out to confirm the amount of siRNA loaded as compared to added siRNA. Assay is important parameter to determine whether any degradation is there or not in final formulations and based on that further potency calculations can be carried out for the *in vitro* and *in vivo* studies. Below given procedure was followed to determine assay of the prepared formulations:

Procedure followed was performed as described in the section **4.2.2.6.** by both gel electrophoresis and UV spectroscopy.

4.3.7. siRNA Entrapment Efficiency

Entrapment of siRNA within liposomes were determined same as described in the section **4.2.2.7.** using both methods viz., gel retardation assay and ultracentrifugation.

4.3.8. Cryo-Transmission Electron Microscopy (Cryo-TEM)

Morphology, lamellarity and intra-liposomal precipitation were studied using Cryo-TEM (TECNAI G2 Spirit BioT WIN, FEI-Netherlands) operating at 200 kV with resolution of 0.27 nm and magnifications of the order of 750,000X. Procedure followed was same as described in the section **4.2.2.10.**

4.3.9. Statistical Analysis

All experiments were performed in triplicates unless otherwise specified. Statistical analyses of data were performed using an ANOVA and Student-t test. Response surface models were analysed by ANOVA using Design Expert 8.0.4. GraphPad Prism (version 5, USA) was used for all other analyses. p value < 0.05 was considered significant.

4.3.10. Results and Discussion

CPE liposomes were in two steps as described earlier i.e. Step-1: formation of calcium phosphate liposomes and step-2: loading of siRNA into the liposomes. Both steps were optimized individually. However, liposomes prepared in step-1 was consequently used step-2 and hence, step-2 relied on the product quality obtained from step-1.

4.3.10.1. Optimization of Calcium Phosphate Entrapped Liposomes

Calcium phosphate liposomes were prepared by the selected TFH method using DPPC, cholesterol, DOPE and mPEG₂₀₀₀-DSPE. Liposomes were optimized to maximize calcium entrapment and minimize particle size. During hydration, calcium entrapment in to liposomes involved transport of calcium ions through bilayer membranes of liposomes and solubilization of calcium into the trapped volume of liposomes. siRNA loading involves incubation at temperature above glass transition temperature of lipids used in the bilayer formation. As seen with the earlier studies, siRNA is prone to degrade at glass transition of higher T_g lipids, i.e. HSPC or DSPC. Subsequently, very flexible lipid is also not suitable (DMPC, T_g= 23 °C). Hence, DPPC was chosen for bilayer formation having T_g = 43-45°C. DOPE was used as a fusogenic lipid to release siRNA in cytoplasm. First of all, various process variables were optimized and then formulation variables were optimized. The results are summarized and discussed in the following sections.

4.3.10.1.1. Optimization of Process Variable:

Process parameter optimization such as vacuum conditions for dry film formation, hydration time, and speed of rotation of flask were optimized for desired results. The effect of one variable was studied at a time keeping other variables constant. All process variables were same as

described in the formulation part of cationic liposomes (Section 4.3.2.2.i). Results were also found to be similar to that of cationic liposomes and hence, were same.

4.3.10.1.2. Optimization of Formulation

All batches of liposomes were prepared according to the formulation variables as shown in Table 4.4.21. All formulations were evaluated for calcium entrapment and particle size, and the results obtained are shown in **Table 4.22**. Table below shows the design matrix for the optimization of Calcium chloride loaded liposomes.

Table 4.22 Design Matrix for Calcium Chloride Loaded Liposome Optimization

Std Run	Run	Factor 1 A:Lipid: Calcium	Factor 2 DPPC: Cholesterol	Factor 3 Concentration of calcium (mg/mL)	Response 1 Calcium Entrapment (%)	Response 2 Particle Size (nm)
19	1	0.10	1.00	125.00	16.98	121.3
26	2	0.30	9.00	125.00	29.75	215.6
27	3	0.50	9.00	125.00	40.98	290.4
17	4	0.30	9.00	100.00	25.14	142.1
31	5	0.30	5.00	100.00	26.80	132.4
21	6	0.50	1.00	125.00	20.01	224.4
22	7	0.10	5.00	125.00	16.83	166.3
10	8	0.10	1.00	100.00	13.61	110.0
16	9	0.10	9.00	100.00	19.31	128.3
32	10	0.30	5.00	100.00	25.40	130.8
11	11	0.30	1.00	100.00	23.13	119.9
24	12	0.50	5.00	125.00	28.73	265.9
8	13	0.30	9.00	75.00	22.93	137.8
3	14	0.50	1.00	75.00	26.72	138.9
25	15	0.10	9.00	125.00	17.63	176.7
5	16	0.30	5.00	75.00	21.61	127.4
12	17	0.50	1.00	100.00	30.61	165.9
20	18	0.30	1.00	125.00	19.32	198.3
30	19	0.30	5.00	100.00	24.50	129.5
15	20	0.50	5.00	100.00	36.20	182.9
9	21	0.50	9.00	75.00	30.11	151.8
1	22	0.10	1.00	75.00	12.42	94.3
7	23	0.10	9.00	75.00	12.17	110.5
2	24	0.30	1.00	75.00	21.42	119.4
18	25	0.50	9.00	100.00	38.12	200.4
6	26	0.50	5.00	75.00	29.83	143.4
4	27	0.10	5.00	75.00	14.90	102.7
13	28	0.10	5.00	100.00	16.24	120.1
14	29	0.30	5.00	100.00	27.10	138.2
29	30	0.30	5.00	100.00	23.40	120.7
23	31	0.30	5.00	125.00	21.92	227.4
28	32	0.30	5.00	100.00	27.90	118.6

i. Statistical Analysis of Response 1 (Calcium Entrapment)

p-value of the different models, p-value for lack of fit in the model, Adjusted R^2 value and Predicted R^2 values are shown in the following **Table 4.23**.

Table 4.23 Summary of ANOVA results for Different Models

Source	Sequential p-value	Lack of Fit p-value	Adjusted R-Squared	Predicted R-Squared	
Linear	< 0.0001	0.0524	0.7817	0.7209	
2FI	0.0050	0.1146	0.8523	0.7579	
Quadratic	0.0100	0.2279	0.8987	0.8061	Suggested
Cubic	0.0393	0.4637	0.9369	0.7974	Aliased***

*** The Cubic Model and higher are Aliased. This shows that the predicted responses would be confounded by the other factors implying that the predicted response would give the wrong idea of the actual response.

As it can be seen from the **Table 4.24**, the best model to fit the experimental results of calcium entrapment in liposomes is quadratic model. The higher model (cubic model) is significant ($p < 0.05$) but the non agreement between the adjusted R^2 value and predicted R^2 value and aliased structure of response prediction rules out the cubic model. **Table 4.24** below shows the ANOVA analysis of the suggested quadratic model.

Table 4.24 ANOVA Table for Response Surface Quadratic Model

Source	Sum of Squares	df	Mean Square	F Value	p-value Prob > F	
Model	1479.77	9	164.42	31.56	< 0.0001	significant
A-Lipid:Calcium	1107.95	1	1107.95	212.66	< 0.0001	
B-DPPC:Cholesterol	149.76	1	149.76	28.74	< 0.0001	
C-Concentration of calcium	22.31	1	22.31	4.28	0.0505	
AB	55.34	1	55.34	10.62	0.0036	
AC	6.59	1	6.59	1.26	0.2730	
BC	62.56	1	62.56	12.01	0.0022	
A ²	0.10	1	0.10	0.020	0.8901	
B ²	0.61	1	0.61	0.12	0.7350	
C ²	63.35	1	63.35	12.16	0.0021	
Residual	114.62	22	5.21			
Lack of Fit	99.92	17	5.88	2.00	0.2279	not significant
Pure Error	14.70	5	2.94			
Cor Total	1594.39	31				

The Model F-value of 31.56 implies the model is significant. There is only a 0.01 % chance that a "Model F-Value" this large could occur due to noise.

Values of "Prob > F" less than 0.0500 indicate model terms are significant. In this case A, B, AB, BC, C² are significant model terms. This signifies that Lipid:Calcium and DPPC:Cholesterol have significant effect on calcium entrapment. There are two way interactions that are significantly affecting the calcium entrapment are AB and BC. Concentration of calcium shows quadratic effect in the response. Values greater than 0.1000 indicate the model terms are not significant. The "Lack of Fit F-value" of 2.00 implies the Lack of Fit is not significant relative to the pure error. There is a 22.79 % chance that a "Lack of Fit F-value" this large could occur due to noise. Non-significant lack of fit implies that selected quadratic model fits the responses.

Table 4.25 Summary of ANOVA results for Quadratic Model

Std. Dev.	2.28	R-Squared	0.9281
Mean	23.80	Adj R-Squared	0.8987
C.V. %	9.59	Pred R-Squared	0.8061
PRESS	309.17	Adeq Precision	21.238

Summary of ANOVA results for selected Quadratic model is shown in **Table 4.25**. The "Pred R-Squared" of 0.8061 is in reasonable agreement with the "Adj R-Squared" of 0.8987. "Adeq Precision" measures the signal to noise ratio. A ratio greater than 4 is desirable. Here ratio of 21.238 indicates an adequate signal. This model can be used to navigate the design space.

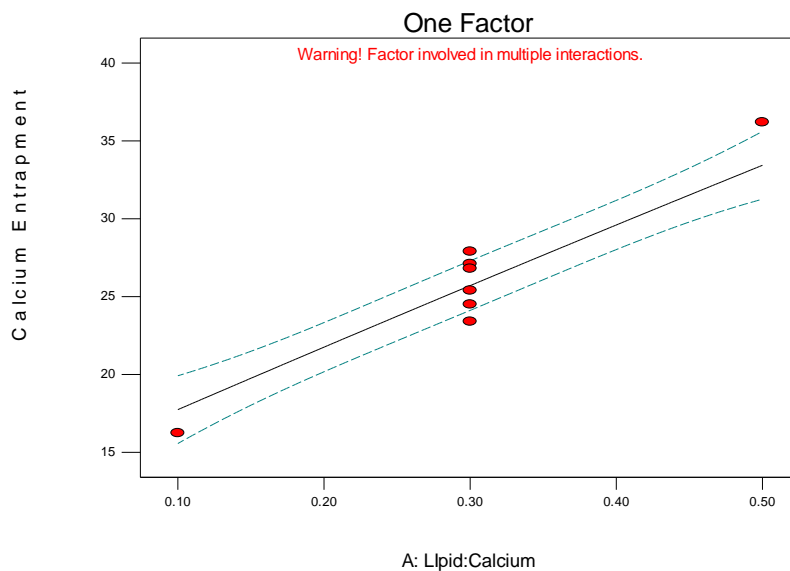


Figure 4.22 Effect of Lipid: Calcium on Calcium Entrapment

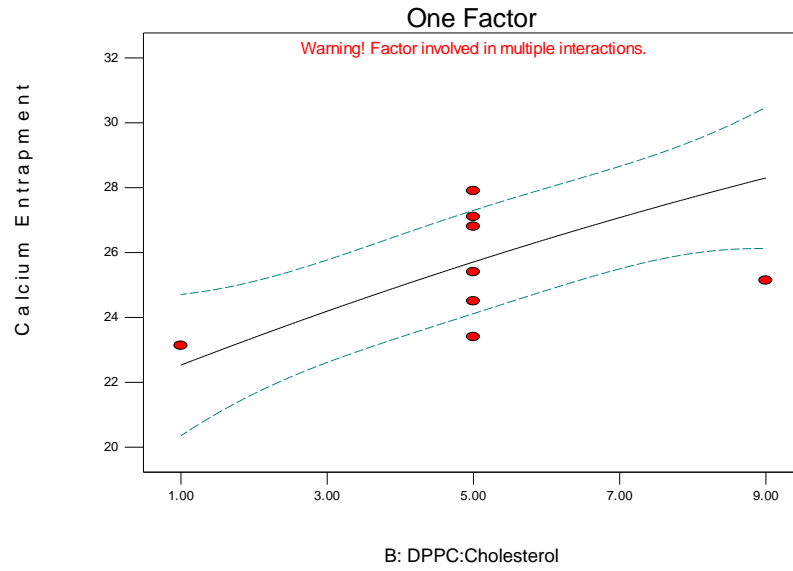


Figure 4.23 Effect of DPPC: Chol on Calcium Entrapment

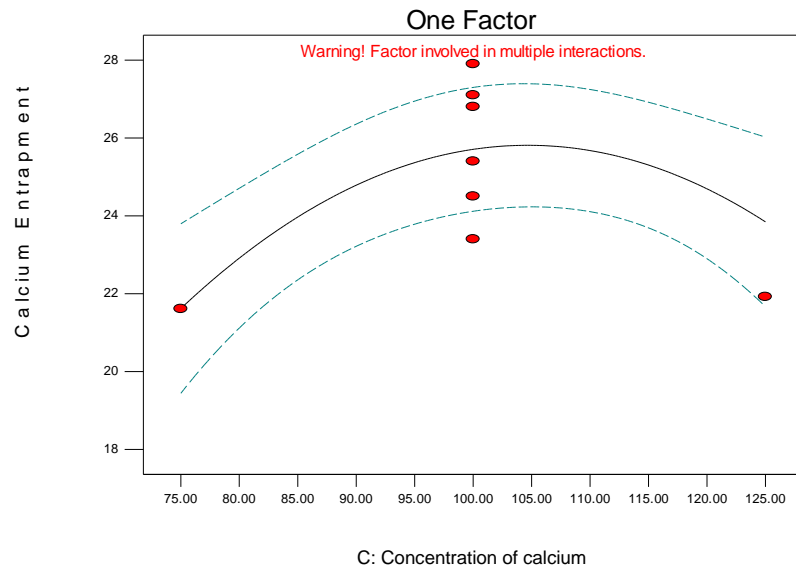


Figure 4.24 Effect of Concentration of Calcium on Calcium Entrapment

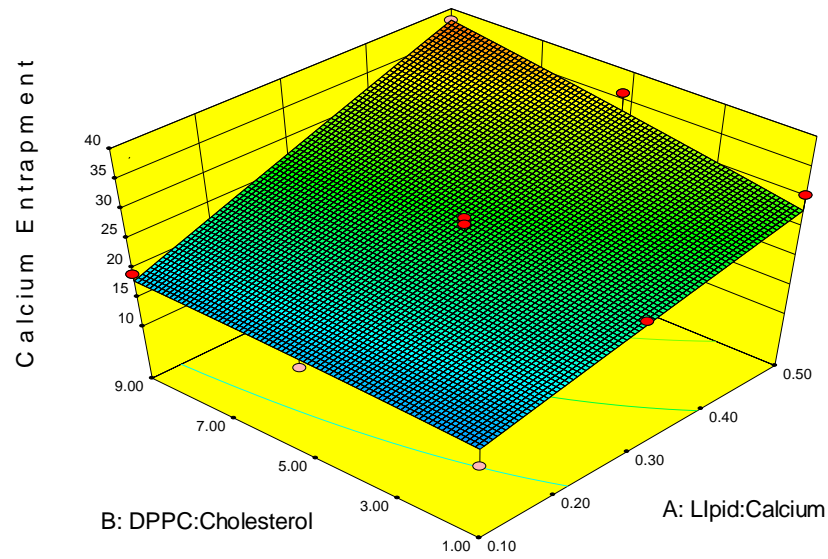


Figure 4.25 Response Surface Showing Combined Effect of Lipid:Calcium and DPPC:Chol on Calcium Entrapment

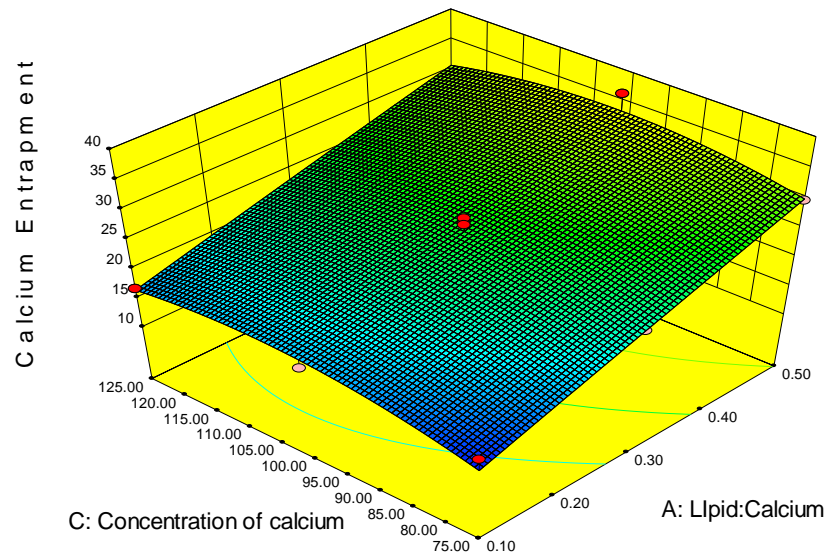


Figure 4.26 Response Surface Showing Combined Effect of Lipid:Caclium and Concentraion of Calcium on Calcium Entrapment

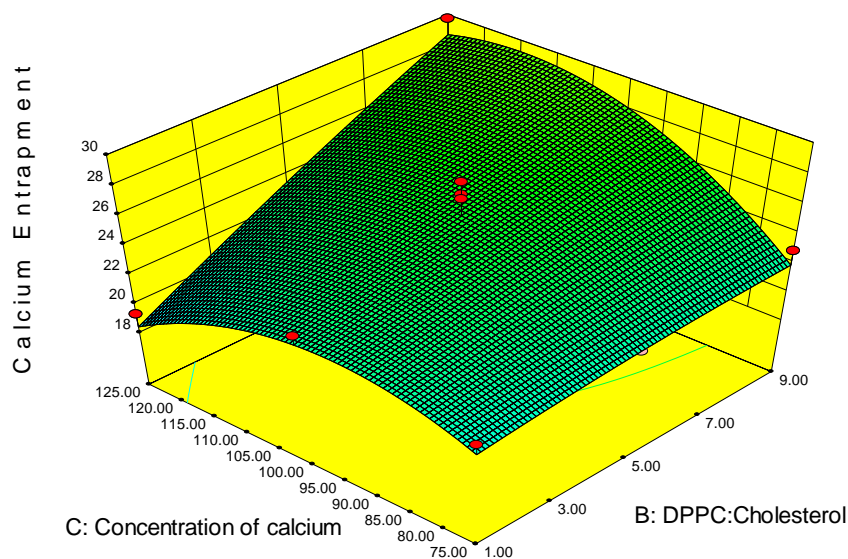


Figure 4.27 Response Surface Showing Combined Effect of Lipid:Caclium and Concentraion of Calcium on Calcium Entrapment

One factor effect plots (**Figure 4.22**, **Figure 4.23** and **Figure 4.24**) of factors A, B, and C show that factor A and B linearly affects the calcium entrapment while factor C has a quadratic effect (curvilinear plot) on the same.

Two-factor response surface plots (**Figure 4.25**, **Figure 4.26** and **Figure 4.27**) of factors AB, AC and BC shows the same effect of C over other factors A and B.

These results show that by increasing the concentration of calcium initially increases the calcium intake but above certain level entrapement goes down. This may be due to limiting loading capacity of calcium inside the liposomal core. Increase in DDPC:cholesterol ratio and lipid:calcium ratio both increased the calcium entrapment inside the liposomes. Increasing the amount of lipid can certainly provide more environment for calcium to reside inside the liposomes.

Predicted response at any point of the plot can be represented by the following equation:

$$\begin{aligned} \text{Calcium Entrapment} = & \\ & -31.45973 \\ & +42.41128* \text{LIpid:Calcium} \\ & -2.18467* \text{DPPC:Cholesterol} \\ & +0.92711* \text{Concentration of calcium} \\ & +2.68437* \text{Lipid:Calcium} * \text{DPPC:Cholesterol} \\ & -0.14817* \text{Lipid:Calcium} * \text{Concentration of calcium} \\ & +0.022833* \text{DPPC:Cholesterol} * \text{Concentration of calcium} \\ & -2.98118* \text{Lipid:Calcium}^2 \\ & -0.018286* \text{DPPC:Cholesterol}^2 \\ & -4.76146\text{E-}003* \text{Concentration of calcium}^2 \end{aligned}$$

ii. Statistical Analysis of Response 2 (Particle size)

p-value of the different models, p-value for lack of fit in the model, Adjusted R² value and Predicted R² values are shown in the following **Table 4.26**.

Table 4.26 Summary of ANOVA results for Different Models

Source	Sequential p-value	Lack of Fit p-value	Adjusted R-Squared	Predicted R-Squared	
Linear	< 0.0001	0.0076	0.7886	0.7527	
2FI	0.0440	0.0119	0.8277	0.7977	
Quadratic	< 0.0001	0.1152	0.9401	0.9017	Suggested
Cubic	0.7504	0.0744	0.9312	0.7549	Aliased**

** The Cubic Model and higher are Aliased. This shows that the predicted responses would be confounded by the other factors implying that the measured response would give the wrong idea of the actual response.

As it can be seen from the **Table 4.27**, the best model to fit the experimental results of calcium entrapment in liposomes is quadratic model.. The table below shows the ANOVA analysis of the suggested quadratic model.

Table 4.27 ANOVA table for Response Surface Quadratic Model

Source	Sum of Squares	df	Mean Square	F Value	p-value Prob > F	
Model	68881.83	9	7653.54	55.03	< 0.0001	significant
A-Lipid:Calcium	22316.80	1	22316.80	160.45	< 0.0001	
B-DPPC:Cholesterol	3790.30	1	3790.30	27.25	< 0.0001	
C-Concentration of calcium	32097.33	1	32097.33	230.77	< 0.0001	
AB	46.02	1	46.02	0.33	0.5710	
AC	3002.00	1	3002.00	21.58	0.0001	
BC	693.12	1	693.12	4.98	0.0361	
A ²	397.23	1	397.23	2.86	0.1052	
B ²	2.42	1	2.42	0.017	0.8962	
C ²	5280.36	1	5280.36	37.96	< 0.0001	
Residual	3059.96	22	139.09			
Lack of Fit	2785.63	17	163.86	2.99	0.1152	not significant
Pure Error	274.33	5	54.87			
Cor Total	71941.80	31				

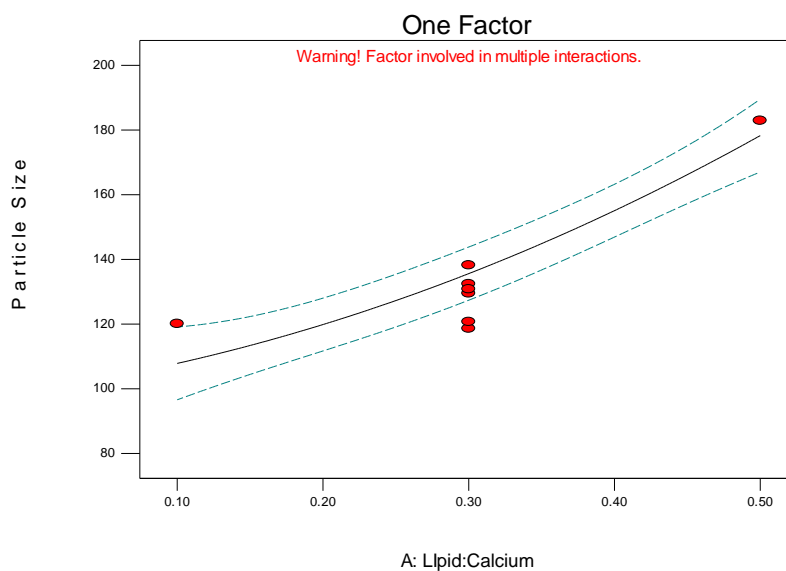
The Model F-value of 55.03 implies the model is significant. There is only a 0.01% chance that a "Model F-Value" this large could occur due to noise.

Values of "Prob > F" less than 0.0500 indicate model terms are significant. In this case A, B, C, AC, BC, C² are significant model terms. This signifies that all the three factors Lipid: Calcium and DPPC: Cholesterol and Calcium concentration have significant effect on particle size. There are two way interactions that are significantly affecting the calcium entrapment are A and BC. Concentration of calcium shows quadratic effect in the response. Values greater than 0.1000 indicate the model terms are not significant. The "Lack of Fit F-value" of 2.99 implies that the Lack of Fit is not significant relative to the pure error. There is a 11.52 % chance that a "Lack of Fit F-value" this large could occur due to noise. Non-significant lack of fit implies that selected quadratic model fits the responses.

Table 4.28 Summary of ANOVA results for Quadratic Model

Std. Dev.	11.79	R-Squared	0.9575
Mean	154.76	Adj R-Squared	0.9401
C.V. %	7.62	Pred R-Squared	0.9017
PRESS	7071.65	Adeq Precision	29.162

Summary of ANOVA results for selected Quadratic model is shown in **Table 4.28**. The "Pred R-Squared" of 0.9017 is in reasonable agreement with the "Adj R-Squared" of 0.9401. "Adeq Precision" measures the signal to noise ratio. A ratio greater than 4 is desirable. Here ratio of 29.162 indicates an adequate signal. This model can be used to navigate the design space.

**Figure 4.28 Effect of Lipid:Caclium on Particle Size**

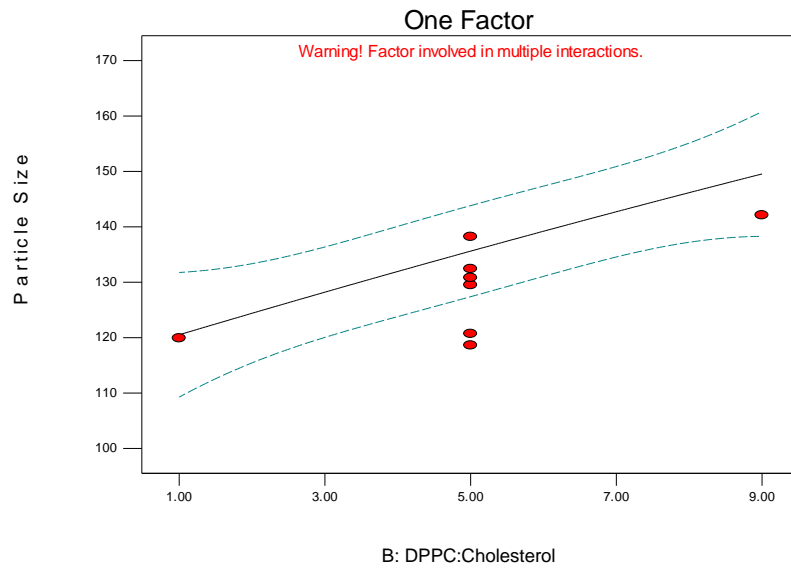


Figure 4.29 Effect of DPPC:Chol on Particle Size

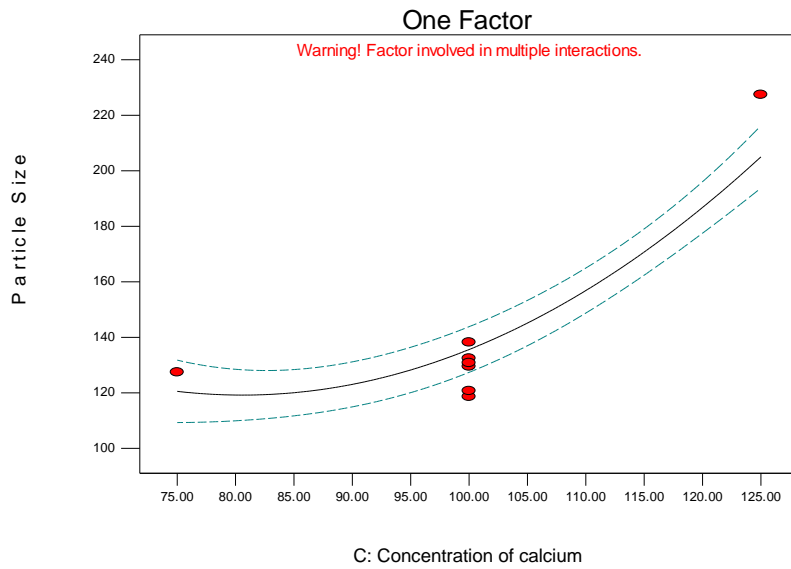


Figure 4.30 Effect of Concentration of Calcium on Particle Size

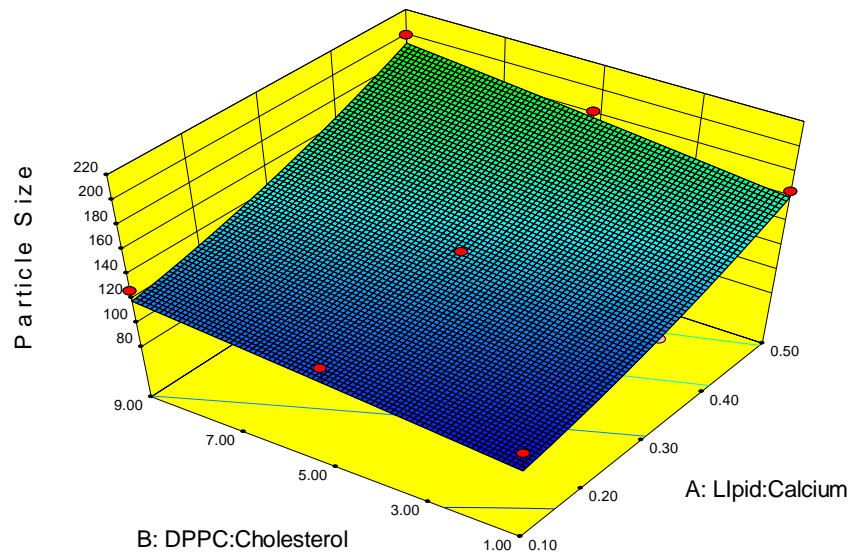


Figure 4.31 Response Surface Showing Combined Effect of Lipid:Calcium and DPPC:Chol on Particle Size

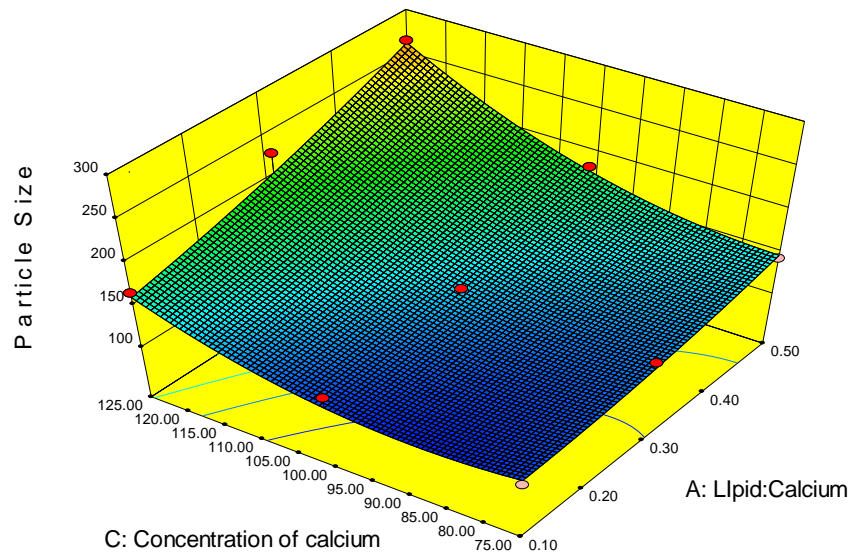


Figure 4.32 Response Surface Showing Combined Effect of Lipid:Calcium and Concentration of Calcium on Particle Size

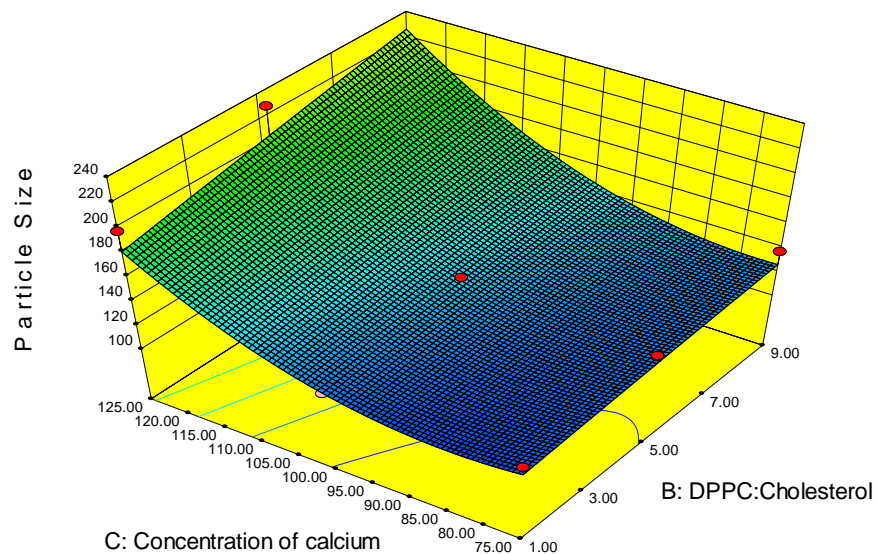


Figure 4.33 Response Surface Showing Combined effect of DPPC:Chol and Concentration of Calcium on Particle Size

One factor effect plots (**Figure 4.28, Figure 4.29 and Figure 4.30**) of factors A, B, and C shows that factor A and B almost linearly affect the particle size while factor C has a quadratic effect (curvilinear plot) on the same. Two-factor surface response plots (**Figure 4.31, Figure 4.32 and Figure 4.33**) of factors AB, AC and BC shows the same effect of C over other factors A and B.

Increase in the magnitude of all factors, showed increased particle size. Increase in the DPPC:cholesterol might cause increased size due to higher levels of lipids. Same effect can be explained for lipid:calcium factor. Increase in the particle size might be due to increased total amount of lipid loaded in unit volume of water. Increased amount of calcium might be causing some ionic interaction with liposomes causing their aggregation and subsequent increase in particle size.

Predicted response at any point of the plot can be represented by the following equation:

$$\begin{aligned} \text{Particle Size} = & \\ & +482.86778 \\ & -264.29155 * \text{Lipid:Calcium} \\ & -4.34302 * \text{DPPC:Cholesterol} \\ & -8.33374 * \text{Concentration of calcium} \\ & +2.44792 * \text{Lipid:Calcium} * \text{DPPC:Cholesterol} \\ & +3.16333 * \text{Lipid:Calcium} * \text{Concentration of calcium} \\ & +0.076000 * \text{DPPC:Cholesterol} * \text{Concentration of calcium} \\ & +186.29032 * \text{Lipid:Calcium}^2 \\ & -0.036358 * \text{DPPC:Cholesterol}^2 \\ & +0.043469 * \text{Concentration of calcium}^2 \end{aligned}$$

iii. Selection of Optimzed Batch

Constraints applied to select the best formulation parameters based on the calcium entrapment and particle size are shown in the following **Table 4.29**.

Table 4.29 Constraints Applied for Selection of Optimized Batch

Name	Goal	Lower Limit	Upper Limit
A:Lipid:Calcium	is in range	0.1	0.5
B:DPPC:Cholesterol	is in range	1	9
C:Concentration of calcium	is in range	75	125
Calcium Entrapment	maximize	12.17	40.98
Particle Size	minimize	94.3	150

All the affecting factors were to be optimized within the range chosen for design matrix. The calcium entrapment was chosen to be maximized while the partizcle size range was chosen to get the particle size between the lowest size obtained in the experiments to 150 nm as optimized formulation from this design was to be used for for further loadign of siRNA. This in turn required the treatment with ethanol and siRNA which will affect the size of the final formulation.

So smaller size was sought to be chosen which will give desired size for *in vivo* use after siRNA loading.

Formulation optimization was based on the desirability which may range from 0 to 1 based on the worst particle size and calcium entrapment to best particle size and calcium entrapment. The desirability plot is shown in the **Figure 4.34**.

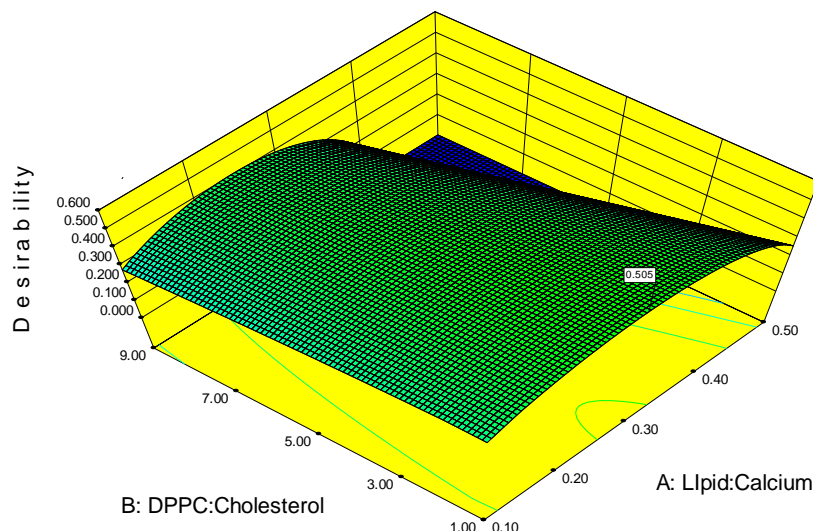


Figure 4.34 Desirability Plot for Selection of Optimized Batch

Based on the maximum desirability, one formulation (desirability 0.505) was chosen for confirmation and further optimization of siRNA loaded liposomes. This optimized batch showed predicted Calcium entrapment of 22.14 % and particle size of 109.04 nm (**Table 4.30**).

Table 4.30 Optimized Batch Parameters Based on Desirability

Lipid: Calcium	DPPC: Cholesterol	Concentration of calcium	Calcium Entrapment	Particle Size	Desirability	
0.29	1.00	87.72	22.1439	109.049	0.505	Selected

iv. Point Prediction and Confirmation:

Table 4.31 below shows predicted response for the solution selected above along with the Standard deviation and 95 % confidence interval of the response. Confirmation of the response was done by carrying out the experiment using the selected factor values in triplicate. **Table 4.32**

shows and confirms that experimental and predicted values are in good agreement concluding the suitability of the selected model for optimization.

Table 4.31 Predicted Responses of the Optimized Batch

Response	Prediction	Std Dev	SE Mean	95% CI low	95% CI high
Calcium Entrapment	22.1439	2.28254	1.06276	19.9399	24.3479
Particle Size	109.049	11.7936	5.49115	97.6607	120.437

Table 4.32 Experimental Confirmation of the Predicted Responses*

Response	Experimental Mean	Std Dev
Calcium Entrapment	23.47	1.173
Particle Size	114.74	3.101

*Experiments were performed in triplicate.

4.3.10.2. Optimization for Loading of siRNA in Calcium Phosphate Entrapped Liposomes

siRNA loaded calcium phosphate encapsulated liposomes (CPE liposomes) were prepared by incubating optimal amount of siRNA in the presence of ethanol. Use of ethanol in this method was to enhance the transport of siRNA inside the liposomal bilayer due to membrane loosening effect of ethanol. First of all, various process variables were optimized and then formulation variables were optimized. The results are summarized and discussed in the following sections.

4.3.10.2.1. Optimization of Process Variable:

Process parameter optimization such as incubation time and temperature were optimized for desired results. The effect of one variable was studied at a time keeping other variables constant. The results are recorded in **Table 4.33** from which the following conclusions were drawn:

i. Incubation time

siRNA entrapment was found to increase by increasing the time of incubation (**Table 4.33**). Up to 20 min of incubation at 48°C temperature significant difference was observed in entrapment as compared to 5 min and 10 min. However, further increase in time did not show any significant change in siRNA entrapment and hence 20 min was selected as optimal time for incubation.

Table 4.33 Effect of incubation time on siRNA Entrapment*

Sr.No.	Incubation time (min)	% siRNA Entrapment
1.	5	21.1
2.	10	34.8
3.	20	54.4
4.	30	55.2

*Experiments were performed in triplicate.

Lipid:Ethanol=2.0, Calcium:siRNA =7.0, siRNA concentration=10 µg/mL, Incubation temperature=48°C

ii. Incubation Temperature:

Incubation at temperature below glass transition temperature of highest bilayer forming lipid is required for efficient transport of siRNA across the liposomal membrane. **Table 4.34** gives the entrapment value below and above glass transition temperature of DDPC. Glass transition temperature of DDPC is between 43-45°C. Maximum amount of siRNA was found inside the liposomes above glass transition temperature only and hence, that temperature was selected for further formulation development.

Table 4.34 Effect of Incubation Temperature on siRNA Entrapment*

Sr.No.	Incubation Temperature	% siRNA Entrapment
1.	25	15.3
2.	37	23.6
3.	48	54.4

*Experiments were performed in triplicate.

Lipid:Ethanol=2.0, Calcium:siRNA =7.0, siRNA concentration=10 µg/mL, Incubation time=20 min.

4.3.10.2.2. Optimization of Formulation

All batches of liposomes were prepared according to the formulation variables as shown in **Table 4.35**. All formulations were evaluated for siRNA entrapment and particle size, and the results obtained are shown in **Table 4.35**. Table below shows the design matrix for the optimization of siRNA loaded liposomes.

Table 4.35 Design Matrix for Optimization of siRNA Entrapment in Calcium Phosphate Loaded Liposomes

Standard Run	Run	Factor 1 Calcium :siRNA	Factor 2 Lipid:Ethano l	Factor 3 siRNA concentration ($\mu\text{g}/\text{mL}$)	Response 1 siRNA entrapment (%)	Response 2 Particle Size (nm)
14	1	7.00	1.50	12.00	73	151.4
20	2	7.00	1.00	14.00	58	302.1
26	3	7.00	2.00	14.00	25	199.3
27	4	9.00	2.00	14.00	14	235.9
12	5	9.00	1.00	12.00	80	335.7
21	6	9.00	1.00	14.00	65	385.8
9	7	9.00	2.00	10.00	61	162.4
5	8	7.00	1.50	10.00	72	157.8
6	9	9.00	1.50	10.00	75	179.9
29	10	7.00	1.50	12.00	83.2	134.6
1	11	5.00	1.00	10.00	73	201.4
31	12	7.00	1.50	12.00	86.9	122.6
7	13	5.00	2.00	10.00	43	110.4
2	14	7.00	1.00	10.00	77	235.2
11	15	7.00	1.00	12.00	72	270.7
13	16	5.00	1.50	12.00	80	122.7
15	17	9.00	1.50	12.00	89	205.1
24	18	9.00	1.50	14.00	57	215.9
25	19	5.00	2.00	14.00	28	158.9
17	20	7.00	2.00	12.00	67	169
18	21	9.00	2.00	12.00	57	197.8
28	22	7.00	1.50	12.00	75	143.6
3	23	9.00	1.00	10.00	85	241.6
22	24	5.00	1.50	14.00	24	132
32	25	7.00	1.50	12.00	80.9	129.4
10	26	5.00	1.00	12.00	66	246.6
23	27	7.00	1.50	14.00	51	169.3
8	28	7.00	2.00	10.00	54	128.9
19	29	5.00	1.00	14.00	49	268.2
30	30	7.00	1.50	12.00	84.3	140.5
4	31	5.00	1.50	10.00	68	135.4
16	32	5.00	2.00	12.00	40	135.7

i. Statistical Analysis of Response 1 (siRNA Entrapment)

p-value of the different models, p-value for lack of fit in the model, Adjusted R^2 value and Predicted R^2 values are shown in the following **Table 4.36**.

Table 4.36 Summary of ANOVA results for Different Models

Sequential Source	Lack of Fit p-value	Adjusted p-value	Predicted R-Squared	R-Squared	
Linear	< 0.0001	0.0155	0.5083	0.4386	
2FI	0.9239	0.0120	0.4595	0.2539	
Quadratic	< 0.0001	0.1559	0.8381	0.7159	Suggested
Cubic	0.4635	0.1377	0.8386	0.3858	Aliased*

* The Cubic Model and higher are Aliased. This shows that the predicted responses would be confounded by the other factors implying that the measured response would give the wrong idea of the actual response.

As it can be seen from the **Table 4.36**, the best model to fit the experimental results of calcium entrapment in liposomes is quadratic model. The higher model (cubic model) is significant but the non agreement between the adjusted R^2 value and predicted R^2 value and aliased structure of response prediction rules out the cubic model. Table below shows the ANOVA analysis of the suggested quadratic model.

Table 4.37 ANOVA table for Response Surface Quadratic Model

Sum of Source	Squares	Mean df	F Square	p-value Value	Prob > F	
Model	11004.93	9	1222.77	18.84	< 0.0001	significant
A-Calcium: siRNA	696.89	1	696.89	10.73	0.0034	
B-Lipid: Ethanol	3094.22	1	3094.22	47.66	< 0.0001	
C-siRNA concentration	3120.50	1	3120.50	48.07	< 0.0001	
AB	36.75	1	36.75	0.57	0.4598	
AC	0.33	1	0.33	5.135E-003	0.9435	
BC	65.33	1	65.33	1.01	0.3267	
A ²	95.81	1	95.81	1.48	0.2373	
B ²	762.84	1	762.84	11.75	0.0024	
C ²	1868.12	1	1868.12	28.78	< 0.0001	
Residual	1428.19	22	64.92			
Lack of Fit	1278.86	17	75.23	2.52	0.1559	not significant
Pure Error	149.34	5	29.87			
Cor Total	12433.12	31				

The Model F-value of 18.84 implies the model is significant. There is only a 0.01 % chance that a "Model F-Value" this large could occur due to noise. Values of "Prob > F" less than 0.0500 indicate model terms are significant. In this case A, B, C, B², C² are significant model terms. This signifies that Calcium: siRNA and Lipid:Ethanol and siRNA concentration have significant effect on siRNA entrapment. There are no two way interactions that are significantly affecting the siRNA entrapment. Lipid:Ethanol ratio and concentration of siRNA show quadratic effect in the response. Values greater than 0.1000 indicate the model terms are not significant. The "Lack of Fit F-value" of 2.52 implies the Lack of Fit is not significant relative to the pure error. There is a 15.59 % chance that a "Lack of Fit F-value" this large could occur due to noise. Non-significant lack of fit implies that selected quadratic model fits the responses.

Table 4.38 Summary of ANOVA results for Quadratic Model

Std. Dev.	8.06	R-Squared	0.8851
Mean	62.92	Adj R-Squared	0.8381
C.V. %	12.81	Pred R-Squared	0.7159
PRESS	3532.38	Adeq Precision	15.577

Summary of ANOVA results for selected Quadratic model are shown in **Table 4.38**. The “Pred R- Squared” of 0.7159 is in reasonable agreement with the “Adj R-squared” of 0.8381. “Adeq Precision” measures the signal to noise ratio. A ratio greater than 4 is desirable. Here ratio of 15.577 indicates an adequate signal. This model can be used to navigate the design space.

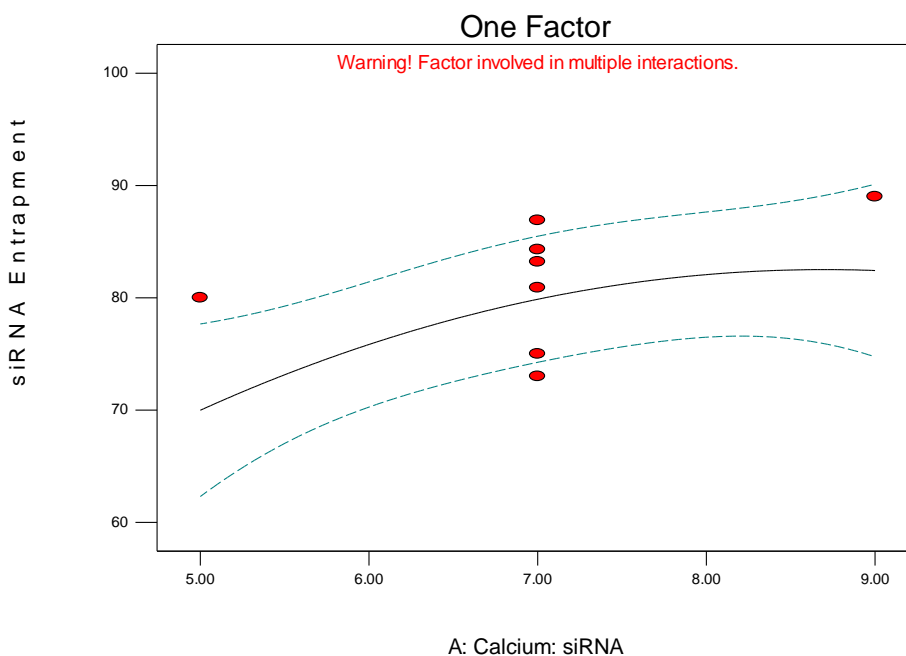


Figure 4.35 Effect of Calcium: siRNA on siRNA Entrapment

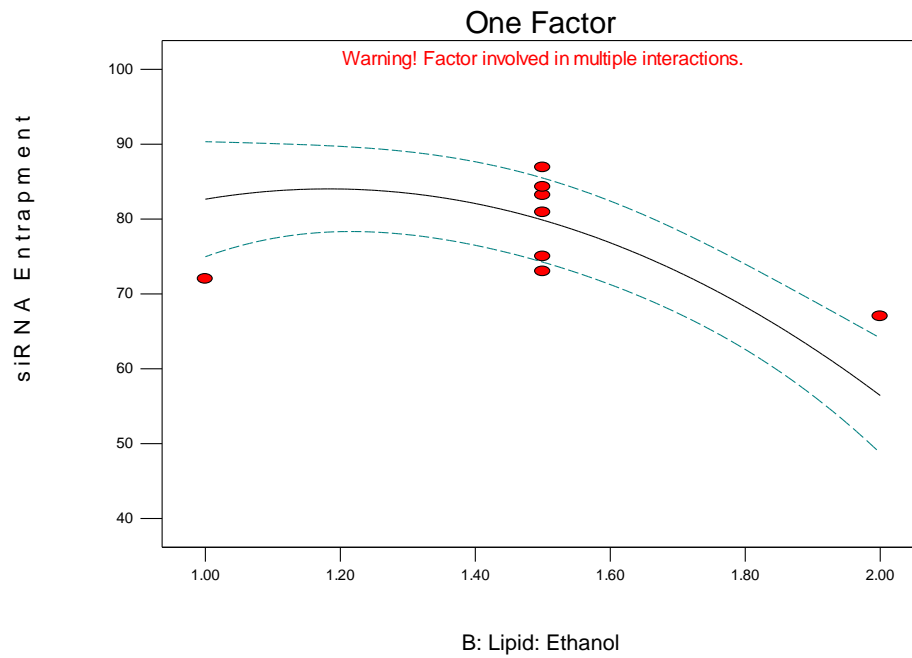


Figure 4.36 Effect of Lipid:Ethanol on siRNA Entrapment

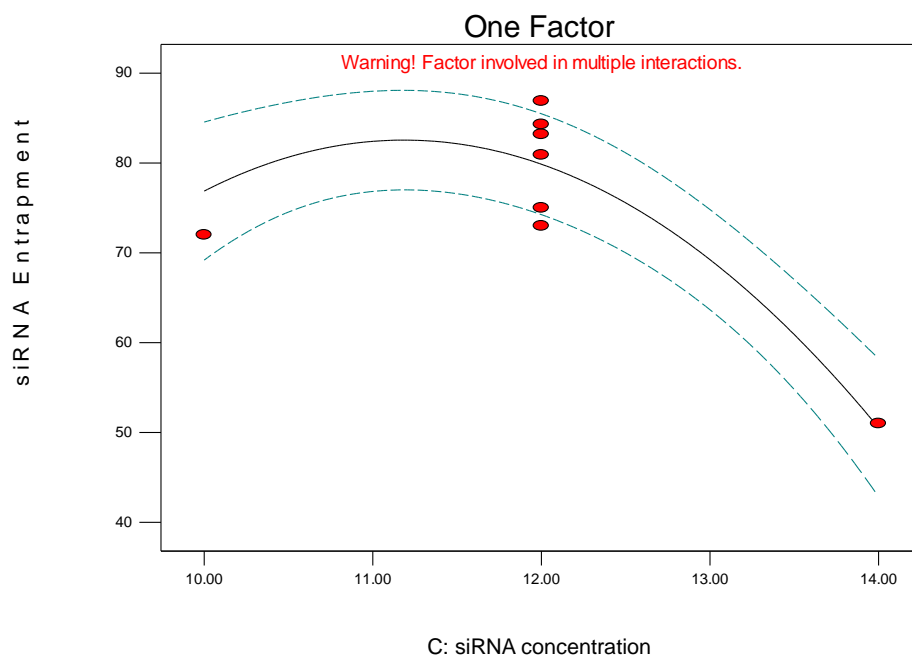


Figure 4.37 Effect of siRNA Concentration on siRNA Entrapment

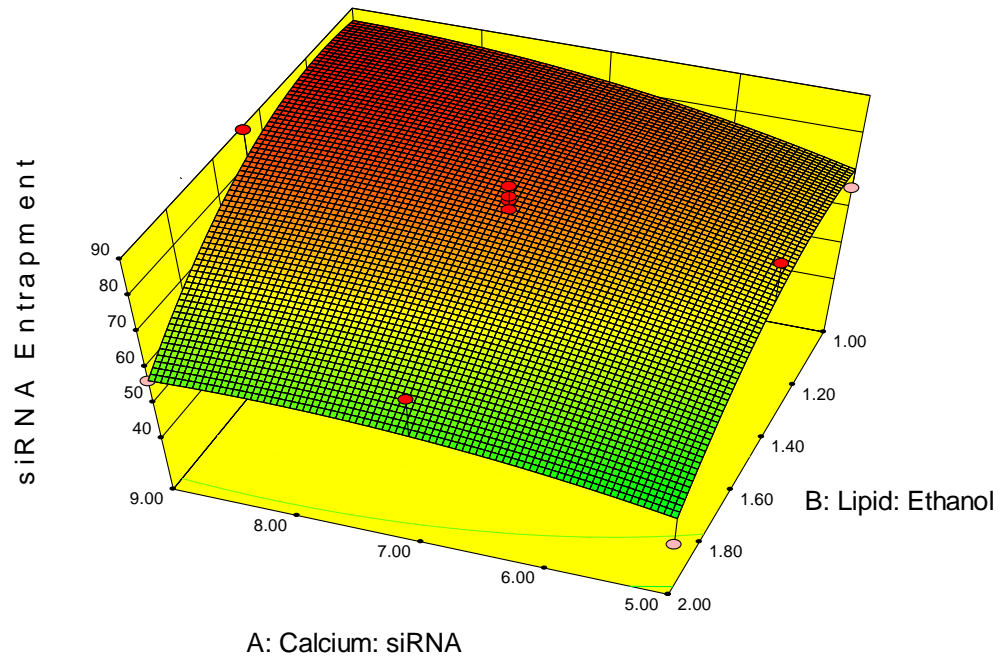


Figure 4.38 Response Surface Showing Combined Effect of lipid: ethanol and Calcium: siRNA on siRNA Entrapment

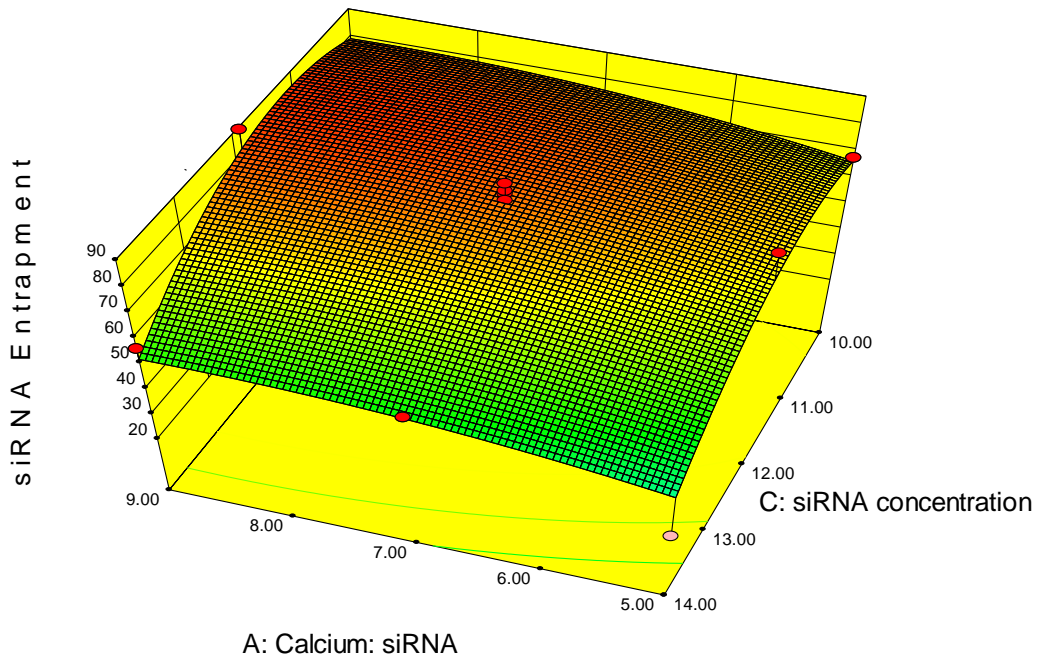


Figure 4.39 Response Surface Showing Combined Effect of Calcium:siRNA and Concentration of Calcium on siRNA Entrapment

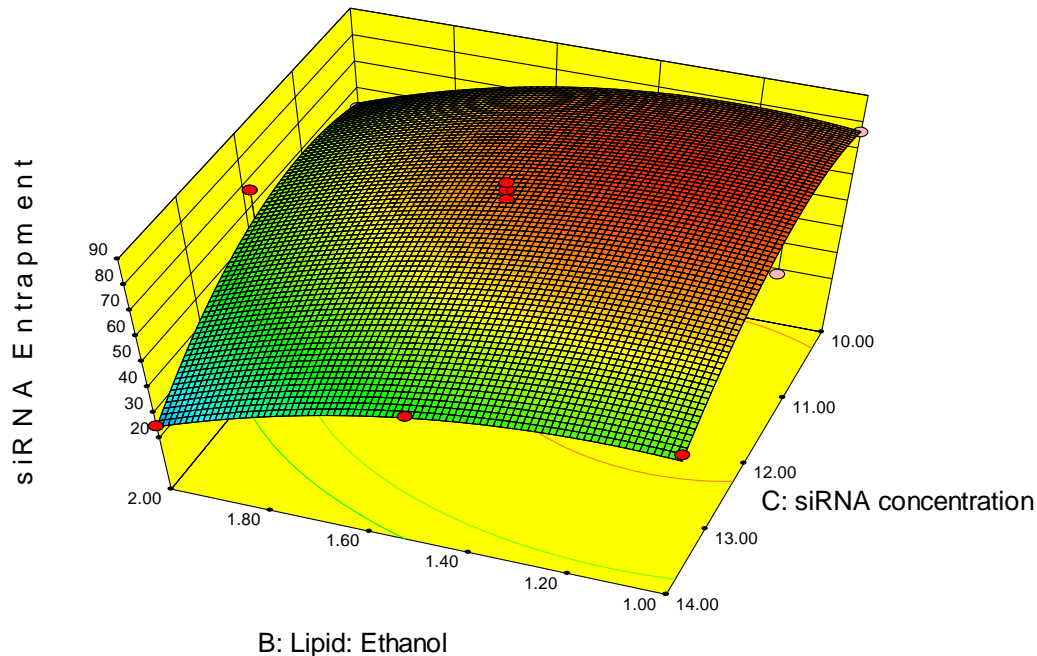


Figure 4.40 Response Surface Showing Combined Effect of Lipid:Ethanol and siRNA Concentration on siRNA Entrapment

One factor effect plots (**Figure 4.35, Figure 4.36 and Figure 4.37**) of factors A, B, and C shows that all the factors affected the siRNA entrapment quadratically, the highest quadratic effect being that of siRNA concentration.

One factor plots and two factor response surfaces (**Figure 4.38, Figure 4.39 and Figure 4.40**) indicated that increasing the calcium:siRNA ratio increased the entrapment of siRNA in to the liposomes while increase in the Lipid:ethanol ratio and siRNA concentration initially increased the siRNA entrapment in to the liposomes but after a particular value they negatively affected the siRNA entrapment. This might be due to reduced ethanol content at higher lipid:ethanol ratio reduced the transfer of siRNA inside the liposomes and at higher siRNA concentration the relative amount of loaded siRNA to unentrapped siRNA would be very high showing less entrapment efficiency of liposomes. Further, after an optimal value ethanol might have an effect on leaching out of the intraliposomal calcium phosphate by membrane disruption effect and led decreased siRNA entrapment. **Figure 4.41, Figure 4.42, Figure 4.43, Figure 4.44, Figure 4.45, Figure 4.46, Figure 4.47, Figure 4.48 and Figure 4.49** given below show the band density of free siRNA of various formulations described in **Table 4.35**.

Gel Electrophoresis of Various Formulations for Free siRNA Quantification:

A: siRNA concentration 10 µg/mL

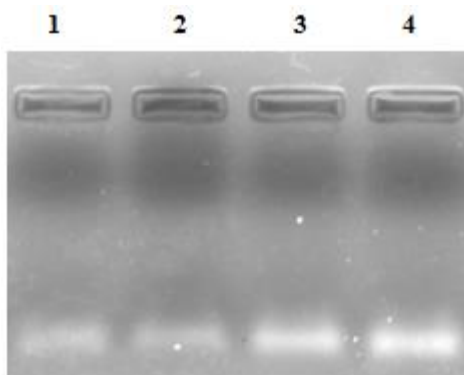


Figure 4.41 Gel electrophoresis for siRNA concentration (Calcium:siRNA = 5)
 4=Naked siRNA, 1=Lipid:Ethanol=2.0, 2=Lipid:Ethanol=1.5, 3=Lipid:Ethanol=1.0
 Calcium:siRNA = 5, siRNA concentration = 10 (µg/mL)

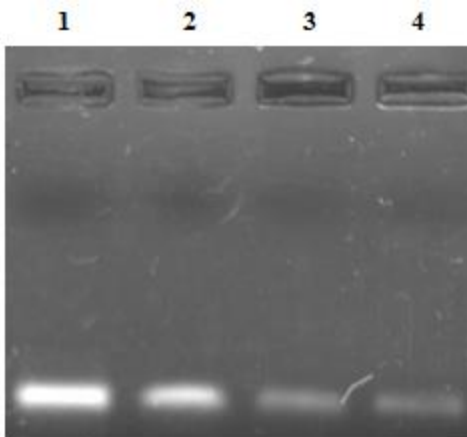


Figure 4.42 Gel electrophoresis for siRNA concentration (Calcium:siRNA = 7)
 1=Naked siRNA, 2=Lipid:Ethanol=2.0, 3=Lipid:Ethanol=1.5, 4=Lipid:Ethanol=1.0
 Calcium:siRNA = 7, siRNA concentration = 10 (µg/mL)

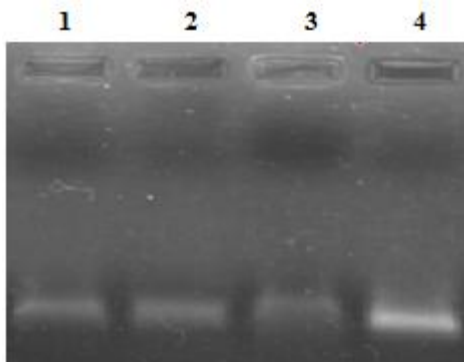


Figure 4.43 Gel electrophoresis for siRNA concentration (Calcium:siRNA = 9)
 1=Lipid:Ethanol=2.0, 2=Lipid:Ethanol=1.5, 3=Lipid:Ethanol=1.0, 4=Naked siRNA
 Calcium:siRNA = 9, siRNA concentration = 10 (µg/mL)

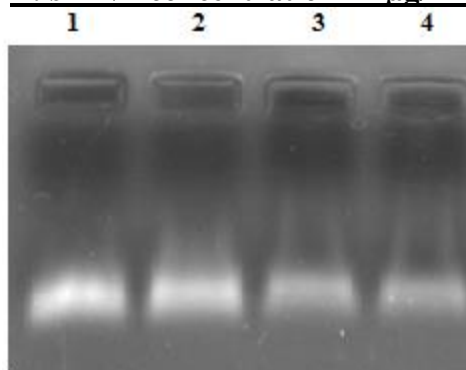
B: siRNA concentration 12 $\mu\text{g/mL}$ 

Figure 4.44 Gel electrophoresis for siRNA concentration (Calcium:siRNA = 5)
 1=Naked siRNA, 2=Lipid:Ethanol=2.0, 3=Lipid:Ethanol=1.5, 4=Lipid:Ethanol=1.0
 Calcium:siRNA= 5, siRNA concentration = 12 ($\mu\text{g/mL}$),

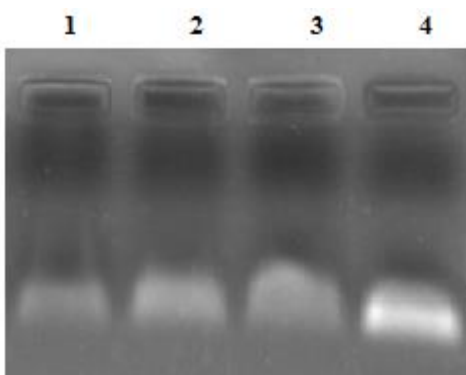


Figure 4.45 Gel electrophoresis for siRNA concentration (Calcium:siRNA = 7)
 1=Naked siRNA, 2=Lipid:Ethanol=2.0, 3=Lipid:Ethanol=1.5, 4=Lipid:Ethanol=1.0
 Calcium:siRNA = 7, siRNA concentration = 12 ($\mu\text{g/mL}$)

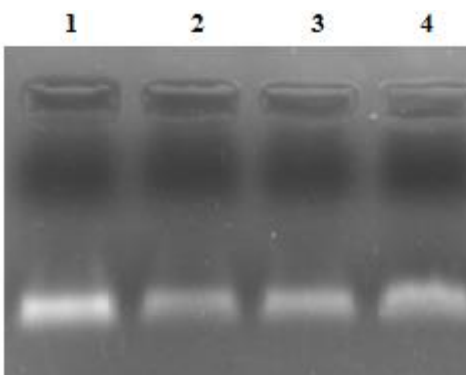


Figure 4.46 Gel electrophoresis for siRNA Concentration (Calcium:siRNA = 9)
 1=Naked siRNA, 2=Lipid:Ethanol=1.0, 3=Lipid:Ethanol=1.5, 4=Lipid:Ethanol=2.0
 Calcium:siRNA = 9, siRNA concentration = 12 ($\mu\text{g/mL}$)

C: siRNA concentration 14 $\mu\text{g/mL}$

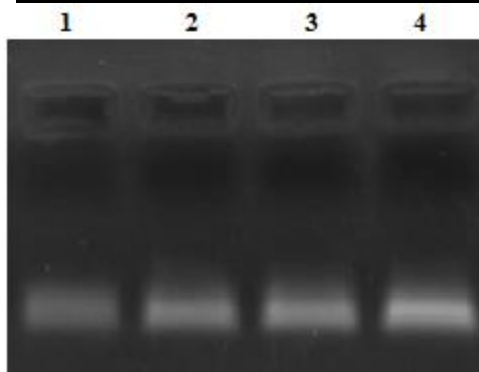


Figure 4.47 Gel electrophoresis for siRNA Concentration (Calcium:siRNA = 5)
 4=Naked siRNA, 1=Lipid:Ethanol=1.0, 2=Lipid:Ethanol=1.5 , 3=Lipid:Ethanol=2.0
 Calcium:siRNA = 5, siRNA concentration = 14 ($\mu\text{g/mL}$)

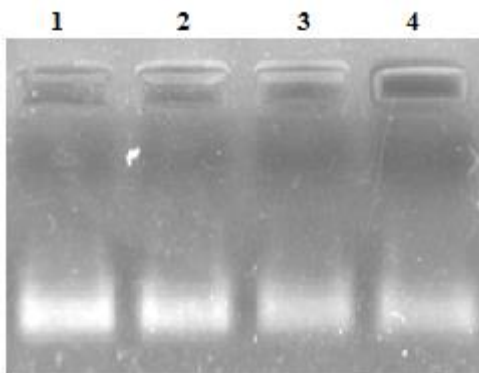


Figure 4.48 Gel electrophoresis for siRNA Concentration (Calcium:siRNA = 7)
 1=Naked siRNA, 2=Lipid:Ethanol=2.0, 3=Lipid:Ethanol=1.5 , 4=Lipid:Ethanol=1.0
 Calcium:siRNA = 7, siRNA concentration = 14 ($\mu\text{g/mL}$)

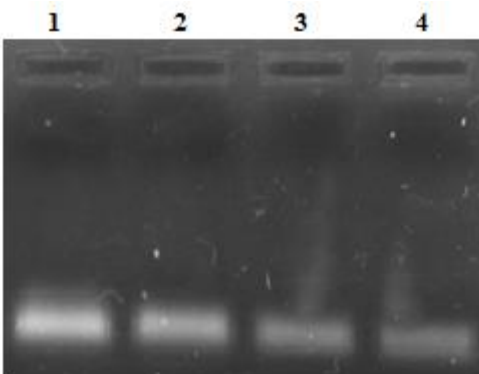


Figure 4.49 Gel electrophoresis for siRNA Concentration (Calcium:siRNA = 9)
 1=Naked siRNA, 2=Lipid:Ethanol=2.0, 3=Lipid:Ethanol=1.5 , 4=Lipid:Ethanol=1.0
 Calcium:siRNA = 9, siRNA concentration = 14 ($\mu\text{g/mL}$)

Final Equation for siRNA Entrapment in Terms of Actual Factors:

$$\begin{aligned}
\text{siRNA Entrapment} = & -606.96340 \\
& +19.04498* \text{ Calcium: siRNA} \\
& +137.94391* \text{ Lipid: Ethanol} \\
& +94.16640* \text{ siRNA concentration} \\
& -1.75000* \text{ Calcium: siRNA * Lipid:Ethanol} \\
& -0.041667* \text{ Calcium: siRNA * siRNA concentration} \\
& -2.33333* \text{ Lipid: Ethanol * siRNA concentration} \\
& -0.91492* \text{ Calcium: siRNA}^2 \\
& -41.30538* \text{ Lipid: Ethanol}^2 \\
& -4.03992* \text{ siRNA concentration}^2
\end{aligned}$$

ii. Statistical Analysis of Response 2 (Particle size)

p-value of the different models, p-value for lack of fit in the model, Adjusted R² value and Predicted R² values are shown in the **Table 4.39**.

Table 4.39 Summary of ANOVA results for Different Models

Source	Sequential p-value	Lack of Fit p-value	Adjusted R-Squared	Predicted R-Squared	
Linear	< 0.0001	0.0018	0.6191	0.5620	
2FI	0.7115	0.0015	0.5958	0.4548	
Quadratic	< 0.0001	0.0708	0.9246	0.8674	Suggested
Cubic	0.0148	0.2198	0.9599	0.8728	Aliased*

* The Cubic Model and higher are Aliased. This shows that the predicted responses would be confounded by the other factors implying that the measured response would give the wrong idea of the actual response.

As it can be seen from the above table that the best model to fit the experimental results of calcium entrapment in liposomes is quadratic model. The higher model (cubic model) is significant but the non agreement between the adjusted R² value and predicted R² value and and aliased structure of response prediction rules out the cubic model.

Table 4.40 below shows the ANOVA analysis of the suggested quadratic model.

Table 4.40 ANOVA table for Response Surface Quadratic Model

Source	Sum of Squares	df	Mean Square	F Value	p-value Prob > F	
Model	1.334E+005	9	14816.80	43.22	< 0.0001	significant
A-Calcium: siRNA	23385.64	1	23385.64	68.21	< 0.0001	
B-Lipid: Ethanol	54340.06	1	54340.06	158.50	< 0.0001	
C-siRNA concentration	14700.41	1	14700.41	42.88	< 0.0001	
AB	259.47	1	259.47	0.76	0.3937	
AC	1675.60	1	1675.60	4.89	0.0378	
BC	609.19	1	609.19	1.78	0.1962	
A ²	1088.37	1	1088.37	3.17	0.0886	
B ²	29947.64	1	29947.64	87.35	< 0.0001	
C ²	105.18	1	105.18	0.31	0.5852	
Residual	7542.70	22	342.85			
Lack of Fit	7008.66	17	412.27	3.86	0.0708	not significant
Pure Error	534.05	5	106.81			
Cor Total	1.409E+005	31				

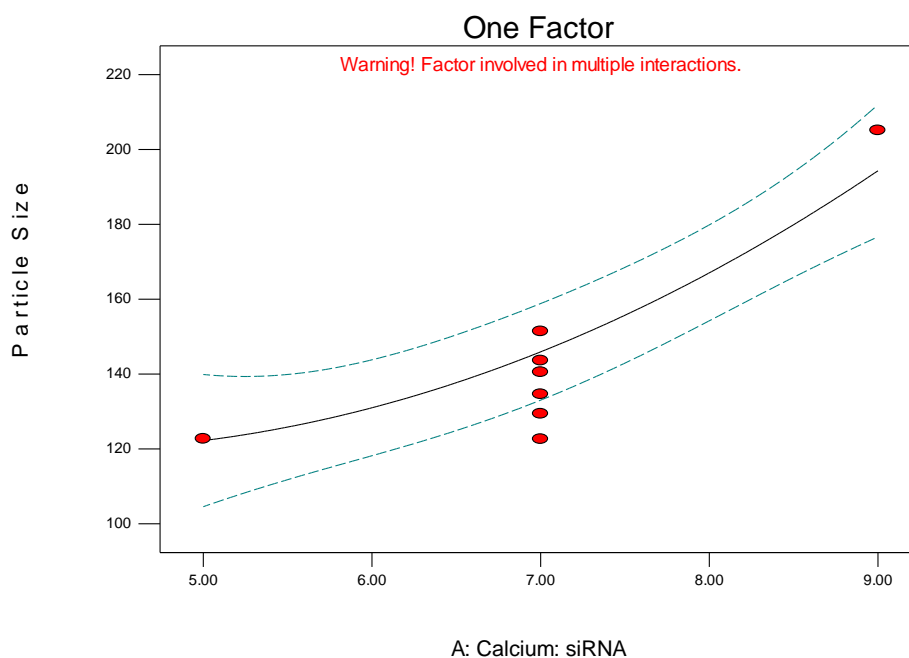
The Model F-value of 43.22 implies the model is significant. There is only a 0.01% chance that a "Model F-Value" this large could occur due to noise.

Values of "Prob > F" less than 0.0500 indicate model terms are significant. In this case A, B, C, AC, B² are significant model terms. This signifies that all the three factors Calcium: siRNA and Lipid:Ethanol and siRNA Concentration have significant effect on particle size. There is a two way interactions that significantly affected the particle size is AC. Concentration of siRNA shows quadratic effect on the response. Values greater than 0.1000 indicate the model terms are not significant. The "Lack of Fit F-value" of 3.86 implies that the Lack of Fit is not significant relative to the pure error. There is a 7.08 % chance that a "Lack of Fit F-value" this large could occur due to noise. Non-significant lack of fit implies that selected quadratic model fits the responses.

Table 4.41 Summary of ANOVA results for Quadratic Model

Std. Dev.	18.52	R-Squared	0.9465
Mean	191.43	Adj R-Squared	0.9246
C.V. %	9.67	Pred R-Squared	0.8674
PRESS	18686.82	Adeq Precision	25.183

Summary of ANOVA results for selected Quadratic model is given in **Table 4.41**. The "Pred R-Squared" of 0.8674 is in reasonable agreement with the "Adj R-Squared" of 0.9246. "Adeq Precision" measures the signal to noise ratio. A ratio greater than 4 is desirable. Here ratio of 25.183 indicates an adequate signal. This model can be used to navigate the design space.

**Figure 4.50 Effect of Calcium: siRNA on Particle Size**

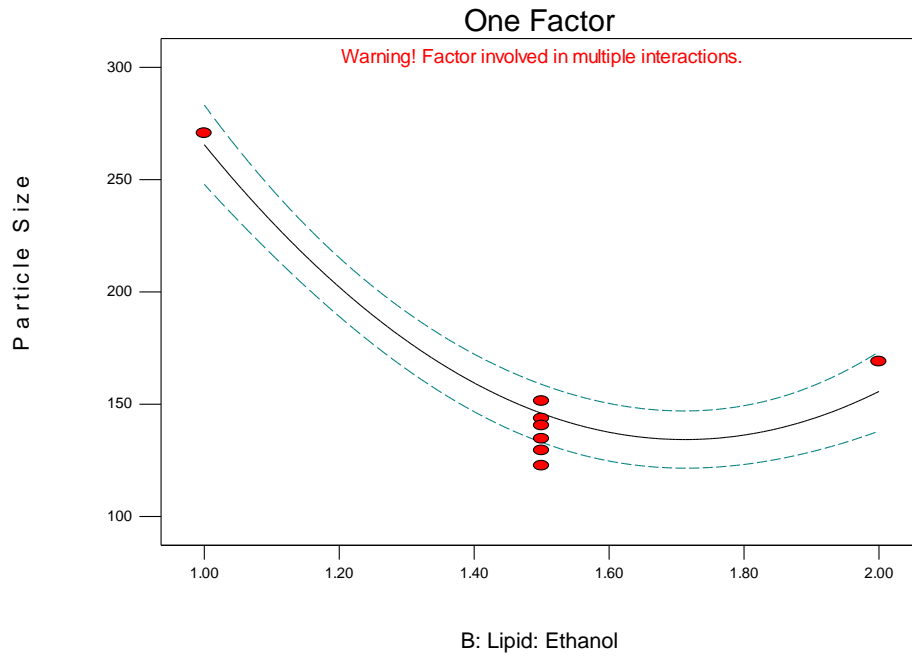


Figure 4.51 Effect of Lipid: Ethanol on Particle Size

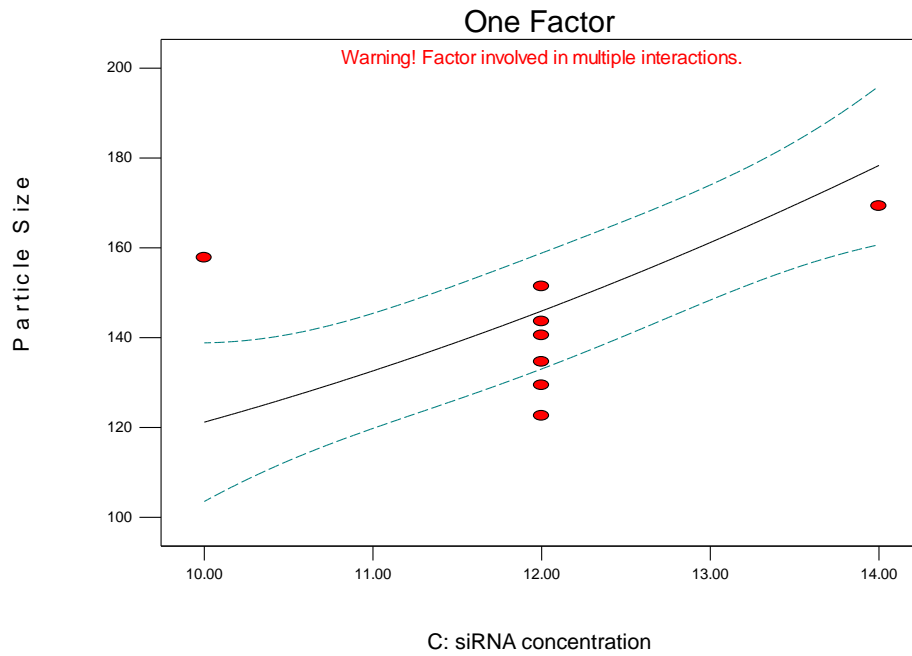


Figure 4.52 Effect of siRNA Concentration on Particle Size

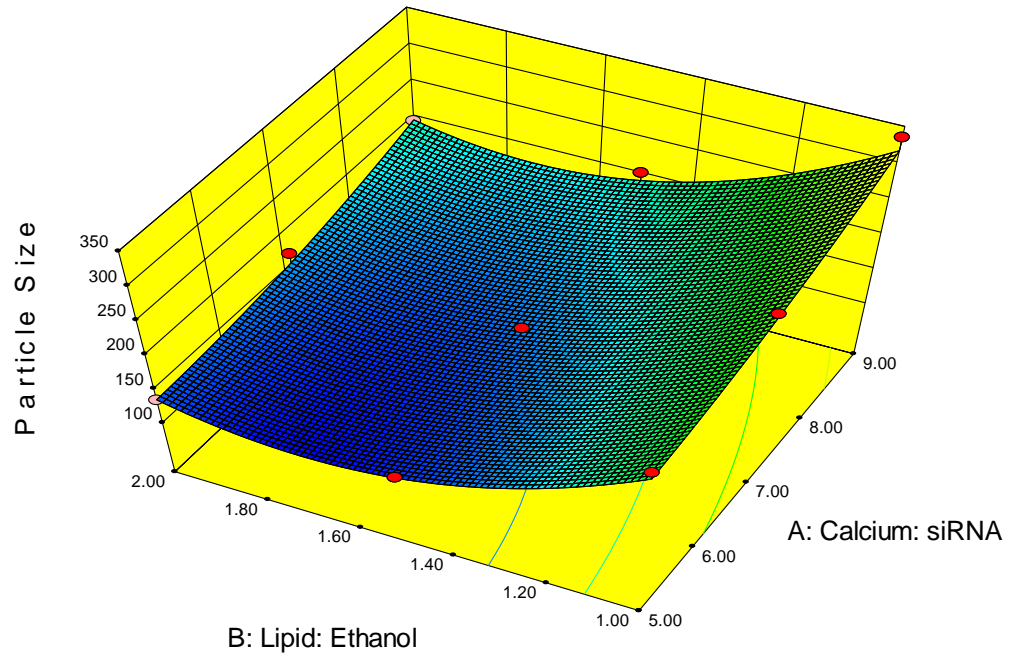


Figure 4.53 Response Surface Showing Combined Effect of Calcium:siRNA and Lipid:Ethanol on Particle Size

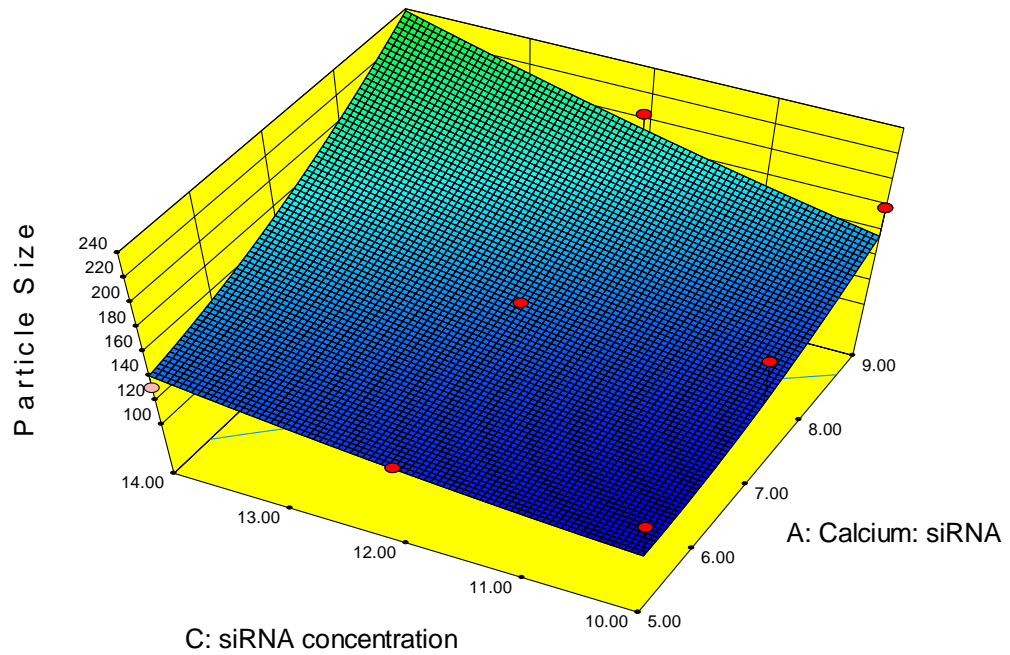


Figure 4.54 Response Surface Showing Combined Effect of Calcium:siRNA and siRNA Concentration on Particle Size

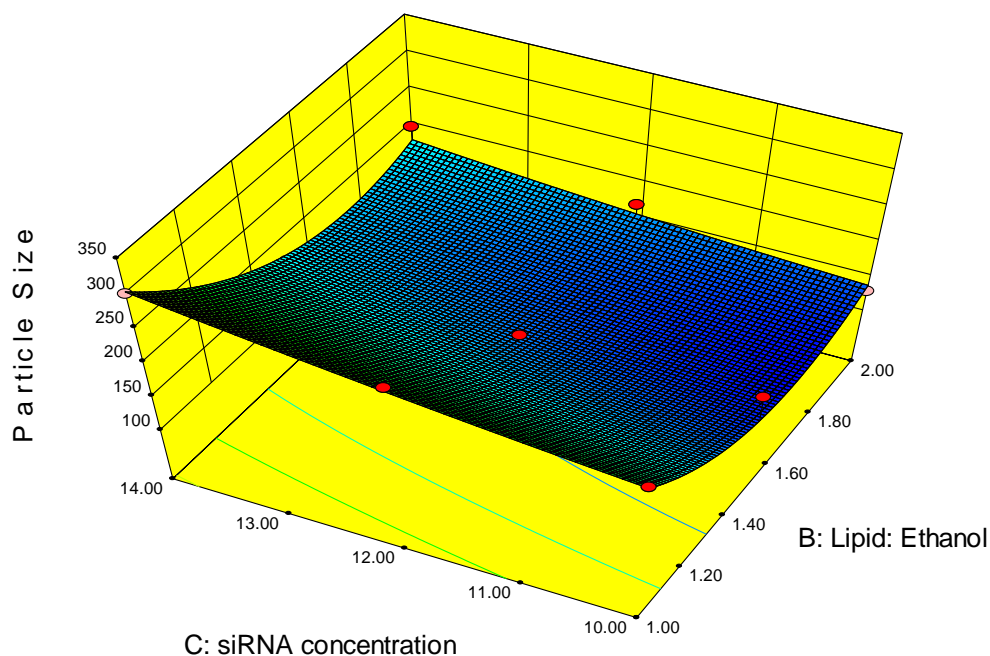


Figure 4.55 Response Surface Showing Combined Effect of Lipid:Ethanol and siRNA Concentration on Particle Size

One factor effect plots (**Figure 4.50**, **Figure 4.51** and **Figure 4.52**) of factors A, B, and C shows that factor C almost linearly affect the particle size while factor A and B has a quadratic effect (curvilinear plot) on the same. Combined effects of A, B and C on particle size are depicted in response surface plots in **Figure 4.53**, **Figure 4.54** and **Figure 4.55**.

Looking at the effects, increase in the Calcium:siRNA ratio and siRNA concentration increased the particle size of liposomes. This may be due to increased siRNA loading inside the liposomes causing the volume of liposomes to expand. In case of Lipid:Ethanol ratio, increase in the ratio decreased the particle size. This might be attributed to the release of calcium from liposomes at lower ratio (higher amount of ethanol) which might be causing increase in particle size due to ionic interaction with liposomes.

Predicted response at any point of the plot can be represented by the following equation:

$$\begin{aligned}
 \text{Particle Size} = & \\
 & +955.67294 \\
 & -53.62321 * \text{Calcium: siRNA} \\
 & -768.25179 * \text{Lipid: Ethanol} \\
 & -18.70923 * \text{siRNA concentration} \\
 & -4.65000 * \text{Calcium: siRNA} * \text{Lipid: Ethanol} \\
 & +2.95417 * \text{Calcium: siRNA} * \text{siRNA concentration} \\
 & -7.12500 * \text{Lipid: Ethanol} * \text{siRNA concentration} \\
 & +3.08360 * \text{Calcium: siRNA}^2 \\
 & +258.80430 * \text{Lipid: Ethanol}^2 \\
 & +0.95860 * \text{siRNA concentration}^2
 \end{aligned}$$

iii. Selection of Optimized Batch:

Constraints applied to select the best formulation parameters based on the siRNA entrapment and particle size are shown in the following **Table 4.42**.

Table 4.42 Constraints Applied for Selection of Optimized Batch

Name	Goal	Lower Limit	Upper Limit
A:Calcium: siRNA	is in range	5	9
B:Lipid: Ethanol	is in range	1	2
C:siRNA concentration	is in range	10	14
siRNA Entrapment	maximize	14	89
Particle Size	minimize	110.4	385.8

Formulation optimization was based on the desirability which may range from 0 to 1 based on the worst particle size and siRNA entrapment to best particle size and siRNA entrapment. The desirability plot is shown in the **Figure 4.56** below.

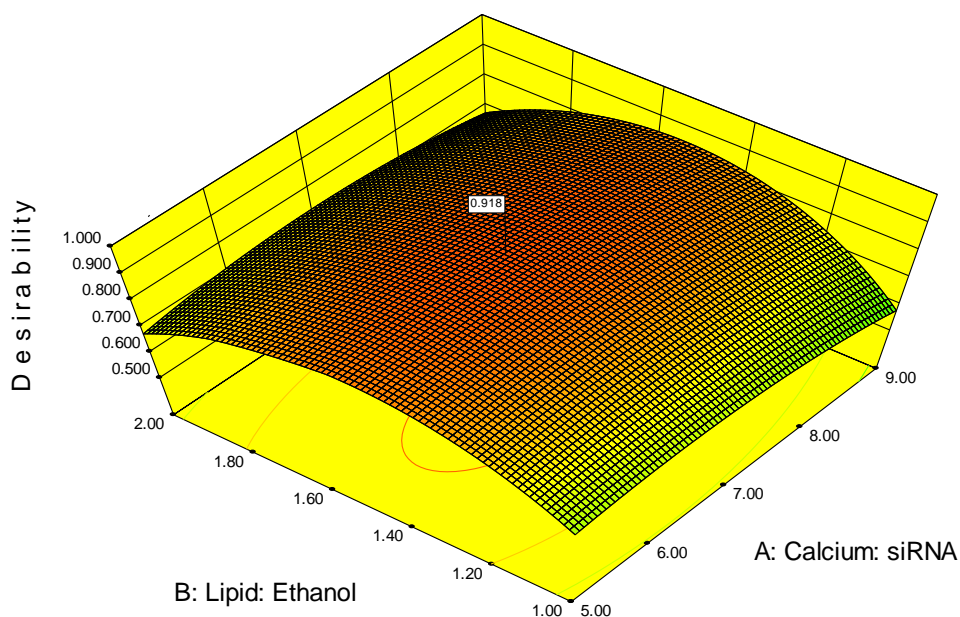


Figure 4.56 Desirability Plot for Selection of Optimized Batch

Based on the maximum desirability, one formulation (desirability 0.918) was chosen for confirmation and further optimization of siRNA loaded liposomes. This optimized batch showed predicted siRNA entrapment of 81.1 % and particle size of 126.6 nm (**Table 4.43**). This batch was prepared for confirmation of the accuracy of predicted response.

Table 4.43 Optimized Batch Parameters Based on Desirability

Number	Calcium: siRNA	Lipid: Ethanol	siRNA concentration	siRNA Entrapment	Particle Size	Desirability
1	6.83	1.51	10.82	81.1119	126.645	0.918

iv. Point Prediction and Confirmation:

Table 4.44 below shows predicted response for the solution selected above along with the Standard deviation and 95 % confidence interval of the responses.

Confirmation of the response was done by carrying out the experiment using the selected factor values in triplicate. The **Table 4.45** shows and confirms that experimental and predicted values

are in good agreement concluding the suitability of the selected model for optimization. Liposomal batch optimized so was used for further modification of surface using RGD peptide.

Table 4.44 Predicted Responses of the Optimized Batch

Response	Prediction	Std Dev	SE Mean	95% CI low	95% CI high
siRNA Entrapment	81.1119	8.05716	2.7368	75.4362	86.7877
Particle Size	126.645	18.5162	6.28946	113.601	139.688

Table 4.45 Experimental Confirmation of the Predicted Responses*

Response	Experiental Mean	Std Dev
siRNA Entrapment	83.855	2.185
Particle Size	117.85	2.150

*Experiments were performed in triplicate.

4.3.10.3. Incorporation of RGD

RGD was incorporated at three different levels, i.e. 1 mole %, 2 mole % and 3 mole % of total incorporated lipid. RGD incorporation does not affect the entrapment efficacy of the CPE liposomes (Table 4.46). RGD grafted CPE liposomes (RGD-CPE liposomes) showed no significant difference in siRNA entrapment as compared to CPE liposomes. Final ratio of lipids is DPPC:DOPE: DSPE-mPEG2000:cholesterol ratio of 1:0.09:0.05:1.

Table 4.46 Effect of RGD Levels on siRNA Entrapment and Particle Size*

Sr. No.	Formulation	siRNA entrapment (%)	Particle size
1.	CPE liposomes	83.86 ± 2.19	117.85 ± 4.02
2.	RGD-CPE liposomes (1%)	81.72 ± 3.02	120.54 ± 3.82
3.	RGD-CPE liposomes (2%)	84.19 ± 2.89	115.71 ± 2.01
4.	RGD-CPE liposomes (3%)	82.93 ± 3.45	125.06 ± 4.90

*Results are expressed as mean±standard deviation (n=3).

4.3.10.4. Calcium Entrapment

Calcium entrapment in the first step of CPE liposomes is very vital for siRNA entrapment later in step-2. Calcium encapsulation was determined using complexometric titration. Effect of various formulation and process parameters on the calcium entrapment inside the liposomes has already been discussed in this chapter in section 4.3.5.1. Liposomes prepared with and without RGD grafting did not show any significant change in calcium entrapment (**Table 4.47**).

Table 4.47 Calcium Entrapment Efficiency of Optimized Liposomes[#]

Sr.No.	Formulation*	Calcium Entrapment (%)
1	CP liposomes	23.470±1.17
2	RGD-CP liposomes (1%)	24.37±1.62
3	RGD-CP liposomes (2%)	23.78±1.09
4	RGD-CP liposomes (3%)	22.81±1.36

* Liposomes obtained after step-1.

[#]Results are expressed as mean±standard deviation (n=3).

4.3.10.5. Assay

Assay was obtained by Phenol/Chloroform extraction method. Extracted siRNA was collected in aqueous layer and quantified using gel densitometry and UV spectroscopy. Both types of formulations showed no degradation of siRNA during processing and in all formulations detected siRNA was within limit (95-105 %) by both methods. Results are summarized in **Table 4.48**.

Table 4.48 Results of Assay of Various siRNA formulations

Sr.No.	Formulation	Assay	
		UV spectroscopy	Gel retardation assay
9.	CPE liposomes	101.87	99.10
10.	RGD-CPE liposomes (1 %)	99.06	98.79
11.	RGD-CPE liposomes (2 %)	102.27	100.21
12.	RGD-CPE liposomes (3 %)	102.35	99.45

Assay results clearly suggest that there is no degradation of siRNA during processing and gel electrophoresis further proves retaining of intact form in final formulation. These data are supported by the studies conducted earlier that no degradation of siRNA was found at 50°C incubation for half an hr. Earlier study at different pH also supports the intact form of siRNA at 8.5 pH. In case of CPE liposomes and RGD-CPE liposomes incubation was carried out at 55°C

for 20 min. And pH was maintained at 8.5. Also siRNA was found to be stable up to half an hr at 60°C and pH 8.5 is also in the safe range. Hence, no degradation was observed in CPE liposomes and RGD-CPE liposomes too as seen with cationic liposomes.

4.3.10.6. siRNA Entrapment Efficiency

All formulations were subjected to study entrapment of siRNA inside the liposomes. Gel retardation assay method provided amount of free siRNA migration and hence, entrapped siRNA was calculated. Optimized formulations were also subjected to ultracentrifuge method to determine siRNA entrapment by direct analysis of liposomal fraction only, because free siRNA was removed from the supernatant after centrifugation. Results are summarised in **Table 4.49**. More than 80 % of entrapment was achieved in all the optimized formulations. RGD grafting did not affect the entrapment efficacy and difference between with and without RGD grafting was insignificant. Effect of various process and formulation parameters on the entrapment efficacy of the CPE liposomes has already been discussed in this chapter in the section 4.3.5.2.

Table 4.49 siRNA Efficiency of Various RGD Grafted Liposomes (as Determined by Various Methods)*

Sr.No.	Formulation	siRNA entrapment (%)		
		Gel retardation assay	Ultracentrifugation	
			UV spectroscopy	Gel electrophoresis
7.	CPE liposomes	83.86±2.19	84.08±3.25	82.42±2.96
8.	RGD-CPE liposomes (1%)	81.72±3.02	83.20±3.72	79.04±3.01
9.	RGD-CPE liposomes (2%)	84.19±2.89	83.35±3.55	82.88±1.73
10.	RGD-CPE liposomes (3%)	82.93±3.45	84.32±2.33	81.61±2.93

*Results are expressed as mean±standard deviation (n=3).

4.3.10.7. Particle size and Zeta Potential

Particle size of the CPE liposomes was mainly dependent on the liposomes obtained in after step-1 i.e. calcium phosphate encapsulated liposomes. **Table 4.50** shows that siRNA loading did not increase the particle size significantly ($p > 0.05$) as seen with the cationic liposomes. This may due to entrapment of siRNA inside the liposomes whereas cationic liposomes entrapped siRNA inside as well as onto the surface due to cationic charge on the liposomal membrane. No significant ($p > 0.05$) difference was observed for zeta potential of various liposomes as well

before and after siRNA loading (Table 4.51). Figure 4.57 shows Malvern particle size analysis report for one of the RGD-CPE (2 %) batch.

Table 4.50 Effect of incorporation of siRNA on Particle Size of Liposomes*

Sr.No.	Formulation	Particle size		Change in Mean Particle size (%)
		Before	After	
1.	CPE liposomes	114.74±3.10	117.85±4.02	2.7
2.	RGD-CPE liposomes (1%)	116.55±3.24	120.54±3.82	3.4
3.	RGD-CPE liposomes (2%)	115.24±3.06	117.71±2.01	2.1
4.	RGD-CPE liposomes (3%)	118.36±3.45	125.06±4.90	5.7

*Results are expressed as mean±standard deviation (n=3).

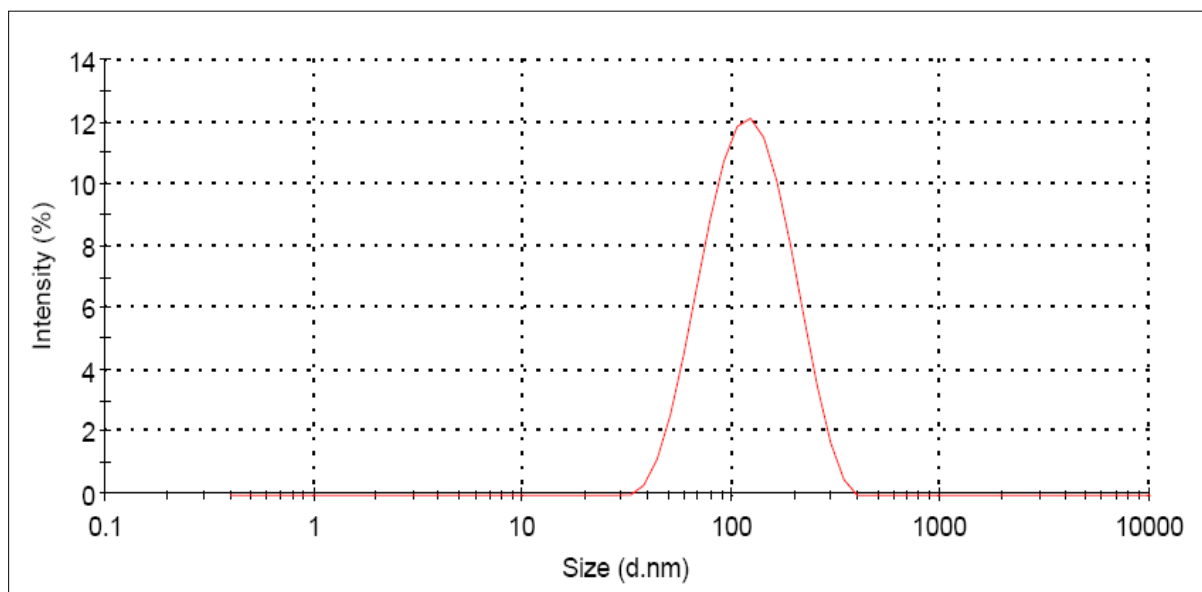


Figure 4.57 Malvern Particle Size Report of One of the RGD-CPE Liposome (2%) Batches

Table 4.51 Effect of incorporation of siRNA on Zeta Potential of Liposomes*

Sr.No.	Formulation	Zeta potential		Change in Meam Zeta Potential (%)
		Before	After	
1.	CPE liposomes	13.92±0.23	11.90±0.52	2.02
2.	RGD-CPE liposomes (1%)	12.41±0.54	12.21±0.13	0.20
3.	RGD-CPE liposomes (2%)	12.01±0.35	11.45±0.44	0.56
4.	RGD-CPE liposomes (3%)	11.78±0.21	11.23±0.31	0.55

*Results are expressed as mean±standard deviation (n=3).

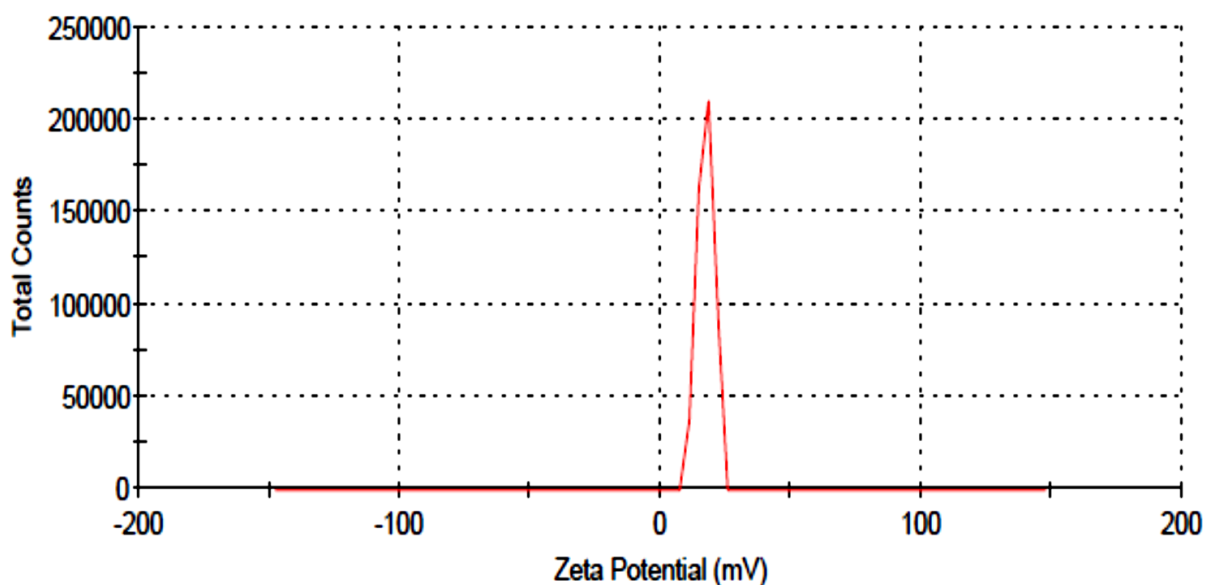


Figure 4.58 Malvern Zeta Potential Report of One of the RGD-CPE Liposome (2%) Batches

Calcium phosphate encapsulated liposomes showed particle size below 150 nm even after encapsulation of siRNA. Change in particle size as well as zeta potential values after siRNA loading was found to be insignificant.

4.3.10.8. Transmission Electron Microscopy

Images obtained by TEM revealed that prepared liposomes are spherical in shape as shown in **Figure 4.59**. All vesicles are unilamellar in structure and having particle size between 100-150 nm. This range can also help in EPR effect for tumor internalization of nano materials [47]. Clear and distinct precipitates were seen during electron microscopy and same can be seen in the image. This result confirms the calcium phosphate precipitation inside the liposomes. Bilayer thickness was also measured and found to be in-between 5-10 nm in size.

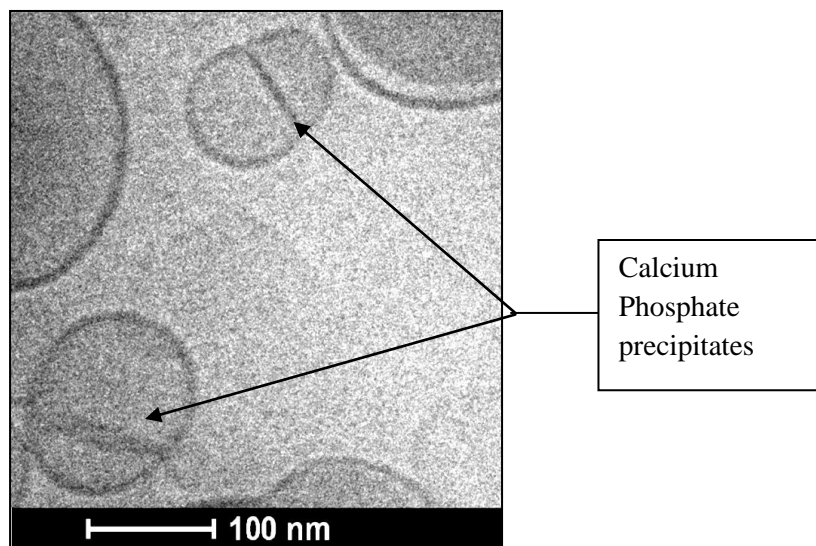


Figure 4.59 TEM Micrograph of Calcium Phosphate Loaded Liposomes

4.4. References

1. Leventis R, Silviu JR. Interactions of mammalian cells with lipid dispersions containing novel metabolizable cationic amphiphiles. *Biochim Biophys Acta*. 1990 Mar 30;1023(1):124-32.
2. Zuidam NJ, Barenholz Y. Electrostatic and structural properties of complexes involving plasmid DNA and cationic lipids commonly used for gene delivery. *Biochim Biophys Acta*. 1998 Jan 5;1368(1):115-28.
3. Zabner J, Fasbender AJ, Moninger T, Poellinger KA, Welsh MJ. Cellular and molecular barriers to gene transfer by a cationic lipid. *J Biol Chem*. 1995 Aug 11;270(32):18997-9007.
4. Yang JP, Huang L. Time-dependent maturation of cationic liposome-DNA complex for serum resistance. *Gene Ther*. 1998 Mar;5(3):380-7.
5. Farhood H, Serbina N, Huang L. The role of dioleoyl phosphatidylethanolamine in cationic liposome mediated gene transfer. *Biochim Biophys Acta*. 1995 May 4;1235(2):289-95.
6. Scarzello M, Smisterova J, Wagenaar A, Stuart MC, Hoekstra D, Engberts JB, et al. Sunfish cationic amphiphiles: toward an adaptative lipoplex morphology. *J Am Chem Soc*. 2005 Jul 27;127(29):10420-9.
7. Zuhorn IS, Bakowsky U, Polushkin E, Visser WH, Stuart MC, Engberts JB, et al. Nonbilayer phase of lipoplex-membrane mixture determines endosomal escape of genetic cargo and transfection efficiency. *Mol Ther*. 2005 May;11(5):801-10.
8. Safinya CR. Structures of lipid-DNA complexes: supramolecular assembly and gene delivery. *Curr Opin Struct Biol*. 2001 Aug;11(4):440-8.
9. Lasic DD. Recent developments in medical applications of liposomes: sterically stabilized liposomes in cancer therapy and gene delivery in vivo. *J Control Release*. 1997 10/13;48(2-3):203-22.
10. Koltover I, Salditt T, Rädler JO, Safinya CR. An Inverted Hexagonal Phase of Cationic Liposome-DNA Complexes Related to DNA Release and Delivery. *Science*. 1998 July 3, 1998;281(5373):78-81.

11. Leal C, Boussein NF, Ewert KK, Safinya CR. Highly efficient gene silencing activity of siRNA embedded in a nanostructured gyroid cubic lipid matrix. *J Am Chem Soc.* 2010 Dec 1;132(47):16841-7.
12. Xu Y, Hui SW, Frederik P, Szoka FC, Jr. Physicochemical characterization and purification of cationic lipoplexes. *Biophys J.* 1999 Jul;77(1):341-53.
13. Zhdanov RI, Podobed OV, Vlassov VV. Cationic lipid-DNA complexes-lipoplexes-for gene transfer and therapy. *Bioelectrochemistry.* 2002 Nov;58(1):53-64.
14. Amenitsch H, Caracciolo G, Foglia P, Fuscoletti V, Giansanti P, Marianecchi C, et al. Existence of hybrid structures in cationic liposome/DNA complexes revealed by their interaction with plasma proteins. *Colloids Surf B Biointerfaces.* 2011 Jan 1;82(1):141-6.
15. Marchini C, Pozzi D, Montani M, Alfonsi C, Amici A, Amenitsch H, et al. Tailoring lipoplex composition to the lipid composition of plasma membrane: a Trojan horse for cell entry? *Langmuir.* 2010 Sep 7;26(17):13867-73.
16. Dokka S, Toledo D, Shi X, Castranova V, Rojanasakul Y. Oxygen radical-mediated pulmonary toxicity induced by some cationic liposomes. *Pharm Res.* 2000 May;17(5):521-5.
17. Lappalainen K, Jaaskelainen I, Syrjanen K, Urtti A, Syrjanen S. Comparison of cell proliferation and toxicity assays using two cationic liposomes. *Pharm Res.* 1994 Aug;11(8):1127-31.
18. Marshall J, Yew NS, Eastman SJ, Jiang C, Scheule RK, Cheng SH. Cationic lipid-mediated gene delivery to the airways. In: Huang L, Hung MC, Wagner E, editors. *Nonviral Vectors for Gene Therapy.* San Diego, California, US: Academic Press; 1999. p. 39-68.
19. Srinivasan C, Burgess DJ. Optimization and characterization of anionic lipoplexes for gene delivery. *J Control Release.* 2009 May 21;136(1):62-70.
20. Roerdink F, Wassef NM, Richardson EC, Alving CR. Effects of negatively charged lipids on phagocytosis of liposomes opsonized by complement. *Biochim Biophys Acta.* 1983 Sep 21;734(1):33-9.
21. Patil SD, Rhodes DG, Burgess DJ. Biophysical characterization of anionic lipoplexes. *Biochim Biophys Acta.* 2005 Jun 1;1711(1):1-11.

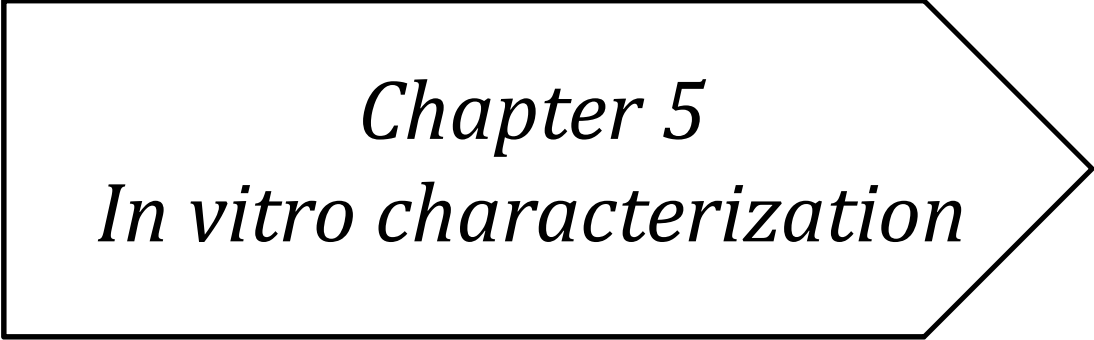
22. Lakkaraju A, Dubinsky JM, Low WC, Rahman YE. Neurons are protected from excitotoxic death by p53 antisense oligonucleotides delivered in anionic liposomes. *J Biol Chem*. 2001 Aug 24;276(34):32000-7.
23. Kulkarni VI, Shenoy VS, Dodiya SS, Rajyaguru TH, Murthy RR. Role of calcium in gene delivery. *Expert Opin Drug Deliv*. 2006 Mar;3(2):235-45.
24. Lasic DD, Templeton NS. Liposomes in gene therapy. *Advanced Drug Delivery Reviews*. 1996 7/26;20(2-3):221-66.
25. Rejman J, Oberle V, Zuhorn IS, Hoekstra D. Size-dependent internalization of particles via the pathways of clathrin- and caveolae-mediated endocytosis. *Biochem J*. 2004 Jan 1;377(Pt 1):159-69.
26. Kim JK, Choi SH, Kim CO, Park JS, Ahn WS, Kim CK. Enhancement of polyethylene glycol (PEG)-modified cationic liposome-mediated gene deliveries: effects on serum stability and transfection efficiency. *J Pharm Pharmacol*. 2003 Apr;55(4):453-60.
27. Dass CR, Choong PF. Selective gene delivery for cancer therapy using cationic liposomes: in vivo proof of applicability. *J Control Release*. 2006 Jun 28;113(2):155-63.
28. Hayes ME, Drummond DC, Hong K, Park JW, Marks JD, Kirpotin DB. Assembly of nucleic acid-lipid nanoparticles from aqueous-organic monophasic systems. *Biochim Biophys Acta*. 2006 Apr;1758(4):429-42.
29. Owens DE, 3rd, Peppas NA. Opsonization, biodistribution, and pharmacokinetics of polymeric nanoparticles. *Int J Pharm*. 2006 Jan 3;307(1):93-102.
30. Zuhorn IS, Engberts JB, Hoekstra D. Gene delivery by cationic lipid vectors: overcoming cellular barriers. *Eur Biophys J*. 2007 Apr;36(4-5):349-62.
31. Stuart DD, Kao GY, Allen TM. A novel, long-circulating, and functional liposomal formulation of antisense oligodeoxynucleotides targeted against MDR1. *Cancer Gene Ther*. 2000 Mar;7(3):466-75.
32. Kohn DB, Sadelain M, Glorioso JC. Occurrence of leukaemia following gene therapy of X-linked SCID. *Nat Rev Cancer*. 2003 Jul;3(7):477-88.
33. Gura T. After a Setback, Gene Therapy Progresses ... Gingerly. *Science*. 2001 March 2, 2001;291(5509):1692-7.

34. Hayes ME, Drummond DC, Kirpotin DB, Zheng WW, Noble CO, Park JW, et al. Genospheres: self-assembling nucleic acid-lipid nanoparticles suitable for targeted gene delivery. *Gene Ther.* 2006 Apr;13(7):646-51.
35. Li S, Rizzo MA, Bhattacharya S, Huang L. Characterization of cationic lipid-protamine-DNA (LPD) complexes for intravenous gene delivery. *Gene Ther.* 1998 Jul;5(7):930-7.
36. Hafez IM, Maurer N, Cullis PR. On the mechanism whereby cationic lipids promote intracellular delivery of polynucleic acids. *Gene Ther.* 2001 Aug;8(15):1188-96.
37. Wolfe-Simon F, Davies P, Anbar A, editors. Did nature also choose arsenic? *Nature Proceedings*; 2008: Nature Publishing Group.
38. Elser JJ, Bracken ME, Cleland EE, Gruner DS, Harpole WS, Hillebrand H, et al. Global analysis of nitrogen and phosphorus limitation of primary producers in freshwater, marine and terrestrial ecosystems. *Ecology letters.* 2007;10(12):1135-42.
39. Redfield A. On the proportions of organic derivatives in sea water and their relation to the composition of plankton. In: Daniel RJ, editor. *The Oceans And Marine Geochemistry*. US: University Press of Liverpool; 1934. p. 177-92.
40. Geider R, La Roche J. Redfield revisited: variability of C:N:P in marine microalgae and its biochemical basis. *European Journal of Phycology.* 2002 //;37(1):1-17.
41. Falkowski PG. Rationalizing elemental ratios in unicellular algae. *Journal of Phycology.* 2000;36(1):3-6.
42. Torčilin VP, Weissig V. Preparation of Liposomes. In: Torčilin VP, Weissig V, editors. *Liposomes: A Practical Approach*. Oxford: Oxford University Press; 2003. p. 33-104.
43. van Winden ECA, Crommelin DJA. Long term stability of freeze-dried, lyoprotected doxorubicin liposomes. *E J Pharm Bio.* 1997 6//;43(3):295-307.
44. Martin FJ. Pharmaceutical Manufacturing of Liposomes. In: Tyle P, editor. *Specialized Drug Delivery Systems: Manufacturing and Production Technology*. New York, USA: Marcel Dekker Inc.; 1990. p. 267-316.
45. Sułkowski WW, Pentak D, Nowak K, Sułkowska A. The influence of temperature, cholesterol content and pH on liposome stability. *Journal of Molecular Structure.* 2005 6/3//;744–747(0):737-47.
46. De Gier J, Mandersloot JG, Van Deenen LLM. Lipid composition and permeability of liposomes. *Biochim Biophys Acta*

- *Biomembranes*. 1968 6/11/;150(4):666-75.

47. Maeda H, Sawa T, Konno T. Mechanism of tumor-targeted delivery of macromolecular drugs, including the EPR effect in solid tumor and clinical overview of the prototype polymeric drug SMANCS. *J Control Release*. 2001 Jul 6;74(1-3):47-61.
48. Cochran WC, Cox GM. *Experimental Design* 2nd Ed. New York: Marcel Dekker; 1992.
49. Fannin TE, Marcus MD, Anderson DA, Bergman HL. Use of a fractional factorial design to evaluate interactions of environmental factors affecting biodegradation rates. *Appl Environ Microbiol*. 1981 Dec;42(6):936-43.
50. Gonzalez-Mira E, Egea MA, Souto EB, Calpena AC, Garcia ML. Optimizing flurbiprofen-loaded NLC by central composite factorial design for ocular delivery. *Nanotechnology*. 2011 Jan 28;22(4):045101.
51. Gonzalez-Rodriguez ML, Barros LB, Palma J, Gonzalez-Rodriguez PL, Rabasco AM. Application of statistical experimental design to study the formulation variables influencing the coating process of lidocaine liposomes. *Int J Pharm*. 2007 Jun 7;337(1-2):336-45.
52. Loukas YL. A 2 (k-p) fractional factorial design via fold over: application to optimization of novel multicomponent vesicular s⁺-stem. *Analyst*. 1997;122:1023-7.
53. Murthy RS, Umrethia ML. Optimization of formulation parameters for the preparation of flutamide liposomes by 3(3) factorial 26-term logit model. *Pharm Dev Technol*. 2004 Nov;9(4):369-77.
54. Padamwar MN, Pokharkar VB. Development of vitamin loaded topical liposomal formulation using factorial design approach: drug deposition and stability. *Int J Pharm*. 2006 Aug 31;320(1-2):37-44.
55. Seth AK, Misra A. Mathematical modelling of preparation of acyclovir liposomes: reverse phase evaporation method. *J Pharm Pharm Sci*. 2002 Sep-Dec;5(3):285-91.
56. Subramanian N, Yajnik A, Murthy RS. Artificial neural network as an alternative to multiple regression analysis in optimizing formulation parameters of cytarabine liposomes. *AAPS PharmSciTech*. 2004 Feb 2;5(1):E4.
57. Vali AM, Toliyat T, Shafaghi B, Dadashzadeh S. Preparation, optimization, and characterization of topotecan loaded PEGylated liposomes using factorial design. *Drug Dev Ind Pharm*. 2008 Jan;34(1):10-23.

-
58. Ducat E, Brion M, Lecomte F, Evrard B, Piel G. The experimental design as practical approach to develop and optimize a formulation of peptide-loaded liposomes. *AAPS PharmSciTech*. 2010 Jun;11(2):966-75.
 59. Naik S, Patel D, Surti N, Misra A. Preparation of PEGylated liposomes of docetaxel using supercritical fluid technology. *The Journal of Supercritical Fluids*. 2010 7//;54(1):110-9.
 60. Singh B, Dahiya M, Saharan V, Ahuja N. Optimizing drug delivery systems using systematic "design of experiments." Part II: retrospect and prospects. *Crit Rev Ther Drug Carrier Syst*. 2005;22(3):215-94.
 61. Xiong Y, Guo D, Wang L, Zheng X, Zhang Y, Chen J. Development of nobiliside A loaded liposomal formulation using response surface methodology. *Int J Pharm*. 2009 Apr 17;371(1-2):197-203.
 62. Stensrud G, Sande SA, Kristensen S, Smistad G. Formulation and characterisation of primaquine loaded liposomes prepared by a pH gradient using experimental design. *Int J Pharm*. 2000 Apr 5;198(2):213-28.
 63. Singh B, Mehta G, Kumar R, Bhatia A, Ahuja N, Katare OP. Design, development and optimization of nimesulide-loaded liposomal systems for topical application. *Curr Drug Deliv*. 2005 Apr;2(2):143-53.
 64. Armstrong NA, James KC. *Understanding Experimental Designs and Interpretation in Pharmaceutics*. London: Ellis Horwood; 1990.
 65. Box GEP, Hunter WG, Hunger JS. *Statistics for Experimenters*. New York: Wiley; 1978.
 66. Mak KWY, Yap MGS, Teo WK. Formulation and optimization of two culture media for the production of tumour necrosis factor- β in *Escherichia coli*. *Journal of Chemical Technology & Biotechnology*. 1995;62(3):289-94.
 67. Box GEP, Wilson KB. On the Experimental Attainment of Optimum Conditions. *Journal of the Royal Statistical Society Series B (Methodological)*. 1951;13(1):1-45.



Chapter 5
In vitro characterization

5.1. Cell-line Studies

Various *in vitro* cell line studies were carried out for further screening of prepared liposomal carriers to achieve maximum siRNA uptake inside the cells with desired transfection.

5.1.1. In Vitro Cytotoxicity Assay (MTT Assay)

This is a colorimetric assay that measures the reduction of yellow 3-(4,5-dimethylthiazol-2-yl)-2,5-diphenyl tetrazolium bromide (MTT) by mitochondrial succinate dehydrogenase. The MTT enters the cells and passes into the mitochondria where it is reduced to an insoluble, coloured (dark purple) formazan product. The cells are then solubilised with an organic solvent (eg. isopropanol) and the released, solubilised formazan reagent is measured spectrophotometrically. Since reduction of MTT can only occur in metabolically active cells the level of activity is a measure of the viability of the cells. Tetrazolium dye reduction is dependent on NAD(P)H-dependent oxidoreductase enzymes largely in the cytosolic compartment of the cell. Therefore, reduction of MTT and other tetrazolium dyes increases with cellular metabolic activity due to elevated NAD(P)H flux. Resting cells such as thymocytes and splenocytes that are viable but metabolically quiet reduce very little MTT. In contrast, rapidly dividing cells exhibit high rates of MTT reduction. It is important to keep in mind that assay conditions can alter metabolic activity and thus tetrazolium dye reduction without affecting cell viability and that different tetrazolium dyes will give different results depending on whether they are reduced intracellularly (MTT, MTS) or extracellularly (WST-1) [1, 2].

Method

The cytotoxicity of siRNA carriers were determined using 3-(4, 5-dimethylthiazole-2-yl)-2,5-diphenyl tetrazolium bromide (MTT; Himedia, India) assays. A549 and H1299 cells were seeded onto 96-well plates at a density of 5×10^3 cells/well. After 24 h, cells were treated separately with DD liposomes, DDC liposomes, DDHC liposomes and RGD-DDHC liposomes at varying N/P ratio ranging from 2.5 to 12.5 in DMEM media containing 10% FBS and antibiotics (**Table 5.1**). In case of CPE liposomes and RGD-CPE liposomes cytotoxicity was carried out using increasing amount of CPE liposomes by varying Ca:siRNA ratio.

In all wells, after 6 hr transfection media was replaced by fresh DMEM containing 10% of FBS and antibiotics. The cells were incubated for 48 hr, and then 20 μ L of 5 mg/mL MTT solution was added to each well. After incubating for 4 hr with MTT solution, the culture medium was removed and 200 μ L of a dimethyl sulfoxide (DMSO) (Sigma, USA) was added. The reduction of viable cells was measured by calorimetry at 570 nm wavelength using an enzyme-linked immunosorbent assay (ELISA) plate reader (Bio-Rad, USA). Cell viability of each group was expressed as a relative percentage to that of control cells.

Cells treated with PBS (Phosphate buffer saline) were considered as negative control and commercially available non-viral lipid transfecting carrier Lipofectamine-2000 (Invitrogen, USA) was kept as positive control (**Table 5.1**).

Table 5.1 Cell-line Treatment Parameters for MTT Assay

Sr.No.	Formulations	Cells	Treatment	Incubation time
1.	DD liposomes	A549 & H1299	100 nM NC siRNA	48 hr
2.	DDC liposomes		100 nM NC siRNA	
3.	DDHC liposomes		100 nM NC siRNA	
4.	RGD-DDHC liposomes (1%)		100 nM NC siRNA	
5.	RGD-DDHC liposomes (2%)		100 nM NC siRNA	
6.	RGD-DDHC liposomes (3%)		100 nM NC siRNA	
7.	CPE liposomes		100 nM NC siRNA	
8.	RGD-CPE liposomes (1%)		100 nM NC siRNA	
9.	RGD-CPE liposomes (2%)		100 nM NC siRNA	
10.	RGD-CPE liposomes (3%)		100 nM NC siRNA	
11.	PBS		-	
12.	Lipofectamine 2000		100 nM NC siRNA	

*Negative control = PBS, Positive control = Lipofectamine 2000

5.1.2. In vitro Cell Uptake Studies

For cellular uptake studies, FAM labelled negative control siRNA (FAM-NC-siRNA) was used. Flow cytometry was utilized for quantitative cell uptake to determine the mean fluorescent intensity while qualitative intracellular accumulation was determined using confocal microscopy.

5.1.2.1. Flow Cytometry

Since the first application of flow cytometry (FCy) in the 1970s [3], the machines have become widely popular in research and clinical diagnostics. In principle, FCy can be combined with

nearly any staining procedure, assay or biotechnological process. Whenever fluorescence is introduced into a microorganism or a cell it can be exploited in flow cytometry for assessing information about the specimen. To a low extent the technology is applied for other objects than microorganisms and cells [4]. But with the combination of fluidics and laser triggered fluorescence detection it is the ideal tool to detect NPs in cells. Subtle changes in scattering and emission of a cell can be observed – which are directly linked to the cellular uptake of fluorescing particles.

In flow cytometry, a fluidics system is coupled with the detection of fluorescence and of light scattering in small and wide angle position. For this application the objects of interest must be prepared as a diluted dispersion commonly not exceeding a concentration of several thousand objects per μl . In the machine, a sample stream is injected into the core of a flowing stream of so called sheath liquid (water or physiological buffer) and a laminar flow is established. The two streams do not mix and the sample flow is surrounded by a layer of sheath liquid flow in a concentric setup. This is termed hydrodynamic focusing. This stream of two concentric layers is directed through the measurement chamber, a narrow glass capillary. In the measurement chamber, the sample stream is hit orthogonally by a laser beam. It is important to note that the objects, e.g. cells, pass this laser beam single-filed. Placed behind an array of filters and mirrors, several detectors successively detect the properties of each cell passing the laser beam. This includes fluorescence signals but also of wide angle (sideward scatter, SSC) and small angle (forward scatter, FSC) scattering. Flow cytometers thus allow for the rapid measuring of individual objects in dispersion. Another obvious advantage is the short exposure of each object to the laser (μs scale), unlike e.g. in microscopy where exposure lasts seconds to minutes. Extremely light sensitive objects can be analyzed by flow cytometry. Within one second, several thousand objects can be measured separately and their number per volume can be counted. But only when one object passes through the beam of the reference laser, data acquisition is triggered. In this instant, a digital event is created and the acquired data from every active channel is assigned to this event i.e. assigned to this particular object. Each event now represents a comprehensive data set, including fluorescence intensities in various channels and scattering intensities at two fixed positions (small and large angle i.e. FSC and SSC). This collected raw data consists of up to hundred thousands of events which represent background (e.g. pieces of cell debris) and wanted objects (cells) alike. Before final data interpretation the signals must be

sorted from the background events. Fluorescence, granularity (SSC) or the presumable size (FSC or SSC) are features which can be applied to identify the wanted objects. Commonly a threshold condition is set on one of the detection channels so that unwanted signals are excluded from detection. In nearly every system a 488 nm laser is present as standard reference, but often additional lasers (e.g. 640 nm, 561 nm, 375 nm) are available.

Method

A549 and H1299 cells were seeded at a density of 5×10^5 cells per well in 24 well plates. After 24 hr of proliferation, formulations (**Table 5.2**) containing FAM-NC-siRNA at a final concentration of 100 nM were exposed to cells and incubated for additional 6 hr at 37°C in humidified air with 5% CO₂. After incubation, the cells were harvested and washed three times with cold PBS having pH = 7.4 and then analysed for mean fluorescence activity using fluorescence activated cell sorter (FACS-BD-AriaIII, BD, USA). Naked FAM-NC-siRNA and Lipofectamine 2000 complexed siRNA were used as negative and positive control respectively.

Table 5.2 Cell-Line Treatment Parameters for Flow-Cytometry

Sr.No.	Formulations	Cells	Treatment	Condition
1	Naked siRNA	A549 & H1299	100 nM FAM-NC siRNA	Incubation time=48 h Temperature = 37°C (5% CO ₂)
2	DDHC liposomes		100 nM FAM-NC siRNA	
3	RGD-DDHC liposomes (1%)		100 nM FAM-NC siRNA	
4	RGD-DDHC liposomes (2%)		100 nM FAM-NC siRNA	
5	RGD-DDHC liposomes (3%)		100 nM FAM-NC siRNA	
6	CPE liposomes		100 nM FAM-NC siRNA	
7	RGD-CPE liposomes (1%)		100 nM FAM-NC siRNA	
8	RGD-CPE liposomes (2%)		100 nM FAM-NC siRNA	
9	RGD-CPE liposomes (3%)		100 nM FAM-NC siRNA siRNA	
10	Lipofectamine		100 nM FAM-NC siRNA	
11	PBS		-	
12	RGD-DDHC liposomes		placebo	
13	RGD-CPE liposomes		Placebo	

5.1.2.2. Confocal Microscopy

Cellular internalization of FAM labelled siRNA in A549 and H1299 cells was monitored by confocal microscopy.

Method

Cells were seeded onto 6-well plates with a glass cover slip at the bottom. Cells were seeded at a density of 10^4 cells/well on flame sterilized 0.17 mm square glass cover slips in a 6 well plate. After 24 hr of seeding, cells were transfected with FAM-NC-siRNA containing formulation (**Table 5.3**) at a final concentration of 100 nM. After 6 hr of incubation, cells were washed with cold PBS immediately and fixed using ice cooled 4% paraformaldehyde solution for 10 min. Cells were stained by cell nuclei stain, DAPI, for next 10 min. Cover slips were mounted on slides after washing with PBS three times and proceeded for confocal microscopy using confocal laser scanning microscope (LSM 710, Carl-Zeiss Inc., USA).

Table 5.3 Cell-Line Treatment Parameters for Confocal Microscopy

Sr.No.	Formulations	Cells	Treatment	Condition
1.	Naked siRNA	A549 & H1299	100 nM FAM-NC siRNA	Incubation time= 6 h Temperature = 37°C (5% CO ₂)
2.	DDHC liposomes		100 nM FAM-NC siRNA	
3.	RGD-DDHC liposomes (2%)		100 nM FAM-NC siRNA	
4.	CPE liposomes		100 nM FAM-NC siRNA	
5.	RGD-CPE liposomes (2%)		100 nM FAM-NC siRNA	
6.	Lipofectamine (Positive control)		100 nM FAM-NC siRNA	
7.	PBS (Negative control)		-	

Live imaging was performed using confocal microscopy to access the potential of RGD grafting on the liposomal surface. Live imaging was carried out in A549 cells using four formulations, i.e. DDHC liposomes, RGD-DDHC liposomes, CPE-liposomes and RGD-CPE liposomes. Naked siRNA was also transfected as such without any liposomal carrier for comparison.

5×10^4 cells were seeded onto confocal microscopic petridish with glass cover slip (Nunc, India). After 24 hr cells were transfected with FAM-NC-siRNA at 100 nM concentration. Soon after transfection imaging was started. Furthermore, the lateral Z-stack images were constructed during imaging from the middle zone of the cells.

5.1.3. Sub-inhibitory concentration (Cell Cycle Analysis)

Cellular growth is considered as successive phases, characterized by specific biochemical processes and called, from one division to the other: 'cell cycle' [5]. Each cell has to replicate its genetic material during the DNA synthesis phase (S phase) before entering the mitotic phase

(M). Moreover, periods of time (gaps) are located between the end of cellular division and DNA synthesis start (G 1 phase) as well as between the end of DNA synthesis and mitosis start (G 2 phase). The mitotic phase is distinguished from other cycle phases (called together interphase). To reach the mitotic phase, cells have to double their whole components, at the same time that their genetic material doubles. Constituent synthesis is generally continuous, with a varying rate during interphase [6]. The growth cycle is considered as distinct from the nuclear cycle and its regulation mechanism seems to be different [7], but these two cycles are closely dependent and have to converge in a synchronous way towards mitosis; otherwise, there is an unbalanced growth [8]. DNA amount in cells is often the single parameter measured for cell cycle studies by flow cytometry. Analyses are performed with fluorescent molecules that bind specifically and stoichiometrically to DNA, in order to obtain a linear relationship between cellular fluorescence intensity and DNA amount [9]. Some dyes possess an intercalative binding mode, such as propidium iodide or ethidium bromide, whereas others present an affinity for DNA A-T rich regions: Hoechst 33342, Hoechst 33258 and DAPI, or G-C rich regions: mithramycin and chromomycin A3.

Method

Chemosensitization is well governed at sub-inhibitory concentration and hence, cell cycle analysis was used to determine the DNA content of cells at varying concentration of RRM1 siRNA i.e. 50 pM, 100 pM, 500 pM and 2.5 nM. RGD-DDHC liposomes only were used to find out the optimal concentration which regulates sub-inhibitory growth of cancer cells in both A549 and H1299 cell lines.

Cells were seeded onto 6-well plates at a density of 10^6 cells/well. After 24 hr of seeding, cells were transfected with RRM1 siRNA containing RGD-DDHC liposomes at varying siRNA concentrations in DMEM media containing 10 % FBS and antibiotics.

In all wells, after 6 hr transfection media was replaced by fresh DMEM containing 10% of FBS and antibiotics. The cells were incubated for 72 hr and then washed with PBS thrice. 10^6 cells were suspended in 1mL of PBS and vortexed gently to obtain a mono-dispersed cell suspension, with minimal cell aggregation. Cells were centrifuged at 200 x g for 5 min at room temperature and again resuspended in 0.5 mL of PBS. Cells were fixed by transferring this suspension into

centrifuge tubes containing 4.5 mL of 70 % ethanol, on ice. Cells were kept in above step for at least 2 h at 4°C. Above ethanolic suspension was centrifuged for 5 min at 300 x *g* and ethanol was decanted thoroughly. Again cells were suspended in 5 mL of PBS and centrifuged at 300 x *g* for 5 min. Finally cell pellet was re-suspended in 1 mL of PI staining solution and kept in the dark at room temperature for 30 min. Samples were transferred to the flow cytometer and cell fluorescence was measured. Maximum excitation of PI bound to DNA was at 536 nm, and emission was at 617 nm. Blue (488 nm) or green light lines of lasers were optimal for excitation of PI fluorescence.

5.1.4. Transfection Studies/Gene expression by real time PCR

In molecular biology, real-time polymerase chain reaction, also called quantitative real time polymerase chain reaction (qPCR) or kinetic polymerase chain reaction is a laboratory technique based on the polymerase chain reaction, which is used to amplify and simultaneously quantify a targeted DNA molecule. For one or more specific sequences in a DNA sample, Real Time-PCR enables both detection and quantification. The quantity can be either an absolute number of copies or a relative amount when normalized to DNA input or additional normalizing genes. The procedure follows the general principle of polymerase chain reaction; its key feature is that the amplified DNA is detected as the reaction progresses in real time. This is a new approach compared to standard PCR, where the product of the reaction is detected at its end. Two common methods for the detection of products in real-time PCR are: (1) non-specific fluorescent dyes that intercalate with any double-stranded DNA, and (2) sequence-specific DNA probes consisting of oligonucleotides that are labelled with a fluorescent reporter which permits detection only after hybridization of the probe with its complementary DNA target. Frequently, real-time PCR is combined with reverse transcription to quantify messenger RNA (mRNA) and non-coding RNA in cells or tissues.

Quantitative PCR is carried out in a thermal cycler with the capacity to illuminate each sample with a beam of light of a specified wavelength and detect the fluorescence emitted by the excited fluorochrome. The thermal cycler is also able to rapidly heat and chill samples thereby taking advantage of the physicochemical properties of the nucleic acids and DNA polymerase. The PCR process generally consists of a series of temperature changes that are repeated 25 – 40 times,

these cycles normally consist of three stages: the first, at around 95 °C, allows the separation of the nucleic acid's double chain; the second, at a temperature of around 50-60 °C, allows the alignment of the primers with the DNA template [10]; the third at between 68 - 72 °C, facilitates the polymerization carried out by the DNA polymerase. Due to the small size of the fragments the last step is usually omitted in this type of PCR as the enzyme is able to increase their number during the change between the alignment stage and the denaturing stage. In addition, some thermal cyclers add another short temperature phase lasting only a few seconds to each cycle in order to reduce the noise caused by the presence of primer dimers when a non-specific dye is used. The temperatures and the timings used for each cycle depend on a wide variety of parameters, such as: the enzyme used to synthesize the DNA, the concentration of divalent ions and deoxyribonucleotides (dNTPs) in the reaction and the bonding temperature of the primers [11].

Method

siRNA mediated transfection was studied by quantifying mRNA knock-down of RRM1 gene by the mean of silencing potential of RRM1 siRNA containing formulations (**Table 5.16** and **Table 5.17**). Real time PCR was utilized to quantify the amount of mRNA present in the transfected cells of both cell lines (A549 & H1299).

A day before transfection, A549 and H1299 cells were seeded onto 24 well plates at a density of 5×10^4 cells/well. After approximately 80% confluency, RRM1 siRNA containing formulations were added to each well. Three different concentrations of siRNA were used i.e. 5 nM, 500 pM and 50 pM. Cells were also transfected with commercially available Lipofectamine 2000 as a positive control according to the manufacturer's instruction. After 48 hr, total RNA was isolated using the TRIzol reagent (Invitrogen, USA) and reverse transcribed into cDNA using RNA to cDNA conversion kit (Invitrogen, USA). The mRNA level was quantified using Step One real time PCR (Applied Biosciences, USA). Each reaction contained SYBR Green Master mix (Applied Biosciences, USA), forward and reverse primer, and 2 ng of cDNA in a total volume of 20 μ L. The mRNA expression level of RRM1 was normalized against housekeeping gene glyceraldehyde-3-phosphate dehydrogenase (GAPDH).

i. Selection of Primers

- ❖ Primers were selected from primer design toll; NCBI (National Center for Biotechnology Information). The primers for RRM1 siRNA were 5'-TGAGCAGCGCCTGGACCTAA-3' for forward and 5'-GCATCGCAGCTAGTGGCTGA-3' for reverse (PCR product 116 bp).
- ❖ Primers for housekeeping gene GAPDH (glyceraldehyde-3-phosphate dehydrogenase) were 5'-TCGCTCTCTGCTCCTCCTGTT-3' for forward and 5'-TGACTCCGACCTTCACCTTCC-3' for reverse (PCR product 103 bp).

ii. RNA Isolation

1. Equal amount of triazole reagent (1 mL/10cm²) was added to each well and incubated at room temperature for 5 min.
2. Each incubated sample was transferred to 2 mL centrifuge tube and 0.2 mL of chloroform for every 1mL of TRIzol was used.
3. Samples were shaken vigorously for 15 sec and incubated at room temperature for 2-3 min.
4. Samples were centrifuged for 15 min at 12,000 x g at 4°C.
5. The aqueous phase was transferred to fresh tubes. The aqueous phase was the colorless upper phase that corresponds to ~60% of the volume of TRIzol used. (The interphase was fairly well-defined.)
6. To each sample 0.5 mL of isopropanol, for every 1 mL of TRIzol used initially, was added to precipitate the RNA.
7. Samples were incubated at room temperature for 10 min and centrifuged for 10 min at 12000 x g at 4°C.
8. The RNA was visible on the side of the tubes.
9. Supernatant was removed and pellet was washed with 1 mL 75 % ethanol for every 1 mL of TRIzol used. At this point samples were mixed by flicking and inverting the tube or vortexing and centrifuged at 7500 x g for 5 min at 4°C.
10. RNA was resolubilized in 40 µL DEPC treated RNase-free deionized water.

RNA isolated from A549 and H1299 showed A260/A280 of 1.83±0.1 and 1.89±0.1 respectively.

Table 5.4 Details of Primers

Primer	Sequence (5'→3')	Template strand	Length	Start	Stop	Tm	GC%	Self complement-arity	Self 3' complement-arity
RRM1 primers									
Forward primer	TGAGCAGCGCCTGGAACCTAA	Plus	21	208	228	61.8	57.14	4.00	1.00
Reverse primer	GCATCGCAGCTAGTGGCTGA	Minus	20	323	304	61.8	60.00	7.00	5.00
Product length	116								
GAPDH primers									
Forward primer	TCGCTCTCTGCTCCTCCTGTT	Plus	21	97	117	60.6	57.14	2.00	0.00
Reverse primer	TGACTCCGACCTTCACCTTCC	Minus	21	199	179	60.7	57.14	3.00	0.00
Product length	103								

iii. RNA to cDNA Conversion

- High Capacity RNA-to-cDNA Kit was utilized to convert RNA into cDNA.
- Kit components were allowed to thaw on ice.
- 1.5 microgram of RNA was used per 20 μ L of reaction.
- The Reaction was set up as given below (**Table 5.5**)

Table 5.5 RNA to cDNA Conversion Parameters

Component	Volume/ Reaction (μ L)
2 \times RT Buffer	10
20 \times RT Enzyme Mix	1
Sample	9
Nuclease-free H ₂ O	q.s. to 20
Total	20

- 20 μ L of RT reaction mix was added into each well of 48 well plate for real time PCR reaction.
- Plate was sealed and centrifuged to settle down the contents and to eliminate air bubble. Plate was placed in the sample holder of real time PCR system and ran according to cycle given below (**Table 5.6**).

Table 5.6 PCR Cycle Steps

Parameters	Step 1	Step 2	Step 3
Temperature (C $^{\circ}$)	37	95	4
Time (min)	60	5	Storage

iv. mRNA Quantification

cDNA from each sample was utilized for mRNA quantification and gene knock down was accessed.

Reaction was set according to below (**Table 5.7**):

Table 5.7 mRNA Quantification – Reaction Parameters

Component	Volume/ Reaction (μ L)
Forward primer	0.5
Reverse primer	0.5
cDNA	0.5
Master Mix	10
Nuclease-free H ₂ O	q.s. to 20
Total	20

- 20 μ L of RT reaction mix was added into each well of 48 well plate for real time PCR reaction.
- Plate was sealed and centrifuged to settle down the contents and to eliminate air bubble. Plate was placed in the sample holder of real time PCR system and ran according cycle given below (**Table 5.8**).

Table 5.8 RT-PCR Cycle Steps

Parameters	Step 1	Step 2	No. of cycles
Temperature ($^{\circ}$ C)	95	60	40
Time (seconds)	15	90	

5.1.5. Statistical Analysis

All analyses were performed in triplicate unless otherwise specified. Statistical analysis of data was performed using an ANOVA and Student-t test. GraphPad Prism (version 5, USA) was used for all analyses and P value < 0.05 was considered significant.

5.1.6. Results and Discussion

5.1.6.1. In Vitro Cytotoxicity Assay (MTT Assay)

In vitro cell line studies for the cytotoxicity of prepared nano-constructs were thoroughly carried out. It was seen that at N/P of 2.5 DDHC (composed of DOTAP, DOPE, HSPC and Cholesterol) and RGD grafted DDHC liposomes were significantly less toxic than lipofectamine 2000 in both cell lines i.e. A549 and H1299. Even at higher N/P ratio of 12.5 at 100 nM siRNA concentrations these liposomes were non-significant in toxicity as compared to L2K. Graphical representation of cell viability against increasing ratio of N/P i.e. charge ratio of cationic lipid to siRNA after treatment with developed formulations was obtained by MTT assay as shown in **Figure 5.1** and **Figure 5.2** Cytotoxicity of blank was used as background. Further there was no significant difference in cell viability by 1%, 2% and 3% RGD incorporation in DDHC liposomes. In both cell lines, RGD-DDHC liposomes showed highest cell viability and hence least toxicity up to N/P ratio of 10.0. All results with mean cell viability at different N/P ratio is given in **Table 5.9** and **Table 5.10**. DDHC and RGD grafted siRNA nano-constructs reduced viability to $85.6 \pm 2.1\%$ and $89.4 \pm 2.2\%$ respectively at N/P ratio of 2.5, while L2K reduced viability to $79.4 \pm 1.7\%$ following 48 h of incubation. At 12.5 N/P charge ratio DDHC and RGD grafted siRNA nano-constructs showed $79.8 \pm 1.4\%$ and $77.8 \pm 4.2\%$ cell viability. Amongst the nano-constructs studied,

DDHC and RGD grafted siRNA nano-constructs showed the highest cell viability at all charge ratio.

Table 5.9 Viability of A549 Cells on Exposure to Cationic Liposomes*

Formulation	% Cell Viability					
	N/P					
		2.50	5.00	7.50	10.00	12.50
DD liposomes	Mean	84.51	70.69	71.15	70.74	68.33
	SEM	3.14	3.04	2.28	3.09	1.18
DDC liposomes	Mean	84.74	76.86	77.84	74.80	67.38
	SEM	0.75	2.25	5.20	1.96	1.79
DDHC liposomes	Mean	85.68	80.98	82.27	78.88	75.44
	SEM	1.50	0.10	1.52	1.99	2.56
RGD-DDHC liposomes (1%)	Mean	88.97	82.82	83.77	78.88	76.31
	SEM	2.09	2.07	2.77	1.82	1.44
RGD-DDHC liposomes (2%)	Mean	89.47	83.32	84.27	79.88	76.82
	SEM	1.59	2.57	3.27	0.82	1.93
RGD-DDHC liposomes (3%)	Mean	88.58	83.87	85.27	80.52	76.42
	SEM	2.48	3.12	2.28	1.46	1.43
Lipofectamine	Mean	79.49	79.49	79.49	79.49	79.49
	SEM	1.22	1.22	1.22	1.22	1.22

*Experiments were performed in triplicate.

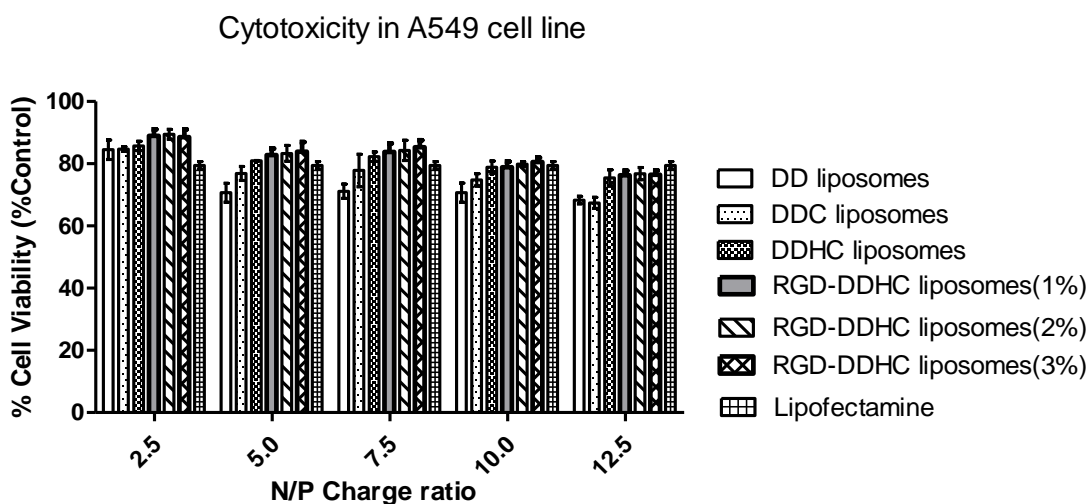


Figure 5.1 Cytotoxicity of Different Cationic Liposomes in A549 Cell-line.

Table 5.10 Viability of H1299 Cells on Exposure to Cationic Liposomes*

Formulations	% Cell Viability					
	N/P					
		2.50	5.00	7.50	10.00	12.50
DD liposomes	Mean	84.51	72.69	72.16	71.82	69.43
	SEM	0.14	1.04	1.27	1.17	1.56
DDC liposomes	Mean	87.24	77.86	80.34	74.83	71.73
	SEM	0.25	1.25	2.70	1.06	1.86
DDHC liposomes	Mean	87.68	82.41	83.93	77.32	76.47
	SEM	3.50	1.33	0.94	1.44	1.40
RGD-DDHC liposomes (1%)	Mean	88.93	85.77	84.77	81.93	77.52
	SEM	1.05	0.87	2.78	0.99	1.53
RGD-DDHC liposomes (2%)	Mean	88.97	86.26	85.31	81.53	78.41
	SEM	1.09	0.38	2.24	0.55	2.53
RGD-DDHC liposomes (3%)	Mean	89.52	86.93	85.98	82.29	78.18
	SEM	0.54	1.05	1.06	1.55	3.76
Lipofectamine 2000	Mean	81.45	81.45	81.45	81.45	81.45
	SEM	2.39	2.39	2.39	2.39	2.39

*Experiments were performed in triplicate.

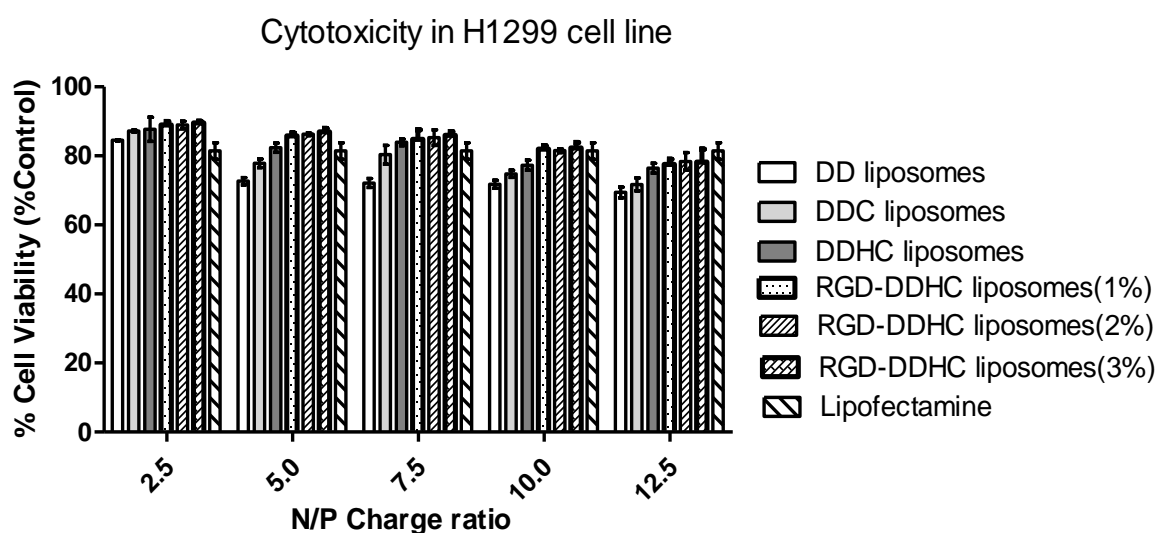


Figure 5.2 Cytotoxicity of Different Cationic Liposomes in H1299 Cell-line.

To access the toxicity of CPE liposomes, increasing ratio of Ca: siRNA i.e. more amount of CPE liposomes containing NC siRNA were exposed to A549 and H1299 cells. Five value for Ca: siRNA i.e. 5.00, 7.50, 10.00, 12.50 and 15.00 were used at 100 nM siRNA concentration. Graphical representation of cell viability against increasing ratio of Ca:siRNA after treatment with developed formulations was obtained by MTT assay as shown in **Figure 5.3** and **Figure 5.4**. Cytotoxicity of blank was used as background. Further there was no significant difference in cell viability by 1%, 2% and 3% RGD incorporation in DDHC liposomes. All results with mean cell viability at different Ca:siRNA ratios is given in **Table 5.11** and Table 5.12. At all ratios, CPE liposomes and RGD-CPE liposomes showed significantly higher cell viability than positive control lipofectamine 2000. Further, there is no significant difference in cell viability by RGD incorporation (1%, 2% and 3%). Taken collectively, CPE liposomes are less toxic as compared to cationic liposomal formulations.

Table 5.11 Viability of H1299 Cells on Exposure to CPE Liposomes*

Formulations	Ca:siRNA					
		5.00	7.50	10.00	12.50	15.00
CPE liposomes	Mean	93.67	90.75	86.24	84.96	83.13
	SEM	1.28	0.75	1.24	2.96	2.18
RGD-CPE Liposomes (1%)	Mean	92.94	91.86	89.35	87.23	84.43
	SEM	2.55	1.25	1.04	2.19	3.81
RGD-CPE liposomes (2%)	Mean	92.84	89.49	88.66	87.99	83.06
	SEM	1.41	1.24	2.12	0.56	2.18
RGD-CPE liposomes (3%)	Mean	90.79	88.21	87.79	82.90	83.39
	SEM	4.46	2.33	0.24	1.43	2.45
Lipofectamine 2000	Mean	79.49	79.49	79.49	79.49	79.49
	SEM	1.22	1.22	1.22	1.22	1.22

*Experiments were performed in triplicate.

Cell cytotoxicity in A549 cell line

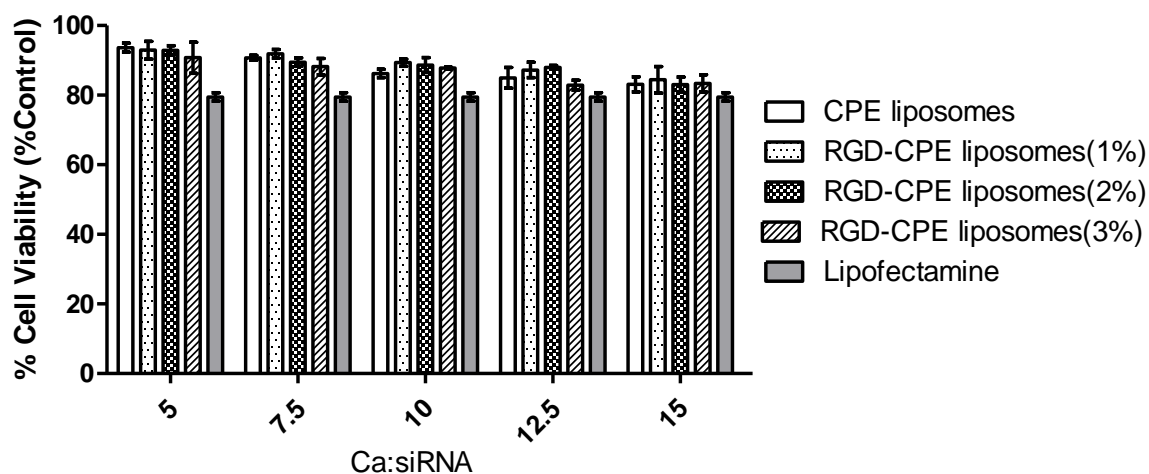


Figure 5.3 Cytotoxicity of Different CPE Liposomes in A549 Cell-line

Table 5.12 Viability of H1299 Cells on Exposure to Various CPE Liposomes*

Formulations	Ca:siRNA					
		5.00	7.50	10.00	12.50	15.00
CPE liposomes	Mean	94.67	92.24	87.24	86.46	84.63
	SEM	2.28	0.75	2.24	1.46	0.68
RGD-CPE liposomes (1%)	Mean	93.94	92.86	90.85	88.23	85.43
	SEM	1.55	2.25	0.46	3.19	4.81
RGD-CPE liposomes (2%)	Mean	93.84	90.99	89.66	89.19	84.56
	SEM	0.41	2.74	1.12	0.65	0.68
RGD-CPE liposomes (3%)	Mean	91.79	89.21	88.79	83.77	83.39
	SEM	3.46	1.33	0.76	2.29	2.45
Lipofectamine 2000	Mean	81.45	81.45	81.45	81.45	81.45
	SEM	2.39	2.39	2.39	2.39	2.39

*Experiments were performed in triplicate.

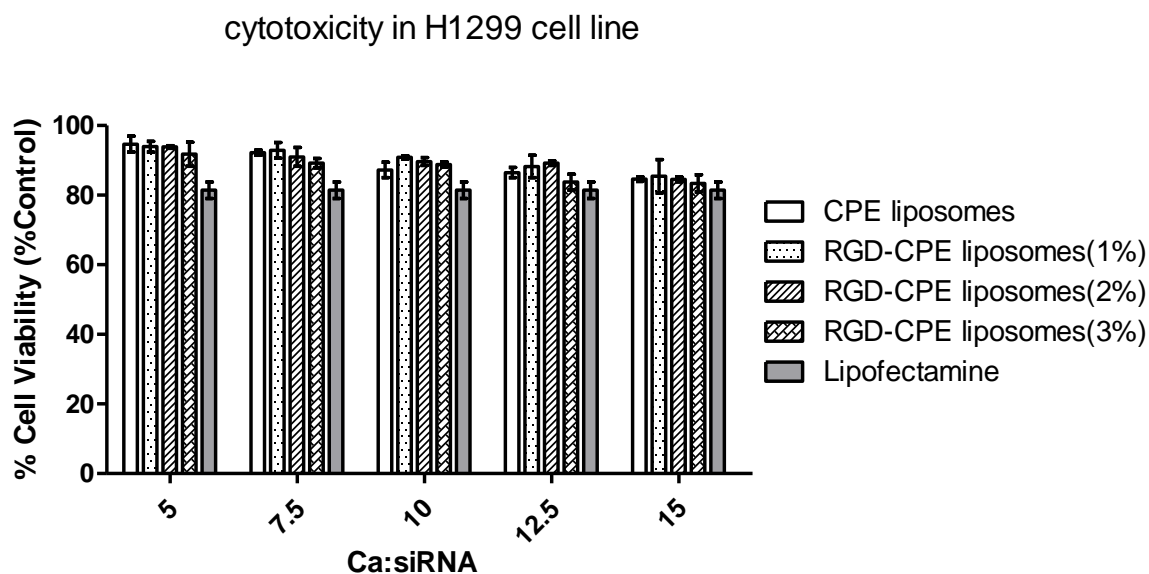


Figure 5.4 Cytotoxicity of Different CPE Liposomes in H1299 Cell-line

In vitro cell line studies for the cytotoxicity of prepared nano-constructs were thoroughly carried out. From the results of MTT assay, it was seen that at N/P of 2.5 DDHC and RGD-DDHC liposomes were significantly ($p < 0.05$) less toxic than lipofectamine. DD liposomes and DDC liposomes showed more toxicity as compared to DDHC liposomes and hence, were not further considered as optimal formulations. CPE liposomes at all concentration showed its potential as a novel siRNA carrier with enhanced margin of safety.

5.1.6.2. *In vitro* cell uptake

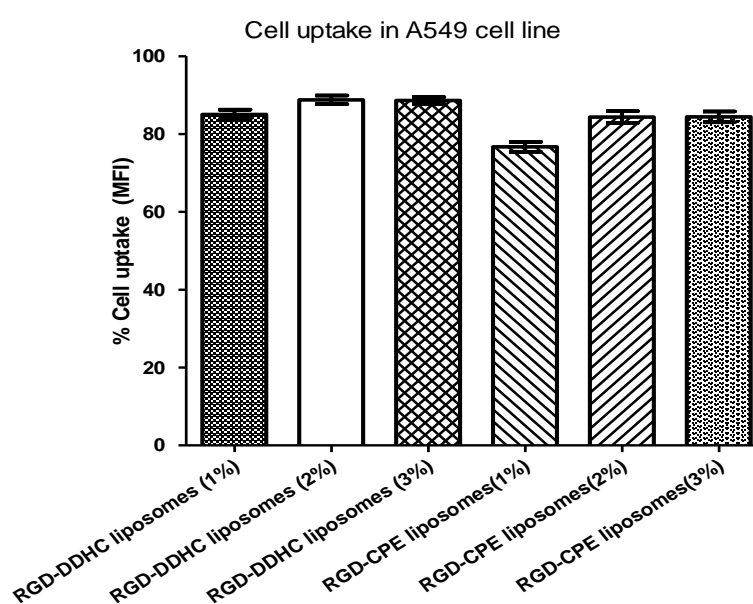
i. Flow Cytometry

RGD was attached on the cell surface to enhance the siRNA uptake inside the cells. Initially, both types of the liposomal formulations, DDHC liposomes and CPE liposomes were studied by grafting 1%, 2% and 3 mole% RGD on the liposomal surface. 2 mole % of RGD was found to be optimal. 2 mole% RGD incorporation showed significantly higher amount of cell uptake as compared to 1 mole% of RGD, while 3 mole% did not show further enhancement in cell uptake (**Figure 5.5** and **Figure 5.6**) and hence, RGD-DDHC liposomes (2%) and RGD-CPE liposomes (2%) were selected for further studies.

Table 5.13 Uptake of Liposomes in A549 Cells

Formulations	MFI	
	Mean	SEM
RGD-DDHC liposomes (1%)	85.03	1.24
RGD-DDHC liposomes (2%)	88.80	1.12
RGD-DDHC liposomes (3%)	88.63	0.87
RGD-CPE liposomes (1%)	76.70	1.27
RGD-CPE liposomes (2%)	84.37	1.51
RGD-CPE liposomes (3%)	84.43	1.38

*Experiments were performed in triplicate.

**Figure 5.5 Uptake of Liposomes in A549 Cells**

As shown in **Figure 5.7** and **Figure 5.9**, the order of fluorescence intensity in cells (**Figure 5.6** and **Figure 5.8**) after treatment with various siRNA formulations was as follows:

in A549 cell line:

Naked siRNA < DDC liposomes < CPE liposomes < Lipofectamine 2000 < RGD-CPE liposomes < DDHC liposomes < RGD-DDHC liposomes

in H1299 cells:

Naked siRNA < DDC liposomes < CPE liposomes < Lipofectamine 2000 < DDHC liposomes < RGD-CPE liposomes < RGD-DDHC liposomes.

It was suggested from these results that nano-constructs could significantly enhance siRNA translocation into cells when compared to that of negatively charged free siRNA. Both types

of the formulations DDHC liposomes and CPE liposomes showed enhanced mean fluorescent intensity by grafting 2mol% of RGD peptide on the liposomal surface. Furthermore, RGD-DDHC liposomes and RGD-CPE liposomes showed significantly more MFI inside the cells (A549 and H1299).

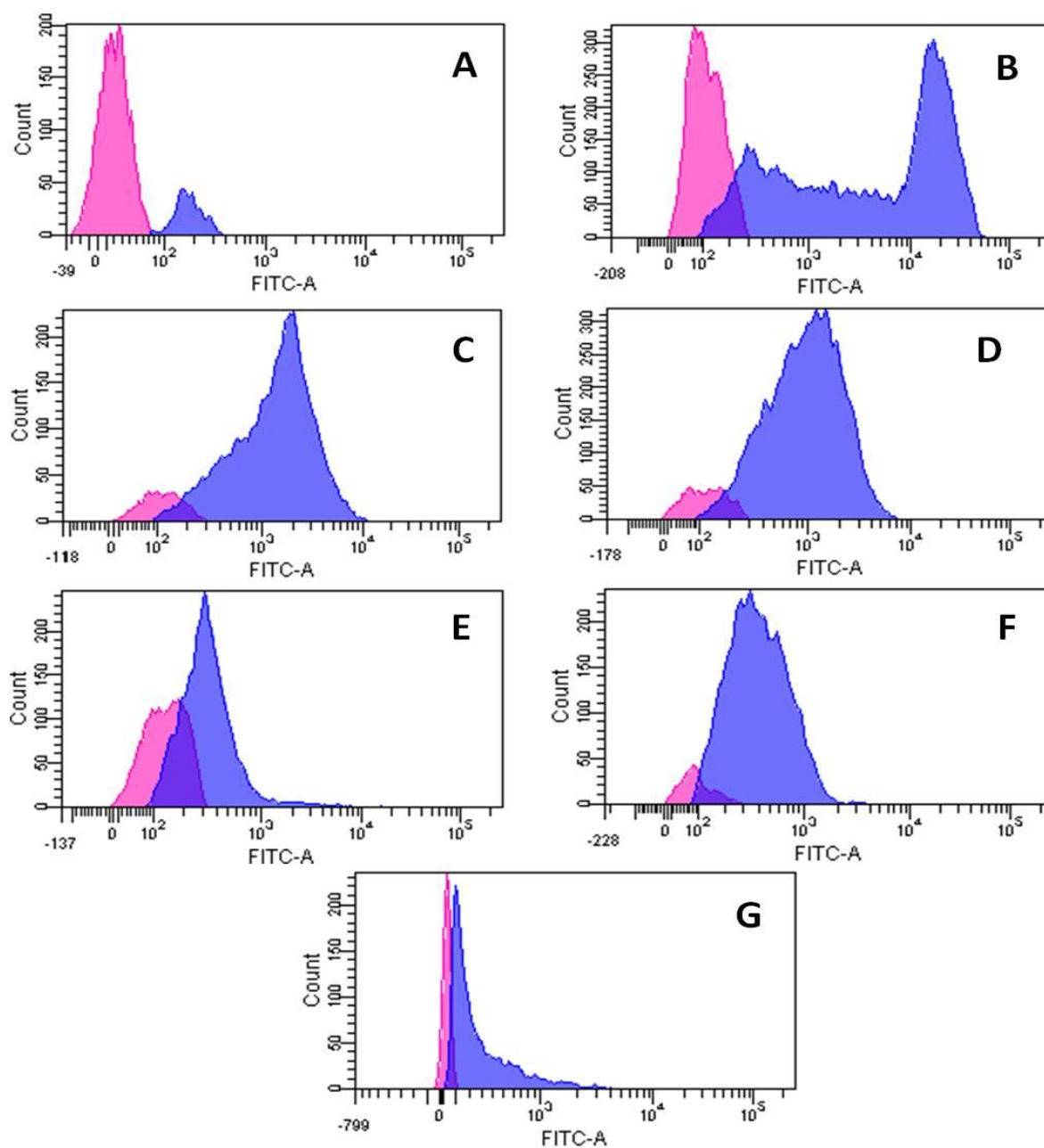


Figure 5.6 Quantification of Mean Fluorescence Intensity in A549 Cells

A=Naked siRNA, B=DDC liposomes, C=DDHC liposomes, D=RGD-DDHC liposomes, E=CPE-liposomes, F=RGD-CPE liposomes, G=Lipofectamine 2000

Table 5.14 Uptake of Cationic Liposomes in A549 Cells

Formulations	MFI	
	Mean	SEM
Placebo-1 (RGD-DDHC liposomes(2%))	1.70	0.15
Placebo-2 (RGD-CPE liposomes(2%))	1.73	0.12
Naked siRNA	13.03	0.35
DDC liposomes	67.97	1.02
DDHC liposomes	83.83	1.01
RGD-DDHC liposomes (2%)	88.67	1.02
CPE liposomes	70.53	1.89
RGD-CPE liposomes(2%)	82.40	1.47
Lipofectamine 2000	74.63	1.39

*Experiments were performed in triplicate.

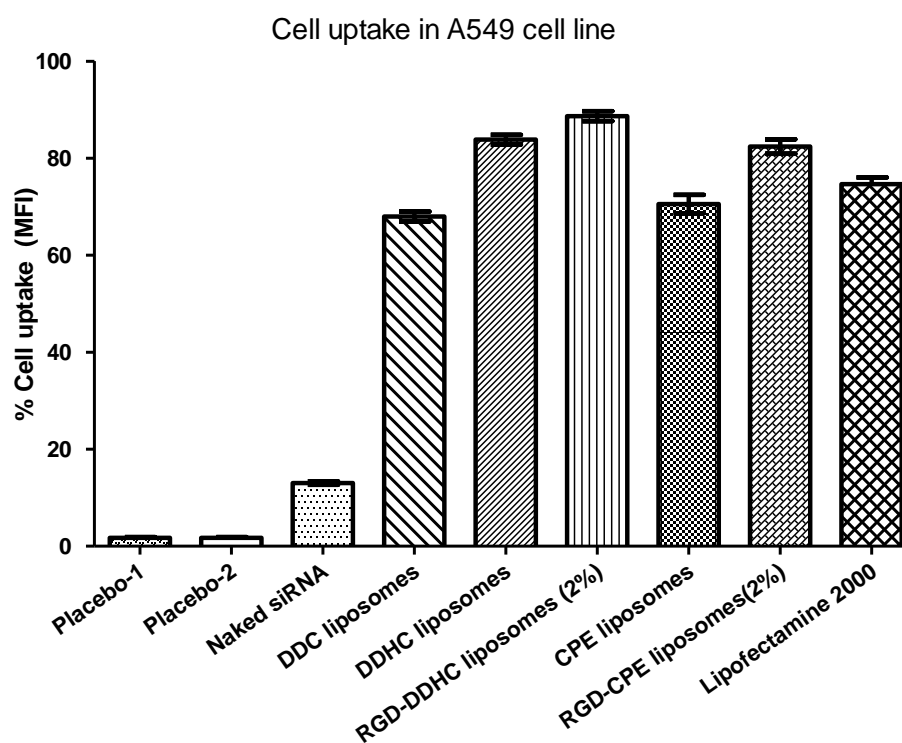


Figure 5.7 Uptake of Liposomes in A549 Cells

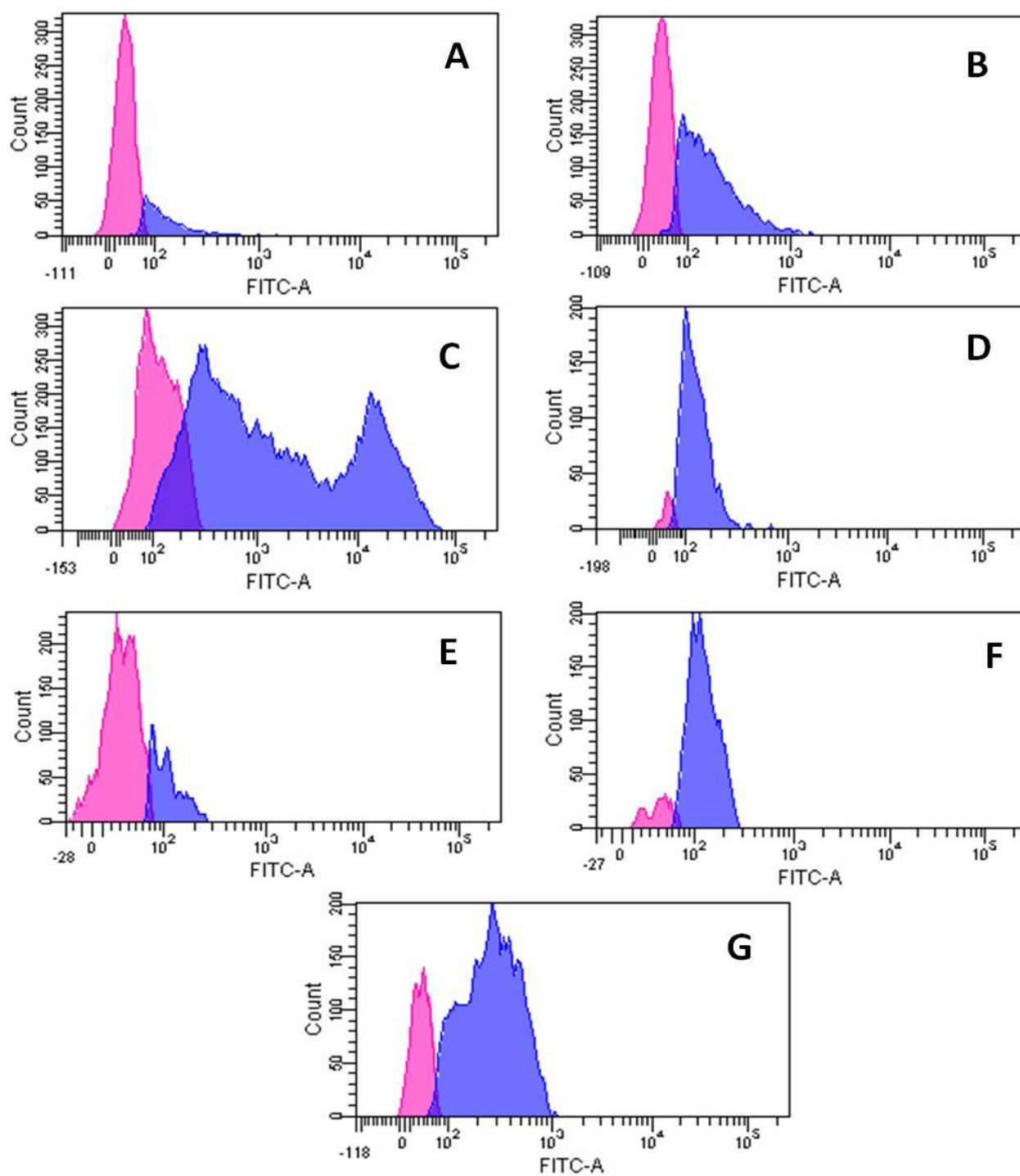


Figure 5.8 Quantification of Mean Fluorescence Intensity in H1299 Cells

A=Naked siRNA, B=DDC liposomes, C=DDHC liposomes, D=RGD-DDHC liposomes, E=CPE-liposomes, F=RGD-CPE liposomes, G=Lipofectamine 2000

Table 5.15 Uptake of Liposomes in H1299 Cells*

Formulations	MFI	
	Mean	SEM
Placebo-1 (RGD-DDHC liposomes (2%))	1.20	0.17
Placebo-2 (RGD-CPE liposomes (2%))	1.57	0.12
Naked siRNA	12.07	0.96
DDC liposomes	53.63	1.03
DDHC liposomes	67.07	0.86
RGD-DDHC liposomes (2%)	80.30	0.70
CPE liposomes	61.37	1.16
RGD-CPE liposomes (2%)	75.83	1.05
Lipofectamine 2000	71.83	1.19

*Experiments were performed in triplicate.

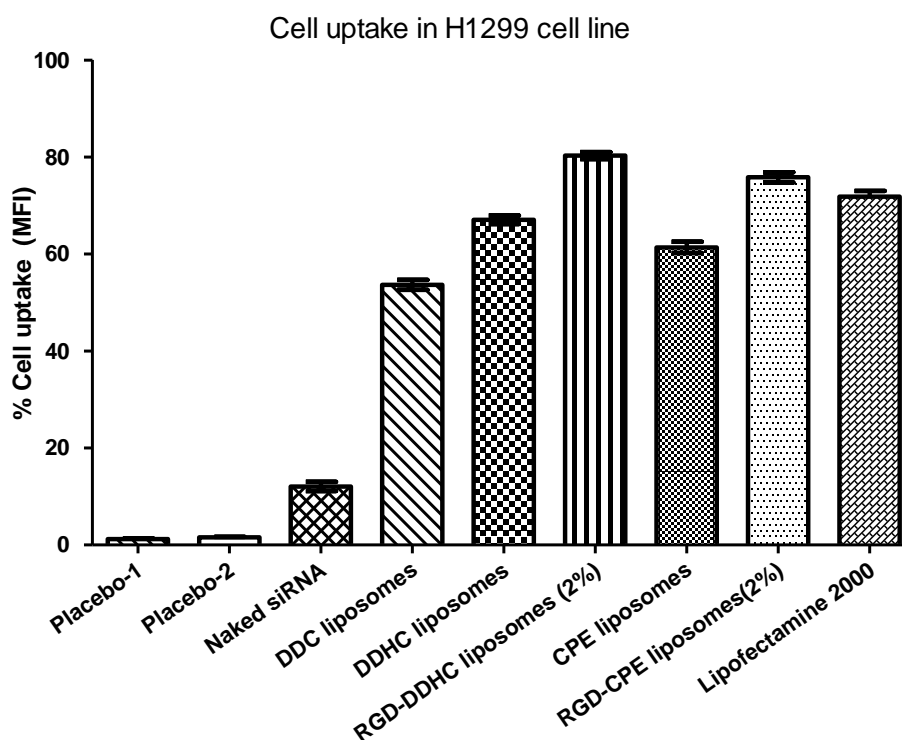


Figure 5.9 Uptake of Liposomes in H1299 Cells

Various reports are available suggesting efficient delivery of siRNA using DOTAP and DOPE but this combination alone is not rigid enough to form physically stable liposomes and that may be one of the reasons for low intracellular accumulation of FAM-NC-siRNA as compared to lipofectamine. However, incorporation of cholesterol and HSPC provided sufficient strength to retain siRNA with positively charged liposomal environment. Significant improvement was achieved in MFI values after incorporation of cholesterol and HSPC as compared to cholesterol alone. RGD grafting shows significant enhancement in cell uptake in both cell lines. Both, quantitative and qualitative, techniques support this hypothesis.

ii. Confocal studies

Results from flow cytometry were well supported by qualitative analysis where intracellular localization of FAM-NC-siRNA (green) was investigated using laser confocal microscope as shown in **Figure 5.10** and **Figure 5.11**. After 6 hr incubation, FAM-NC-siRNA was mainly observed in cytoplasm with a relative uniform distribution. Confocal microscopy also showed that RGD grafting helps to enhance the cellular localization in both cell lines.

To investigate the mechanism or pattern of uptake by the mean of RGD grafting, live uptake was monitored for DDHC liposomes, RGD-DDHC liposomes, CPE liposomes and RGD-CPE liposomes. Naked siRNA uptake was also monitored in live mode. Live images (**Figure 5.12**, **Figure 5.13**, **Figure 5.14**, **Figure 5.15** and **Figure 5.16**) revealed that naked siRNA only bound to the surface or lie outside of the cells. DDHC liposomes and CPE liposomes get accumulated inside the liposomes soon after transfection but RGD-DDHC and RGD-CPE liposomes showed different pattern for uptake. They initially bound to the cell surface and surface bound liposomes further taken up inside by the mean of phagocytosis. Live images with Z-stacking (**Figure 5.17**, **Figure 5.18**, **Figure 5.19** and **Figure 5.20**) showed marginal different pattern of intracellular localization with RGD grafted liposomes as compared to non-grafted formulations and naked siRNA.

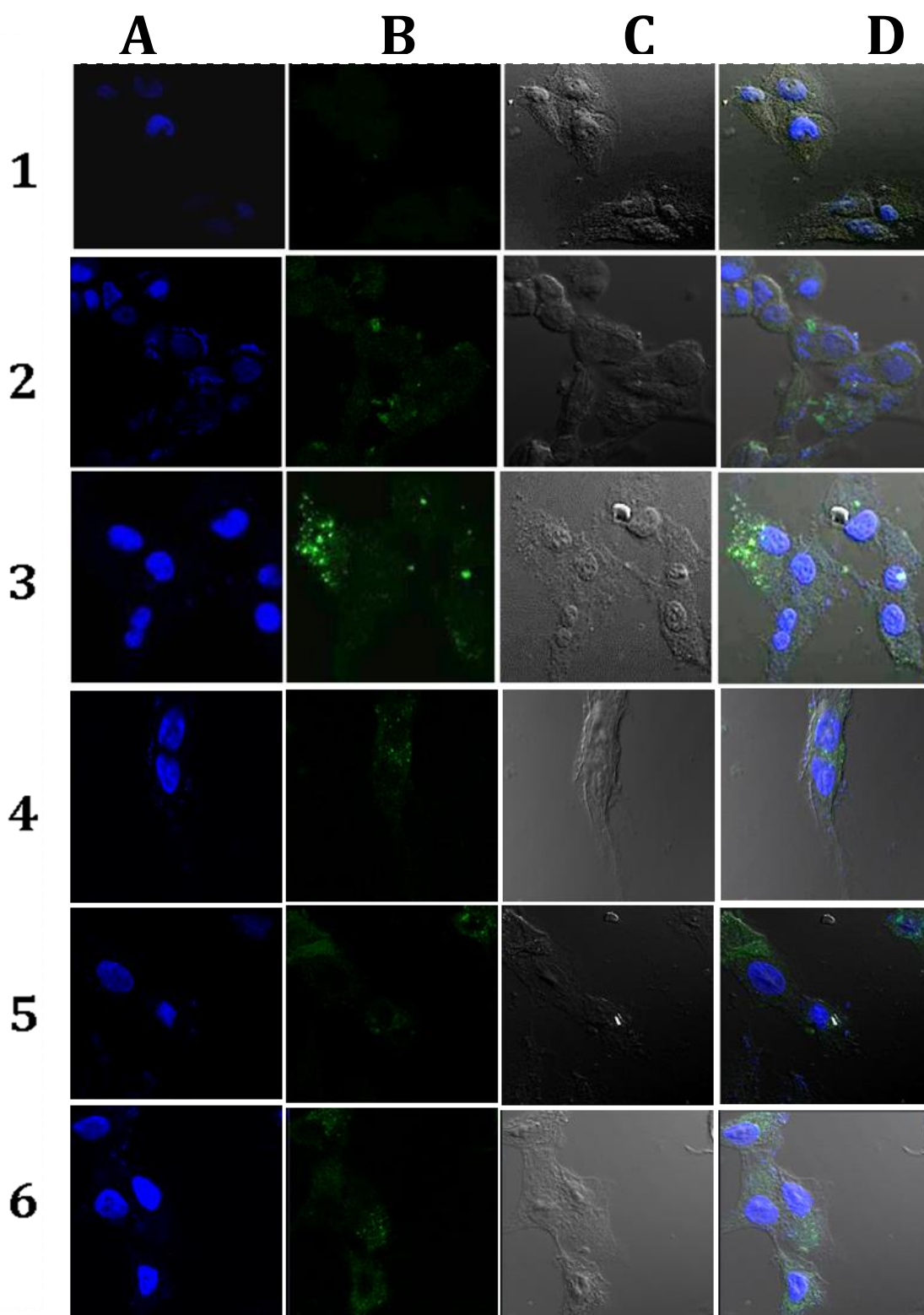


Figure 5.10 Cell Uptake in A549 Cell Line
1=Naked siRNA, 2=DDHC liposomes, 3=RGD-DDHC liposomes, 4=CPE liposomes, 5=RGD-CPE liposomes, 6=Lipofectamine 2000

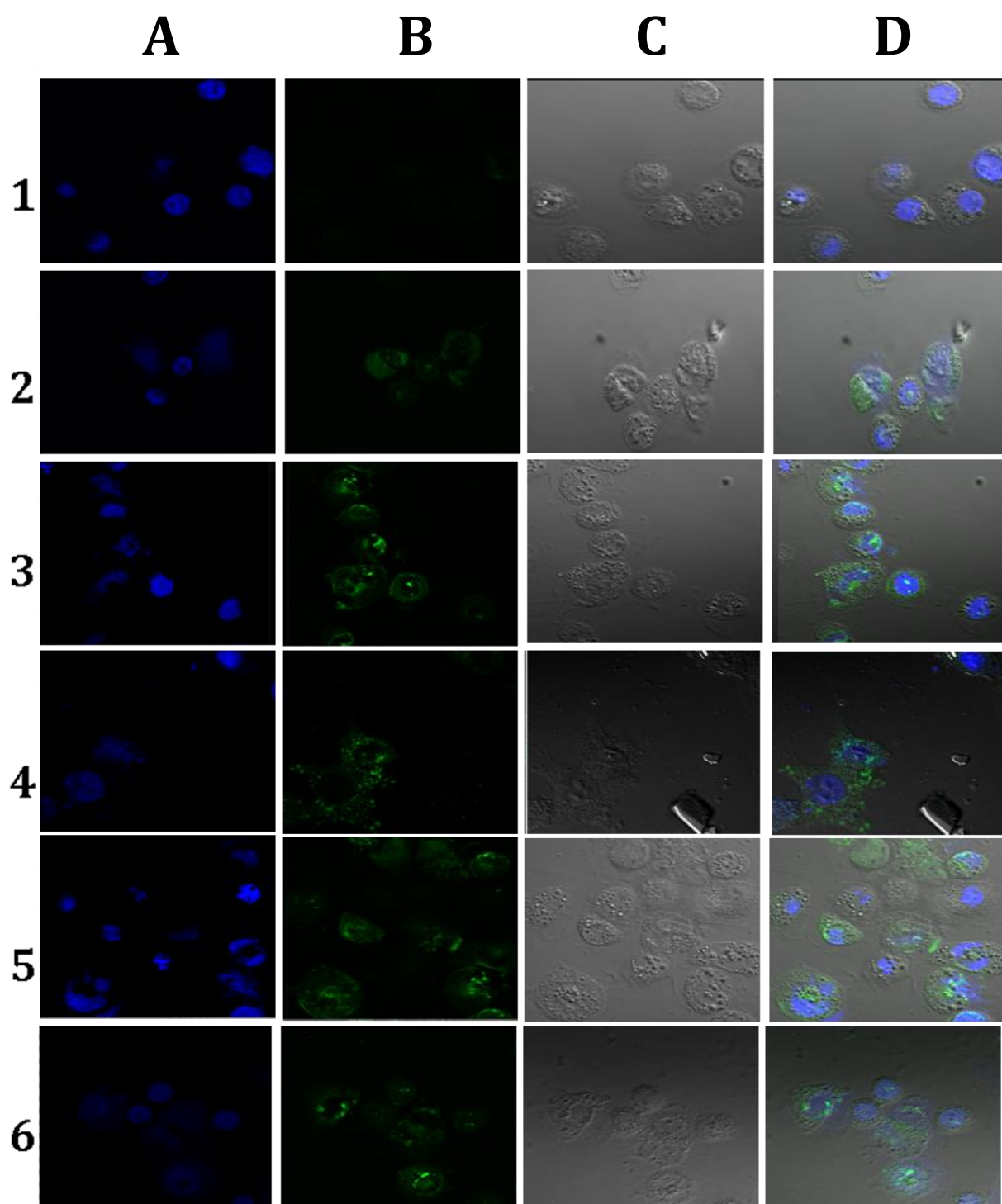


Figure 5.11 Cell Uptake in H1299 Cell Line

1=Naked siRNA, 2=DDHC liposomes, 3=RGD-DDHC liposomes, 4=CPE liposomes,

5=RGD-CPE liposomes, 6=Lipofectamine 2000

A=DAPI, 2=FAM-NC-siRNA, 3=Bright field, 4=Merged

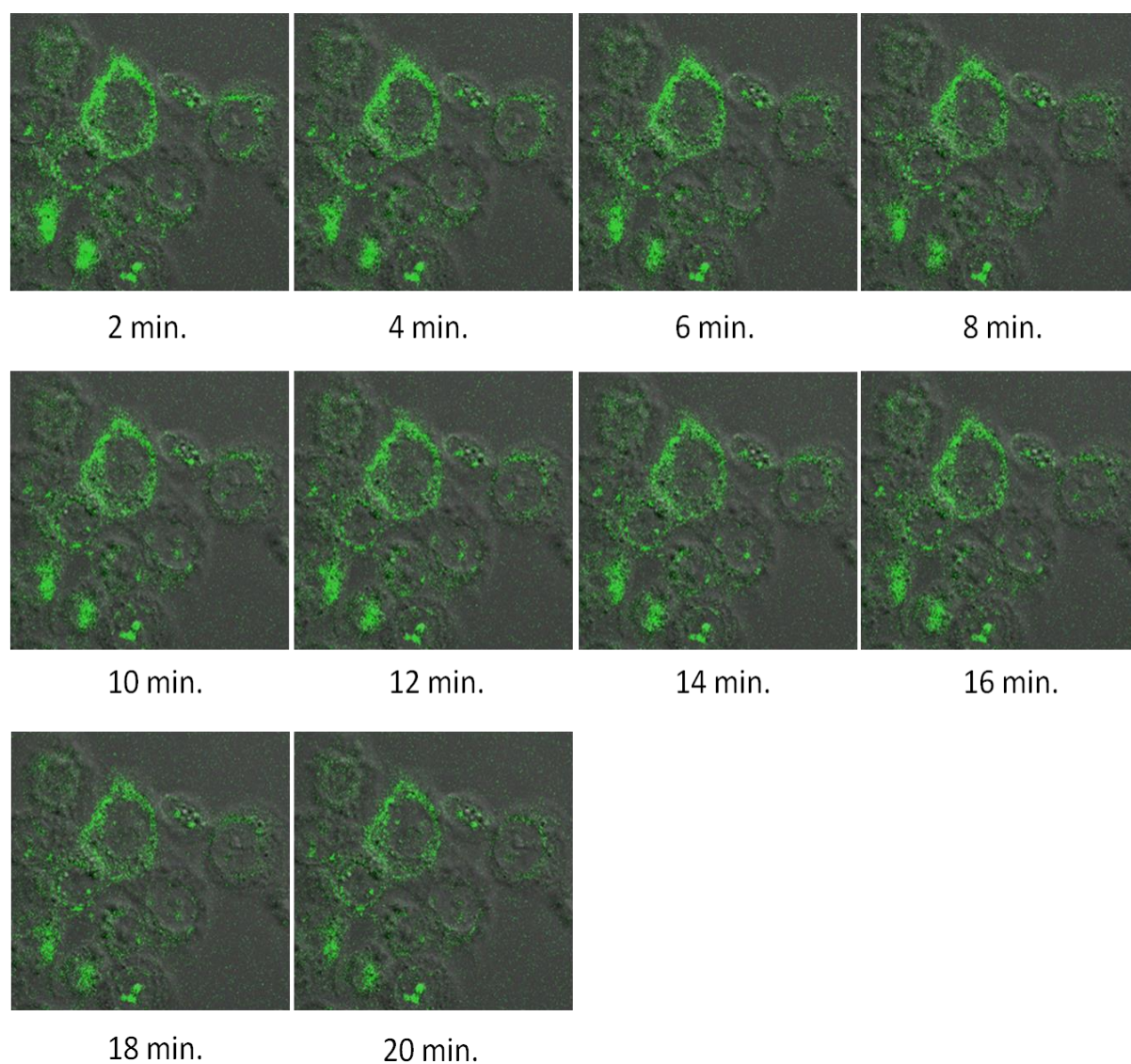


Figure 5.12 Live Uptake of Naked siRNA in A549 Cells

Above figure shows that naked siRNA resides on the surface only and does not give effective intracellular fluorescence.

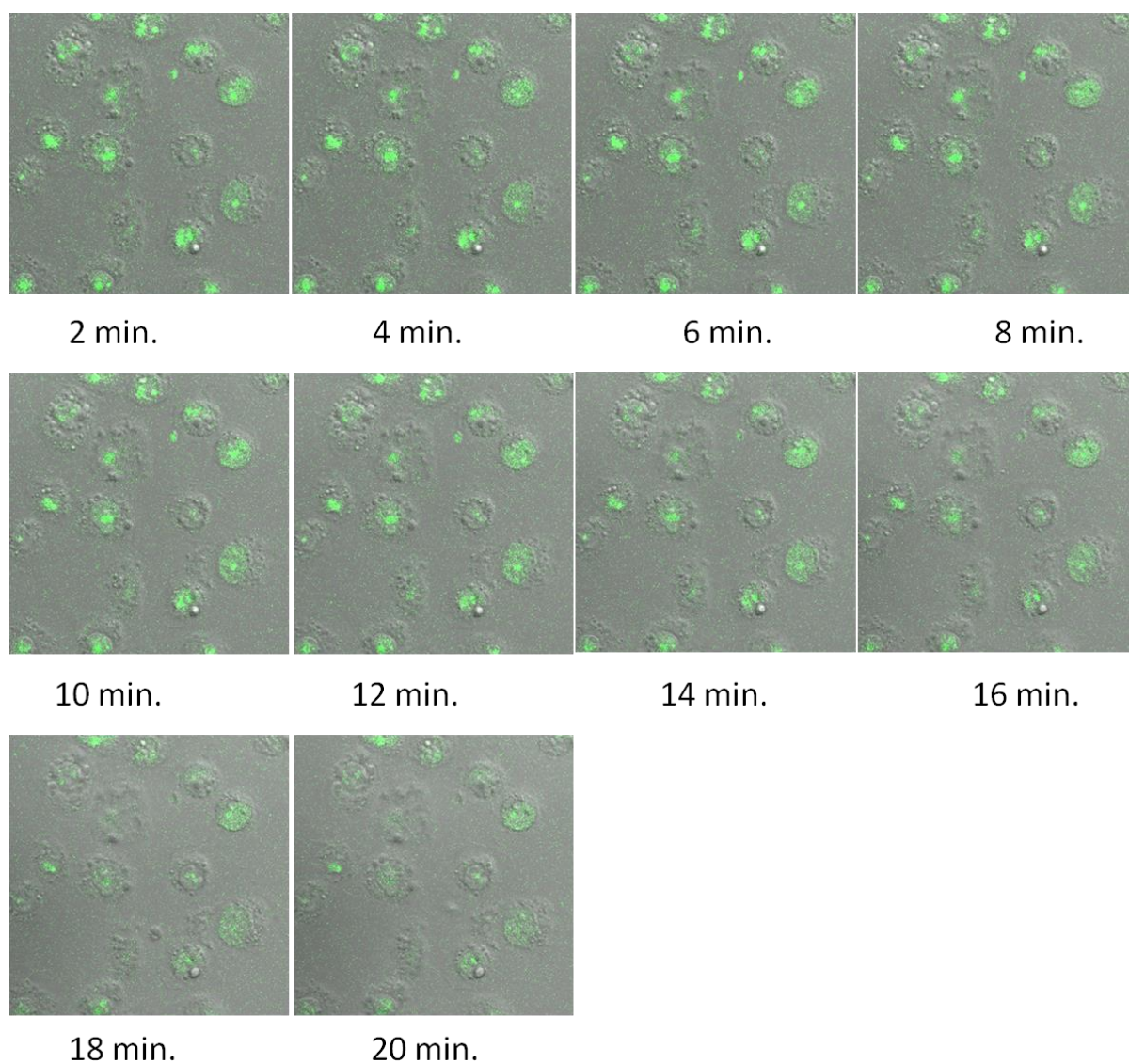


Figure 5.13 Live uptake of DDHC liposomes in A549 cells

Fluorescence was found inside the cells soon after transfection with DDHC liposomes.

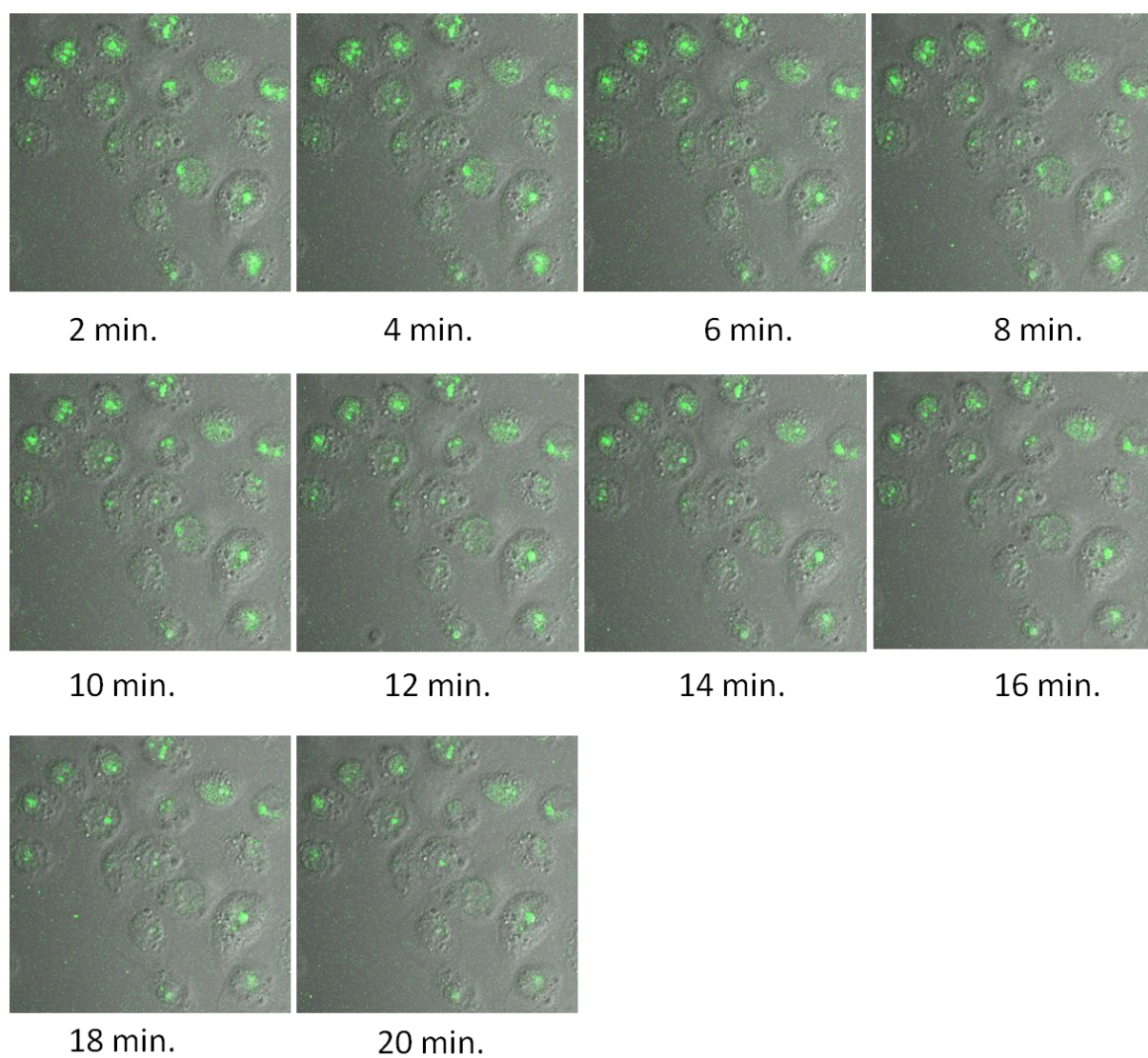


Figure 5.14 Live uptake of CPE liposomes in A549 cells

Fluorescence was found inside the cells soon after transfection with CPE liposomes.

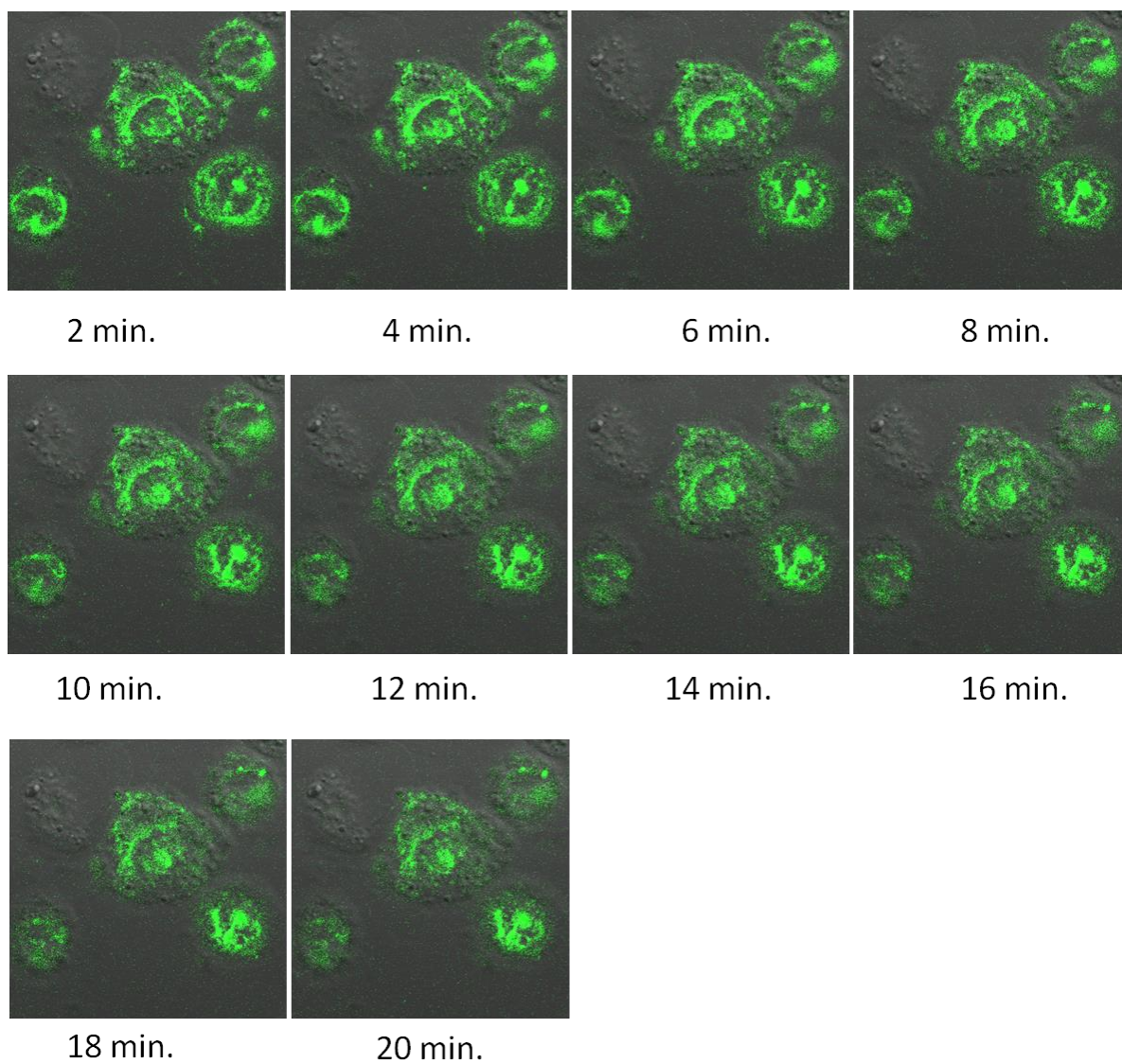


Figure 5.15 Live uptake of RGD-DDHC liposomes in A549 cells

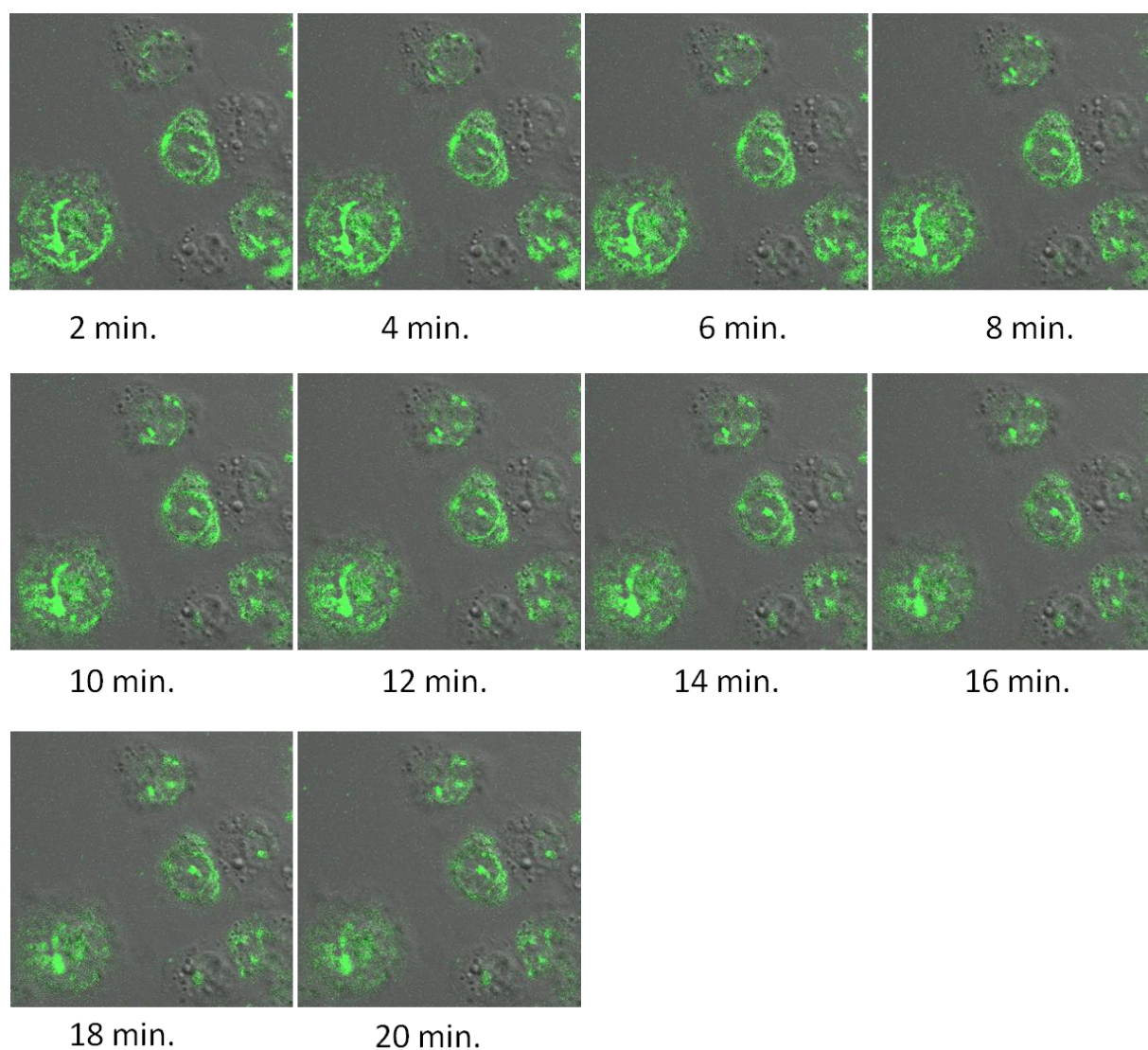


Figure 5.16 Live Uptake of RGD-CPE Liposomes in A549 cells

Figure 5.12, Figure 5.13, Figure 5.14, Figure 5.15 and **Figure 5.16** describe the efficacy of liposomal carrier for intracellular localization. Naked siRNA was found onto the cell surface throughout the uptake duration, starting from initial to 20 min. DDHC liposomes and CPE liposomes helped siRNA to get internalized into the cells immediately soon after transfection. siRNA was found to localize inside the cell from very beginning and this siRNA stayed as such till end. However, at the end after 16 min, fluorescence was found to decrease due to constant exposure of laser. RGD grafted liposomal formulations, RGD-DDHC liposomes and RGD-CPE liposomes initially helped siRNA to locate onto the cell surface. However, part of siRNA was also internalized as seen with DDHC and CPE liposomes. After some time siRNA translocated from surface to the intracellular region of the cells. These results suggest the receptor based translocation of liposomal siRNA inside the cell. This is

due to grafting of RGD on the liposomal surface which is detected by the cell surface. RGD have shown to have selective binding affinity against integrin for treatments of human tumor metastasis and tumor-induced angiogenesis. Due to cytoadhesion, cytoinvasion and partial lysosomal accumulation, RGD-mediated drug delivery may provide improved intracellular availability of conjugated liposomal systems [12]. Taken collectively, live imaging with Z-stack at different time points confirmed that siRNA is not localized to the apical surface of the cells; rather it travelled through the cell membrane inside the cell and thus reveals the targeting potency of RGD towards cancer cells.

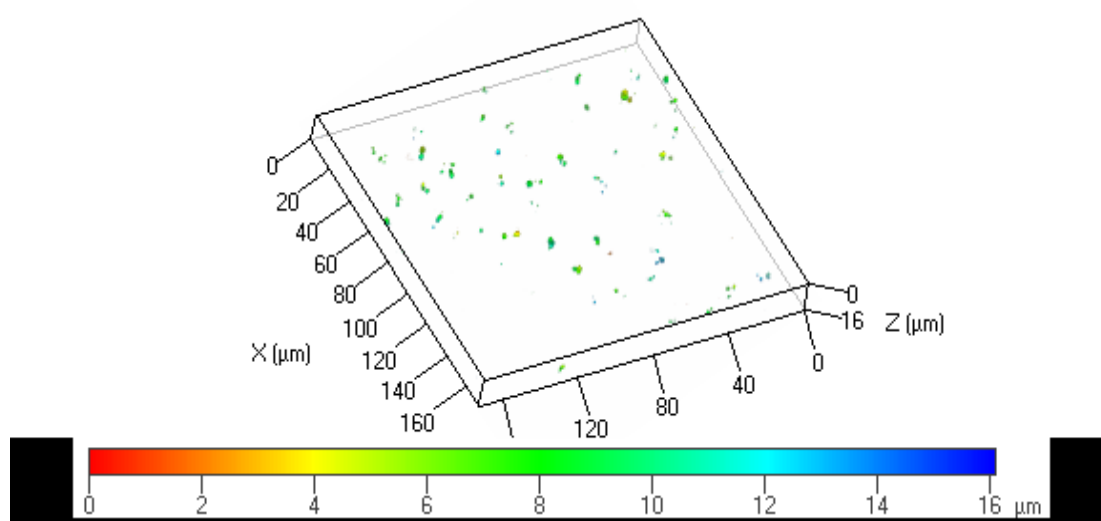


Figure 5.17 3D Z-stack image for DDHC liposomes uptake

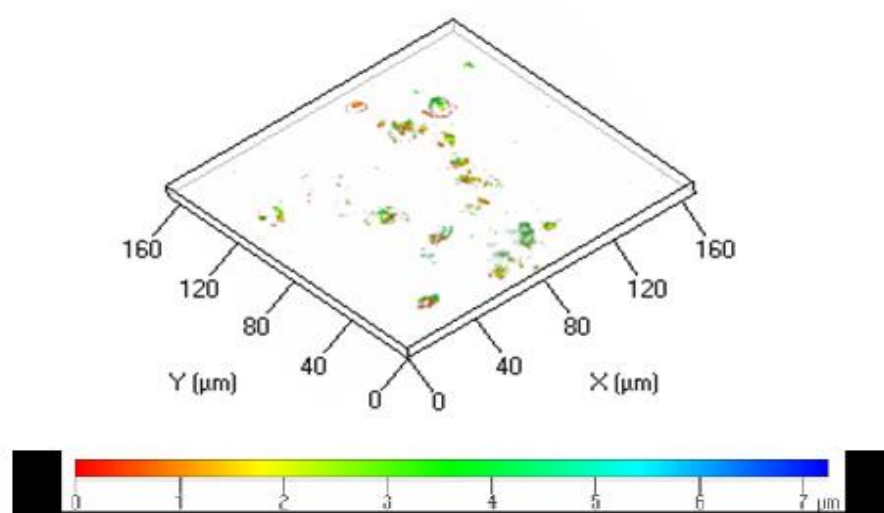


Figure 5.18 3D Z-stack image for CPE liposomes uptake

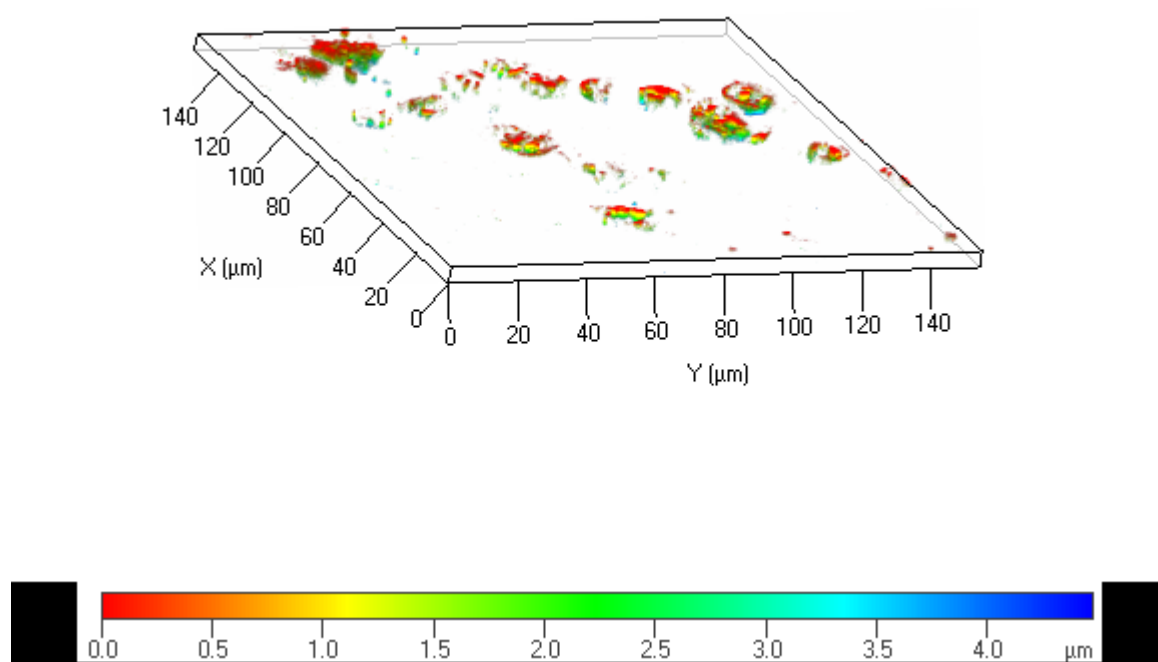


Figure 5.19 3D Z-stack Image for RGD-DDHC Liposomes Uptake

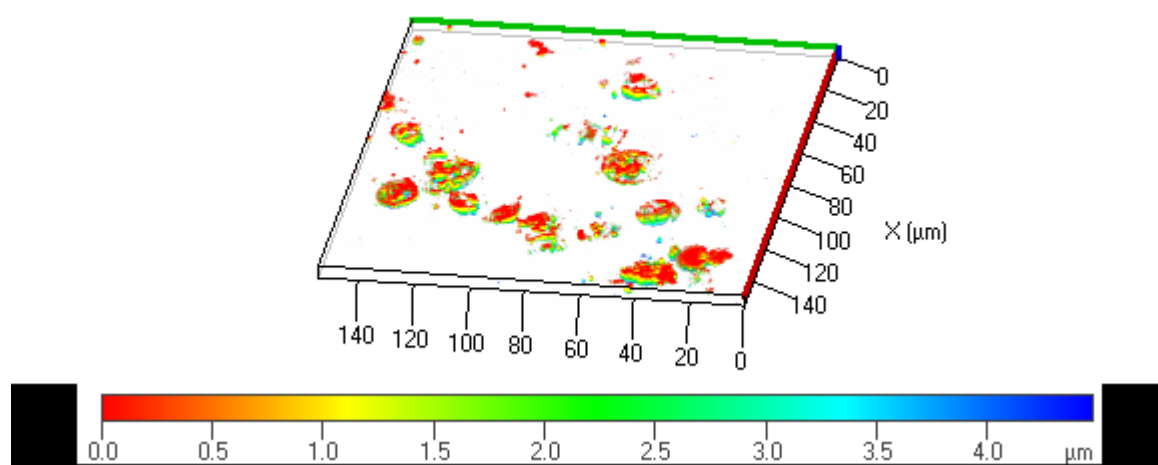


Figure 5.20 3D Z-stack Image for RGD-CPE Liposomes Uptake

Figure 5.19 and **Figure 5.20** show receptor based localization in case of RGD-DDHC liposomes and RGD-CPE liposomes. Red color indicates the surface intensity of FAM labelled siRNA. In case of DDHC liposomes and CPE liposomes, very less surface fluorescence was seen (**Figure 5.17** and **Figure 5.18**) while in case of RGD grafted

liposomal carriers surface as well as intracellular both kind of fluorescence were seen. This shows the ability of RGD for invading the siRNA by surface receptor binding mechanism.

5.1.6.3. Sub-inhibitory concentration (Cell Cycle Analysis)

Cell cycle analysis revealed that cell growth inhibition occurs at higher concentration i.e. 500 pM and 2.5 nM only (Figure 5.21 and Figure 5.22). However, lower concentrations, 50 pM and 100 pM, did not show any marked inhibition. Both types of cells (A549 and H1299) showed similar pattern of inhibition. Control siRNA showed no inhibition at 2.5nM concentration.

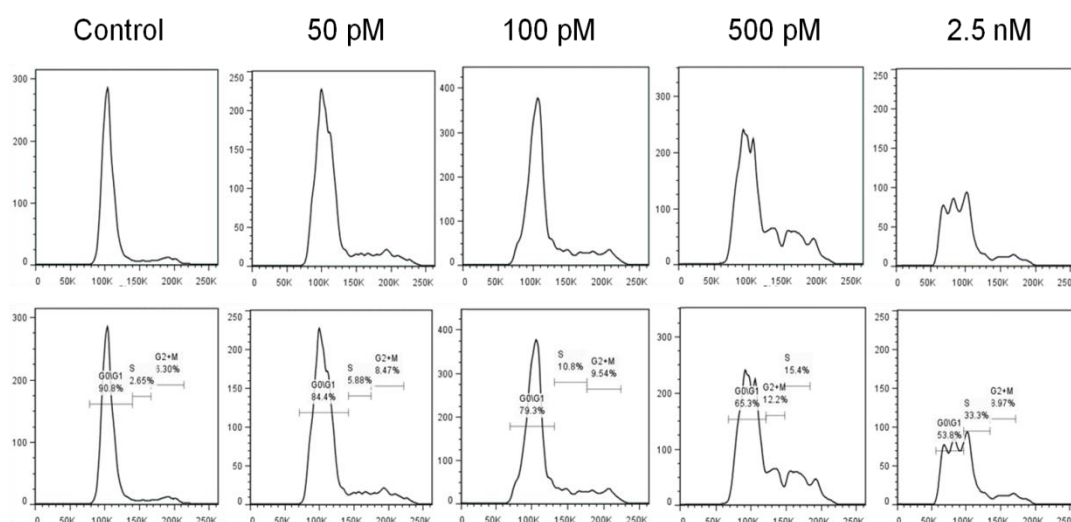


Figure 5.21 Cell Growth Inhibition in A549 Cells

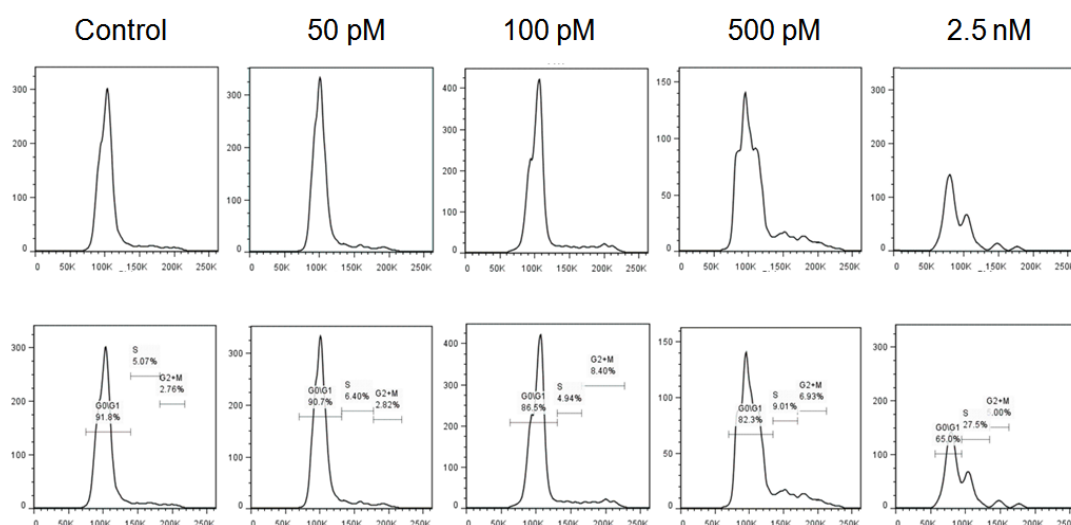


Figure 5.22 Cell Growth Inhibition in H1299 Cells

These results suggested that 50 pM of RRM1 siRNA concentration can be taken for chemosensitization. These results can be utilized for further studies to evaluate chemosensitization of a chemotherapeutic drug Gemcitabine HCl because; earlier reports have described the utility of sub inhibitory growth concentration of RRM1 for chemosensitization [13]. Further, this fact was reassessed using transfection study by the mean of gene knock down effect and that study also supported the results obtained from cell cycle analysis. Hence, 50 pM was used for chemosensitization of cancer cells for further studies.

5.1.6.4. Transfection Studies

Gene knock down was studied using Real time PCR system. **Figure 5.24, Figure 5.25** and **Figure 5.26** show the amplification plot for RRM1 and housekeeping gene GAPDH. Threshold value for amplification was 0.81 and 0.31 for GPDH and RRM1, respectively. After completion of amplification, high resolution melt curve was also studied. This HRM curve signifies the quality of generated mRNA and justifies the mRNA quantification. Both mRNAs, RRM1 and GAPDH showed sharp peak in HRM curve. RRM1 showed melt temperature of 82.89°C while GAPDH showed 83.34°C.

Using optimized transfection conditions, cells were transfected at final siRNA concentration of 5 nM, 500 pM and 50 pM. RRM1 gene knock down was certainly dependent on the siRNA concentration used and at 5nM concentration maximum silencing was achieved. Results for gene silencing by both types of liposomal formulations, with and without RGD, along with positive and negative control are shown in **Table 5.16/Figure 5.27** and **Table 5.17/Figure 5.28** for A549 cells and H1299 cells respectively.

RGD grafted formulations showed significantly higher mRNA knock down ($p < 0.05$) than ungrafted liposomes in both cell lines and also more transfection was achieved as compared to lipofectamine 2000 at 5 nM concentrations. At 5 nM concentration RGD-DDHC liposomes and RGD-CPE liposomes showed 23.2 ± 2.6 and 24.2 ± 3.4 % while naked siRNA exhibited 83.50 ± 2.5 % gene expression in A549 cells while 23.05 ± 2.85 for RGD-DDHC liposomes, , 23.95 ± 3.55 for RGD-CPE liposomes and 85.9 ± 2.5 for naked siRNA in H1299 cells. There was no significant difference ($p > 0.05$) between nano-construct and L2K at 5 nM concentration. At lower concentrations, 500 pM and 50 pM, inhibition was markedly decreased with both nano-constructs and L2K. Naked form demonstrated very poor gene

silencing at lower concentrations i.e. 96.45 ± 3.35 , 97.6 ± 5.60 respectively for 500 pM and 50 pM in A549 cells while 96.55 ± 2.65 and 101.15 ± 2.05 for 500 pM and 50 pM in H11299 cells. Results suggest that 50 pM is the sub-growth inhibitory concentration which was utilized for further Chemosensitization studies.

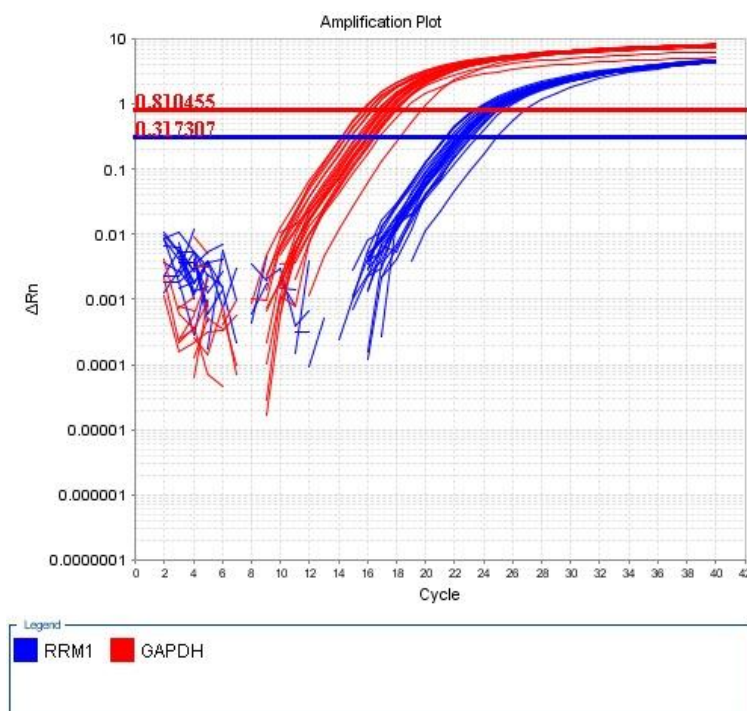


Figure 5.23 Amplification Plot for RRM1 and GAPDH mRNA

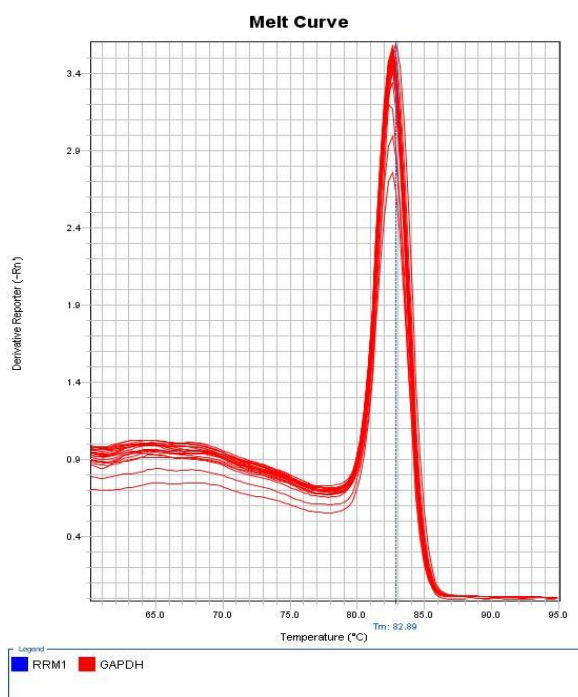


Figure 5.24 High Resolution Melt Curve for RRM1

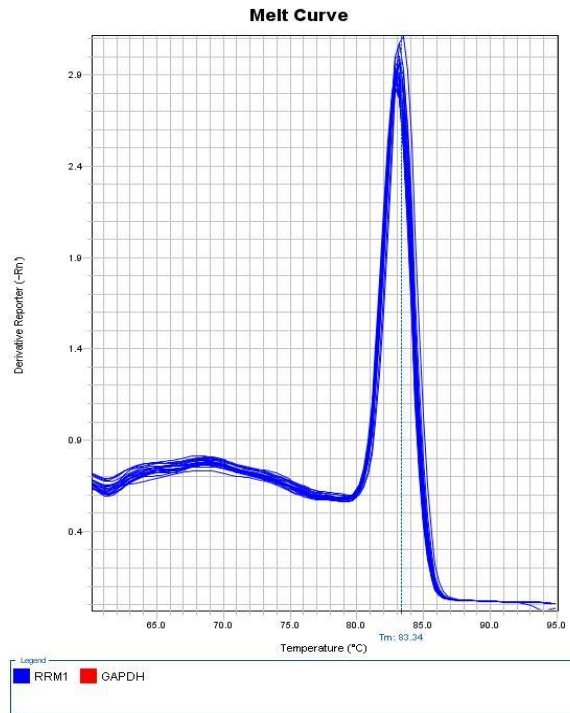


Figure 5.25 High Resolution Melt Curve for GAPDH

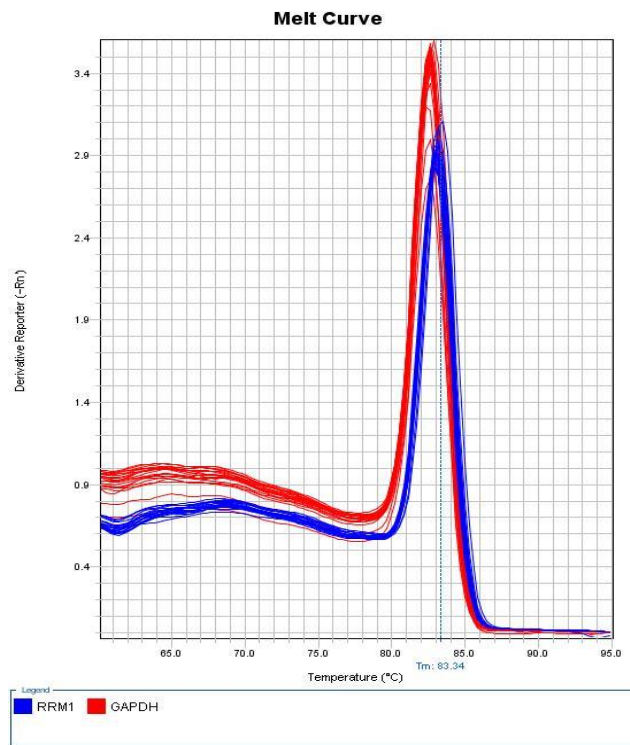


Figure 5.26 High Resolution Melt Curve for RRM1 and GAPDH

Table 5.16 Transfection in A549 Cells*

Formulations	% Transfection			
	siRNA Concentration	5 nM	500 pM	50 pM
Control	Mean	99.15	99.15	99.15
	SEM	0.85	0.85	0.85
Naked siRNA	Mean	83.5	99.45	97.6
	SEM	2.5	3.35	5.6
DDHC liposomes	Mean	27.15	74.65	91.2
	SEM	1.85	3.35	1.1
RGD-DDHC liposomes(2%)	Mean	23.2	67.3	88.25
	SEM	2.6	3	0.95
CPE liposomes	Mean	29.75	75.3	93.6
	SEM	1.75	2.2	1.6
RGD-CPE liposomes(2%)	Mean	24.1	73.1	90.65
	SEM	3.4	2.1	1.45
Lipofectamine 2000	Mean	26.35	72.15	91.5
	SEM	1.55	2.95	1.5

*Experiments were performed in triplicate.

Transfection in A549 cell line

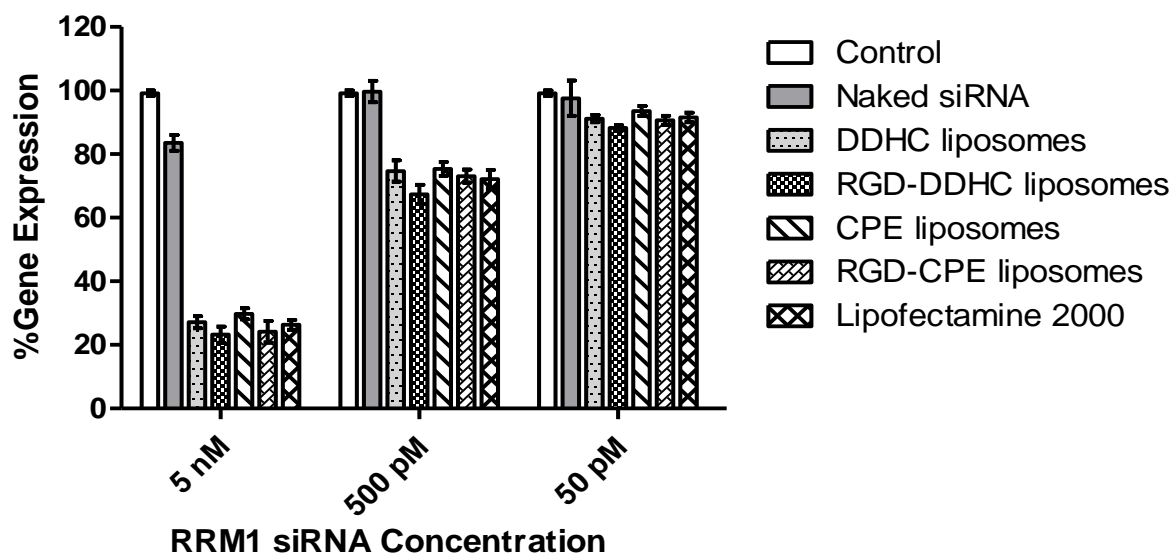


Figure 5.27 Transfection in A549 Cells

Table 5.17 Transfection in H1299 Cells*

Formulations	% Transfection			
	siRNA Concentration	5 nM	500 pM	50 pM
Control	Mean	99.2	99.2	99.2
	SEM	1.1	1.1	1.1
Naked siRNA	Mean	85.9	96.55	101.15
	SEM	2.5	2.65	2.05
DDHC Liposomes	Mean	28.25	76.35	89.3
	SEM	1.05	3.95	1.5
RGD-siRNA Liposomes	Mean	23.05	67.3	86.845
	SEM	2.85	3	1.755
CPE-Liposomes	Mean	32.8	75.3	91.55
	SEM	3	2.2	1.95
RGD-CPE-Liposomes	Mean	23.95	72.25	89
	SEM	3.55	2.95	0.4
Lipofectamine 2000	Mean	31.85	73.7	88.8
	SEM	1.65	4.5	1.2

*Experiments were performed in triplicate.

Transfection in H1299 cell line

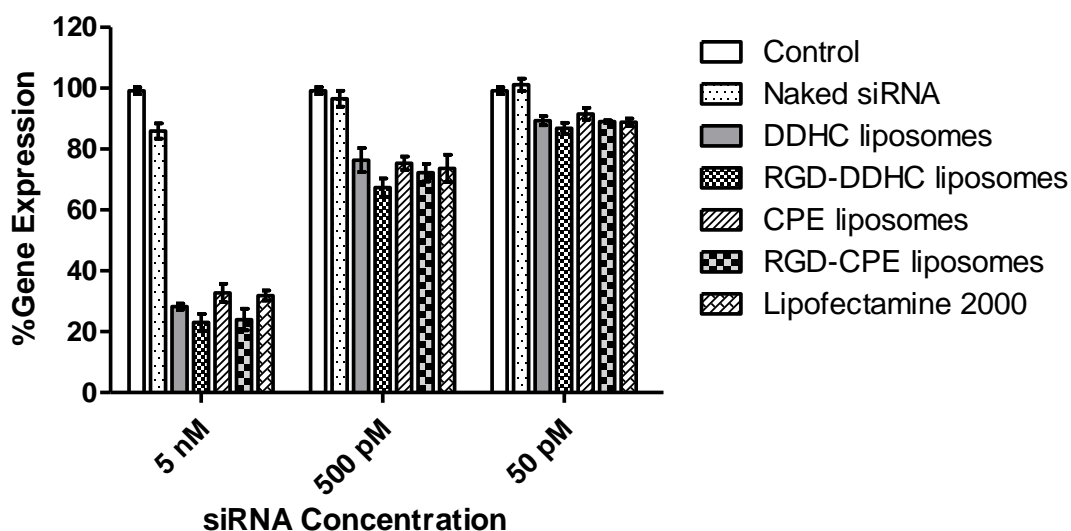


Figure 5.28 Transfection in H1299 Cells

Gene expression studies reveals transfection efficacy of RGD grafted siRNA nano-constructs targeting RRM1 gene. Transfection at 5 nM strongly down regulates the RRM1 concentration as compared to 500 pM and 50 pM. From the gene expression study it can be seen that 50 pM is sub growth inhibitory concentration. No significant difference was

observed at 5 nM concentration for gene expression using L2K and nano-constructs. But, RGD grafting marginally enhances the gene silencing efficacy. At lower concentration of RRM1 siRNA i.e. 50 pM the knockdown efficacy was unaffected. Hence, 50 pM was utilized for the chemosensitization studies.

5.2. Chemosensitization Studies

Although a number of chemotherapeutic treatments have been shown to be effective at inhibiting or eliminating cancer cell growth in preclinical studies, clinical applications are often limited due to the toxic side effects associated with anticancer drugs. Patients are often unable to tolerate the level of a drug needed to effectively eliminate malignant cells while levels that can be tolerated are insufficient therapeutically. As a result, chemo-resistance and subsequent tumor recurrence are often the outcome of such therapies. An example of this all too common event is the use of taxanes (paclitaxel and its semi-synthetic analogue, docetaxel) in the treatment of a variety of cancers including ovarian, breast, prostate, and non-small cell lung cancers [14, 15]. While surgery along with taxane- and platinum-based chemotherapy for advanced ovarian cancer has allowed up to 80% of women to achieve a clinical response [16], cancers in most patients initially diagnosed with late stage disease eventually recur. Development of methods to circumvent resistance may ultimately improve the impact of adjuvant therapy, resulting in prolonged disease-free intervals and survival. Novel targeted therapies that interfere with specific molecular signalling pathways affecting cancer cell survival are being developed as potential treatment options to render cancer cells more sensitive to cytotoxic chemotherapy. Targeted therapies that increase cancer cell sensitivity to chemotherapies offer the benefits of lowering unwanted side effects and increasing the likelihood of destroying resistant cells while avoiding healthy cells where there is little or no expression of the targeted entity.

5.2.1. Method

In vitro cytotoxicity of anticancer drug Gemcitabine HCl at sequential concentrations was assessed with pre-treatment of RGD grafted siRNA nano-constructs (RGD-DDHC liposomes and RGD-CPE liposomes) in A549 and H1299 cells. Gemcitabine HCl solution (Gem. sol.) and Gemcitabine HCl liposomes (Gem. lipo.) were used as chemotherapeutic agents. Gemcitabine solution was obtained by reconstituting lyophilized injection of Gemcitabine HCl (Gemtaz, Sun Pharma Ind. Ltd., India) with saline solution. Lyophilized injection was composed of Gemcitabine HCl, sodium acetate and mannitol. Gemcitabine liposomes were prepared and obtained by Mohan Rathi and Ambikanadan Misra, Pharmacy dept., The M. S. University of Baroda. Liposomes were made up of DPPC, DSPG, cholesterol, mPEG-DSPE₂₀₀₀ (5.6: 2: 2: 0.4) with mean particle size of 150 nm. Entrapment efficiency of prepared liposomes was 60.6±4.32%.

Aliquots of 10^6 cells were seeded in 60 mm petri dishes. After 24 hr proliferation, the cells were transfected with RRM1 siRNA containing RGD-DDHC liposomes and RGD-CPE liposomes in antibiotics and serum free medium. Lipofectamine 2000 was used as a positive control. The final concentration of RRM1 siRNA was 50 pM. After 6 hr transfection, the culture medium was replaced with fresh DMEM supplemented with 10% FBS and antibiotics. Following next 42 hr of incubation, cells were harvested and seeded in 96-well plates at a density of 5×10^3 cells per well. After 24 hr proliferation, cells were treated with a series of concentrations of Gemcitabine solution or Gemcitabine liposomes for 48 hr, and 20 μ l of a 5 mg/ml MTT was added to detect IC_{50} values. Along with these sets of experiments, sets of samples without pre-exposure to RRM1 siRNA were also investigated and IC_{50} values were determined.

5.2.2. Result and Discussion

MTT assay was used to determine IC_{50} values of Gemcitabine HCl in A549 and H1299 cells pre-treated with RGD grafted siRNA nano-constructs at final RRM1 siRNA concentration of 50 pM in both cell lines. Cell viability was accessed in a range of Gemcitabine HCl concentration i.e. 0.005 nM to 250 nM. Cell viability at these concentrations after 48 hr with and without pre-exposure to RRM1 siRNA by the mean of RGD-DDHC liposomes, RGD-CPE liposomes and lipofectamine 2000 is given in **Table 5.18** and **Table 5.19**. Viability of A549 and H1299 Cells on exposure of various formulations is graphically represented in **Figure 5.29** and **Figure 5.30**.

H1299 cell line showed more amount of viable cells after 48 hr as compared to A549 cells. In both types of cells, Gem. sol. (without pre-exposure to RRM1 siRNA) showed highest IC_{50} values of 6.28 ± 0.37 and 19.26 ± 1.07 in A549 and H1299 cells, respectively. The order of IC_{50} values for Gemcitabine HCl in both A549 and H1299 cells were as follow (**Table 5.20**):

Gem. sol. < Gem. lipo. < RGD-CPE liposomes+Gem. sol. < Lipofectamine + Gem. sol. < RGD-DDHC liposomes+Gem. sol. < Lipofectamine+Gem. lipo. < RGD-CPE liposomes+Gem. lipo. < RGD-DDHC liposomes+Gem. lipo

siRNA pre-treated Gemcitabine liposomes and siRNA pre-treated Gemcitabine solution exposed cells showed significantly less IC_{50} values as compared to IC_{50} values of cells

treated with Gemcitabine liposomes and Gemcitabine solution alone. Results strongly suggest the chemosensitization effect by pre-exposure of siRNA in liposomal forms at picomolar concentration (**Table 5.21, Table 5.22 and Table 5.23**).

Table 5.18 Chemosensitization of Gemcitabine HCl in A549 Cells*

Formulation	Gemcitabine Concentration (log nM)										
		-2.30	-1.60	-1.30	-0.60	-0.30	0.40	0.70	1.40	1.70	2.40
RGD-DDHC liposomes(2%)+Gem. lipo.	Mean	98.32	93.39	73.55	60.80	44.45	38.00	33.35	30.95	24.25	22.45
	SEM	2.05	1.92	2.25	1.30	0.85	2.60	1.05	1.95	1.05	0.95
RGD-DDHC liposomes(2%)+Gem. sol.	Mean	101.95	93.61	74.20	63.10	47.20	40.00	38.90	33.20	30.50	29.50
	SEM	1.95	3.29	3.88	5.20	4.00	3.60	3.50	0.90	1.50	2.00
RGD-CPE liposomes(2%)+Gem. Lipo.	Mean	100.39	93.24	74.05	61.35	45.30	39.80	36.10	31.70	26.95	25.85
	SEM	0.01	1.76	1.25	1.85	1.70	0.80	0.60	1.50	1.45	1.55
RGD-CPE liposomes(2%)+Gem. sol	Mean	100.50	94.00	76.30	64.80	48.50	42.30	40.90	34.60	31.40	30.20
	SEM	0.50	3.68	5.98	3.50	5.30	1.30	5.50	0.50	2.40	1.30
Lipofectamine+Gem. lipo	Mean	101.79	94.89	73.40	60.75	47.70	43.70	37.90	33.15	28.30	26.40
	SEM	1.41	3.42	0.60	1.25	0.80	0.60	2.40	1.95	2.00	1.00
Lipofectamine+Gem. Sol.	Mean	100.50	97.50	71.50	59.40	48.10	41.80	39.70	35.40	31.75	29.55
	SEM	0.50	7.18	1.18	8.90	4.90	1.80	4.30	1.30	2.45	1.95
Gem. lipo	Mean	102.40	97.05	90.00	80.13	71.05	60.45	57.10	51.85	45.65	41.62
	SEM	1.52	1.65	0.40	0.72	2.35	2.15	1.80	1.65	1.15	2.30
Gem. sol.	Mean	100.78	95.78	88.35	80.02	72.40	68.20	64.60	58.40	50.00	44.42
	SEM	1.08	2.94	5.17	0.52	6.81	7.01	1.40	2.10	2.31	2.79

*Experiments were performed in triplicate.

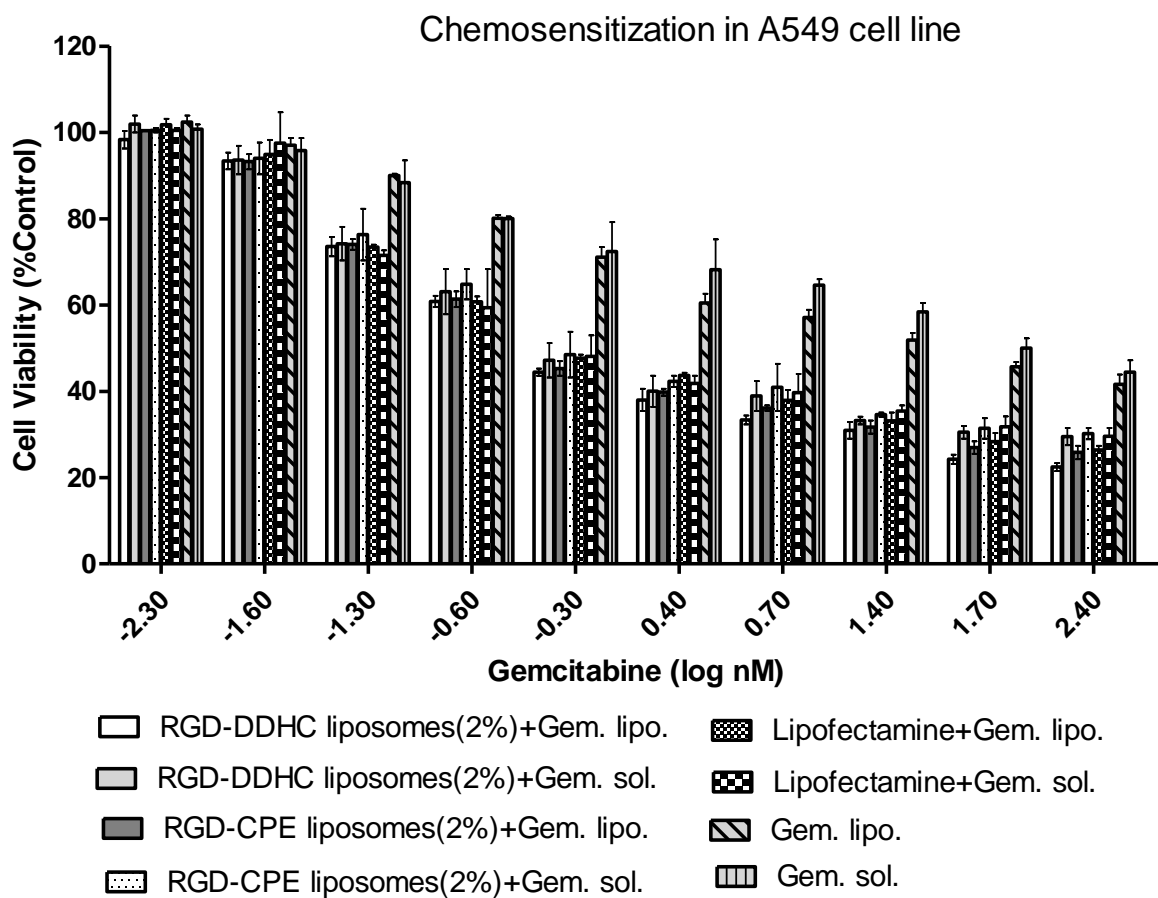


Figure 5.29 Chemosensitization of Gemcitabine in A549 Cells by siRNA

Table 5.19 Chemosensitization of Gemcitabine HCl in H1299 Cells*

Formulation	Gemcitabine Concentration (log nM)											
		-2.30	-1.60	-1.30	-0.60	-0.30	0.40	0.70	1.40	1.70	2.40	2.70
RGD-DDHC liposomes(2%)+Gem. lipo	Mean	101.34	93.95	87.70	76.90	64.10	62.65	53.25	51.30	46.80	44.50	39.60
	SEM	0.97	1.65	0.30	2.00	1.60	1.45	0.15	1.10	1.00	0.30	1.60
RGD-DDHC liposomes(2%)+Gem. sol.	Mean	101.40	99.00	87.30	80.30	68.70	60.90	55.60	52.10	50.50	43.80	41.50
	SEM	1.40	3.40	1.60	2.80	2.10	0.80	2.70	2.90	2.90	1.50	0.60
RGD-CPE liposomes(2%)+Gem. lipo.	Mean	100.39	93.65	88.80	77.05	67.90	62.50	55.05	51.31	45.60	43.05	39.50
	SEM	0.01	1.35	1.40	1.25	2.20	1.60	1.65	1.09	1.10	0.95	1.00
RGD-CPE liposomes(2%)+Gem. sol.	Mean	99.70	95.60	92.30	78.40	70.90	63.90	55.70	54.60	46.10	43.90	40.90
	SEM	0.30	1.60	1.10	2.10	2.00	1.70	0.40	2.00	0.10	0.80	2.50
Lipofectamine+Gem. lipo.	Mean	100.35	95.10	87.75	77.00	68.25	63.70	55.30	51.65	46.00	43.25	39.10
	SEM	0.55	0.50	0.35	0.10	0.75	0.60	0.00	1.85	0.10	0.65	0.20
Lipofectamine+Gem. sol.	Mean	101.50	97.65	90.40	79.33	72.50	62.75	56.30	53.15	47.85	44.76	41.45
	SEM	0.60	1.05	0.80	1.52	1.70	1.55	1.00	1.05	1.05	0.84	1.65
Gem. lipo.	Mean	100.19	96.85	91.35	85.85	77.95	74.10	71.45	66.55	61.15	48.90	45.15
	SEM	0.69	1.85	0.95	0.55	1.55	1.10	1.15	1.25	0.85	1.70	1.15
Gem. sol.	Mean	99.00	98.30	94.20	84.20	80.30	76.90	74.20	68.90	61.40	57.90	46.30
	SEM	0.30	1.60	2.20	2.20	3.70	2.00	2.10	3.10	1.90	3.00	2.00

*Experiments were performed in triplicate.

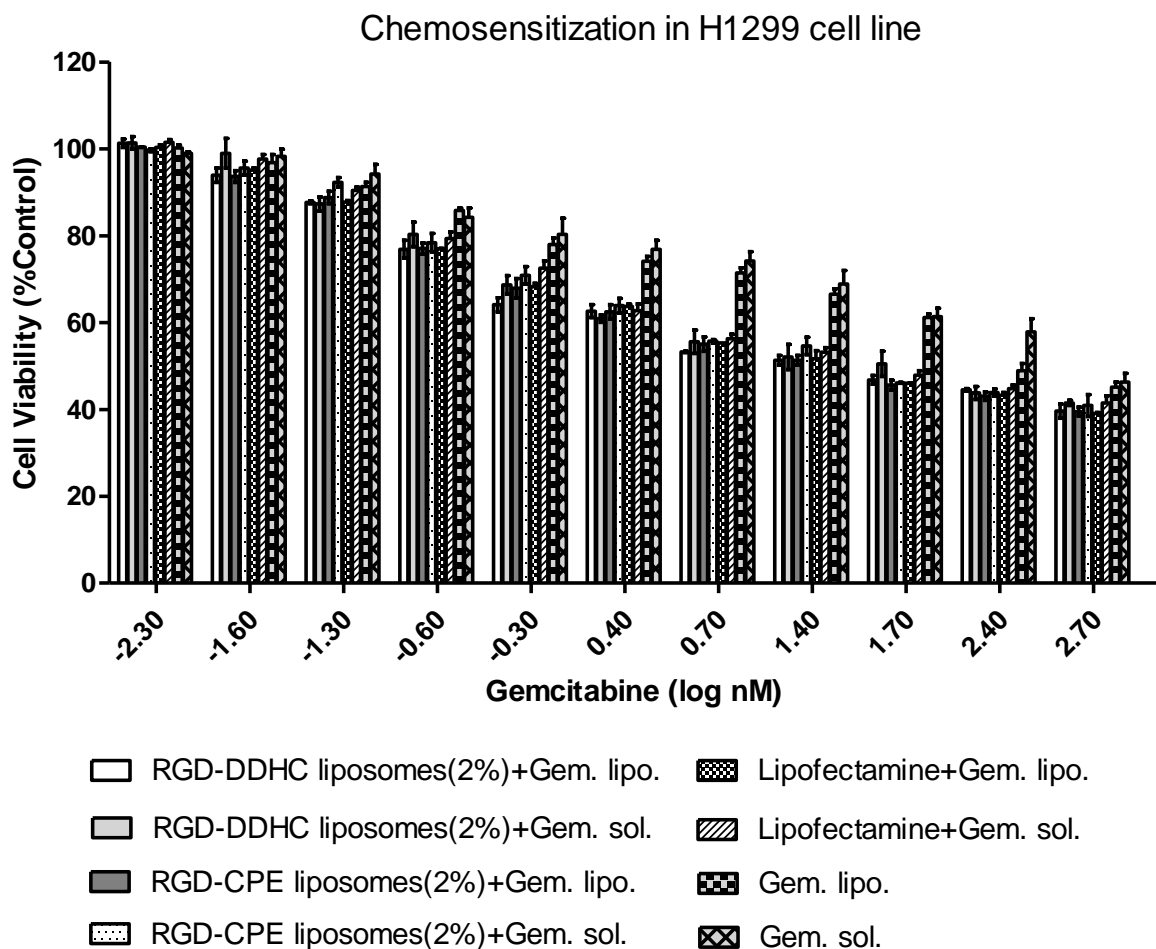


Figure 5.30 Chemosensitization of Gemcitabine in H1299 Cells by siRNA

Table 5.20 IC₅₀ values of Various Formulations with or without siRNA *

Sr.No.	Formulation	IC ₅₀	
		A549	H1299
1.	RGD-DDHC liposomes(2%)+Gem. lipo	1.23±0.12	4.42±0.28
2.	RGD-DDHC liposomes(2%)+Gem. sol.	1.35±0.56	4.97±0.19
3.	RGD-CPE liposomes(2%)+Gem. lipo.	1.27±0.10	4.59±0.46
4.	RGD-CPE liposomes(2%)+Gem. sol.	1.53±0.12	5.30±0.51
5.	Lipofectaine+Gem. lipo.	1.32±0.17	4.70±0.36
6.	Lipofectaine+Gem. sol.	1.44±0.10	5.10±0.44
7.	Gem. lipo.	3.93±0.25	12.50±0.93
8.	Gem. sol.	6.28±0.37	19.26±1.07

*Results are expressed as mean±

Chemosensitization effect is described by the fold change in IC₅₀ values when siRNA was pre-exposed in different formulations. Fold change in IC₅₀ values are given in Table 5.21, Table 5.22, Table 5.23 and **Table 5.24**. Highest chemosensitization (fold change=5.11) was observed in cells pre-treated with RGD-DDHC liposomes followed by treatment with Gem. lipo. as compared to treatment with Gem. sol. alone. The order of fold change in IC₅₀ values for RGD-DDHC liposomes is more as compared lipofectamine 2000 and no significant difference was observed between RGD-CPE-liposomes and lipofectamine 2000.

Table 5.21 Change in IC₅₀ of Gemcitabine HCl after Chemosensitization by RGD-DDHC Liposomes(2%)

Sr.No.	Fold change in IC ₅₀		
	RRM1 siRNA Pre-exposure with RGD-DDHC liposomes(2%)	A549	H1299
1.	Gem. sol./RGD-DDHC liposomes(2%)-Gem. lipo.	5.11	4.36
2.	Gem. sol./RGD-DDHC liposomes(2%)-Gem. sol.	4.65	3.88
3.	Gem. lipo./RGD-DDHC liposomes(2%)-Gem. lipo.	3.20	2.83
4.	Gem. lipo./RGD-DDHC liposomes(2%)-Gem. sol.	2.91	2.52

Table 5.22 Change in IC₅₀ of Gemcitabine HCl After Chemosensitization by RGD-CPE Liposomes(2%)

Sr.No.	Fold change in IC ₅₀		
	RRM1 siRNA Pre-exposure with RGD-CPE liposomes(2%)	A549	H1299
1.	Gem. sol./RGD-CPE liposomes(2%)-Gem. lipo.	4.94	4.20
2.	Gem. sol./RGD-CPE liposomes(2%)-Gem. sol.	4.10	3.63
3.	Gem. lipo./RGD-CPE liposomes(2%)-Gem. lipo.	3.09	2.72
4.	Gem. lipo./RGD-CPE liposomes(2%)-Gem. sol.	2.57	2.45

Table 5.23 Change in IC₅₀ of Gemcitabine HCl After Chemosensitization by Lipofectamine 2000

Sr.No.	Fold change in IC ₅₀		
	RRM1 siRNA Pre-exposure with Lipofectamine 2000	A549	H1299
1.	Gem. sol./Lipofectamine-Gem. lipo.	4.76	4.10
2.	Gem. sol./Lipofectamine-Gem. sol.	4.36	3.78
3.	Gem. lipo./Lipofectamine-Gem. lipo.	2.98	2.66
4.	Gem. lipo./Lipofectamine-Gem. sol.	2.73	2.45

Fold change of 1.10 & 1.12, 1.20 & 1.15 and 1.09 & 1.09 was observed for RGD-DDHC liposomes(2%)- Gem. sol./ RGD-DDHC liposomes(2%)-Gem. lipo., RGD-CPE liposomes(2%)- Gem. sol./ RGD-CPE liposomes(2%)-Gem. lipo. and Lipofectamine-Gem.Sol/ Lipofectamine-Gem.Lipo., respectively, as compared to 1.60 & 1.54 for Gem. sol./Gem. lipo. By comparing the fold change in IC₅₀ values of Gem. sol. vs Gem. lipo. in with and without pre-exposure for in all formulations, it can be said that pre-exposure of siRNA has dominating effect in fold change as compared to liposomal vs solution form. However, one should not neglect the beneficial effect of liposomal for over simple solution.

Table 5.24 Comparison of Change in IC₅₀ Value of Various Formulation

Sr.No.	Fold change in IC ₅₀		
	Gem. Sol. vs Gem. lipo.	A549	H1299
1.	Gem. sol./Gem. lipo.	1.60	1.54
2.	RGD-DDHC liposomes(2%)- Gem. sol./ RGD-DDHC liposomes(2%)-Gem. lipo.	1.10	1.12
3.	RGD-CPE liposomes(2%)- Gem. sol./ RGD-CPE liposomes(2%)-Gem. lipo.	1.20	1.15
4.	Lipofectamine-Gem. sol./ Lipofectamine-Gem. lipo.	1.09	1.09

The 5-fold increase in Gemcitabine sensitivity following sub-growth inhibitory RRM1 knockdown using siRNA nano-constructs correlates well with a previous report [13], where stably expressed shRNAs were used to knockdown RRM1. Additionally, Gemcitabine liposome showed significantly less IC₅₀ value (P < 0.05) as compared to Gemcitabine solution in both with and without pre-siRNA treatment. This also demonstrates the application of gemcitabine

liposome as a substitute for Gemcitabine solution. Due to the higher dose of Gemcitabine HCl, it is very difficult to load sufficient amount of drug inside the liposomes. But, present studies open a vista for chemotherapy at lower dose and at that point it may be possible to formulate clinically suitable liposomes of Gemcitabine HCl with sufficient drug loading. Studies have also demonstrated that transfection with as little as 2.5 nM siRNA caused cell growth inhibition while 50 pM concentrations resulted in a noticeable chemosensitization of the drug Gemcitabine. Taken collectively results suggest that prepared siRNA liposomal formulations may be a novel therapeutic strategy for reducing a dose of Gemcitabine with combination therapy or alone as a chemotherapeutic agent.

5.3. Serum Stability Study (*In vitro* Release)

For siRNAs to retain their functional activity, they must resist degradation prior to cellular internalization. The half-life reported for unmodified siRNAs in serum ranges from several minutes to around an hour [17]. The susceptibility to degradation by nucleases present in serum appears to preclude the systemic application of naked, unmodified siRNAs through clinically feasible administration routes. Chemical modifications to the nucleotides (e.g., 2'-F, 2'-OMe, LNA) or the backbone (e.g., phosphorothioate linkages) have been used successfully to enhance nuclease stability and prolong siRNA half-life in serum while still enabling siRNA function [18]. The effects of nuclease stabilization should be most dramatic in situations where the siRNAs can directly interact with nucleases present in the extracellular environment such as the bloodstream. However, transfection of cultured cells is accomplished most effectively using carrier-mediated delivery, often through cationic lipid encapsulation of the siRNAs to enhance cellular uptake. Because the siRNAs are protected by the carrier prior to cellular uptake, *in vitro* studies most aptly highlight the effects of intracellular processes on the activity of transfected siRNAs. A similar situation should be expected *in vivo* when delivery vehicles are used to transport the siRNAs to the target cells. However, hydrodynamic injection (HDI) provides a unique situation in which naked siRNAs can be successfully delivered systemically *in vivo* [19]. The duration of the exposure to the bloodstream prior to cellular uptake by cells such as hepatocytes is not precisely known, although the rapid degradation of unmodified siRNAs in serum indicates that even a short exposure can be sufficient to degrade a portion of the injected unmodified siRNAs, while nuclease-stabilized siRNAs should be affected to a much lesser extent by this serum exposure.

5.3.1. Methods

The siRNA liposomes were studied for the integrity of complexed siRNA in presence of serum for possible *in vivo* degradation because of degradation during circulation, and degradation due to extracellular and intracellular RNase. Naked siRNA, RGD-DDHC liposomes and RGD-CPE liposomes containing 2.6 µg of siRNA were incubated with 50 µL non-heat inactivated FBS at 37°C for various time periods to give a 50 % serum concentration in final incubation volume having pH of 7.4. Incubated samples were processed as per following two protocols:

1. The samples were then vortexed with 100 μ L of phenol/chloroform (1:1 v/v) and were subsequently spun at 14,000 rpm at 4°C for 10 min. 25 μ L from the aqueous layer was then mixed with 5 μ L loading buffer and was loaded onto 2 % agarose gel to check the integrity of siRNA and protection offered by prepared liposomal formulations against serum.
2. Samples were collected and ultracentrifuged to separate out liposomal fraction from serum and other aqueous media. Liposomes were processed to determine the remaining amount of encapsulated siRNA using phenol/chloroform extraction and analysis by UV spectroscopy as described in analytical methods in **Chapter 3**.

5.3.2. Result and discussion

Structural stability study of siRNA in serum condition was carried out at higher serum conditions. Naked siRNA and liposomal siRNA formulations were incubated in 50 % serum containing medium, and the degradation of siRNA was analysed by gel electrophoresis. Figure 5.31 shows gel electrophoresis analysis for naked siRNA and siRNA entrapped within RGD-DDHC liposomes(2%) and RGD-CPE liposomes(2%).

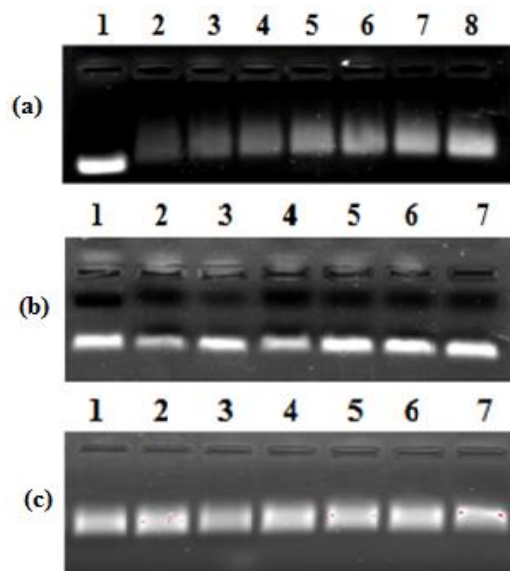


Figure 5.31 Gel Electrophoresis of Serum Stability

- (a) Naked siRNA; 1=0h, 2=6h, 3=3h, 4=2.5h, 5=2h, 6=1.5h, 7=1.0h, 8=0.5h
 (b) RGD-DDHC liposomes (2%); 1=0h, 2=24h, 3=20h, 4=16h, 5=8h, 6=4h, 7=2h
 (c) RGD-CPE liposomes (2%); 1=0h, 2=24h, 3=20h, 4=16h, 5=8h, 6=4h, 7=2h

An essential property of liposomes designed in present investigation for further applications is the ability to protect the encapsulated siRNA from degradation by serum nucleases (mainly RNase). Therefore, serum stability of RGD grafted liposomal formulations were determined by incubating them in FBS at 37°C.

Table 5.25 Serum Stability of Liposomes*

Time (hr)	RGD-DDHC liposomes (% total siRNA remained)		RGD-CPE liposomes (% total siRNA remained)	
	Mean	SEM	Mean	SEM
0	100.00	0.00	100.00	0.00
2	98.04	2.84	101.01	1.90
4	96.72	3.72	98.28	3.62
8	92.93	2.24	96.52	2.87
16	82.64	1.36	96.95	3.15
20	78.40	2.93	95.02	2.03
24	75.82	3.01	94.33	1.74

*Experiments were performed in triplicate.

Table 5.26 Serum Stability of Naked siRNA*

Time (hr)	Naked siRNA (% total siRNA remained)	
	Mean	SEM
0	100.00	0.00
0.5	88.620	1.57
1.0	75.300	1.20
1.5	67.450	2.05
2.0	61.850	1.350
2.5	53.850	2.650
3.0	41.200	1.900
6.0	16.900	1.000

*Experiments were performed in triplicate.

Gel retardation assay showed that degradation was started within half an hour after incubation of siRNA with FBS. At 0.5 hr more than 10% of siRNA was degraded, which reached up to 60% within 3 hr. After 6 hr less than 20 % of siRNA was remained as compared to initially loaded siRNA. RGD-DDHC liposomes and RGD-CPE liposomes encapsulated siRNA was stable even after 24 hr and more than 75 % of siRNA was seen on agarose gel (Figure 5.31). This result indicates that prepared liposomal formulations successfully protected the encapsulated siRNA from enzymatic degradation. Results are summarised in **Table 5.25** and **Table 5.26**. Results suggest that there is significant difference in stability of siRNA against serum nucleases by comparing naked siRNA to that of liposomal formulations at every time points. Further,

significant increase in stability was seen in RGD-CPE liposomes as compared to RGD-DDHC liposomes. This may be due to encapsulation of siRNA within the liposomal aqueous compartment as contrast to the cationic liposomal formulation, where siRNA mainly complexed to the surface.

After every time points remaining siRNA was detected and plotted against time points (**Figure 5.32**). Results are summarised in **Table 5.27**. Amount remained in the liposomes are showing same results as was seen with serum stability study. Results suggest that both liposomes protect siRNA inside within the formulation at blood pH (7.4) and serum condition. Upto 6 hr most of the siRNA is being preserved in cationic liposomes; however these liposomes failed to maintain the rigidity upto 24 hr. It is generally observed that most of the liposomal formulations are distributed to different tissue within 6 hr of injection and hence, prepared cationic formulation will be able to face *in vivo* fate. In case of RGD-CPE liposomes, rigid structure was maintained even after 24 hr and hence, this formulation was proved to be superior in maintaining the stability at blood pH and serum conditions.

Table 5.27 *In vitro* Release in Serum at pH 7.4*

Time (hr)	RGD-DDHC liposomes (% siRNA in liposomes)		RGD-CPE liposomes (% siRNA in liposomes)	
	Mean	SEM	Mean	SEM
0	99.450	1.450	100.100	1.099
2	96.850	2.849	98.399	2.799
4	95.350	1.650	97.650	1.349
8	95.100	2.700	95.450	3.149
16	86.100	1.799	95.000	3.699
20	82.300	2.299	94.085	2.215
24	76.650	1.250	95.100	1.400

*Experiments were performed in triplicate.

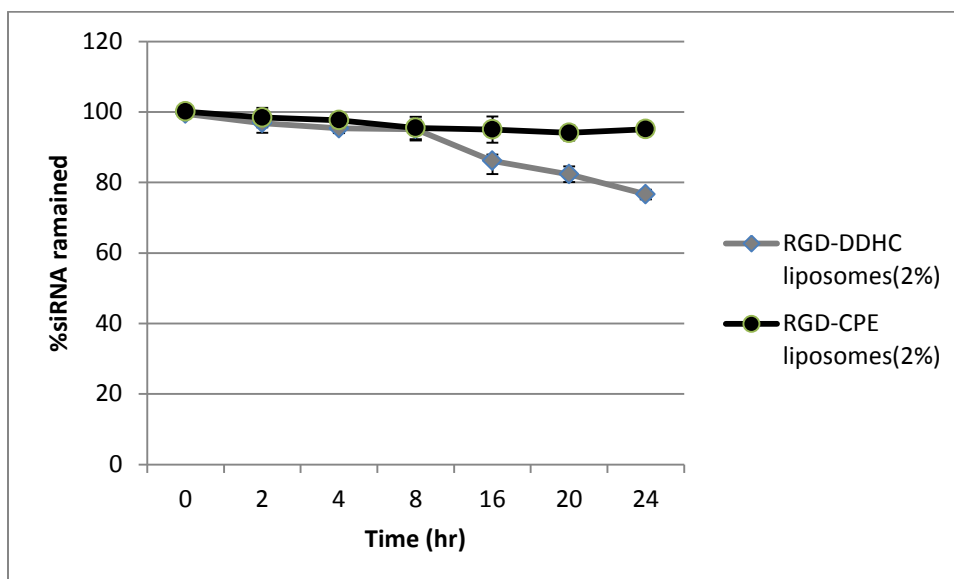


Figure 5.32 *In vitro* Release of siRNA from Liposomes

Optimized liposomal formulations exhibited almost no structural loss of siRNA after 24 hr incubation and successfully protected the encapsulated siRNA from enzymatic degradation. Prepared formulations also showed great potential for maintaining the rigid structure during blood circulation without releasing significant amount of siRNA into the blood.

5.4. Haemolysis Study

Due to their resemblance with biological membranes liposomes are acceptable and essentially nontoxic to blood cells. But sometimes haemolytic activity is seen with the liposomal components [20-22]. It has been also reported that various lipids including short-chain phosphatidylcholines and lipid metabolites like free fatty acids and lysophosphatidylcholine induce erythrocyte lysis by some non-specific destruction of cell wall causing various Sodium(Na^+) and potassium(K^+) ion permeability defects [21, 23, 24]. This might be related to the haemolytic activity of various liposomes and lipid component. Apart from this cationic lipids (DOTAP, DOTMA etc) can induce formation of pores in the erythrocyte membrane [25]. In addition fusogenic proteins used along with cationic lipids in delivery of genes can promote cationic lipid mediated pore formation [25]. Such pore formation can induce haemoglobin leakage and consequent haemolysis.

Phospholipids are prone to undergo various physicochemical changes on exposure to different conditions [26, 27]. Chemically phospholipids are susceptible to hydrolytic reactions at the ester bonds. Hydrolysis induces formation of lysophosphatidylcholine and free fatty acids [28] and causes increase in membrane permeability [29]. Such changes also induce changes in organization of liposomes causing transformation to micellar solutions [29]. Such components as described earlier can cause erythrocyte lysis by getting incorporated in erythrocyte membrane and causing ion permeability defects. This necessitates the evaluation of haemolysis potential of liposomes.

Haemolytic toxicity of formulated liposomes was checked by incubating the formulation with Red Blood Cells separated from Rat blood by centrifugation at low speed [30] and analysing the samples for haemoglobin release at 541 nm [20]. The haemolysis with different formulations were compared with that obtained with Triton-X100 as a positive control [31].

5.4.1. Method

In vitro haemolysis test as described by Oku and Namba [20] was used with some modifications. Blood samples were collected in 2 mL Eppendorff tubes from the Sprague Dawley Rats by retro-orbital puncture. All blood samples were heparinised. The blood samples were washed with

normal saline (0.9 % w/w Sodium Chloride in water) 3 times before use to remove plasma components. For washing, each mL of blood samples was treated with 1 mL normal saline and gently stirred up and then centrifuged on Remi Lab Centrifuge at low speed (3000 rpm) to separate the red blood cells (RBCs). The RBC pellet separated was resuspended in normal saline and washed the same way.

Final pellet was used to prepare 0.5 % v/v dispersion of RBCs based on the final volume. 25 μ L of RBC pellet was resuspended in 2 mL of normal saline taken in a 10 mL Centrifuge tube. Specific volumes of different liposomal formulations were sampled in these centrifuge tubes and the volume was made up to 5 mL with normal saline. This will make the final concentration of RBCs 0.5 % v/v. Volumes of different liposome components/formulations were chosen to get the final concentrations to range from 0.01 mM to 5 mM on lipid basis (Semilog increase in concentration to check haemolysis potential over a large concentration range).

Positive Control was prepared by getting 100 % haemolysis of RBCs by using 0.5 % Triton-X100 (20 μ L in 5 mL) instead of formulation treatment. Negative Control was prepared by using the dilutions without any formulation treatment (Dilution only with normal saline).

Different components of liposomes were evaluated separately and incorporated in liposomes for their potential to cause haemolysis.

- Blank DOTAP liposomes
- DOTAP liposomes
- PEGylated DOTAP liposomes
- RGD-grafted PEGylated DOTAP liposomes
- Blank calcium phosphate loaded liposomes
- Calcium phosphate loaded liposomes
- PEGylated calcium phosphate loaded liposomes
- RGD-grafted PEGylated calcium phosphate loaded liposomes

Depending on the total lipid content of the each liposomal dispersion, appropriate volumes of each was used to treat blood cells to get semi-log concentration range. After treatment with each liposomal formulation, RBC dispersion was gently stirred for effective suspension of RBCs. The

treated dispersions were incubated at 37°C for 30 min in incubator. After incubation all the samples were centrifuged at low speed (3000 rpm for 5 min) to separate the RBC mass and the solutions were analysed for UV absorbance at 541 nm wavelength against normal saline as a measure of haemolysis. Percentage of haemolysis was determined for different samples considering the absorbance value of sample treated with Triton-X100 to represent 100 % haemolysis.

5.4.2. Results and Discussion

The haemolysis observed with different formulations as compared to that with Triton-X100 are shown in **Table 5.28** and **Table 5.29**. Relative haemolytic potentials are also shown graphically in **Figure 5.33** and **Figure 5.34**.

Table 5.28 Haemolysis by Cationic Liposomes*

mM of lipid	%Relative Haemolysis									
	DD liposomes (Placebo)		DDHC liposomes (Placebo)		DDHC liposomes (non-PEGylated)		DDHC liposomes		RGD-DDHC liposomes(2%)	
	Mean	SEM	Mean	SEM	Mean	SEM	Mean	SEM	Mean	SEM
0.01	4.160	1.140	2.850	0.350	2.700	0.300	2.000	0.099	1.900	0.100
0.05	7.250	0.550	5.200	0.500	4.450	0.550	4.000	0.500	3.800	0.600
0.10	11.650	0.749	9.650	1.250	4.850	0.550	4.450	0.450	3.950	0.950
0.5	14.300	1.100	12.950	0.550	7.100	0.700	5.800	0.600	5.550	0.550
1	19.400	1.500	15.900	0.500	12.550	0.449	8.000	0.199	7.750	0.350
5	27.600	1.300	19.200	1.200	14.600	0.799	9.150	0.250	8.900	0.400

*Experiments were performed in triplicate.

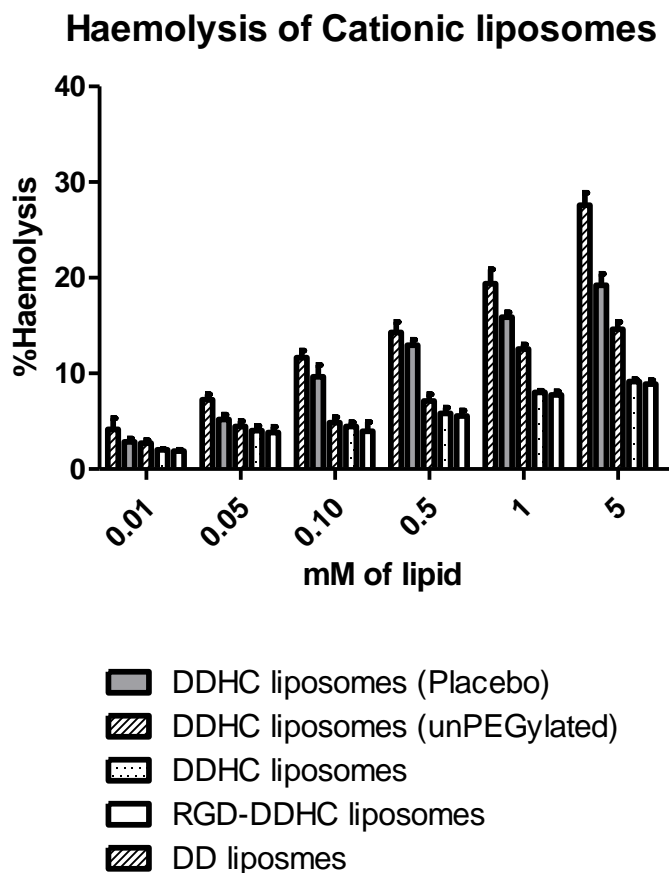


Figure 5.33 Haemolytic Potential of Cationic Liposomes

Table 5.29 Haemolysis in CP liposomes*

mM of lipid	%Relative Haemolysis							
	CPE liposomes (Placebo)		CPE liposomes(Non-PEGylated)		CPE liposomes		RGD-CPE liposomes	
	Mean	SEM	Mean	SEM	Mean	SEM	Mean	SEM
0.01	1.050	0.250	1.100	0.200	0.400	0.0999	0.200	0.100
0.05	1.900	0.400	1.950	0.250	0.300	0.200	0.300	0.100
0.10	2.250	0.450	2.400	0.100	1.500	0.100	1.465	0.165
0.5	3.350	0.150	2.480	0.120	1.800	0.0999	1.725	0.125
1	3.700	0.100	2.600	0.100	2.300	0.100	2.200	0.300
5	3.925	0.075	3.150	0.150	2.670	0.07	2.645	0.045

*Experiments were performed in triplicate.

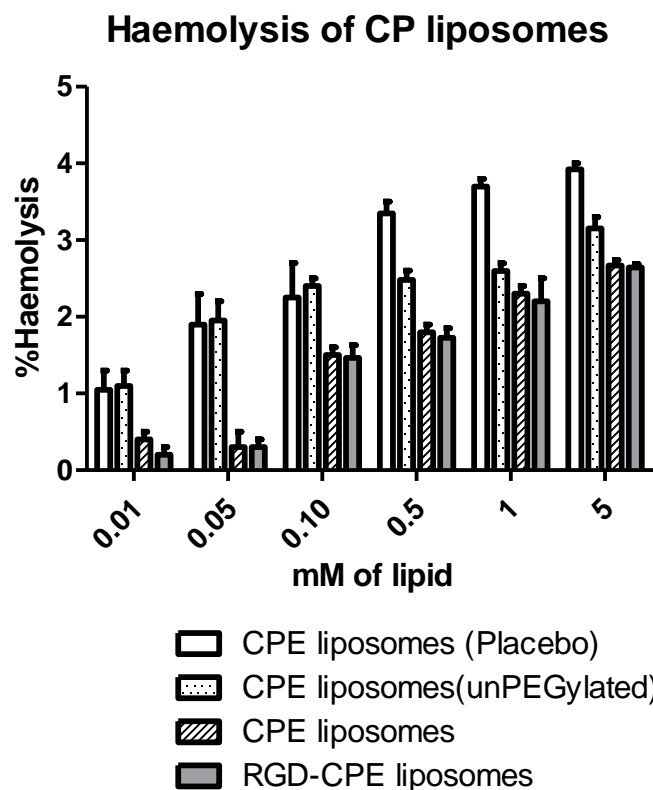


Figure 5.34 Haemolytic potential of calcium phosphate loaded liposomes

As it can be seen from the **Figure 5.33** blank DD liposomes showed highest haemolytic potential ranging from 4.16 ± 1.14 % at 0.01 mM lipid concentration to 27.6 ± 1.3 % at 5 mM lipid concentration. This might be due to the positively charged DOTAP which causes pore formation in erythrocyte membrane causing leaching of haemoglobin from erythrocytes. Further fusogenic lipid, DOPE, promotes pore formation effect of DOTAP causing enhanced haemolysis. siRNA loaded liposomes exhibited less haemolysis as compared to blank liposomes. This can be explained by complexation of DOTAP to negatively charged siRNA molecules. This is in agreement with previous study by van der Woude et al. [25].

PEGylation of liposomes showed substantially reduced haemolysis which can be attributed to the reduced interaction of DOTAP and DOPE to surface of erythrocytes due to coating of liposome surface by PEG chains.

Calcium phosphate loaded liposomes exhibited very less haemolysis (**Figure 5.34**) as compared to DOTAP liposomes, showing only <4 % haemolysis at 5 mM lipid concentration of blank

liposomes. The haemolysis occurring may be due to liposomal components or calcium leaking out of liposomes. As in the case of DOTAP liposomes, PEGylation of these liposomes reduced the hemolytic potential. Further RGD grafting has also shown minor reduction in haemolysis. At all concentrations haemolysis was found to be very less.

Thus we conclude from the observations that optimized batches of PEGylated liposomes prepared with DOTAP and calcium phosphate have very less potential to cause haemolysis at therapeutic concentrations of lipids body would be exposed with.

5.5. Electrolyte induced flocculation test

Particle aggregation refers to formation of clusters in a colloidal suspension and represents the most frequent mechanism leading to destabilization of colloidal systems. During this process, which normally occurs within short periods of time (seconds to hours), particles dispersed in the liquid phase stick to each other, and spontaneously form irregular particle clusters, flocks, or aggregates. This phenomenon is also referred to as coagulation or flocculation and such dispersion is also called unstable. Particle aggregation can be induced by adding salts or another chemical referred to as coagulant or flocculant [32]. Some people refer to specifically to flocculation when aggregation is induced by addition of polymers or polyelectrolytes, while coagulation is a more widely used term. Numerous experimental techniques have been developed to study particle aggregation. Most frequently used are time-resolved optical techniques that are based on transmittance or scattering of light [33]. Light scattering techniques are based on probing the scattered light from an aggregating suspension in a time-resolved fashion. Static light scattering yields the change in the scattering intensity, while dynamic light scattering the variation in the apparent hydrodynamic radius. At early-stages of aggregation, the variation of each of these quantities is directly proportional to the aggregation rate constant k [34]. At later stages, one can obtain information on the clusters formed (e.g., fractal dimension) [35]. Light scattering works well for a wide range of particle sizes. Multiple scattering effects may have to be considered, since scattering becomes increasingly important for larger particles or larger aggregates. Such effects can be neglected in weakly turbid suspensions. Aggregation processes in strongly scattering systems have been studied with backscattering techniques or diffusing-wave spectroscopy.

5.5.1. Method

Prepared liposomal formulations in three different categories, i.e. without pegylation, with pegylation and with RGD grafting, were studied for electrolyte induced flocculation test. This test confirms the stability of liposomal formulations in presence of electrolyte *in vivo*. This also proves the efficacy of pegylation effect governed by mPEG₂₀₀₀-DSPE on the liposomal surface. siRNA containing liposomal formulations were incubated at varying concentration of sodium chloride ranging from 1% to 5% w/v. Liposomal formulations were used at 100 nM

concentration of NC (negative control) siRNA. After 1 hr of incubation at 37°C particle size was determined. Results are summarised in **Table 5.30** and **Table 5.31**.

5.5.2. Results and Discussion

Sodium chloride is one of the most electrolytes used to check efficacy of pegylation. **Figure 5.35** and **Figure 5.36** depict changes in particle size at different concentration of sodium chloride. Salt induced flocculation measures the efficacy of steric hindrance provided by mPEG₂₀₀₀-DSPE. Particle size of un-PEGylated liposomes was found to increase significantly at all concentration of added salt in both, cationic and CPE, types of liposomal formulations. However, again in both cases, incorporation of 5 mol% of mPEG₂₀₀₀-DSPE did help in maintaining the particle size. Up to 2% NaCl addition was found to maintain particle size of DDHC and RGD-DDHC liposomes below 150 nm. Addition of three per cent and above concentration of salt increased the particle size up to 300 nm. Particle size of the CPE and RGD-CPE liposomes was maintained below 150 nm up to 3% electrolyte addition. Even 5 % salt treatment did not cross 200 nm particle sizes and these results show the stability of CPE and RGD-CPE liposomes in presence of electrolyte as compared to cationic liposomes. The probable reason behind inferior stability of cationic liposomes is presence of positive groups on the liposomal surface, i.e. free amino groups of DOTAP. These provide ease of interaction between electrolyte and liposomal surface.

Table 5.30 Electrolyte Induced Flocculation of DDHC Liposomes*

% NaCl	Particle Size (nm)					
	DDHC liposomes-without mPEG-DSPE		DDHC liposomes		RGD-DDHC liposomes(2%)	
	Mean	SEM	Mean	SEM	Mean	SEM
0	165.750	2.550	145.110	2.089	147.500	2.000
1	187.350	2.049	143.050	1.250	144.800	1.599
2	204.900	4.599	147.850	1.049	145.700	1.800
3	305.100	2.399	177.100	1.799	177.800	1.500
4	357.400	6.899	203.550	2.250	207.900	2.500
5	425.900	4.300	293.050	5.449	296.400	4.800

*Experiments were performed in triplicate.

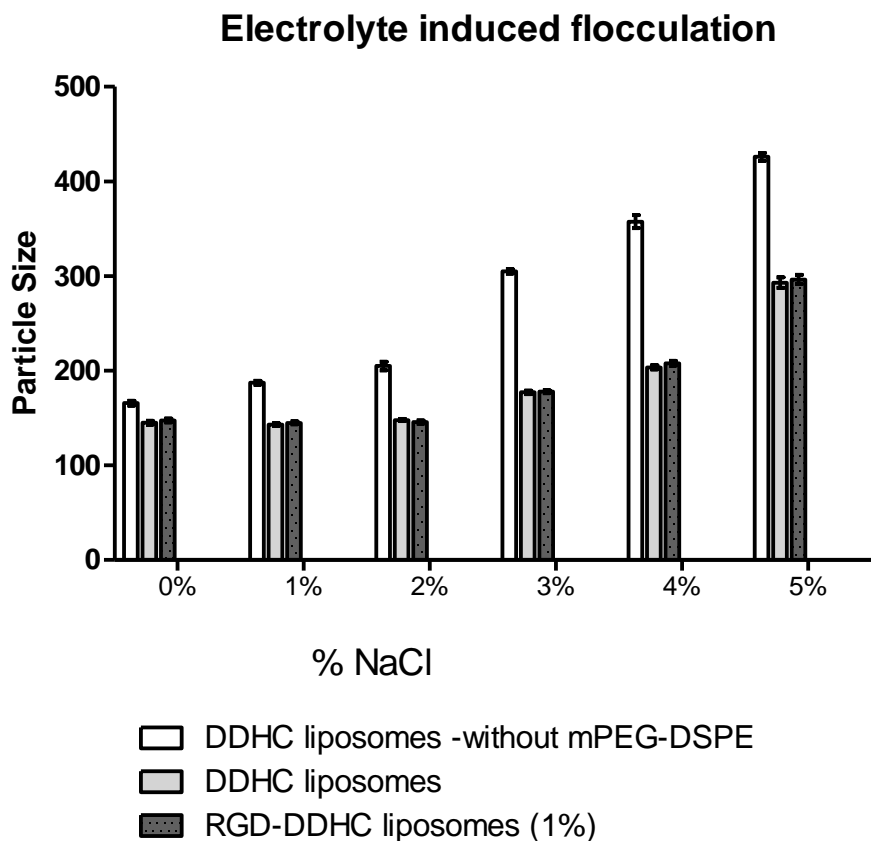


Figure 5.35 Electrolyte Induced Flocculation of DDHC Liposomes

Table 5.31 Electrolyte Induced Flocculation of CPE Liposomes*

% NaCl	Particle Size (nm)					
	CPE liposome-without mPEG-DSPE		CPE liposomes		RGD-CPE liposomes(2%)	
	Mean	SEM	Mean	SEM	Mean	SEM
0	185.050	4.449	114.555	3.195	114.350	2.349
1	200.000	1.300	117.100	1.799	119.050	1.250
2	230.050	2.250	123.650	2.750	130.000	1.300
3	261.800	2.900	142.400	3.400	147.700	1.699
4	296.550	6.250	161.150	1.349	166.150	2.150
5	349.250	1.450	164.350	1.049	170.350	2.849

*Experiments were performed in triplicate.

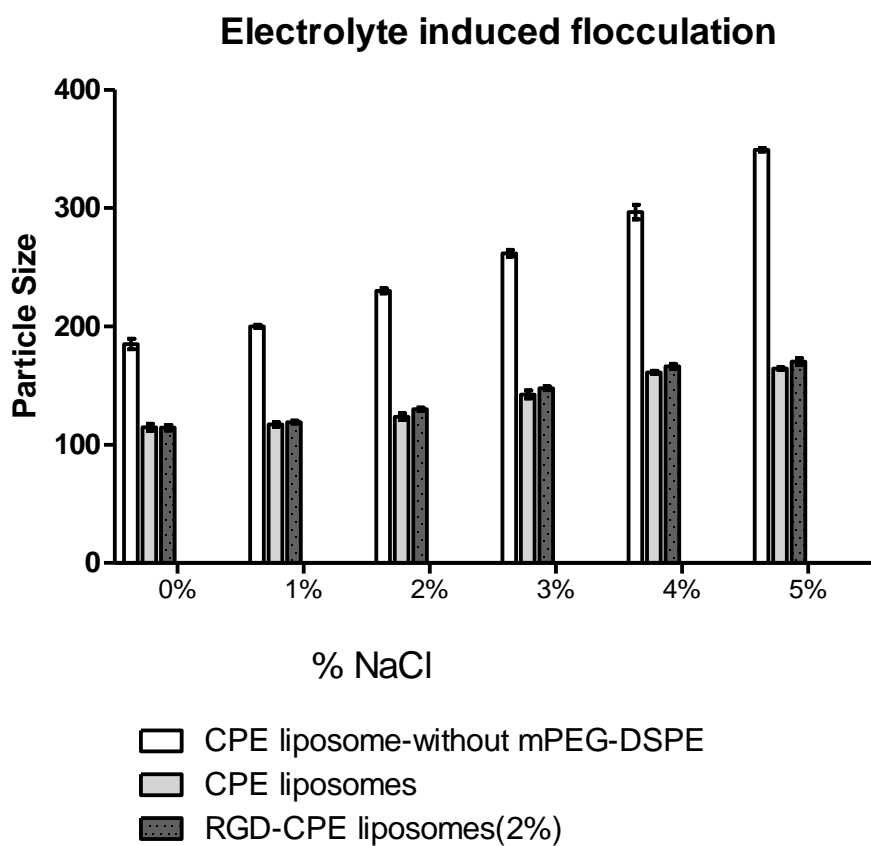


Figure 5.36 Electrolyte Induced Flocculation of CPE Liposomes

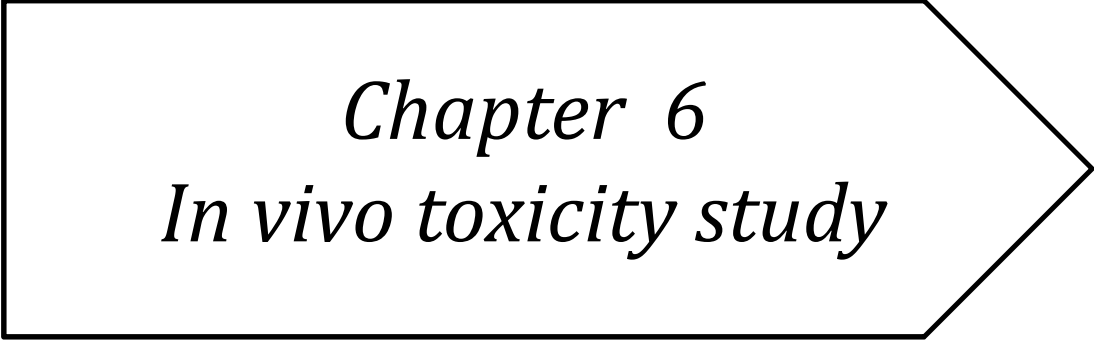
Thus, prepared liposomal formulations of siRNA were found to be stable in presence of electrolytes.

5.6. References

1. Berridge MV, Herst PM, Tan AS. Tetrazolium dyes as tools in cell biology: new insights into their cellular reduction. *Biotechnol Annu Rev.* 2005;11:127-52.
2. Berridge MV, Tan AS. Characterization of the cellular reduction of 3-(4,5-dimethylthiazol-2-yl)-2,5-diphenyltetrazolium bromide (MTT): subcellular localization, substrate dependence, and involvement of mitochondrial electron transport in MTT reduction. *Arch Biochem Biophys.* 1993 Jun;303(2):474-82.
3. Van Dilla MA, Truiullo TT, Mullaney PF, Coultex JR. Cell Microfluorometry: A Method for Rapid Fluorescence Measurement. *Science.* 1969 March 14, 1969;163(3872):1213-4.
4. Lauer SA, Nolan JP. Development and characterization of Ni-NTA-bearing microspheres. *Cytometry.* 2002 Jul 1;48(3):136-45.
5. Baserga R. Recombinant DNA approaches to studying control proliferation: an overview. In: Stein GS, Stein JL, editors. *Recombinant Dna and Cell Proliferation.* UK: Academic Press; 1984. p. 337-60.
6. Hochhauser SJ, Stein JL, Stein GS. Gene Expression and Cell Cycle Regulation. In: G.H. Bourne JFD, Jeon KW, editors. *International Review of Cytology:* Academic Press; 1981. p. 95-243.
7. Baserga R. Introduction to Cell Growth: Growth in Size and DNA Replication. In: Baserga R, editor. *Tissue Growth Factors:* Springer Berlin Heidelberg; 1981. p. 1-12.
8. Tyson JJ. The coordination of cell growth and division — intentional or Incidental? *BioEssays.* 1985;2(2):72-7.
9. Kerker M, Van Dilla MA, Brunsting A, Kratochvil JP, Hsu P, Wang DS, et al. Is the central dogma of flow cytometry true: that fluorescence intensity is proportional to cellular dye content? *Cytometry.* 1982 Sep;3(2):71-8.
10. Rychlik W, Spencer WJ, Rhoads RE. Optimization of the annealing temperature for DNA amplification in vitro. *Nucleic Acids Res.* 1990 Nov 11;18(21):6409-12.
11. Sambrook J, Russel DW. *Molecular Cloning: A Laboratory Manual.* New York, US: Cold Spring Harbor Laboratory Press; 2001.

12. Danhier F, Breton AL, Pr at V. RGD-Based Strategies To Target Alpha(v) Beta(3) Integrin in Cancer Therapy and Diagnosis. *Molecular Pharmaceutics*. 2012 2012/11/05;9(11):2961-73.
13. Bepler G, Kusmartseva I, Sharma S, Gautam A, Cantor A, Sharma A, et al. RRM1 modulated in vitro and in vivo efficacy of gemcitabine and platinum in non-small-cell lung cancer. *Journal of clinical oncology*. 2006 Oct 10;24(29):4731-7.
14. Saloustros E, Mavroudis D, Georgoulis V. Paclitaxel and docetaxel in the treatment of breast cancer. *Expert Opin Pharmacother*. 2008 Oct;9(15):2603-16.
15. Lyseng-Williamson KA, Fenton C. Docetaxel: a review of its use in metastatic breast cancer. *Drugs*. 2005;65(17):2513-31.
16. McGuire WP, 3rd, Markman M. Primary ovarian cancer chemotherapy: current standards of care. *Br J Cancer*. 2003 Dec;89 Suppl 3:S3-8.
17. Dykxhoorn DM, Palliser D, Lieberman J. The silent treatment: siRNAs as small molecule drugs. *Gene Ther*. 2006 Mar;13(6):541-52.
18. Layzer JM, McCaffrey AP, Tanner AK, Huang Z, Kay MA, Sullenger BA. In vivo activity of nuclease-resistant siRNAs. *RNA*. 2004 May;10(5):766-71.
19. McCaffrey AP, Meuse L, Pham TT, Conklin DS, Hannon GJ, Kay MA. RNA interference in adult mice. *Nature*. 2002 Jul 4;418(6893):38-9.
20. Oku N, Namba Y. Glucuronate-modified, long-circulating liposomes for the delivery of anticancer agents. *Methods Enzymol*. 2005;391:145-62.
21. Lundbaek JA, Andersen OS. Lysophospholipids modulate channel function by altering the mechanical properties of lipid bilayers. *J Gen Physiol*. 1994 Oct;104(4):645-73.
22. Niki E, Komuro E, Takahashi M, Urano S, Ito E, Terao K. Oxidative hemolysis of erythrocytes and its inhibition by free radical scavengers. *J Biol Chem*. 1988 Dec 25;263(36):19809-14.
23. Tanaka Y, Mashino K, Inoue K, Nojima S. Mechanism of human erythrocyte hemolysis induced by short-chain phosphatidylcholines and lysophosphatidylcholine. *J Biochem*. 1983 Sep;94(3):833-40.
24. Bierbaum TJ, Bouma SR, Huestis WH. A mechanism of erythrocyte lysis by lysophosphatidylcholine. *Biochim Biophys Acta*. 1979 Jul 19;555(1):102-10.

25. van der Woude I, Visser HW, ter Beest MB, Wagenaar A, Ruiters MH, Engberts JB, et al. Parameters influencing the introduction of plasmid DNA into cells by the use of synthetic amphiphiles as a carrier system. *Biochim Biophys Acta*. 1995 Nov 22;1240(1):34-40.
26. Grit M, Crommelin DJ. Chemical stability of liposomes: implications for their physical stability. *Chem Phys Lipids*. 1993 Sep;64(1-3):3-18.
27. Heurtault B, Saulnier P, Pech B, Proust JE, Benoit JP. Physico-chemical stability of colloidal lipid particles. *Biomaterials*. 2003 Oct;24(23):4283-300.
28. Zuidam NJ, Crommelin DJA. Differential scanning calorimetric analysis of dipalmitoylphosphatidylcholine-liposomes upon hydrolysis. *International Journal of Pharmaceutics*. 1995 12/29;126(1-2):209-17.
29. Zuidam NJ, Gouw HK, Barenholz Y, Crommelin DJ. Physical (in) stability of liposomes upon chemical hydrolysis: the role of lysophospholipids and fatty acids. *Biochim Biophys Acta*. 1995 Nov 22;1240(1):101-10.
30. Bosch FH, Werre JM, Roerdinkholder-Stoelwinder B, Huls TH, Willekens FL, Halie MR. Characteristics of red blood cell populations fractionated with a combination of counterflow centrifugation and Percoll separation. *Blood*. 1992 Jan 1;79(1):254-60.
31. Prete PS, Malheiros SV, Meirelles NC, de Paula E. Quantitative assessment of human erythrocyte membrane solubilization by Triton X-100. *Biophys Chem*. 2002 May 23;97(1):1-5.
32. Elimelech M, Jia X, Gregory J, Williams R. Particle Deposition & Aggregation: Measurement, Modelling and Simulation. US: Elsevier Inc.; 1995.
33. Gregory J. Monitoring particle aggregation processes. *Adv Colloid Interface Sci*. 2009 Mar-Jun;147-148:109-23.
34. Holthoff H, Schmitt A, Fernandez-Barbero A, Borkovec M, Cabrerizo-Vilchez Ma, Schurtenberger P, et al. Measurement of Absolute Coagulation Rate Constants for Colloidal Particles: Comparison of Single and Multiparticle Light Scattering Techniques. *Journal of Colloid and Interface Science*. 1997;192(2):463-70.
35. Lin MY, Lindsay HM, Weitz DA, Ball RC, Klein R, Meakin P. Universality in colloid aggregation. *Nature*. 1989 06/01/print;339(6223):360-2.



Chapter 6
In vivo toxicity study

6.1. Acute Toxicity Study

In vivo acute toxicity studies on animals are an essential part of drug development process. Such acute toxicity studies are carried out for various objectives i.e.

1. To determine the Median Lethal Dose (LD_{50}) after a single dose administered through one or more routes, one of which is the intended route of administration in humans.
2. To determine Maximum Tolerated Dose (MTD) and No Observable Effect Level (NOEL).
3. To identify potential target organs for toxicity, determine reversibility of toxicity, and identify parameters for clinical monitoring.
4. To help select doses for repeated-dose toxicity tests.

A number of methods are available to have an insight about the acute toxicity of any chemical or drug product. These include classical Litchfield and Wilcoxon method (Dosing of animals of both sex with increasing amounts of chemical and plotting dose-response curve to determine LD_{50} /MTD). This type of study has a disadvantage that it uses a large number of animals. So two methods are available now as alternatives which reduces the use of animals i.e. Fixed Dose Procedure (FDP) [1] and Up-Down Procedure (UDP) [2]. Both methods produce data consistent with classical LD_{50} methods [3, 4]. Among these methods Up-Down procedure requires the least number of animals (6-10) of single sex and provides results in terms of LD_{50} along with data for the hazard classification system, unlike FDP that does not estimate results in terms of LD_{50}^{value} [5]. Instead FDP gives better evaluation of the maximum tolerated dose of drug/drug product.

MTD of a drug can be defined as the highest dose of a drug or treatment that does not cause unacceptable side effects. The maximum tolerated dose is determined in clinical trials by testing increasing doses on different groups of people until the highest dose with acceptable side effects is found. Toxicity parameters to be considered include,

1. Mortality
2. Clinical pathology
3. Gross necropsy
4. Weight change

5. Signs of toxicity – convulsions, rashes, akinesia, licking, tremors

Drug doses at or below this level should not induce [6]

- Overt toxicity, for example appreciable death of cells or organ dysfunction,
- Toxic manifestations that are predicted materially to reduce the life span of the animals except as the result of neoplastic development or
- 10% or greater retardation of body weight gain as compared with control animals.

In some studies, toxicity that could interfere with a carcinogenic effect is specifically excluded from consideration.

For determination of MTD of siRNA loaded liposomes, fixed dose procedure of OECD-Organization for Economic Cooperation and Development was used. Typical protocol includes administration of a drug/drug product in escalating doses through intravenous route and observing animals for any signs of toxicity.

6.2. Description of the Methods

All experiments and protocol described in the present study were approved by the Institutional Animal Ethical Committee (IAEC) of Pharmacy Department, The M. S. University of Baroda and with permission from committee for the purpose of control and supervision of experiments on Animals (CPCSEA), Ministry of Social Justice and Empowerment, Government of India.

6.2.1. Selection of Animals Species

Female Swiss Albino mice (Wistar Strain) were used for the study as females are generally slightly more sensitive to such studies [4]. Healthy young adult animals (with 8-12 weeks age) which were nulliparous and non-pregnant were used for study.

6.2.2. Housing and Feeding Conditions

The temperature in the animal room was 20-25°C. Artificial lighting with the sequence of 12 hr light and 12 hr dark was kept in animal housing. The animals were housed individually. For feeding, conventional rodent laboratory diets was used with an unlimited supply of drinking water.

6.2.3. Preparation of Animals

The animals were randomly selected, marked to permit individual identification, and kept in their cages for at least 5 days prior to dosing for acclimatisation to the laboratory conditions.

6.2.4. Preparation of Doses

Test substances (siRNA loaded Liposomes) were administered in a constant dose volume of 20 mL/kg by varying the concentration of the dosing preparation. (The dosing volume was chosen such that the volume did not exceed 2 mL/100g bodyweight). All doses were prepared prior to administration. Above certain dose, only liposomal carrier was tested to ascertain the safety profile of developed liposomal carrier systems.

siRNA loaded liposomes' lyophilized formulation was reconstituted with sufficient quantities of normal saline to produce siRNA concentrations desired for administration. All the test substances were sterilized by filtering through 0.2 μ membrane filter prior to administration.

6.2.5. Procedures

6.2.5.1. Administration of Doses

Prior to dosing, all the animals were fasted by withholding food but not water for 3-4 hr. The fasted body weight of each animal was determined and the dose was calculated according to the body weight.

The test substances were administered via tail vein of animals using sterile single use disposable polystyrene syringes. In the circumstance that a single dose was not possible, the dose was given in smaller fractions over a period not exceeding 24 hr at 1hr time gap between two doses.

After the substances were administered, mice were withheld from food for 1-2 hr except for the case where dosing is done in fractions.

6.2.5.2. Main Test

The test substance was administered in a single dose by intravenous injection using a polystyrene single-use disposable injection. In the unusual circumstance that a single dose was not possible, the dose was given in smaller fractions over a period not exceeding 24 hr.

Animals should be fasted prior to dosing (e.g. with the rat, food but not water was withheld overnight; with the mouse, food but not water was withheld for 3-4 hr). Following the period of fasting, the animals weighed and the test substance was administered. After the substance was administered, food was withheld for a further 3-4 hr in rats or 1-2 hr in mice. Where a dose was administered in fractions over a period of time, animals were provided with food and water depending on the length of the period.

6.2.5.3. Sighting Study

The purpose of the sighting study was to allow selection of the appropriate starting dose for the main study. The test substance was administered to single animals in a sequential manner starting from DOSE_{first} to DOSE_{last}. The sighting study was completed when a decision on the starting dose for the main study was made (or if a death is seen at the lowest fixed dose).

The starting dose for the sighting study was selected from the fixed dose levels as described in Table 6.1. Starting dose selection was obtained from the available literature showing toxicological data for specific chemicals.

6.2.5.4. MTD Determination

Single animals were dosed in sequence usually at 48 hr interval. The first animal was dosed at a level selected from the sighting study. A period of at least 24 hr was allowed between the dosing of each animal. All animals were observed for at least 14 days for any signs of toxicity.

If the animal survived, the second animal received a higher dose. If the first animal died or appeared moribund (Moribund status: being in a state of dying or inability to survive, even if treated), the second animal was administered a lower dose.

Animals were euthanized by intraperitoneal injection of pentobarbital (50 mg/ml) after study or if moribund status (inability to ambulate, inflammation, anorexia, dehydration, or more than 20% weight loss) was observed. The weight of each animal was recorded immediately before intravenous injection, 1 day after injection, and at the end of study.

6.2.5.5. Numbers of Animals and Dose Levels

1. The action to be taken following testing at the starting dose level is indicated based on the observations. One of three actions will be required; either stop testing and assign the appropriate hazard classification class, test at a higher fixed dose or test at a lower fixed dose. However, to protect animals, a dose level that caused death in the sighting study was not revisited in the main study.
2. A total of five animals of female sex were used for each dose level investigated. The five animals were made up of one animal from the sighting study dosed at the selected dose level together with an additional four animals.
3. The time interval between dosing at each level was determined by the onset, duration, and severity of toxic signs. Treatment of animals at the next dose was delayed until there was confidence of survival of the previously dosed animals. A period of 3 or 4 days between dosing at each dose level is recommended, if needed, to allow for the observation of delayed toxicity. The time interval may be adjusted as appropriate, e.g., in case of inconclusive response.

6.2.5.6. Observations

Animals were observed individually after dosing at least once during the first 30 min, periodically during the first 24 hr, with special attention given during the first 4 hours, and daily thereafter, for a total of 14 days, except where they needed to be removed from the study and humanely killed for animal welfare reasons or were found dead.

Observations included were changes in skin and fur, eyes and mucous membranes, and also respiratory, circulatory, autonomic and central nervous systems, and somatomotor activity and behavior pattern. Attention was directed to observations of tremors, convulsions, salivation,

diarrhea, lethargy, sleep and coma. Animals found in a moribund condition and animals showing severe pain or enduring signs of severe distress were humanely killed.

Loss of weight, if more than 20% of initial, or death of animal was considered a positive response at short term outcome (during first 24 hr). For long term outcome death was used as a termination point to stop the test. The duration of observation was determined by the toxic reactions, time of onset and length of recovery period. The times at which signs of toxicity appear and disappear were considered important, especially if there was a tendency for toxic signs to be delayed [7]. All observations were systematically recorded, with individual records being maintained for each animal.

6.3. Results and Discussion

Liposomal formulations, RGD-DDHC liposomes and RGD-CPE liposomes were administered intravenously to the female Swiss Albino mice with and without siRNA loading as given below (**Table 6.1**) during sighting study in single mice. At the dose 0.75 mg/kg of siRNA, lipid concentrations was found to be about 40 mg/kg and 150 mg/kg for RGD-DDHC and RGD-CPE liposomes respectively. Hence, to determine the starting dose for liposomal carrier only, 50 mg/kg (RGD-DDHC liposomes) and 200 mg/kg (CPE-DDHC liposomes) of lipids were used.

Table 6.1 Sighting Study: Dosing protocol

Sr.No.	Formulation	Dose (mg/kg)		
		0.5 mg/kg of siRNA	0.75 mg/kg of siRNA	-
1.	RGD-DDHC liposomes	0.5 mg/kg of siRNA	0.75 mg/kg of siRNA	-
2.	RGD-CPE liposomes	0.5 mg/kg of siRNA	0.75 mg/kg of siRNA	-
3.	RGD-DDHC liposomes (Placebo)	50 mg/kg of lipids	100 mg/kg of lipids	150 mg/kg of lipids
4.	RGD-CPE liposomes (Placebo)	200 mg/kg of lipids	300 mg/kg of lipids	400 mg/kg of lipids
5.	Normal Saline	-	-	-

All animals were found healthy and no sign of any toxicity was appeared. Results for sighting studies are summarized in **Table 6.2**.

Table 6.2 Results of Sighting Study

Formulation	Animal No.	Dose	Observation	
			Toxicological Signs/symptoms*	Mortality
RGD-DDHC liposomes	1.	0.5 mg/kg of siRNA	None	None
	2.	0.75 mg/kg of siRNA	None	None
RGD-CPE liposomes	3.	0.5 mg/kg of siRNA	None	None
	4.	0.75 mg/kg of siRNA	None	None
RGD-DDHC liposomes (Placebo)	5.	50 mg/kg of lipids	None	None
	6.	100 mg/kg of lipids	None	None
	7.	150 mg/kg of lipids	None	None
RGD-CPE liposomes (Placebo)	8.	200 mg/kg of lipids	None	None
	9.	300 mg/kg of lipids	None	None
	10.	400 mg/kg of lipids	None	None

*Observations included were changes in skin and fur, eyes and mucous membranes, respiratory distress, symptoms related to autonomic and central nervous systems including tremors, convulsions etc., lethargy, and coma.

After performing the sighting study maximum dose in each group was selected as a starting dose and main test was performed using the dosing protocol shown in **Table 6.3**. Due to lack of literature available for exact therapeutic concentration of RRM1 siRNA, 0.75 mg/kg was selected as maximum dose for MTD study. However, chemosensitization may be governed at very less concentration as compared to this dose. Dosing sequences were limited to 300 mg/kg and 600 mg/kg for RGD-DDHC liposomes (Placebo) and RGD-CPE liposomes (Placebo) respectively. At these much higher doses, amount of siRNA loading would be much higher than that required for therapeutic efficacy and hence sufficient to prove safety profile for the developed non-viral siRNA delivery lipid carriers.

Table 6.3 MTD Study: Dosing Protocol

Sr.No.	Group No.	Formulation	Dose		
1.	1	Normal Saline	-		
2.	2	RGD-DDHC liposomes	0.75 mg/kg of siRNA		
3.	3	RGD-CPE liposomes	0.75 mg/kg of siRNA		
4.	4A,4B,4C	RGD-DDHC liposomes (Placebo)	150 mg/kg of lipids (4A)	200 mg/kg of lipids (4B)	300 mg/kg of lipids (4C)
5.	5A,5B,5C	RGD-CPE liposomes (Placebo)	400 mg/kg of lipids (5A)	500 mg/kg of lipids (5B)	600 mg/kg of lipids (5C)

Results for the MTD study is summarised in **Table 6.4**. MTD study was performed in group of five mice, where one mouse was collected from sighting study. All groups showed no sign of toxicity after administration of test substance. In all groups MTD values were considered as greater than maximum administered dose i.e. >0.75 mg/kg of siRNA for both; RGD-DDHC liposomes and RGD-CPE liposomes, >300 Mg/kg of total lipids for RGD-DDHC liposomes (placebo), > 600 mg/kg of total lipids for RGD-CPE liposomes (placebo).

Table 6.4 Results for MTD study

Sr.No.	Group No.	Weight (g) (Mean \pm SEM)			Observation	
		Initial	After 1 day	After 14 days	Toxicological Signs/symptoms*	Mortality
1.	1	30.1 \pm 0.13	29.7 \pm 0.38	30.3 \pm 0.17	None	None
2.	2	29.7 \pm 0.24	30.1 \pm 0.43	30.2 \pm 0.38	None	None
3.	3	31.4 \pm 0.22	31.2 \pm 0.33	31.4 \pm 0.31	None	None
4.	4A	30.4 \pm 0.37	30.7 \pm 0.35	30.7 \pm 0.14	None	None
5.	4B	29.5 \pm 0.19	29.0 \pm 0.27	30.1 \pm 0.26	None	None
6.	4C	30.2 \pm 0.16	29.6 \pm 0.30	30.4 \pm 0.41	None	None
7.	5A	31.6 \pm 0.10	31.8 \pm 0.29	31.9 \pm 0.39	None	None
8.	5B	30.5 \pm 0.38	31.3 \pm 0.38	32.1 \pm 0.20	None	None
9.	5C	30.2 \pm 0.23	29.5 \pm 0.33	29.7 \pm 0.25	None	None

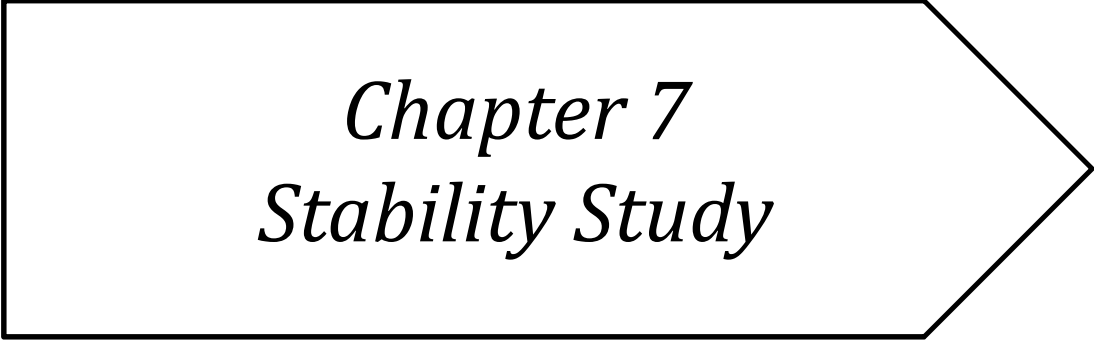
*Experiments were performed in triplicate.

All excipients (except DOTAP and DOPE) used in the formulations are approved for intravenous route according to USFDA and were used at a concentration below IIG limit. DOTAP is a cationic lipid and many literatures have described the in-vitro toxicity for the use of DOTAP as a transfecting agent. However, incorporation of DOTAP in to liposomal bilayer and use of very less quantity as compared to total lipids used in formulation, make this substance safe at above tested concentrations. DOPE is a non-ionic lipid and did not impart toxicity at the above tested concentrations. Conclusively, both the developed liposomal carriers are safe for in-vivo application.

From the results of the study, it can be concluded that optimized siRNA liposomal formulations were non-toxic at therapeutic concentrations to be used for chemosensitization.

6.4. References

1. OECD GUIDELINE FOR TESTING OF CHEMICALS Fixed Dose Procedure, Guideline 420, 1-14 (2001).
2. OECD GUIDELINE FOR TESTING OF CHEMICALS Up-and-Down Procedure, Guideline 425, 1-14 (2001).
3. Whitehead A, Curnow RN. Statistical evaluation of the fixed-dose procedure. *Food and Chemical Toxicology*. 1992 4//;30(4):313-24.
4. Lipnick RL, Cotruvo JA, Hill RN, Bruce RD, Stitzel KA, Walker AP, et al. Comparison of the up-and-down, conventional LD50, and fixed-dose acute toxicity procedures. *Food Chem Toxicol*. 1995 Mar;33(3):223-31.
5. Festing MF. The design and statistical analysis of animal experiments. *ILAR J*. 2002;43(4):191-3.
6. IUPAC. Compendium of Chemical Terminology netGBCbADMaAWBSP, Oxford (1997). XML on-line corrected version: <http://goldbook.iupac.org> (2006-) created by M. Nic, J. Jirat, B. Kosata; updates compiled by A. Jenkins. ISBN 0-9678550-9-8. doi:10.1351/goldbook.
7. Chan PK, Hayes AW. Acute Toxicity and Eye Irritation. In: Hayes AW, editor. Principles and Methods of Toxicology. New York, US: Raven Press, Ltd.; 1994.



Chapter 7
Stability Study

7.1. Stability Studies of Liposomes

For liposomal products an attention has been focused on two processes affecting the quality and therefore acceptability of liposomes [1]. Especially, with liposomal product to see the market it should stable during the shelf life (storage or transport). In general, a shelf life of at least one year is a minimum prerequisite criterion for a commercial product. First leakage of entrapped molecules from the vesicles may take place into the extra liposomal compartment. Secondly, there is a possibility of liposomal aggregation and/or fusion, which leads to formation of larger particles [2-5]. These parameters will alter the *in vivo* fate, affecting therapeutic index of the entrapped biomacromolecules. Hydrolysis of phospholipids is one of the parameters like to cause the formation of fatty acids and lysophospholipids [6, 7]. Although under dehydrated storage, there is least possibility of the formulation to encounter hydrolytic degradation. Another aspect to be considered is liposome oxidation [8]. Stability is considered as chemical stability of drug substance in a dosage form. However, the performance of liposomal formulation is not only dependent upon the content of the drug substance, but also dependent on reproducible *in vivo* performance of the formulations. Formulations under stability studies were considered chemically stable by evaluating the siRNA leakage from liposomes. The stability protocol was designed as per ICH guidelines [9] for countries falling under zone III (hot, dry) and zone IV (very hot, humid) [10].

7.2. Method

Comparative stability studies were carried out of the potential liposomal formulations at accelerated condition ($25^{\circ}\text{C} \pm 2^{\circ}\text{C}$, $60\% \text{ RH} \pm 5\% \text{ RH}$) for six months and at long-term conditions ($2-8^{\circ}\text{C}$) up to six months. Liposomal formulations were filled into type-1 tubular glass vials, purged with nitrogen, sealed and stored at the above mentioned condition [11-18]. At each sampling time different vial was used for the stability testing.

The liposomal formulations were examined visually for the evidence of discoloration. The content of the vials were tested for percentage siRNA entrapment, particle size, zeta-potential, assay and water content (for RGD-DDHC liposomes (2%) only). The stability results are summarized in **Table 7.1** and **Table 7.2**.

7.3. Results and Discussion

The physical stability of liposomes is one of the biggest obstacles in formulation commercially viable product [19]. Liposomes should be stable for 1-2 years preferably at room temperature or refrigerated condition, whichever is storage temperature, to be pharmaceutically acceptable with high siRNA retention within liposome and the particle size should be maintained during storage time, hence the siRNA leakage, particle size growth, change in zeta-potential and the chemical stability of siRNA were studied at accelerated condition ($25^{\circ}\text{C} \pm 2^{\circ}\text{C}$, $60\% \text{ RH} \pm 5\% \text{ RH}$) for six months and at long-term conditions ($2-8^{\circ}\text{C}$) up to six months. No significant differences ($p > 0.05$) were found in all above mentioned parameters at refrigerated condition.

7.3.1 Stability Testing of RGD-DDHC Liposomes(2%)

The stability testing of prepared **RGD-DDHC liposomes(2%)** was performed at accelerated condition ($25^{\circ}\text{C} \pm 2^{\circ}\text{C}$, $60\% \text{ RH} \pm 5\% \text{ RH}$) for six months and at long-term conditions ($2-8^{\circ}\text{C}$) up to six months and the effect on various parameters was studied. Results of the study are reported below (**Table 7.1**).

At both accelerated and refrigerated conditions, Assay and siRNA entrapment values were found to be within range (95-105% of initial) and change was non-significant ($p > 0.05$). There was no significant increase ($p > 0.05$) in particle size after six month at both conditions and same results were shown by zeta potential values. Water content was increased to a significant extent ($p < 0.05$) at accelerated condition while refrigerated condition maintained the water content value even after six months of storage. Thus, formulation is stable at both conditions after six months.

Table 7.1 Stability Testing Data of RGD-DDHC Liposomes (2%)*

Sampling time (Month)	Description	Assay (%)	siRNA entrapment (%)	Water content (%)	Particle size (d.nm)	Particle distribution Index	Zeta potential (mV)
Initial	White lyophilized cake	102.67 ±3.74	98.20 ±3.34	1.89 ±0.10	147.5 ±2.13	0.164	12.26 ±0.65
Accelerated condition (25°C ± 2°C, 60% RH ± 5% RH)							
1	White lyophilized cake	100.09 ± 2.25	97.83 ±3.10	1.96 ±0.17	148.5 ±2.04	0.120	12.36 ±0.72
2	White lyophilized cake	99.42 ± 1.48	97.73 ±2.52	2.51 ±0.34	156.2 ±2.82	0.204	13.48 ±1.23
3	White lyophilized cake	97.33 ± 2.04	96.51 ±1.95	3.09 ±0.24	174.7 ±3.79	0.147	12.39 ±1.21
6	White lyophilized cake	97.79 ± 4.03	96.03 ±0.97	3.79 ±0.19	169.3 ±3.20	0.103	13.37 ±1.10
Long-term conditions (2-8°C)							
1	White lyophilized cake	101.07 ± 2.83	97.36 ±1.69	1.86 ±0.18	148.9 ±2.02	0.173	12.73 ±1.20
2	White lyophilized cake	100.34 ± 3.22	98.01 ±2.30	1.91 ±0.33	158.0 ±3.71	0.242	12.08 ±1.73
3	White lyophilized cake	102.32 ± 2.20	96.32 ±2.75	2.14 ±0.20	163.3 ±1.98	0.121	13.83 ±1.16
6	White lyophilized cake	101.28 ±2.03	96.06 ±3.02	2.52 ±0.31	162.4 ±2.90	0.239	13.73 ±1.43

*Results are expressed as mean±standard deviation (n=3).

7.3.2 Stability Testing of RGD-CPE Liposomes (2%)

The stability testing of prepared **RGD-CPE liposomes(2%)** was performed at accelerated condition (25°C ± 2°C, 60% RH ± 5% RH) for six months and at long-term conditions (2-8°C) up to six months and the effect on various parameters was studied. Results of the study are reported below (**Table 7.2**).

At accelerated condition, Assay value and siRNA entrapment were found to decrease significantly as compared to initial values ($p < 0.05$). Particle size was also increased significantly ($p < 0.05$) from first month only. These effects might be due to degradation of siRNA in liquid state as 25°C. Recommended storage is also at refrigerated condition or below in liquid state. In case of 2-8°C condition, Assay and siRNA entrapment values were found to decrease in a non-significant ($p > 0.05$) manner and found within range (95-105% of initial value). However, particle size was found to decrease but it was maintained below

150 nm. Taken collectively, these result suggest that RGD-CPE liposomes are stable at 2-8°C but not at accelerated condition after six month.

Table 7.2 Stability Testing Data of RGD-CPE Liposomes(2%)

Sampling time (Month)	Description	Assay (%)	siRNA entrapment (%)	Particle size [Z-Average (d.nm)]	Particle distribution Index	Zeta potential (mV)
Initial	Translucent liposomal dispersion	102.27 ±2.86	84.19 ±2.89	115.71 ±2.01	0.104	11.45 ±0.44
Accelerated condition (25°C ± 2°C, 60% RH ± 5% RH)						
1	Translucent liposomal dispersion	101.08 ±3.71	81.53 ±2.64	152.14 ± 2.42	0.297	13.53 ±1.73
2	Translucent liposomal dispersion	98.54 ±2.03	80.62 ±3.24	164.26 ±2.82	0.138	12.94.6 ±1.30
3	Translucent liposomal dispersion	96.02 ±3.82	76.39 ±3.07	173.05 ±3.17	0.232	13.30 ±2.82
6	Translucent liposomal dispersion	94.62 ±2.90	75.80 ±1.87	189.52 ±3.74	0.184	12.47 ±2.04
Long-term conditions (2-8°C)						
1	Translucent liposomal dispersion	101.04 ±3.32	83.09 ±2.42	129.5 ±3.43	0.135	11.29 ±0.89
2	Translucent liposomal dispersion	99.82 ±2.88	84.35 ±2.34	124.4 ±3.08	0.270	12.42 ±2.38
3	Translucent liposomal dispersion	98.60 ±1.98	81.93 ±3.02	135.7 ±2.26	0.120	12.35 ±1.02
6	Translucent liposomal dispersion	98.04 ±2.95	80.04 ±3.59	147.8 ±3.53	0.327	13.84 ±1.93

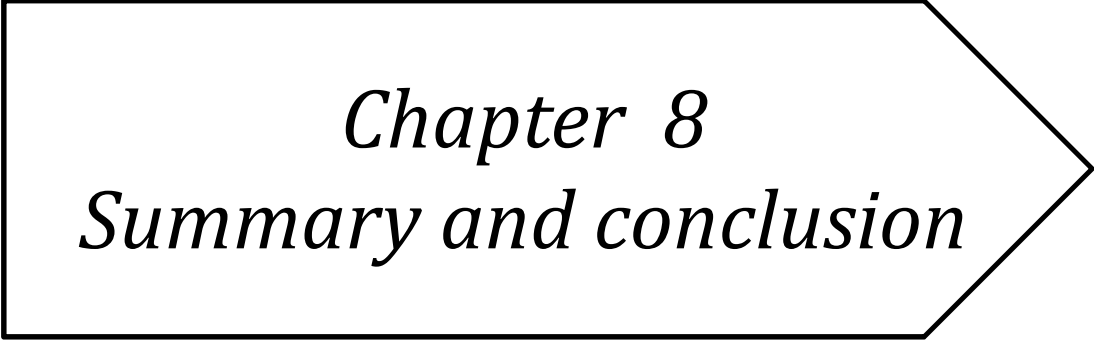
*Results are expressed as mean±stadard deviation (n=3).

Assay, percentage siRNA entrapment, particle size and zeta-potential were found to be in range but increase in water content suggest that RGD-DDHC liposomes should be stored at refrigerated condition, because water content may start degrading the siRNA on aging at accelerated condition (25°C ± 2°C, 60% RH ± 5% RH). The decrease in assay, percentage siRNA entrapment, particle size and zeta-potential suggest that RGD-CPE liposomes should be stored at refrigerated condition (2-8°C) only.

7.4. References

1. Talsma H, Crommelin DJ. Liposomes as Drug Delivery Systems, Part III: Stabilization. *Pharmaceutucial Technology*. 1992;17:48-59.
2. Grit M, Crommelin DJ. The effect of aging on the physical stability of liposome dispersions. *Chem Phys Lipids*. 1992 Sep;62(2):113-22.
3. Cliff RO, Ligler F, Goins B, Hoffmann PM, Spielberg H, Rudolph AS. Liposome encapsulated hemoglobin: long-term storage stability and in vivo characterization. *Biomater Artif Cells Immobilization Biotechnol*. 1992;20(2-4):619-26.
4. Fang JY, Lin HH, Hsu LR, Tsai YH. Characterization and stability of various liposome-encapsulated enoxacin formulations. *Chem Pharm Bull (Tokyo)*. 1997 Sep;45(9):1504-9.
5. Slabbert C, Plessis LH, Kotze AF. Evaluation of the physical properties and stability of two lipid drug delivery systems containing mefloquine. *Int J Pharm*. 2011 May 16;409(1-2):209-15.
6. Mowri H, Nojima S, Inoue K. Effect of lipid composition of liposomes on their sensitivity to peroxidation. *J Biochem*. 1984 Feb;95(2):551-8.
7. Grit M, Zuidam NJ, Underberg WJ, Crommelin DJ. Hydrolysis of partially saturated egg phosphatidylcholine in aqueous liposome dispersions and the effect of cholesterol incorporation on hydrolysis kinetics. *J Pharm Pharmacol*. 1993 Jun;45(6):490-5.
8. Frokjaer S, Hjorth EL, Worts O. Stability testing of liposomes during storage. In: Gregoriadis G, editor. *Liposome Technology: Preparation of Liposomes*. Boca Raton, Florida, US: CRC Press; 1984. p. 235-45.
9. Singh S. Drug stability testing and shelf-life determination according to international guidelines. *Pharm Technol*. 1999;23:68-88.
10. US FDA (CDER), Draft Guidance for Industry Liposome Drug Products. CMC Documentation.
11. Ugwu S, Zhang A, Parmar M, Miller B, Sardone T, Peikov V, et al. Preparation, characterization, and stability of liposome-based formulations of mitoxantrone. *Drug Dev Ind Pharm*. 2005 Jan;31(2):223-9.
12. Winterhalter M, Lasic DD. Liposome stability and formation: experimental parameters and theories on the size distribution. *Chem Phys Lipids*. 1993 Sep;64(1-3):35-43.

13. Changsan N, Chan HK, Separovic F, Srichana T. Physicochemical characterization and stability of rifampicin liposome dry powder formulations for inhalation. *J Pharm Sci.* 2009 Feb;98(2):628-39.
14. Yang T, Cui FD, Choi MK, Lin H, Chung SJ, Shim CK, et al. Liposome formulation of paclitaxel with enhanced solubility and stability. *Drug Deliv.* 2007 Jul;14(5):301-8.
15. Anderson M, Omri A. The effect of different lipid components on the in vitro stability and release kinetics of liposome formulations. *Drug Deliv.* 2004 Jan-Feb;11(1):33-9.
16. Manosroi A, Podjanasoonthon K, Manosroi J. Stability and release of topical tranexamic acid liposome formulations. *J Cosmet Sci.* 2002 Nov-Dec;53(6):375-86.
17. Manosroi A, Kongkaneramt L, Manosroi J. Characterization of amphotericin B liposome formulations. *Drug Dev Ind Pharm.* 2004 May;30(5):535-43.
18. Bhalerao SS, Raje Harshal A. Preparation, optimization, characterization, and stability studies of salicylic acid liposomes. *Drug Dev Ind Pharm.* 2003 Apr;29(4):451-67.
19. Fildes F. Liposomes: The Industrial view point. In: *Liposomes from Physical Structure to Therapeutic Applications*. Knight C, editor. New York, US: Elsevier Biomedical Press; 1998.



Chapter 8
Summary and conclusion

8.1. Summary

Lung cancer is the most common cancer in developed and developing nations. India faces about 10% of the world lung cancer incidents. The most common etiological factor for the cause of lung cancer is smoking, which is on the rise in India. Lung cancer carried mostly by long term exposure to tobacco smoke accounts for more than 1.5 million deaths worldwide annually, with 80% mortality within a year of diagnosis. Lung cancer is currently treated with intravenous administration of chemotherapeutic agents but is non-selective as it cannot differentiate between host cells and cancer cells leading to normal cell toxicity. Further, the diagnostic tools available currently can inadequately detect the tumors and hence render the condition dejected. This provides impetus to pursue the research for effectively treating the lung cancer.

Lung cancer is well characterized by uninhibited cell growth in lung tissues leading to metastases, invasion to adjacent tissue and infiltration beyond the lungs. The two most common histological types of lung carcinoma include Non-small cell lung carcinoma (NSCLC) and small-cell lung carcinoma (SCLC). NSCLC generally leads to high mortality and hence proves to be very hostile. Although surgery is a preferred method of cancer removal, it cannot remove the tissue completely and is required to be supplemented by multi-drug chemotherapy and/or radiation as preferred treatment of choice. The chief chemotherapeutic agents used in the treatment of NSCLC are camptothecin, paclitaxil, carboplatin, cisplatin, docetaxel, topotecan, etoposide, gemcitabine etc., with their known reported toxicities. The medications are available as injections for systemic use and result in hazardous side effects due to their non specificity on the dividing cells in the body. Intracellular transport of different biologically active molecules is one of the key problems in drug delivery in general. Currently the anticancer agents have poor intracellular concentration in the cancer cells. However, response to consequent systemic treatment is approximately 10% for single agents after the failure of initial therapy. Thus, resistance to systemic therapy does majorly rely on molecular characteristics of individual tumors rather than all-or-none phenomenon.

Ribonucleotide Reductase Subunit 1 (RRM1) gene encodes the regulatory subunit of ribonucleotide reductase, an essential enzyme that catalyses the reduction of ribonucleoside diphosphates to the corresponding deoxyribonucleotides. It is the molecular target of Gemcitabine (2, 2-difluorodeoxycytidine), an antimetabolite with

activity in several malignancies including NSCLC. Previously researchers had suggested that patients with low level of tumoral RRM1 expression had improved survival when treated with Gemcitabine-based chemotherapy as compared to high level of tumoral RRM1 expression. In addition, continuous exposure of lung cancer cell lines to increasing amounts of Gemcitabine resulted in increased RRM1 expression. There are proteins residing inside the cells responsible for the activation and metabolism, and thought to be a sole responsible for drug's action. Gemcitabine is activated in cells by nucleoside kinases to Gemcitabine diphosphate (dFdCDP) and Gemcitabine triphosphate (dFdCTP). The cytotoxic effect of Gemcitabine has been attributed to the combination of two actions that lead to inhibition of DNA synthesis and subsequent apoptosis. First, dFdCDP inhibits ribonucleotide reductase which is required for augmenting the reactions that generate the deoxynucleotides for DNA synthesis and repair. Then, dFdCTP competes with dCTP for incorporation into DNA during replication, which results in a termination of chain elongation.

Recently, one study suggested that resistance to gemcitabine HCl is associated with Ribonucleotide reductase overexpression in several cancer cells. In particular, an increase in the expression of the RRM1 has been associated with gemcitabine resistance in NSCLC cell lines, while clinical studies demonstrated that NSCLC patients with low mRNA expression benefited from gemcitabine chemotherapy.

RNA interference (RNAi) is the process of mRNA degradation that is induced by double stranded RNA in a sequence-specific manner. RNA interference (RNAi) is a conserved cellular mechanism by which a small double stranded RNA (dsRNA) directs the degradation of complementary mRNA and therefore inhibits the expression of a specific gene. The ability to induce RNAi in mammalian cells using synthetic small interfering RNA (siRNA) has stimulated great interest in therapeutic applications of RNAi. In numerous studies, siRNAs have shown promise for treating a variety of diseases, including influenza and HIV infection, cancer and genetic defects. The double stranded RNA-based molecule, siRNA, has a high potential as therapeutic agent but efficient delivery into target cells is a key challenge in RNAi-based therapy. siRNA is generally having 21 nucleotides and highly charged surface with limited diffusion across the cell membrane. Further, siRNA is prone to degradation by nucleases in the circulation and interstitial space. The genetic consequences of cancer strongly support the rationale

behind the use of siRNA-mediated gene therapy in the cancer treatment. Numbers of siRNAs have been designed and investigated to target specific malfunctionally regulated oncogenes, or viral proteins involved in carcinogenesis. Furthermore, researchers have envisaged that therapeutic siRNAs can be utilized for silencing target molecules against tumor–host interactions and tumor resistance to chemotherapy and/or radiotherapy.

During the past few years, RGD peptides have become very popular agent for targeting of therapeutics and imaging agents to cancer tissue over expressing integrin. Various chemical modifications have been applied to attach RGD peptides and its modified forms to liposomes, polymers, peptides and radiotracers. RGD grafted liposomes have been investigated as an impending carrier for tumor targeting of chemotherapeutics. The present research work was aimed to develop stable siRNA nano-constructs using suitable lipid carrier in liposomal form and chemosensitization of the anticancer agent Gemcitabine HCl by pre exposure of siRNA encapsulated liposomes. RGD conjugated siRNA liposomes were used to target non-small cell lung cancer cells to achieve receptor based uptake of liposomal formulations and hence to avoid non selective distribution of siRNA in other tissues.

Spectrophotometric method was used for determination of siRNA content in the formulation. The determination was based on the zero order UV spectra of siRNA at the λ_{max} of 260 nm, developed in nuclease-free water to preserve integrity of siRNA against nucleases. Calibration plot showed a straight line expressed by the equation, $y = 0.0193x + 0.0504$ at 8-40 ppm concentration, with regression coefficient of 0.9994. UV-spectrophotometric method was evaluated for precision and accuracy by determining % recovery and relative standard deviation (%RSD) respectively. The % recovery was found to be between 99.5% to 100.5% and % RSD of interday and intraday measurements were below 1%, and hence, the method was found to comply with FDA and ICH guidelines on accuracy and precision of an analytical method validation.

Direct complexometric titration method was used for analysis of calcium content of liposomes. The determination was based on the formation of 1:1 complex between calcium and ethylene diamine tetraacetic acid (EDTA). Method was found to be linear having r^2 value of 0.9994 and had high accuracy and precision. Calibration plot showed a straight line expressed by the equation, $y = 0.0214x + 0.0757$.

Agarose gel electrophoresis was used for relative quantification of free siRNA migrated on the gel due to differences in the surface charge. Gel electrophoresis was carried out in TBE buffer at 100 and bands were visualized using ethidium bromide. was utilized for gel electrophoresis. The gel electrophoresis data showed that siRNA can be quantified at a minimum of 20 pmole concentration. At lower concentrations (below 20 pmole) the bands were not accurately quantifiable while at higher concentrations distinct bands were observed. To develop a calibration curve for the quantitation of siRNA, relative quantification was used i.e., the band density at highest siRNA concentration (50 pmole) being taken as 1 and evaluating band density of lower concentrations relative to the former. The results were found to be linear with regression coefficient of 0.9952 and the equation representing line was $y = 0.1703x + 0.133$. %recovery and %relative standard deviation of the method were found to be $102.7 \pm 2.6\%$ and 2.55% concluding the adequacy of the analytical method for quantification of siRNA.

Two prototypes of formulations were developed for siRNA delivery i.e. cationic siRNA liposomes and calcium phosphate encapsulated siRNA liposomes.

siRNA containing cationic liposomes were prepared by incubating siRNA with preformed liposomes. Preformed liposomes were prepared by thin film hydration method containing HSPC, cholesterol, DOTAP, DOPE and mPEG₂₀₀₀-DSPE as lipid components and nuclease free water as hydration media. The size of liposomes was the reduced using successive extrusion through 1, 0.4, 0.2 and 0.1 μm polycarbonate membrane filter. Optimized liposomes were grafted with 1, 2 and 3 mole% of RGD by incorporation RGD-mPEG₂₀₀₀-DSPE into the liposome during initial stage of film formation. Liposomes were characterised for particle size and zeta potential, assay, entrapment of siRNA and surface morphology. Process parameters such as organic solvent composition, solvent evaporation time, speed of rotation, hydration time and vacuum applied were optimized to obtain desired formulation characteristics. N/P ratio was optimized to achieve complete complexation of free siRNA with cationic preformed liposomes. Liposomes were developed by incorporating different types of lipids in varying concentrations and finally DD liposomes (containing DOTAP and DOPE), DDH liposomes (containing DOTAP, DOPE and HSPC), DDC liposomes (containing DOTAP, DOPE and cholesterol), DDHC liposomes (containing DOTAP, DOPE, HSPC and cholesterol) and RGD-DDHC liposomes (containing DOTAP, DOPE, HSPC, cholesterol and RGD) were screened on

the basis of optimized N/P ratio for further studies. Here said all screened liposomes were sterically stabilized using mPEG₂₀₀₀-DSPE. Further optimization was performed on the basis of particle size of liposomes after complexation with siRNA. Optimized liposomes showed complete complexation of siRNA above N/P=2.0. However, D liposomes and DD liposomes showed loose complexation at this N/P level and hence were found to be inferior. Particle size of D liposomes, DD liposomes and DDH were found to increase more than 200 nm after complexation with siRNA, while DDC liposomes, DDHC liposomes showed particle size of 174.3±6.7 nm and 145.9±8.7 nm, respectively. RGD grafting on the liposomal surface (1, 2, and 3 mole %) did not affect the size of liposomes significantly as compared to DDHC liposomes and showed particle size below 150 nm. Zeta potential of liposomes were found to decrease after complexation with siRNA. Mean zeta potential values for D liposomes (15.84±0.64 mV), DD liposomes (16.24±0.76 mV), DDH liposomes (13.39±0.87 mV), DDC liposomes (13.52±0.68 mV), DDHC liposomes (12.90±0.68 mV) and RGD-DDHC liposomes were found to lie between 11 to 17 mV as compared to initial values, which were lying between 33-39 mV. Cationic liposomes were lyophilized using sucrose as a cryoprotectant in a concentration of 50 mg/mL.

Assay was determined by Phenol/Chloroform extraction method. Extracted siRNA was collected in aqueous layer and quantified using gel densitometry and UV spectroscopy. All formulations showed no degradation of siRNA during processing and in all formulations, detected siRNA was within limit (95-105%).

All formulations were subjected to study entrapment of siRNA, either encapsulated within liposomes or complexed to the surface. Gel retardation assay method provided amount of free siRNA migration and hence, entrapped siRNA was calculated by deducting the free siRNA from initially added siRNA. Optimized formulations were also subjected to ultracentrifuge method to determine siRNA entrapment by direct analysis of liposomal fraction only, because free siRNA was removed from the supernatant after centrifugation. DDC liposomes and DDHC liposomes showed entrapment efficiency of 97.5±3.60 % and 98.2±1.89 %, respectively, as detected by gel retardation assay. More than 95% of entrapment was achieved in all the optimized formulations and that can be considered as complete complexation of siRNA with pre-formed liposomes. RGD grafting did not affect the entrapment efficacy and difference between with and without RGD grafting was insignificant.

Images obtained by Transmission Electron Microscopy revealed that prepared liposomes were spherical in shape. All vesicles are unilamellar in structure and having particle size below 200 nm. Bilayer thickness was also measured and found to be in-between 5-10 nm in size.

siRNA containing CPE liposomes were prepared in two steps; Step-1: Preparation of calcium phosphate liposomes and Step-2 : Loading of siRNA in calcium phosphate entrapped liposomes. Both steps were optimized individually. However, liposomes prepared in step-1 were consequently used in step-2 and hence, step-2 relied on the product quality obtained from step-1. Calcium phosphate liposomes were prepared by the selected TFH method using DPPC, cholesterol, DOPE and mPEG₂₀₀₀-DSPE. Liposomes were hydrated using calcium chloride solution and Particle size of liposomes was reduced using successively passing through 1, 0.4, 0.2 and 0.1 μm polycarbonate membranes. Unentrapped calcium was removed by passing through sephadex column. Calcium entrapped liposomes were made permeable by addition of ethanol and incubated with disodium hydrogen phosphate solution. This addition allowed formation of calcium phosphate precipitates inside as well as outside of the liposomes. Outer precipitates were removed by centrifugation and unreacted phosphate was removed by passing through sephadex column. These liposomes were added with siRNA in presence of ethanol and incubated at 48°C for 20 minutes. Optimal formulation was further improved by incorporation of cyclic RGD peptide for its capability to target tumor cells. Prepared CPE liposomes were characterised for calcium entrapment by complexometric titration, Assay, entrapment of siRNA, particle size and zeta potential and surface morphology. The size of Liposomes was measured by dynamic light scattering with a Malvern Zetasizer. Assay and entrapment of siRNA were detected as mentioned in above summarised cationic liposomal section.

Liposomes were optimized to maximize entrapment and minimize particle size. Calcium phosphate liposomes (step-1) and siRNA loading (step-2) was optimized using 3³ factorial design by varying lipid:calcium molar ratio (0.1, 0.3 and 0.5), DPPC: cholesterol molar ratio (1.0, 5.0 and 9.0), and concentration of calcium (75, 100 and 125 mg/mL) for step-1 and by varying Calcium:siRNA molar ratio (5.0, 7.0 and 9.0), Lipid:Ethanol molar ratio (1.0, 1.5 and 2.0), and siRNA concentration (10.0, 12.0 and 14.0 $\mu\text{g/mL}$) for step-2 at 3

different levels as low (-1), medium (0) and high (1), by keeping all other process and formulation parameter invariant.

RSM was applied to fit second order polynomial equations, obtained by multiple linear regression analysis (MLRA) approach. Two dimensional contour plots and three dimensional response surface plots were established by varying levels of two factors and keeping the third factor at fixed levels at a time. Optimized formulation was derived by specifying goal and importance to the formulation variables and response parameters.

For calcium phosphate liposomes (obtained from step-1), the optimized batch (lipid:calcium molar ratio= 0.29, DPPC:cholesterol molar ratio = 1.0, and concentration of calcium = 87.72 mg/mL) showed calcium entrapment of 23.470 ± 1.173 and particle size of 114.745 ± 3.101 . Final formulation i.e. calcium phosphate encapsulated siRNA liposomes (step-2) with optimized batch (Calcium:siRNA molar ratio = 6.83, Lipid:Ethanol molar ratio = 1.51, and siRNA concentration = 10.82) showed siRNA entrapment of 83.86 ± 2.19 and particle size 117.85 ± 2.15 .

P-value > 0.05 indicates the differences between predicted and experimental values are statistically insignificant. In checkpoint analysis higher r^2 values (0.9947 and 0.9995 for PDE and PR respectively) of the linear correlation plots suggest excellent goodness of fit and high predictive capability of RSM.

Assay values for CPE and RGD-CPE liposomes were found to lie within the limit i.e. 95-105%. Incorporation of RGD at 1, 2 and 3 mole% did not affect the calcium and siRNA entrapment efficiencies. Calcium entrapment for 1, 2 and 3 mole % RGD incorporated liposomes was found to be 24.37 ± 1.62 %, 23.78 ± 1.09 % and 22.81 ± 1.36 % respectively, while siRNA entrapment was 81.72 ± 3.02 %, 84.19 ± 2.89 % and 82.93 ± 3.45 % respectively. Zeta potential values for CPE liposomes, RGD-CPE liposomes(1%), RGD-CPE liposomes(2%), RGD-CPE liposomes(3%) were found to be 11.90 ± 0.52 , 12.21 ± 0.13 , 11.45 ± 0.44 and 11.23 ± 0.31 respectively. Clear and distinct precipitates were seen during electron microscopy and same can be seen in the images taken from microscopy. Bilayer thickness was also measured and found to be in-between 5-10 nm in size.

Prepared liposomal formulations were characterised for *in vitro* cell line studies. The cytotoxicity of siRNA carriers were determined using 3-(4, 5-dimethylthiazole-2-yl)-2,5-di-phenyl tetrazolium bromide (MTT) assay. cells were treated separately with DD

liposomes, DDC liposomes, DDHC liposomes and RGD-DDHC liposomes at varying N/P ratio ranging from 2.5 to 12.5 in DMEM media containing 10% FBS and antibiotics. In case of CPE liposomes and RGD-CPE liposomes cytotoxicity was carried out using increasing amount of CPE liposomes by varying Ca:siRNA ratio (5.0 to 15.0). Cells treated with PBS were considered as negative control and commercially available non-viral lipid transfecting carrier Lipofectamine 2000 was kept as positive control. It was seen that at N/P of 2.5 DDHC (composed of DOTAP, DOPE, HSPC and Cholesterol) and RGD grafted DDHC liposomes were significantly less toxic than lipofectamine 2000 in both cell lines i.e A549 and H1299. Even at higher N/P ratio of 12.5 at 100 nM siRNA concentrations these liposomes were non-significant in toxicity as compared to Lipofectamine 2000. At all ratios, CPE liposomes and RGD-CPE liposomes showed significantly higher cell viability than positive control lipofectamine 2000. Further, there was no significant difference in cell viability by RGD incorporation (1%, 2% and 3%).

For cellular uptake studies, FAM labelled negative control siRNA (FAM-NC-siRNA) was used. Flow cytometry was utilized for quantitative cell uptake to determine the mean fluorescent intensity while qualitative intracellular accumulation was determined using confocal microscopy. Liposomal formulations containing FAM-NC-siRNA at a final concentration of 100 nM were exposed to A549 and H1299 cells and analysed for mean fluorescence activity using fluorescence activated cell sorter. Naked FAM-NC-siRNA and Lipofectamine 2000 complexed siRNA were used as negative and positive control respectively. 2 mole% of RGD was found to be optimal for both types of liposomal formulations in A549 as well as H1299 cells. Fluorescence intensity in A549 cells after treatment with various siRNA formulations was as follow: Naked siRNA < DDC liposomes < CPE liposomes < Lipofectamine 2000 < RGD-CPE liposomes < DDHC liposomes < RGD-DDHC liposomes. In H1299 cells the order of fluorescence intensity in cells after treatment with various siRNA formulations was as follow: Naked siRNA < DDC liposomes < CPE liposomes < Lipofectamine 2000 < DDHC liposomes < RGD-CPE liposomes < RGD-DDHC liposomes. Maximum MFI in A549 cells were found to be 88.67 ± 1.02 and 82.40 ± 1.47 for RGD-DDHC liposomes (2%) and RGD-CPE liposomes (2%) respectively while, Maximum MFI in H1299 cells were found to be 80.30 ± 0.70 and 75.83 ± 1.05 for RGD-DDHC liposomes (2%) and RGD-CPE liposomes (2%), respectively. MFI values for Lipofectamine 2000 in A549 and H1299 were 74.63 ± 1.39 and 71.83 ± 1.19 respectively.

Cellular internalization of FAM labelled siRNA in A549 and H1299 cells was monitored by confocal microscopy. Cells were transfected with liposomal formulations containing 100nM of FAM labelled siRNA. Cells were also stained with nucleus staining dye DAPI and proceeded for confocal microscopy using confocal laser scanning microscope. Further, Live imaging was performed using confocal microscopy to access the potential of RGD grafting on the liposomal surface. After 6 h incubation, FAM-NC-siRNA was mainly observed in cytoplasm with a relative uniform distribution. Confocal microscopy also showed that RGD grafting helps to enhance the cellular localization in both cell lines. Live images revealed that naked siRNA only bound to the surface or lie outside of the cells. DDHC liposomes and CPE liposomes get accumulated inside the liposomes soon after transfection but RGD-DDHC and RGD-CPE liposomes showed different pattern for uptake. They initially bound to the cell surface and surface bound liposomes further taken up inside the cells. These results suggest the receptor based translocation of liposomal siRNA inside the cell.

Chemosensitization is well governed at sub-inhibitory concentration and hence, cell cycle analysis was used to determine the DNA content of cells at varying concentration of RRM1 siRNA i.e. 50 pM, 100 pM, 500 pM and 2.5 nM. Cells were transfected with RRM1 siRNA containing RGD-DDHC liposomes at varying siRNA concentrations. Cells were fixed by ethanol, stained with propidium iodide and analysed using FACS. Results suggested that 50 pM of RRM1 siRNA concentration is sub-inhibitory concentration and can be taken for chemosensitization.

siRNA mediated transfection was studied by quantifying mRNA knock-down of RRM1 gene by the mean of silencing potential of RRM1 siRNA containing formulations. Real time PCR (RT-PCR) was utilized to quantify the amount of mRNA present in the transfected cells of both cell lines (A549 & H1299). RGD grafted formulations showed significantly higher mRNA knock down ($p < 0.05$) than non-grafted liposomes in both cell lines and also more transfection was achieved as compared to lipofectamine 2000 at 5 nM concentrations. At 5 nM concentration RGD-DDHC liposomes and RGD-CPE liposomes showed $23.2 \pm 2.6\%$ and $24.2 \pm 3.4\%$ gene expression, while naked siRNA exhibited $83.50 \pm 2.5\%$ gene expression in A549 cells. In H1299 cells, gene expression was found to be $23.05 \pm 2.85\%$ for RGD-DDHC liposomes, $23.95 \pm 3.55\%$ for RGD-CPE liposomes and $85.9 \pm 2.5\%$ for naked siRNA. At lower concentrations, 500 pM and 50 pM, inhibition was

markedly decreased with both liposomal formulations and Lipofectamine 2000. RT-PCR also suggested that 50 pM is the sub-growth inhibitory concentration which was utilized for further Chemosensitization studies.

Chemosensitization effect was evaluated by studying the cytotoxic effect of Gemcitabine HCl in RRM1 siRNA pre-exposed lung cancer cells. *In vitro* cytotoxicity of anticancer drug Gemcitabine HCl at sequential concentrations was assessed with pre-treatment of RGD grafted siRNA nano-constructs (RGD-DDHC liposomes and RGD-CPE liposomes) in A549 and H1299 cells. Gemcitabine HCl solution (Gem.sol.) and Gemcitabine HCl liposomes (Gem. lipo.) were used as chemotherapeutic agents. IC₅₀ values for these different sets of cells were used to compare the chemosensitization efficacy. Chemosensitization effect was described by the fold change in IC₅₀ values when siRNA liposomes were pre-exposed in different sets of cells. The order of IC₅₀ value for Gemcitabine HCl in both A549 and H1299 cells were as follow: Gemcitabine solution < Gemcitabine liposomes < RGD-CPE liposomes (2%) + Gemcitabine solution < Lipofectamine 2000 + Gemcitabine solution < RGD-DDHC liposomes(2%)+ Gemcitabine solution < Lipofectamine 2000+ Gemcitabine liposomes < RGD-CPE liposomes(2%)+ Gemcitabine liposomes < RGD-DDHC liposomes(2%)+ Gemcitabine liposomes.

Highest chemosensitization for cationic liposomes (fold change=5.11 in A549 and 4.94 in H1299) was observed in cells pre-treated with RGD-DDHC liposomes (2%) followed by treatment with Gemcitabine liposomes as compared to treatment with Gemcitabine solution alone while, RGD-CPE liposomes (2%) showed 4.94 and 4.20 fold change in IC₅₀ value in A549 and H1299 cells respectively in same sets of cells. The order of fold change in IC₅₀ values for RGD-DDHC liposomes was more as compared lipofectamine 2000 and no significant difference was observed between RGD-CPE-liposomes and lipofectamine 2000. Results suggest the efficacy of developed formulation for chemosensitization of lung cancer cells against Gemcitabine HCl by pre-exposure of RRM1 siRNA in liposomal form.

The siRNA liposomes were studied for the integrity of incorporated siRNA in presence of serum at pH 7.4 for possible *in vivo* degradation because of degradation during circulation, and degradation due to extracellular and intracellular RNase. Naked siRNA, RGD-DDHC liposomes (2%) and RGD-CPE liposomes (2%) were incubated with non-heat inactivated FBS at 37°C for various time periods. At 0.5 h more than 10% of siRNA was degraded,

which reached up to 60% within 3 h. siRNA release at blood pH was also ascertain to maintain the siRNA within liposomes and hence to achieve the intracellular localization. After 6 h less than 20% of siRNA was remained as compared to initially loaded siRNA. RGD-DDHC liposomes and RGD-CPE liposomes encapsulated siRNA was stable even after 24 h and more than 75% of siRNA was preserved. Upto 8 hrs > 95% of the siRNA was preserved in both types of liposomes. It is generally observed that most of the liposomal formulations are distributed to different tissue within 6 hrs of injection and hence, prepared cationic formulation will be able to face *in vivo* fate.

Haemolytic toxicity of formulated liposomes was checked by incubating the formulation with erythrocyte separated from rat blood by centrifugation at low speed and analysing the supernatant at 541 nm. The haemolysis with different formulations was compared with that obtained with Triton-X100 as a positive control. RGD-DDHC liposomes (2%) showed $8.90\pm 0.40\%$ haemolysis while RGD-CPE liposomes (2%) showed only $2.645\pm 0.05\%$ haemolysis. Maximum haemolysis was observed with DD placebo liposomes i.e. $27.6\pm 1.30\%$.

Prepared liposomal formulations in three different categories, i.e. without PEGylation, with PEGylation and with RGD grafting, were studied for electrolyte induced flocculation test. This test confirms the stability of liposomal formulations in presence of electrolyte *in vivo*. siRNA containing liposomal formulations at (100 nM) were incubated at varying concentration of sodium chloride i.e. 1, 2, 3, 4 and 5%. After 1 hr of incubation at 37°C particle size was determined. Particle size of non-pegylated liposomes was found to increase significantly at all concentration of added salt in both, cationic and CPE, types of liposomal formulations. However, again in both cases, incorporation of 5 mol% of mPEG₂₀₀₀-DSPE did help in maintaining the particle size. Upto 2% NaCl addition was found to maintain particle size of DDHC and RGD DDHC liposomes below 150 nm. Addition of 3% and above concentration of salt increased the particle size upto 300 nm. Particle size of the CPE and RGD-CPE liposomes was maintained below 150 nm upto 3% electrolyte addition. Even 5 % salt did not able to cross particle size beyond 200 nm.

In vivo toxicity of developed liposomal formulations were evaluated in female swiss albino mice. For determination of maximum tolerated dose (MTD) of siRNA loaded liposomes, Fixed Dose Procedure of OECD-Organization for Economic Cooperation and Development was used. Typical protocol includes administration of a drug/drug product in

escalating doses through intravenous route and observing animals for any signs of toxicity. Fixed dose test substances (siRNA loaded liposomes) were administered in a constant dose volume of 20 mL/kg. All doses were prepared prior to administration. Above maximum therapeutic doses of siRNA loaded liposomes (0.75 mg/kg of siRNA), only liposomal carrier (without siRNA loading) was tested to ascertain the safety profile of developed liposomal carrier systems. MTD values for RGD-DDHC liposomes and RGD-CPE liposomes were found to be > 0.75 mg/kg of siRNA, whereas RGD-DDHC liposomes (placebo) and RGD-CPE liposomes (placebo) showed MTD values of >300 mg/kg and >600 mg/kg of total lipids respectively.

The stability testing of prepared liposomal formulations, RGD-DDHC liposomes and RGD-DDHC liposomes was performed at accelerated condition ($25^{\circ}\text{C} \pm 2^{\circ}\text{C}$, 60% RH \pm 5% RH) for six months and at long-term conditions ($2-8^{\circ}\text{C}$) up to six months. Various parameters, i.e. assay, siRNA entrapment, particle size and zeta potential, were evaluated after each predetermined time points (1, 2, 3 and 6 month). Apart from these, water content was also determined for RGD-DDHC liposomes. In case of RGD-DDHC liposomes both accelerated and refrigerated conditions, Assay and siRNA entrapment values were found within range (95-105% of initial) and change was non-significant. There was no significant increase in particle size and zeta potential after six month at both conditions. Water content was increased to a significant extent ($3.79 \pm 0.19\%$ w/w at 6 month) at accelerated condition while refrigerated condition maintained the water content value < 3% w/w even after six months of storage. While in case of RGD-CPE liposomes, accelerated condition showed that Assay value (94.62 ± 2.90 at 6 month) and siRNA entrapment (75.80 ± 1.87 at 6 month) were found to decrease significantly as compared to initial values. Particle size was also increased significantly from first month only. At $2-8^{\circ}\text{C}$ condition, Assay and siRNA entrapment values were found to lie within range (95-105% of initial value) and particle size was also maintained below 150 nm.

8.2. Conclusions

To conclude, RRM1 siRNA encapsulated nanoconstructs in liposomal forms were successfully prepared. Two types of liposomal formulations were developed, i.e. cationic liposomes containing DOTAP as a key cationic lipid and calcium phosphate encapsulated liposomes containing calcium phosphate complexed siRNA inside the liposomes. Both formulations were optimized to achieve maximum siRNA encapsulation. Particle size of

the liposomes was also chosen as one of the optimization parameters as particle size was found to increase in case of cationic liposomes due to complexation between cationic lipid and siRNA. Developed formulations were well characterised using Cryo-TEM and proved the bilayer structure of liposomes with uni-lamellarity. Presence of calcium phosphate precipitates inside the RGD-CPE liposomes was clearly observed. Both the formulations showed less cell cytotoxicity at therapeutic and higher concentrations. RGD grafting on liposomal surface was found to increase the cell uptake of siRNA. Optimal RGD concentration was found to be 2 mole%. RGD grafted liposomes significantly increased intracellular localization of siRNA as compared to non RGD grafted liposomes. Further, RGD also governed the cell uptake via receptor mediated pathway, which was shown by live uptake studies. Sub-inhibitory concentration (50 pM) was obtained by cell cycle analysis and transfection studies. mRNA quantification after 2.5 nM concentration of siRNA showed transfection efficacy of developed liposomal formulations. More than 75% of gene silencing was obtained with both liposomal formulations and hence transfection efficacy was proven. Pre-exposure of siRNA liposomes at 50 pM concentration sensitized the lung cancer cells against Gemcitabine HCl up to 5 fold in both the lung cancer cells. Haemolysis study showed that PEGylation markedly decreased the haemolysis of erythrocyte. RGD-DDHC liposomes(2%) and RGD-CPE liposomes(2%) at very high lipid concentration (5 mM) showed less than 10% of haemolysis as compared to >25% haemolysis with DOTAP:DOPE placebo liposomes. This high percentage of haemolysis might be due to amount of free DOTAP lipid, which is carrying very high positive surface charge. RGD-DDHC and RGD-CPE both liposomes preserved the siRNA in the liposomal forms against serum nucleases and less than 5% of siRNA was released within 8 hrs in presence of serum at pH 7.4. Effect of addition of electrolyte to govern flocculation was well studied and PEGylation was found to maintain the particle size against added electrolyte for maintaining the particle size. Both formulations showed non-significant change in particle size (below 150 nm) upto 2% addition of electrolyte. However, RGD-CPE liposomes maintained the particle size (below 200 nm) even upto 5% of electrolyte concentration. *In vivo* toxicity studies revealed that developed RGD grafted formulations are safe to administer even at much higher concentrations than required for achieving therapeutic effect. Stability studies indicated that both formulations should be stored at 2-8°C/refrigerated condition. At 25C±2°C / 60±5RH% condition, RGD-DDHC liposomes in

lyophilized form showed increase in water content and RGD-CPE liposomes showed decrease in assay and entrapment values. Hence, refrigerated condition was recommended. Present investigation shows a promising way to treat lung cancer using genomic approach with enhanced margin of safety and reduced dose dependent toxicity of the Gemcitabine HCl. Pre-exposure of RGD grafted siRNA liposomes targeting RRM1 protein caused sensitization of cancer cells. Developed liposomes are stable in presence of serum and delivered the siRNA inside the cells along with efficient transfection. Sub-inhibitory concentration of siRNA will avoid toxicity related to localization of siRNA in unwanted sites. Taken collectively, suggested approach will definitely open a vista in the era of cancer treatment with reduced dosing profile.

List of Publications

Patents:

- 1) "Preparation of Liposomal Amphotericin-B by Super Critical Fluid Technology" Indian Patent - Application No-391/MUM/2008, Publication date: 25/02/2008
- 2) "Novel Non-viral Vector for Delivery of Small Interfering RNA" Indian Patent - Application No-560/MUM/2012, Publication date: 22/02/2012.
- 3) "Small Interfering RNA Nanoconstructs for Chemosensitization in the Treatment of Lung Cancer". Indian Patent - Application No-559/MUM/2012, Publication date: 22/02/2012.

Publications:

- 4) **N. I. Khatri**, M. N. Rathi, D. P. Baradia, S. Trehan and A. R. Misra. In vivo delivery aspects of miRNA, shRNA and siRNA, Critical Reviews™ in Therapeutic Drug Carrier Systems. 29(6), 487-527 (2012).
- 5) **Nirav I. Khatri**, Mohan N. Rathi et al. Patents Review in siRNA Delivery for Pulmonary Disorders, Recent Pat Drug Deliv Formul. 2012 Apr 1;6(1):45-65.
- 6) Dipesh Baradia, **Nirav Khatri**, Sonia Trehan, Ambikanandan Misra. Inhalation therapy to treat Pulmonary Arterial Hypertension, Pharmaceutical Patent Analyst. Pharm. Pat. Analyst (2012) 1(5)
- 7) **Khatri N**, Misra A. Development of siRNA lipoplexes for intracellular delivery in lung cancer cells. J Pharm Bioall Sci 2012;4:1-3.
- 8) Desai J, **Khatri N**, Chauhan S, Seth A. Design, development and optimization of selfemulsifying drug delivery system of an antiobesity drug. J Pharm Bioall Sci 2012;4:21-2.
- 9) **N. I. Khatri** and A.N. Misra. Application of polymers in parenteral drug delivery. In 'Application of polymers in drug delivery' Misra A.N. (Ed.), iSmithers publisher, London, UK under preparation.
- 10) **N. I. Khatri.**, M. N. Rathi, D. P. Baradia, and A. N. Misra. siRNA Nano-Constructs for chemosensitization of Gemcitabine HCl in lung cancer treatment, Pharm Research. (Revision Submitted)
- 11) **Nirav Khatri**, Dipesh Baradia, Imran Vhora, Mohan Rathi, Ambikanandan Misra, cRGD Grafted Liposomes Containing Inorganic Nano-Precipitate Complexed siRNA for Intracellular Delivery in Cancer Cells, Journal of Controlled Release. (Revision Submitted)
- 12) Imran Vhora, **Nirav Khatri**, Jagruti Desai, Hetal Thakkar. Caprylate Conjugated Cisplatin for Development of Novel Liposomal Formulation. AAPS PharmSciTech. 2013. (Accepted Manuscript)
- 13) Priyanka Bhatt, **Nirav Khatri**, Dipesh Bardia, Ambikanandan Misra, Microbeads mediated oral plasmid DNA delivery using polymethacrylate vectors: An effectual groundwork for colorectal cancer, Drug Delivery. (Under Review, Manuscript Id:UDRD-2013-0399)
- 14) **Nirav Khatri**, Dipesh Baradia, Imran Vhora, Ambikanandan Misra, Development and Characterization of siRNA Lipoplexes: Effect of Different Lipids, In Vitro Evaluation in Cancerous Cell Lines and In Vivo Toxicity Study,. AAPS PharmSciTech (Under Review, Manuscript Id: AAPSPT-D-13-00569)